UNIVERSITY OF TRENTO - Italy

International PhD Program in Biomolecular Sciences

Department of Cellular, Computational and Integrative Biology – CIBIO

XXXI Cycle

Biological and microbiological properties of dental implants and their relation to peri-implant diseases

Tutor

Prof. Nicola Segata
CIBIO (Department of Cellular, Computational and Integrative Biology), University of Trento

Advisors

Dr. Francesco Tessarolo
Department of Industrial Engineering, University of Trento

Prof. Cristiano Tomasi
Department of Periodontology, Institute of Odontology, University of Gothenburg

Ph.D. Thesis of

Paolo Ghensi
CIBIO (Department of Cellular, Computational and Integrative Biology), University of Trento

Academic Year 2017/2018

Contents

Table of Contents

Declaration of authorship

Declaration

I Paolo Ghensi confirm that this is my own work and the use of all material from other sources has been properly and fully acknowledged.

Abstract

With the increasing use of dental implants in the population, the past three decades have seen a dramatic growth in the prevalence of two new oral diseases: peri-implantitis which affects both soft and hard tissues surrounding the implant, and mucositis which precedes peri-implantitis and involves instead only soft tissues. Mucositis affects 50% to 90% of implants, while almost 20% of implants develop peri-implantitis that can lead over time to implant loss.

The underlying hypothesis of this research project is that dental implant properties and their interaction with surrounding soft and hard tissues and oral microbiome play an important role in the maintenance of peri-implant health. Regarding specific characteristics of dental implants, experimental data are in part still lacking on biochemical behavior of implant surfaces and of possible new coatings able to reduce bacterial colonization. From the microbiological viewpoint, based on the lessons learned from the study of periodontal diseases, there are reasons to believe that specific members of the oral microbial communities represent a prerequisite for the development of peri-implant diseases. A thorough profiling of the microbial organisms associated with disease is thus the first step to undertake in order to develop novel prevention and therapeutic strategies. Currently available studies, however, adopted a study design which is not accounting for inter-subject variability, focused on few cultivable microbes only, or used low-resolution microbial profiling. Overall, there are thus several open questions on implant characteristics and microbiologic aspects that need to be addressed for the next generation of implant care.

Because these aspects are tightly interconnected, in this thesis I employed an integrated approach to study multiple aspects of biological and microbiological properties of dental implants and their relation to peri-implant diseases. Starting from implant surfaces, we evaluated the biochemical behavior of a specific type of moderately rough surface. We found that, *in-vitro,* this surface called OGI (Osteo Growth Induction) positively acts on osteogenic and angiogenic commitment of mesenchymal stem cells (MSC). Still in the field of implant surfaces, we developed and tested *in-vitro* a potential anti-biofilm sericin-based coating obtaining very promising bacterial inhibition values. Finally, we investigated *in-vivo* through shotgun metagenomics the plaque microbiome associated with peri-implant health and disease unraveling specific microbial and functional signatures associated with these conditions and identifying specific disease-associated microbiome features.

In this work we showed that peri-implant diseases are connected with the specific composition of the plaque microbiome and that implant surfaces, in addition to a potential strong bioactive role, if properly treated can significantly reduce microbial adhesion on them. Stressing that maintenance therapy always remains something essential, new scenarios for the future are possible. Besides the need of employing implants with adequate micro- and macro-characteristics, the ever more in-depth knowledge of the peri-implant microbiome will allow to implement increasingly effective anti-biofilm implant surfaces and to introduce microbiome-based protocols of diagnosis, prevention and personalized therapy.

1. Introduction

Since the late 70s, the use of osseointegrated implants for replacing missing teeth has become a clinical practice increasingly common and accessible to the population. Over the years, innovations that have concerned both the surgical technique and the materials used have allowed to make implant therapy more and more predictable and usable by the population; to date, millions of implants are placed every year worldwide, exceeding one million units in Italy alone (Carr 1998; Klinge et al. 2015). Dental implants have very high survival rate (> 90%) over a 10-year period, however, in line with other medical disciplines, also oral implantology is not free from complications. The past 3 decades have seen the emergence of 2 new oral diseases: peri-implant mucositis and peri-implantitis (Moraschini et al. 2015). These peri-implant inflammations represent serious diseases connected with dental implant treatment, which affect both the surrounding hard and soft tissue. Due to its potential fast progression, peri-implantitis can lead to the loss of the implant if not associated with multilateral prevention and therapeutic interventions. Specific continuous check-ups with evaluation and elimination of risk factors (e.g. periodontitis, smoking, systemic diseases) are effective precautions (Smeets et al. 2014; Berglundh et al. 2018; Heitz-Mayfield and Salvi 2018a; Schwarz et al. 2018).

I am introducing below the different aspects connected with peri-implant diseases that are the basis for the work in my thesis.

Unclear role of implant surface roughness as potential modifying factor for peri-implant diseases. In the first age of implant osseointegration studies, the so-called age of smooth surfaces, the complication most frequently responsible for failure was represented by problems with the dental implant osseointegration (Wiskott et al. 1999; Quirynen et al. 2002; Esposito et al. 2014). In order, therefore, to improve the osseointegration process, since the beginning of the 90s, implant surfaces began to be chemically treated to make them rougher and more bioactive towards the bone tissue. This innovation allowed to make the osseointegration process more and more predictable, also reducing drastically the waiting time for loading endosseous implants (Trisi et al. 1999; Schwartz et al. 2005). Some authors have suggested that the prevalence of peri-implant diseases began to increase gradually and significantly over the years after introduction of rough surfaces (Quirynen et al. 2002; Martines et al. 2008). However, it is currently still unclear to what extent the increased incidence of peri-implant diseases is due to rough surfaces; what is demonstrated in animal experiments is that rough surfaces significantly influence the rate of progression and severity of peri-implantitis being much more easily attacked by the bacterial biofilm compared to smooth surfaces when they are exposed to the oral environment (Albouy et al. 2012; Carcuac et al. 2013). It should be however taken into account that, compared to the first implant age, indications and techniques of oral implantology over the years have been exasperated and users, even unskilled, have significantly increased, thereby increasing the risk of biological and mechanical complications and failures (Sakka et al. 2012; Heitz-Mayfield et al. 2013).

Need for a shared solution for the growing prevalence of peri-implant diseases. To date, peri-implant diseases result to be very consolidated and evidence indicates that mucositis occurs in 50% to 90% of implants, while almost 20% of implants with an average function time of 5 to 11 years develop peri-implantitis. This means that approximately a fifth of all inserted dental implants are suffering from a disease, which may lead over time to implant loosening or

to the need for implant removal (Smeets et al. 2014; Derks and Tomasi 2015; Derks et al. 2016; Berglundh et al. 2018). Within the scientific community there is an open debate about how to address and resolve this issue: some researchers advocate a return to smooth surfaces or at least significantly less rough surfaces (Simion et al. 2015a, 2015b); others suggest improving the mucosal seal around implants that is considered the true entrance door of bacteria (Silverstein et al. 1994; Bumgardner et al. 2011); finally, others have suggested that new surfaces or coatings with antibacterial properties should be developed (Qin et al. 2018; Chouirfa et al. 2019). Moreover, some scientists believe that a revision of the indications and criteria of modern implantology is needed (Pinchi et al. 2014). Peri-implantitis is therefore a well-established disease and urges for new strategies, procedures and devices able to counteract or prevent its occurrence. It is therefore anticipated that research activities in the field oral implantology will particularly focus on peri-implant diseases in the near future.

Need for further investigations on the role of the oral microbiome in peri-implant diseases. What is well established is that peri-implant diseases are microbial biofilm-induced but precise mechanisms of onset and progression remain however still not completely known, including the specific bacteria underlying these diseases (Takanashi et al. 2004; Tabanella et al. 2009; Rakic et al. 2016; Lafaurie et al. 2017; Teles 2017). Bacterial colonization is a key requisite although there remains debate about the precise role of host response in the onset and progression of mucositis and peri-implantitis (Heitz-Mayfield and Lang 2010). To date, therapeutic interventions and prognostic algorithms for peri-implant diseases were based on a paradigm of clinical similarity with periodontal diseases (Mombelli et al. 1995; Shibli et al. 2008; Dabdoub et al. 2013). However, the outcomes of these therapies have been modest, with disturbingly high rates of disease recurrence, suggesting that peri-implantitis and periodontitis might not be as similar as previously thought (Renvert et al. 2009; Esposito et al. 2012; Dabdoub et al. 2013; Carcuac et al. 2016). Although certain known periodontal pathogens may also be associated with the etiology of peri-implantitis, apparently there are many differences between these two clinical conditions, involving distinct microorganisms (Faveri et al. 2015). Moreover, recent studies, while maintaining the association of Gram-negative anaerobic microorganisms with peri-implantitis as in periodontitis, revealed new microbial signatures that might be uniquely associated with peri-implantitis (Kumar et al. 2012a). Further investigations on the diversity of peri-implant microbiome would be essential in order to define effective preventive and therapeutic strategies (Faveri et al. 2015).

Evolution of the techniques for the study of microbial organisms: from cultivation to metagenomics. Investigations of the oral microorganisms with crucial roles in oral diseases are being performed since decades, but the recent evolution in technologies for “reading” the DNA revolutionized the field. By sequencing the genetic material present in an oral sample (e.g. from a swab of the supragingival or subgingival plaque) it is possible to study the ecosystem of bacterial, viral, micro-eukaryotic, and archaeal organisms - the microbiome - present in the dental environment. Such techniques, called metagenomics, have the crucial advantage that they avoid completely the cultivation step which is very time consuming and can target only a small fraction of microbes with known cultivation protocols (Segata et al. 2013; Quince et al. 2017). This led to the recent definition of the current map of the microbiome in healthy individuals within the largest metagenomic sequencing effort performed so far (the Human Microbiome Project) (Consortium and The Human Microbiome Project Consortium 2012).

Metagenomics as a powerful tool to better study microbiome - peri-implant diseases connection. Although the study of the microbiome gained a lot of popularity in the last ten years, only recently the research community improved the sequencing and analysis approaches to profile the oral microbiome at very high resolution (Donati et al. 2016). Preliminary studies on peri-implant diseases adopted, in fact, a study design which was not accounting for inter-subject variability and used low-resolution microbiome profiling (Charalampakis and Belibasakis 2015). To date, at the best of our knowledge, shotgun metagenomic sequencing has never been used in any study of peri-implant diseases; apart from cultivation-based approaches, the most advanced method to investigate the peri-implant microbiome to date was the 16S rRNA deep sequencing (Heuer et al. 2012; Kumar et al. 2012a; Dabdoub et al. 2013; Maruyama et al. 2014; Schaumann et al. 2014; Faveri et al. 2015; Tsigarida et al. 2015; Zheng et al. 2015; Robitaille et al. 2016; Sanz-Martin et al. 2017; Schincaglia et al. 2017). However, even the studies in which the 16S rRNA sequencing was used followed a questionable and not very effective methodology and have led to conflicting results leaving unaddressed crucial aspects such as whether the microbial risk factors or peri-implantitis are similar to those of periodontitis. Moreover, it is still unclear which are the most relevant organisms from which the material of the implant should try to be protective; this may allow to develop specific materials that are most effective against the most harmful microbial bacterial organisms. Altogether, there is now the opportunity to gain crucial insights into the relation between oral microorganisms and peri-implant diseases with the latest advances in metagenomic approaches and analysis techniques.

1.1 Aims and main contributions of the thesis

Based on the high incidence of peri-implant biological complications in the population and the current unknown aspects in their mechanisms of onset and progression, the works presented in this thesis aim to analyze peri-implant diseases and their related factors from different perspectives in order to give a contribution toward the biochemical characterization of moderately rough implant surfaces, the development of new coatings able to reduce microbial adhesion and the deep understanding of peri-implant microbiome. Each chapter will deal with a distinct topic and will have a specific aim, while trying to maintain a logical thread. The main contribution of this thesis to the field of dental implants and connected diseases are described in **Chapters 3, 4**, and **5**, and their respective aims are:

- investigate biochemical properties of a specific moderately rough implant surface and their influence on the angiogenic and osteogenic behaviors of mesenchymal stem cells (MSCs);
- develop and test a sericin-based coating with anti-biofilm properties for dental implants;
- identify microbiome features associated with the onset and progression of peri-implant diseases;

All of the chapters in this thesis are based on articles (published, or under submission) that are fully reported in **Chapters 3**, **4**, and **5**.

There are different implant surfaces on the market, but those that are moderately rough (1 µm<Sa<2 µm) have been suggested as clinically ideal as they are supposed to limit bacterial

colonization if they are exposed to the oral environment. However, there is less evidence regarding their biological characteristics. **Chapter 3** therefore explores the biochemical behavior of a specific type of moderately rough surface. Specifically, we tested *in-vitro* (Ghensi et al. 2017a, 2017b) the influence of this surface on the osteogenic and angiogenic commitment of MSC (mesenchymal stem cells).

Some authors have suggested that new implant surfaces or coatings with anti-bacterial properties should be developed in order to prevent and drastically reduce the incidence of peri-implant diseases. **Chapter 4** describes the development and testing of a new potential anti-biofilm coating based on sericin, one of the two main silk proteins, whose antibacterial efficacy is still debated. Different experimental protocols are evaluated in order to find the most suitable sericin-based coating on medical grade titanium (Ti) able to reduce microbial adhesion and biofilm formation on the dental implant surface (Ghensi et al. 2019).

Chapter 5 investigates the plaque microbiome associated with peri-implant health and peri-implant diseases through a shotgun metagenomic sequencing approach coupled with the novel computational methods developed in the host laboratory (Ghensi et al., under submission). The final aim is to unravel specific microbial organisms, genes, and virulence factors associated with these conditions and to identify disease-associated microbiome features for new diagnostic and therapeutic approaches.

Finally, in the Conclusions (**Chapter 6**) I summarize the overall results of each chapter.

2. Background

For a better overall understanding, in this chapter I will discuss the concept of dental implant (**2.1 Dental implants**) and its characteristics (**2.2 Dental implant surface** and **2.3 Dental implant-abutment connection**) also in relation to the surrounding tissues (**2.4 Peri-implant tissues**), so as to be able to understand in the following chapters as these implant micro- and macro-characteristics may influence the onset and progression of peri-implant biological complications (**2.5 Peri-implant diseases**). Finally, I report the current state-of-the-art regarding the peri-implant plaque microbiome in healthy and diseased implants (**2.6 The plaque microbiome in healthy and diseased implants)**.

2.1 Dental implants

A dental implant is one of the treatment options to replace missing teeth. It is a structure made of an alloplastic biomaterial that is surgically inserted into the upper or lower jaw bone to solve a patient's functional and / or aesthetic problems (Shemtov-Yona and Rittel 2015). The use of dental implants in the treatment of partial and complete edentulism has become an integral treatment modality in modern dentistry. A typical dental implant, as shown in Figure 1, includes the implant body to be surgically inserted in the bone. The abutment is the part of the implant that is applied to support and / or retain the superstructure (i.e., removable or fixed prosthesis) (Misch 2014).

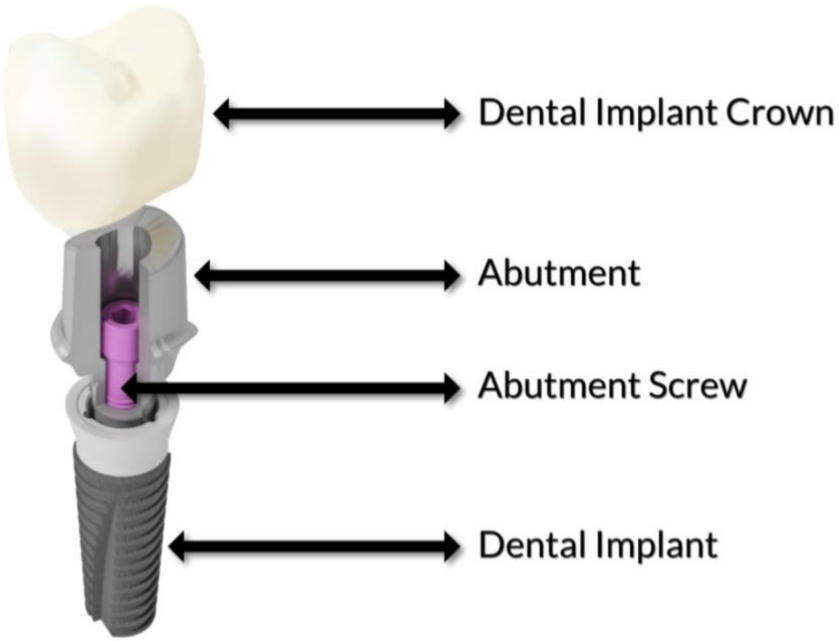

Figure 1. Dental implant components (source www.feedx.club/hashtag-overview/dentalclinicdubai)

Despite the recent advent of alternative materials such as zirconia, most dental implants today are made of commercially pure titanium (CP-Ti grade 4 or 5) or titanium alloy Ti-6Al-4V (Bosshardt et al. 2017; Liu et al. 2017; Koizumi et al. 2019). This material selection is based on the well-documented properties of biocompatibility and corrosion resistance of those materials and on the excellent bone-titanium bonding. Titanium, in fact, bonds incredibly effectively with bone because a thin film of titanium oxide (TiO_2) forms on its surface when it is exposed to air (Fleck and Eifler 2010). This film not only provides the means of bonding the metal to human tissue, the so-called “osseointegration”, but it prevents the corrosion of the metal beneath, ensuring durability (Kingston and Webster 2013). Osseointegration implies an anchoring mechanism, in which titanium components can be reliably and predictably incorporated into living bone and this direct structural and functional connection between bone and the endosseous implant can persist in all normal loading conditions (Brånemark et al. 1969b).

Modern dental implantology begins with the work of Professor Per-Ingvar Brånemark at the University of Gothenburg, Sweden, and Professor Andre´ Schroeder at the University of Bern, Switzerland. Professor Brånemark was the first to observe the unique property of titanium in osseointegration. From this observation, he then had the further understanding that titanium could be used as a material for endosseous dental implants (Greenberg 2015).

Continuous scientific research in the basic science of bone biology, dental implant surfaces and metallurgy has allowed continuous developments in the field of implant dentistry making this procedure highly accessible to the general population. After more than four decades, dental implantology can be considered a well-established therapeutic solution in the treatment of partial or complete edentulism (Guillaume 2016). The technique is reliable and drastically reduce the use of partial and complete removable dentures, which may not be well tolerated by all patients (Rissin 1978; Carr and Laney 1987; Carlsson 1998).

The reliability of oral implantology is mainly based on the general analysis of the patient's clinical situation and the appropriate use of the different surgical-prosthetic options. Currently available dental implants meet strict criteria of manufacturing and two main parameters distinguish them from each other apart from the external design (Guillaume 2016). The first is the implant's surface characteristics, and the second, of a more macroscopic nature, is the junction between the implant and the abutment, the so-called implant-abutment connection. This connection should provide a high quality, intimate union between the two components ensuring stability, effective mechanical coupling and an adequate seal against bacteria entering the interface (Jaworski et al. 2012; Machado et al. 2013; Nassar and Abdalla 2015; Mishra et al. 2017).

2.2 Dental implant surface

The control of the surface characteristics of dental implants is a topic of great relevance and importance in the field of dental implantology and the surface morphology has been and is still nowadays the workhorse of many innovations and new proposals (Hosseini et al. 2000; Morra et al. 2003) (Figure 2).

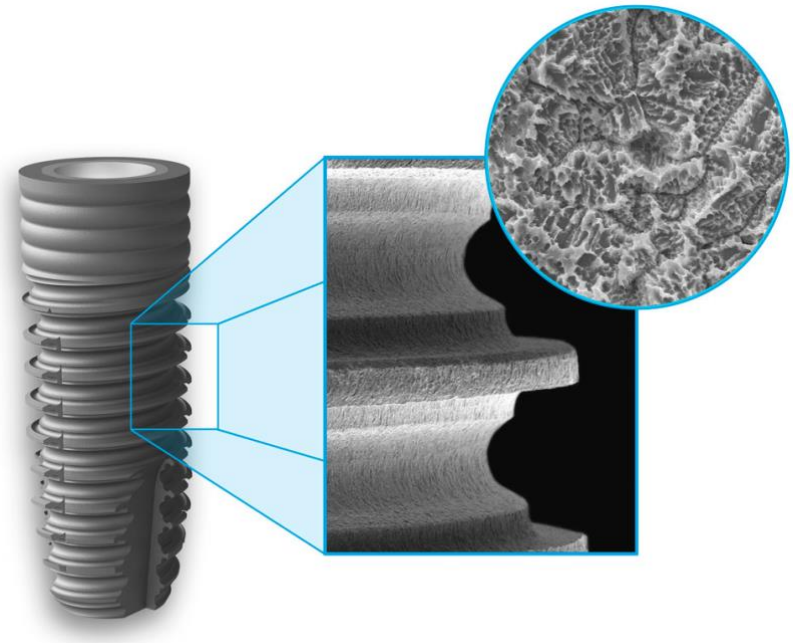

Figure 2. Dental implant surface at different magnifications (source www.clcscientific.com/it/clc-conic)

In the pioneering era of implantology, the first implant surfaces were smooth, obtained by turning processes of titanium able to confer a high anisotropy in the distribution of surface irregularities, and with a dominant direction (Albrektsson and Sennerby 1991; Eckert et al. 1997; Davies et al. 2009). The first Brånemark studies based on implants with such machined surface demonstrated that, although the surface was extremely smooth, it was possible to achieve adequate osseointegration. (Brånemark et al. 1969b). However, in order to further improve and accelerate implant osseointegration, numerous treatments have been suggested and applied over time aiming at increasing surface bioactive properties (Sykaras et al. 2000).

So, over the years, various processes have been introduced to obtain roughened implant surfaces characterized by a greater surface area (Ivanoff et al. 1997; Grassi et al. 2006; Shibli et al. 2007). It is known that the treatments applied to the implant surface induce modifications not only in the chemical composition, but also in the topography (Larsson et al. 1996). These modified surfaces are much rougher and more isotropic, that is with numerous irregularities, accentuated, irregular, and without a dominant direction (Wennerberg and Albrektsson 2009).
The research in this field has focused on obtaining surfaces that allow greater bone-to-implant contact (BIC) (Cochran et al. 1998b; Bigerelle et al. 2002). The implant surface represents in all respects the link between the human body and the implant prosthesis; through this interface the occlusal forces are discharged during the function. Implant surface, therefore, must not only promote bone healing, but also maintain it over time (Davies et al. 2009).

There are many human histological studies who have investigated how different roughness levels can influence the process of osseointegration. Overall, these studies have shown that implants with a rough surface allow the establishment of micromechanical retentions between the implant and the bone tissue, and above all how they present a percentage of contact bone-implant (BIC) greater than that of smooth implants (Wennerberg et al. 1996b; Cochran et al. 1998b; Davies et al. 2009). This allows to achieve a faster and stronger osseointegration and an increase in the primary stability of the implant upon insertion (Ivanoff et al. 1997; Gotfredsen et al. 2000; Hallgren Höstner 2001).

A concept widely established by the science of medical materials is that cell-material contact does not take place directly, but through the medium of proteins that bind to the surface in the first moments of exposure of the implant to the biological fluid (Wojciechowski 1996). Since protein molecules have a much smaller size than cells, they have a much higher diffusion coefficient and transfer rate, and are always the first to reach the surface. The cell therefore does not encounter a titanium surface, but a surface covered by a bed of adsorbed proteins, some of which, having chemical structures capable of binding to cells receptors, are able to mediate cell adhesion (Ellingsen 1991). Since the composition of the protein bed depends on the surface characteristics, it is clear that cell adhesion is also tightly bound (Morra et al. 2003).

In the chain of events leading to osseointegration of an endosseous implant the surface characteristics therefore play a major role: in this regard, a paper by Albrektsson et al dating back to 1981 (Albrektsson et al. 1981) already underlined how the quality of the implant surface represented one of the six key factors able to influence the healing of the surgical wound and consequently the process of osseointegration.

2.2.1 Classification of dental implant surfaces

The surface modification methods can be generally divided into two broad categories: subtractive and additive processes (Rupp et al. 2018) (Figure 3). Among the additive processes, titanium deposition by plasma spray, hydroxyapatite and calcium-phosphate coatings and sinterization are just some of the available methods. The main subtractive processes, on the other hand, are represented by grit-blasting, acid etching by strong mineral acids (hydrochloric acid-HCl and sulfuric acid-H_2SO_4 are among the few acids able to react with titanium oxide), anodic oxidation or several combinations of these techniques, e.g., combined grit-blasted/acid etched surfaces. These subtractive processes determine a modification of the free surface energy and, consequently, of the implant roughness (Davies et al. 2009; Rupp et al. 2018).

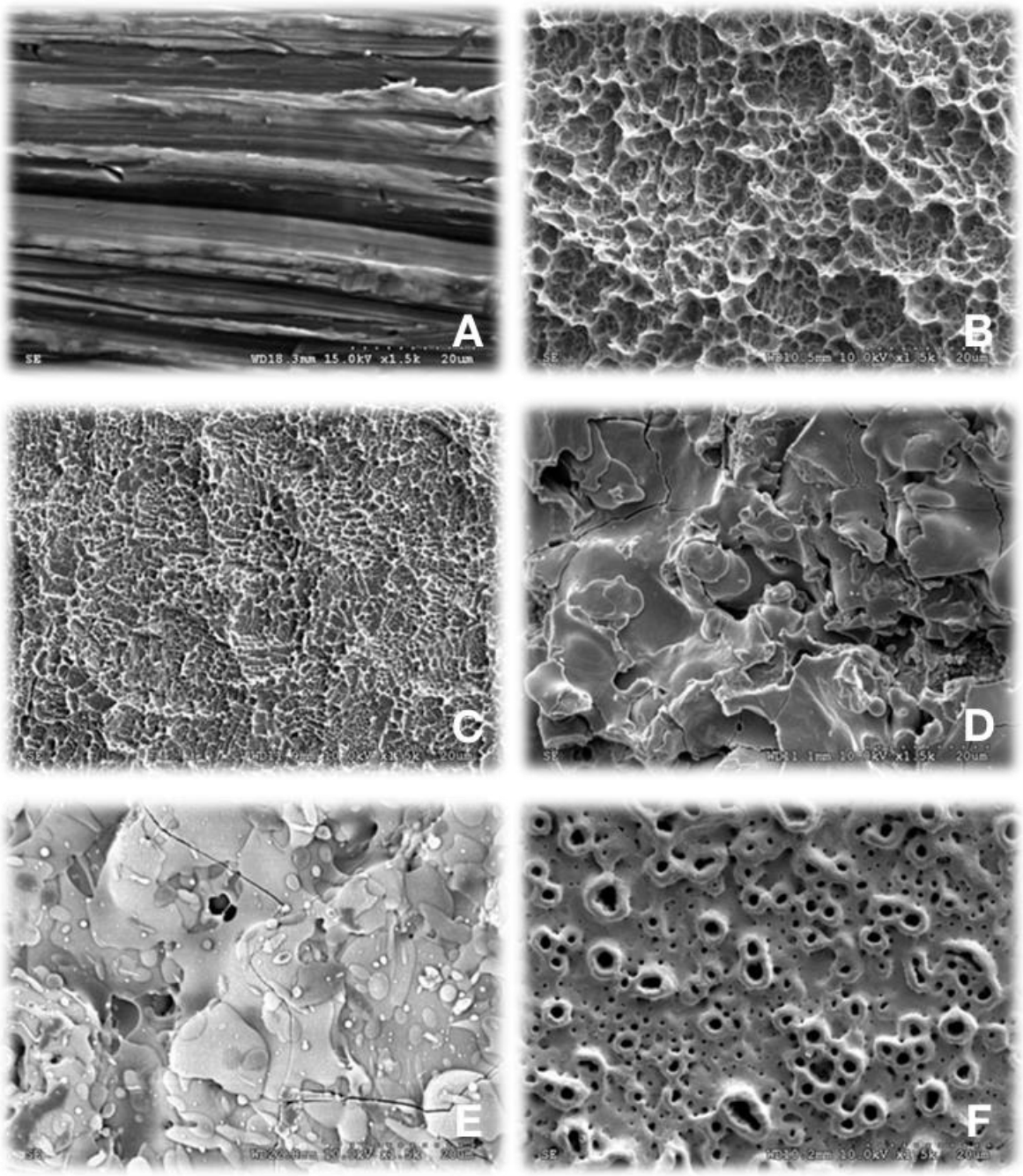

Figure 3. Different dental implant surfaces. A) machined; B) grit-blasted; C) grit-blasted and acid etched; D) titanium plasma-sprayed; E) hydroxyapatite coated; F) anodized

2.3 Dental implant-abutment connection

As already mentioned, one of the features that differentiates the various implant systems is the design of the connection that allows the prosthetic superstructure to be connected to the implant (Gracis et al. 2012) (Figure 4). The implant-abutment connection is related to the possible formation of abutment micromovements causing microgaps at the interface and bacterial leakage (contamination from the abutment to the external environment) (Herrero-Climent et al. 2014; Zipprich et al. 2016; Zipprich et al. 2018). For this reason, it is considered a fundamental factor in the maintenance of peri-implant health (Koutouzis 2019). Although there are a number of trade names, implant-abutment connection designs can be summarized in two main categories: external and internal connections (Bonfante and Coelho 2016) (Figure 5).

Figure 4. Connection between the dental implant and its abutment (source www.clcscientific.com/it/clc-conic)

2.3.1 Classification of dental implant-abutment connections

The most common type of external connection is the hexagonal one; changes in height and width affect the tactile perception and stability (more often, anti-rotational) of the superstructure. The octagonal connection and the spline interface, with its projections and its interdigitating slots, are other examples of external connection. The category of internal connections includes, instead, the internal hexagon, the internal octagon and the conical interface (Sykaras et al. 2000).

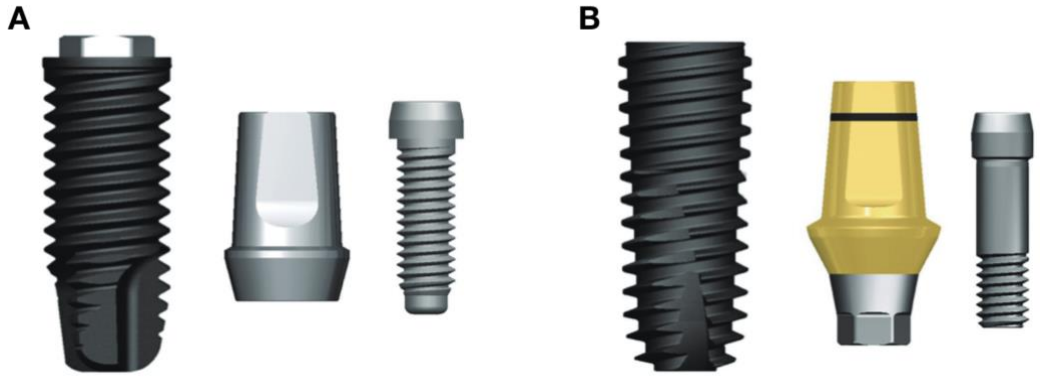

Figure 5. Implant/abutment connections: (A) External type; (B) Internal type (from Cho et al. 2015)

External connections, particularly the hexagonal ones, have been used since the dawn of modern implantology, through the implant system introduced by Professor Brånemark (Lemos et al. 2018). Although still widely used today, this type of connection has some drawbacks, in particular the biomechanical behavior when exposed to off-axis loads (Gracis et al. 2012). Therefore, it was hypothesized that, under high occlusal loads, the external hexagon could lead to micromovements and instability of the abutment, which has been associated with mechanical complications (Camargos Gde et al. 2012; Lemos et al. 2018). Internal connections were developed to eliminate or eventually decrease the micromovements at the interface level and to reduce stress transferred to the peri-implant bone (Ceruso et al. 2017). Long-term clinical data support this hypothesis demonstrating how internal connection remarkably lowers the rotation center and improves the mechanical stability reducing screw loosening and fracture and enhancing stress dissipation around the implant (Sailer et al. 2009; Mangano et al. 2015; Santiago et al. 2016). However, the European Association for Osseointegration Consensus Conference, suggested that more research and clinical studies are needed to evaluate the differences in peri-implant bone loss between different implant-abutment connections (Gotfredsen et al. 2012; Lemos et al. 2018).

Regardless of whether the connection is internal or external, the abutment and implant can have equal diameters, or an abutment with a narrower diameter (“platform switching” concept) can be used. Platform switching therefore transfers the connection between the implant and the prosthetic abutment towards the center of the implant. In this way the mechanical and microbial irritations, responsible for a persistent inflammatory infiltration at the implant-abutment interface (Broggini et al. 2003; Broggini et al. 2006), are kept away from the bone crest, the biological width moves from a vertical to a horizontal plane, and the thinner abutment also leaves more space for peri-implant soft tissues (Weng and Richter 2005; Lazzara and Porter 2006) (Figure 6).

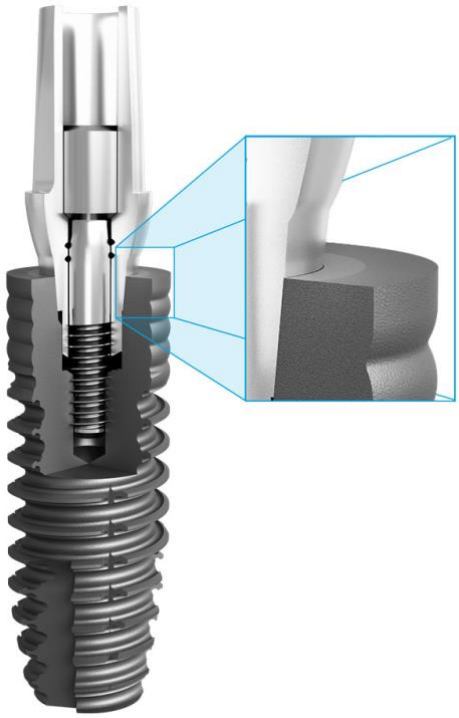

Figure 6. Platform switching: the connection between the implant and the prosthetic abutment is shifted towards the center of the implant (source www.clcscientific.com/it/clc-conic)

2.4 Peri-implant tissues

For the long-term success of implant therapy, a crucial role is played by the peri-implant mucosa (Atsuta et al. 2016). The development of this soft tissue barrier, at the point of passage with the oral environment, represents an important phase of the tissue integration process: the preservation over time of the health and efficiency of this mucosal seal is a critical factor for the functioning and the survival of the implant (Ivanovski and Lee 2018).

Results from animal experiments have revealed that the established mucosal attachment to the implant is comprised of one 1.5- to 2-mm- high epithelial portion and one 1- to 1.5-mm-high connective tissue portion (Berglundh et al. 1991; Abrahamsson et al. 1996; Berglundh and Lindhe 1996b). The formation of such mucosal attachment starts with the formation of a blood clot and the induction of an inflammatory process that leads to tissue formation and remodeling (Berglundh et al. 2007; Eming et al. 2007; Sculean et al. 2014).

The healing process takes several weeks and begins when the implant is inserted in case of transmucosal implants, and at the time of abutment connection in case of two-stage implants (Tomasi et al. 2014). Oral epithelium located on the edge of surgical flaps adapted to the implant neck or abutment proliferates and migrates in a corono-apical direction to cover the underlying connective tissue and adheres to the surface forming a junctional epithelium. The mucosal seal thus formed prevents bacteria and products deriving from their metabolism from

penetrating inside the body (Sculean et al. 2014). Its stability was observed in the presence of an effective chemical and mechanical regimen of oral hygiene and bacterial plaque control (Heitz-Mayfield 2008) .

In ensuring an effective seal between the intraoral environment and the endosseous portion of the implant, the supracrestal connective tissue, that resembles a scar tissue in composition, fibre orientation, and vasculature, appears to be the most important component of the peri-implant soft tissue barrier (Sculean et al. 2014). Apically to the junctional epithelium, this connective layer can be schematically divided into two parts. The first, with a thickness of 50-100 µm, is in direct contact with the implant surface and is characterized by few and scattered cellular elements and scarce vessels, but it is rich in collagen fibers, which run mostly parallel to the implant surface and can assume a circular pattern; in the remaining part of supracrestal connective tissue, external with respect to the previous one, the connective fibers, on the other hand, run in different directions and there is a greater cellular and vascular component (Buser et al. 1992).

Peri-implant tissues have many similarities, as well as some anatomical differences with gingival tissues around teeth (Figure 7). Peri-implant junctional epithelium appears to be similar to that found in natural dentition, whereas there are considerable differences in the connective tissue layer, mainly in the cellular composition and fiber orientation (Yeung 2008). Peri-implant connective tissue has, in fact, a lower cellular concentration and a higher fibre content than that of gingiva around teeth. Moreover, collagen fibres are organized parallel to the implant surface in contrast to that of the gingiva which tend to insert into the root cementum in a perpendicular direction (Berglundh et al. 1991; Çomut et al. 2001).

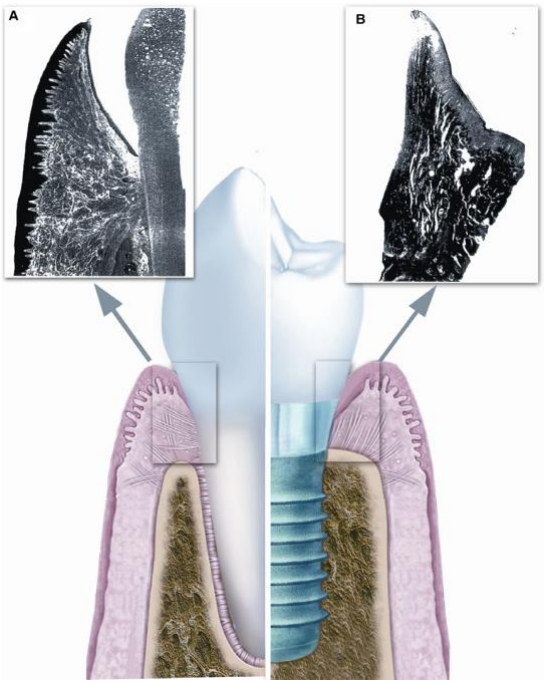

Figure 7. Anatomical differences between A) dentoalveolar region and B) peri-implant bone and mucosa (source Ivanovski and Lee 2018)

2.4.1 Peri-implant supracrestal attached tissues

The dimension of the peri-implant supracrestal attached tissues, formerly named peri-implant biological width, is a concept introduced in the early 90s through the study of Berglundh and Lindhe (1996) and, as already pointed out, its minimum value corresponds to about 3-3.5 mm, 2 of which are represented by the junctional epithelium and 1-1.5 mm from the supracrestal connective tissue (Berglundh and Lindhe 1996b) (Figure 8). These authors have demonstrated that even if the supracrestal attached tissues are experimentally reduced to less than 3 mm, the healing process, however, restores a dimension equal to 3 mm, through a certain degree of resorption of the bone crest.

The dimension of supracrestal attached tissues does not seem to be affected either by the placement of the implants in a one-stage or a two-stage procedure (Ericsson et al. 1996; Abrahamsson et al. 1999), nor by the type of implant system adopted (Abrahamsson et al. 1996).

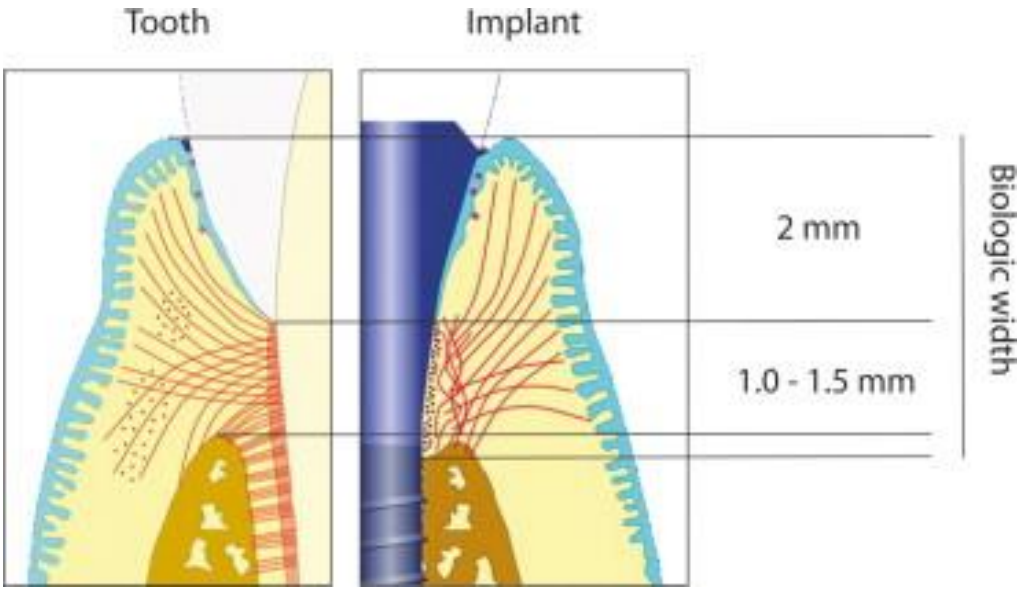

Figure 8. Supracrestal attached tissues around teeth and implants (source Gruber and Bosshardt 2015)

Results from histological analysis in regards to dimensional and qualitative changes in the peri-implant mucosa over time in humans were consistent with those reported from animal experiments (Tomasi et al. 2014, 2016). A mucosal attachment adjacent to titanium implant units was formed and developed completely in 8 weeks and soft tissue dimension was about 3.6 mm and included a barrier epithelium of 1.9 mm and a connective tissue portion of 1.7 mm (Tomasi et al. 2014).

2.5 Peri-implant diseases

The use of osseointegrated implants to support removable and fixed prostheses is a widely

accepted treatment modality of high satisfaction and predictability (Aglietta et al. 2009). However, despite high implant survival and success rates, it has long been established that dental implants may suffer from biological complications (van Steenberghe et al. 1993). Similarly to teeth, in fact, dental implants can be colonized by plaque biofilm, which is the etiological factor of periodontal diseases (gingivitis and periodontitis), leading to peri-implant diseases. (Zitzmann and Berglundh 2008a; Trombelli et al. 2018). Two clinical varieties may be distinguished: peri-implant mucositis and peri-implantitis (Schwarz et al. 2018) (Figure 9). Peri-implant diseases were first defined and described at the First European Workshop on Periodontology in Ittingen in 1993 (Albrektsson and Isidor 1994; Heitz-Mayfield and Salvi 2018a) and scientific interest in this area has increased dramatically, especially over the last 10 years, as evidenced by an increase in the number of publications addressing the definition, prevalence, and treatment of these peri-implant biological complications (Klinge et al. 2018).

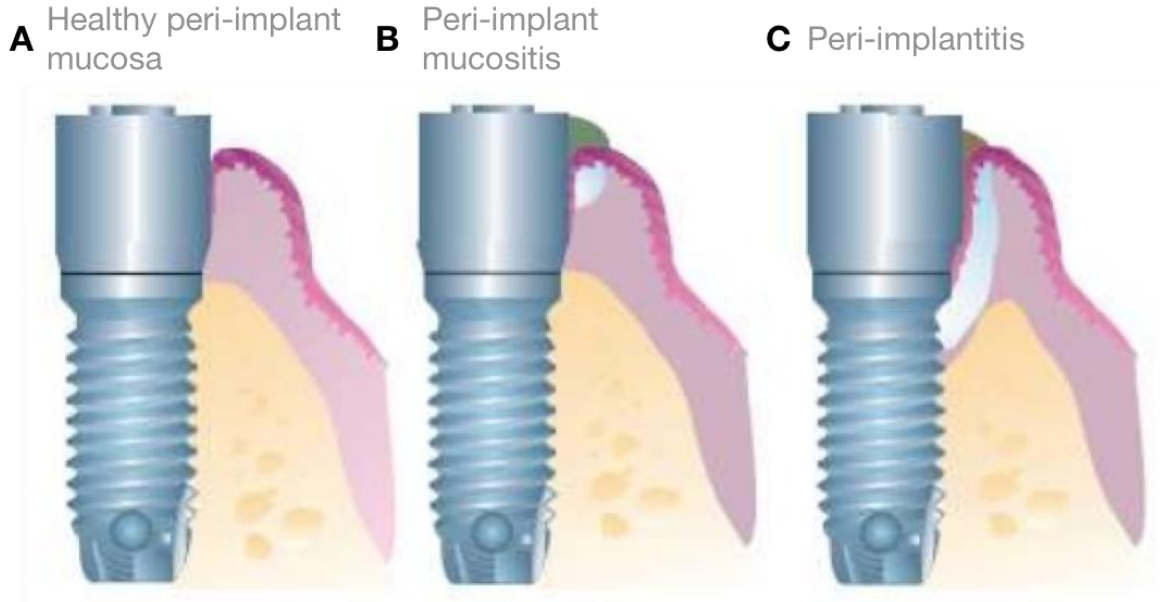

Figure 9. A) Peri-implant health; B) Peri-implant mucositis; C) Peri-implantitis (source www.artedentalclinic.com/en/dental-implants-peri-implantitis/)

Poor plaque control, lack of regular maintenance therapy, history of previous periodontitis, diabetes, alcohol consumption, smoking and genetics are all considered possible risk factors for the onset of peri-implant diseases (Ferreira et al. 2006; Daubert et al. 2015; Gurgel et al. 2017).

The prevalence of peri-implant diseases represents a debated issue since data deriving from different scientific studies are divergent and indicate a wide range in prevalence, making it difficult to globally estimate the magnitude of the problem (Tarnow 2016; Salvi et al. 2017). One of the main reasons from which these inconsistencies arise reflecting the lack of consensus in epidemiological research is found in the differences applied in the various published studies for case definitions (Sanz et al. 2012; Tomasi and Derks 2012). Derks & Tomasi, in a recent systematic review with meta-analyses, tried to clarify this issue and reported patient-based estimated weighted mean prevalences and ranges for peri-implant

diseases. Prevalence of peri-implant mucositis was reported at 43% (range: 19 - 65 %), whereas of peri-implantitis it amounted to 22% (range: 1 - 47 %) (Derks and Tomasi 2015). Results from other recent epidemiological studies not included in this systematic review reported prevalences for peri-implant diseases within ranges comparable to those reported by Derks and Tomasi (Aguirre-Zorzano et al. 2015; Daubert et al. 2015; Dalago et al. 2017; Rokn et al. 2017; Schwarz et al. 2017).

2.5.1 Mucositis

Mucositis has been described as an inflammatory reaction of the peri-implant mucosa surrounding an osseointegrated implant with absence of bone loss beyond crestal bone level or changes resulting from initial peri-implant bone remodeling (Berglundh et al. 2018; Heitz-Mayfield and Salvi 2018a) (Figure 10). Current literature indicates that peri-implant mucositis is the precursor of peri-implantitis in the same way that gingivitis is the precursor of periodontitis (Renvert and Polyzois 2018). Data suggest that patient diagnosed with peri-implant mucositis may develop peri-implantitis especially in the absence of regular maintenance care (Berglundh et al. 2018).

Figure 10. Bleeding on probing (BOP) in a peri-implant mucositis (source www.oapublishinglondon.com/article/743)

Mucositis develops from a healthy peri-implant mucosa and bacterial plaque accumulation is considered the main etiological factor. Host response to the bacterial exposure may vary

between individuals (Berglundh et al. 2018). A strong cause–effect relationship between experimental biofilm accumulation and the development of experimental mucositis was demonstrated in animal and human experimental studies, and upon plaque removal, peri-implant mucosal health can be achieved although complete resolution might not be expected in every case (Salvi et al. 2017; Heitz-Mayfield and Salvi 2018a).

The main clinical characteristic of peri-implant mucositis is bleeding on probing, while additional signs may include erythema, swelling and/or suppuration. An increase in peri-implant probing depth is often observed in the presence of mucositis due to swelling or decrease in probing resistance (Berglundh et al. 2018).

2.5.2 Peri-implantitis

Similarly to mucositis also peri-implantitis is a plaque-associated pathological condition occurring in tissues around dental implants, but unlike mucositis it is not only characterized by inflammation in the peri-implant connective tissue but also by a subsequent progressive loss of supporting bone (Berglundh et al. 2018) (Figure 11). Patients having poor plaque control and not attending regular supportive therapy are at higher risk of developing peri-implantitis. Despite it is preceded by an untreated or unsuccessfully treated mucositis, the characteristics or conditions that promote this conversion have not been currently identified (Schwarz et al. 2018).

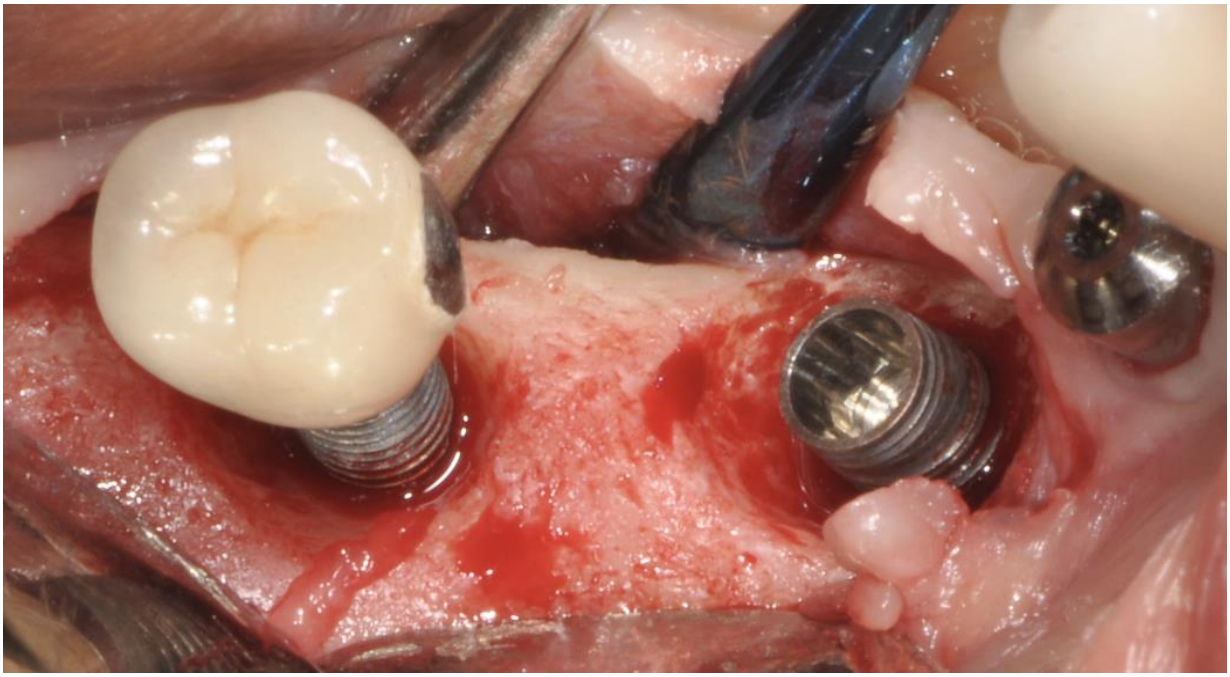

Figure 11. Extensive bone loss around two dental implants affected by peri-implantitis

Peri-implantitis corresponds to periodontitis at natural teeth but progression appears to be faster and, in the absence of treatment, seems to have a non-linear and accelerating pattern (Derks et al. 2016). Furthermore, unlike periodontitis, no specific or unique bacteria or proinflammatory cytokines have been identified associated with peri-implantitis (Berglundh et

al. 2018). Its main clinical features are represented by clinical signs of inflammation, bleeding on probing and/or suppuration, increased probing depths and/or recession of the mucosal margin in addition to radiographic bone loss compared to previous examinations. In the absence of previous examination data diagnosis of peri-implantitis can be based on the combination of bleeding and/or suppuration on probing, probing depths ≥6 mm, bone levels ≥3 mm apical of the most coronal portion of the intraosseous part of the implant (Berglundh et al. 2018).

2.6 The plaque microbiome in healthy and diseased implants

Over the years, different methods have been applied to characterize the peri-implant plaque microbiome. Culture-dependent methods have been the gold standard, but molecular methods have also been introduced to avoid the time-consuming and costly process for isolation and laboratory culture of individual species. As technology improves, sequencing methods, including the latest next-generation sequencing, have emerged to unravel in more detail differences between healthy and diseased oral microbiomes (Charalampakis and Belibasakis 2015).

Investigations have studied whether microbial biofilm profiles of implants are similar to teeth or if they represent another type of bacterial colonization (Ebadian et al. 2012; Koyanagi et al. 2013; Lafaurie et al. 2017). Although peri-implant diseases were considered a counterpart of periodontal diseases at implant sites, early investigations of periopathogens were generally unable to establish a clear microbiologic profile associated with peri-implantitis and it was suggested that, in addition to immunopathologic ones (Berglundh et al. 2011), also microbiologic profiles of peri-implantitis and periodontitis present some differences (Rakic et al. 2016). Therefore, more recent studies have been directed toward comprehensive analyses of the microbiome in peri-implantitis (Kumar at al. 2012, Dabdoub et al. 2013, Koyanagi et al. 2013, Tamura et al. 2013, da Silva et al. 2013).

In the same way the bacterial profile differences of healthy and diseased dental implants have also been investigated (Pérez-Chaparro et al. 2016; Rakic et al. 2016; Lafaurie et al. 2017; Teles 2017). Biofilm profiles of peri-implantitis and healthy implants have shown controversial results mainly related to the methodologic design of studies: investigations of microbiologic profiles of peri-implant biofilms at healthy and diseased sites in the same subject differ from studies with parallel design (Canullo et al. 2015, 2016; Lafaurie et al. 2017). Microbiological methods used also appear to influence results of microbial profile studies (Lafaurie et al. 2017).

Results from 11 studies included in a recent systematic review aimed at elucidating the microorganisms closely associated to peri-implantitis concluded that the bacterial species mostly associated with peri-implantitis are identified as some known periodontal pathogens (*Tannerella forsythia*, *Treponema denticola*, *Porphyromonas gingivalis*) enriched with other pathogenic species (*Campylobacter rectus*, *Prevotella intermedia*) (Teles 2017).

These results are confirmed by a recent study, where the microbiome of healthy and diseased implants was compared and the core peri-implant microbiome was determined through 16S rRNA sequencing (Sanz-Martin et al. 2017; Teles 2017). A sharp difference was described between healthy and peri-implantitis microbiological samples at all taxonomic levels. *Treponema* and *Porphyromonas* were significantly more abundant in peri-implantitis while

Neisseria and *Rothia* were higher in health. The core peri-implant microbiome included *Campylobacter*, *Parvimonas*, *Fusobacterium*, genera that are traditionally associated with periodontal inflammation. *Porphyromonas gingivalis* and *Treponema denticola* levels were significantly higher in peri-implantitis, as well as *Treponema maltophilum*, *Fretibacterium fastidiosum and Filifactor alocis (Teles 2017).* In general, these results underline that peri-implantitis microbiome is commensal-depleted and pathogen-enriched, including traditional pathogenic species (Socransky's red and orange complexes (Socransky et al. 1998b) (Figure 12)) and newly proposed pathogenic microorganisms, several of which have not yet been cultivated. Future studies should be conceived with appropriate inclusion of cases and controls and the adoption of state-of-the-art "omics" techniques, such as metagenomics (Teles 2017).

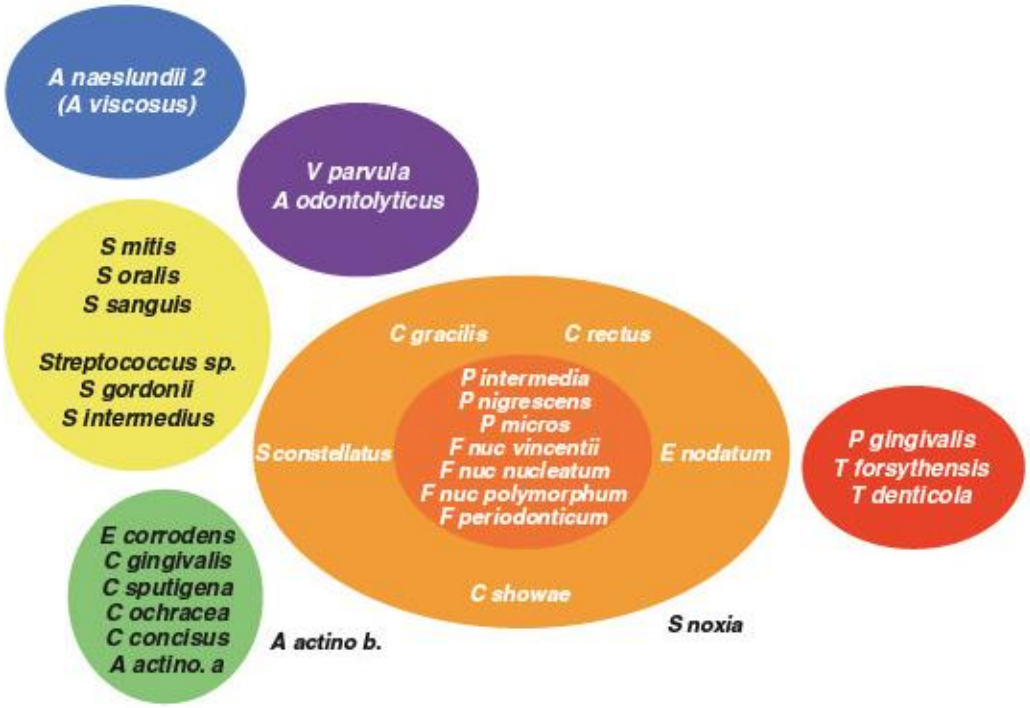

Figure 12. Socransky's microbial complexes in subgingival biofilm: diagrammatic representation of the relationships of species within microbial complexes and between the microbial complexes (source Socransky et al. 1998)

3. Moderately rough implant surfaces positively act on osteogenic and angiogenic commitment of mesenchymal stem cells (MSCs)

Rationale

The topography and roughness of implant surface have been progressively optimized during the last forty years to continuously improve biological surface properties, which can enhance the mechanism of osseointegration (Buser et al. 2004; Lang et al. 2011; Meng et al. 2016). A broad range of modifications has been developed and applied on commercially available dental implants with the purpose to positively affect the host-to-implant tissue response leading to significantly higher bone-to-implant contact percentages at earlier time points following implant placement (Coelho et al. 2009; Bosshardt et al. 2017).

Surface roughness is often described in terms of 3-dimensional S_a (arithmetic mean surface roughness) and implant surfaces are classified into four different categories, according to their roughness: smooth (S_a < 0.5 µm); minimally rough (S_a between 0.5 and 1.0 µm), moderately rough (S_a between 1.0 and 2.0 µm), and rough (S_a > 2.0 µm) (Albrektsson and Wennerberg 2004; De Bruyn et al. 2017). Today, most marketed implant surfaces are moderately rough with S_a values between 1.1 and 2 µm (Jordana et al. 2018). Some authors have speculated that there is an ideal surface roughness window from 1 to 1.5 µm, for which there is a compromise between engineering and clinical outcomes (Albrektsson and Wennerberg 2004; De Bruyn et al. 2017), but to date there is no clear scientific evidence about this.

It has been suggested that implants with relatively smooth surfaces should be used also in order to prevent biological complications (Quirynen et al. 2002). Despite the proven clinical benefit of the currently available, surface-modified implants, there is evidence, in fact, that increasing implant surface roughness induces qualitative and quantitative changes in biofilm formation and may play a decisive role in the development of peri-implant diseases (Socransky and Haffajee 2002; Teughels et al. 2006; Cavalcanti et al. 2015). In this regard, although data on oral biofilm adherence to different implant surfaces are scarce, there is recent moderate scientific consensus towards a tendency to smoother and bioactive implant surfaces. The demonstrated influence of plaque deposits on implant and abutment surfaces and patient's oral hygiene habits in the etiology of peri-implant diseases (Berglundh et al. 2018) make the rationale of this tendency very clear (Sanz et al. 2019).

This chapter describes, precisely, the chemical and biological characterization of a particular type of moderately rough surface (OGI surface, S_a = 1.3 µm) obtained by large grit sandblasting with white corundum followed by double acid etching with a mixture of mineral acids. In collaboration with the Department of Biomedical Sciences of University of Padova two *in-vitro* studies were conducted, regarding the influence that this OGI surface exerts on the commitment of MSC (mesenchymal stem cells) derived from dental pulp and HUVEC (Human Umbilical Vein Endothelial Cells). Results were very clear and showed that OGI surface positively acts on mesenchymal stem cells inducing an increase in their osteogenic and angiogenic commitment.

My contribution

In the scientific works included in this chapter I dealt mainly with the execution of laboratory experiments and the interpretation of *in-vitro* results.

The chapter is based on the following articles:

Ghensi P, Bressan E, Gardin C, Ferroni L, Ruffato L, Caberlotto M, Soldini C, Zavan B

Osteo Growth Induction titanium surface treatment reduces ROS production of mesenchymal stem cells increasing their osteogenic commitment

Materials Science and Engineering: C (2017)

Ghensi P, Bressan E, Gardin C, Ferroni L, Soldini MC, Mandelli F, Soldini C, Zavan B

The biological properties of OGI surfaces positively act on osteogenic and angiogenic commitment of mesenchymal stem cells

Materials (Basel) (2017)

3.1 Osteo Growth Induction titanium surface treatment reduces ROS production of mesenchymal stem cells increasing their osteogenic commitment

Ghensi P, Bressan E, Gardin C, Ferroni L, Ruffato L, Caberlotto M, Soldini C, Zavan B

Osteo Growth Induction titanium surface treatment reduces ROS production of mesenchymal stem cells increasing their osteogenic commitment

Materials Science and Engineering: C (2017)

Abstract

Surface characteristics play a special role for the biological performance of implants and several strategies are available to this end. The OGI (Osteo Growth Induction) titanium surface is a surface, obtained by applying a strong acid onto the blasted surface. The aim of this in-vitro study is to evaluate in-vitro the osteoproperties of OGI surfaces on Mesenchymal Stem cells derived from dental pulp. Our results confirm that this treatment exerts a positive effect on mitochondrial homeostasis, as shown by a decrease in ROS production related to environmental stress on the mitochondria. Morphological and molecular biology analyses confirmed moreover that the DPSC cultured on the OGI surfaces appeared more spread in comparison to those grown on control titanium surface and real time PCR and biochemical data clearly demonstrated the increase of osteoconductive properties of the OGI treatment. In conclusion, our results suggest that mesenchymal stem cells sensitively respond to surface properties related to OGI treatment enhancing their osteogenic activities.

Keywords: DPSc; osteogenesis; dental pulp; dental implant; titanium

3.1.1 Introduction

Implant dentistry has undergone a slow but steady growth during the last 40 years. When teeth are missing for caries, periodontal disease or agenesis, dental implants, such as dentures, are used either to replace the missing elements or to support complex prostheses (Palmquist et al. 2010). The first generation of successfully used clinical titanium implants, which were machined with a smooth surface texture; now approach 40 years in clinical use. The second generation of clinically used implants underwent chemical and topographical modifications, usually resulting in a moderately increased surface topography. Many of these oral implant systems now approach 25 years of clinical use (Pattanaik et al. 2012).

Surface characteristics play a special role for the biological performance of implants. Whereas mechanical properties such as Young's modulus and fatigue properties are mainly determined by the bulk of the material, chemical and biological interactions between the material and the host tissue are closely associated with the material surface properties (Palmquist et al. 2010). Characteristics such as surface composition, surface topography, surface roughness, and surface energy affect the mechanical stability of the implant/tissue interface (Smith et al. 1991; Kieswetter et al. 1996; Deligianni et al. 2001). It was found that cell attachment and proliferation were surface roughness sensitive, and increased as the roughness of Ti-6Al-4V increased

(Jemat et al. 2015). Many works have been carried out on surface treated commercial titanium implants to enhance the osseointegration function (Albrektsson and Wennerberg 2004). Experimental evidence from *in-vitro* and in vivo studies strongly suggests that some types of surface modifications promote a more rapid bone formation than do machined surfaces. This could depend on an altered surface chemistry and or an increased texture on the micrometer scale (Ellingsen et al. 2006; Jr et al. 2010; Palmquist et al. 2010). Methods for altering surface texture can be classified as either techniques that add particles on the biomaterial, creating a surface with bumps(additive methods), and techniques that remove material from the surface, creating pits or pores (subtractive methods) (Liu et al. 2004).

The additive methods employed the treatment in which other materials are added to the surface, either superficial or integrated, categorized into coating and impregnation, respectively. Meanwhile, the subtractive techniques are the procedure to either remove the layer of core material or plastically deform the superficial surface and thus roughen the surface of core material. The common subtractive techniques are large-grit sands or ceramic particle blasts, acid etch, and anodization (Lohmann et al. 2002; Palmquist et al. 2010).

The OGI (Osteo Growth Induction) titanium surface is a surface, obtained (Kim et al. 2008) by applying a strong acid onto the blasted surface. This treatment combines blasting with large-grit sand particles and acid etching sequentially to obtain macro roughness and micro pits to increase the surface roughness as well as osseointegration (Lohmann et al. 2002; Zavan et al. 2009; Ferroni et al. 2015). The aim of this in-vitro study is to evaluate *in-vitro* the osteoproperties of OGI surfaces on Mesenchymal Stem cells derived from dental pulp; namely: Dental Pulp Stem Cell (DPSC) with a great attention to evaluate even long-term cultures could affect the efficiency of the commitment of the cells. We'll here focus our effort also in evaluation on the anti-aging properties of the surfaces eventually exerted through variation on ROS production.

3.1.2 Material and Methods

3.1.2.1 Biomaterial

This study cell activity on 2 implant surfaces was evaluated. We utilized implants with grit-blasted surfaces (control) and OGI surfaces (CLC implant, Italy). OGI samples are obtained by surface treatment by large grit sandblasting followed by double acid etching and relevant cleaning cycles. The materials involved sandblasting medium is corundum and the double acid etching involves a mixture of mineral acids. In this process, the acids used in the double acid etching steps that follow sandblasting remove sandblasting particles. All experimental surfaces were cleaned and sterilized by γ-rays.

3.1.2.2 Analysis of the surface chemistry by XPS (X-ray photoelectron spectroscopy)

XPS analysis was performed using a Perkin Elmer PHI 5400 ESCA spectrometer. This is equipped with an X-ray source with an Mg anode, maintained at 20 kV with a nominal power rating of 200 W. The depth analyzed is approx. 5 nm. The pressure inside the analysis chamber has been maintained at approx. 10–9 Torr. The analysis results are expressed in atomic percentages. Two treated and cleaned samples were tested by XPS.

3.1.2.3 Analysis of surface topography by SEM (scanning electron microscopy)

The surface topography of the implants was evaluated by scanning electron microscope. Analysis was conducted using an EVO MA 10 SEM (Zeiss). The electron acceleration voltage was maintained at 15kV, the working distance at 15mm. These parameters are reported in the images, along with the level of magnification (MAG) and the kind of detector utilized (Signal A = SE1 or CZ BSD). Images were acquired in both conventional mode (Signal A = SE1) and in backscattered electron mode (Signal A = CZ BSD), allowing improved contrast between different chemical elements.

Stereo-SEM (SSEM), using dedicated software to convert conventional SEM images into three-dimensional data (Mex 4.2, Alicona Imaging), evaluated roughness quantitatively. In particular, this evaluation exploits the basic principle of stereovision. Basically, two images of the same field of view are acquired after eucentric rotation by a given angle. This is obtained by changing the angle between the sample and the electrons, by tilting the table that holds the sample. The tilting angle is set and controlled by the instrument control software. The couple of images obtained (stereopair), the size of the field of view and the tilting angle are the incoming data, that the software converts into a single three-dimensional image, where each data point is characterized by the values of the x, y, z coordinates. The image obtained by this process allows then to measure height profiles (roughness profiles) and to calculate the different roughness parameters defined by relevant literature and standards.

3.1.2.4 Dental pulp extraction and differentiation

Human dental pulps were extracted from healthy molar teeth, which had been extracted because of mucosal inflammation (impacted teeth with pericoronitis) or for orthodontic reasons from adult subjects aged 16. The pulps were classified into 6 age groups (12 teeth per group). Each subject gave informed written consent for the use of their donor of dental pulps. The Ethical Committee of Padua Hospital approved the research protocol. Before extraction, each subject was checked for systemic and oral infections or diseases. Only disease-free subjects were selected for pulp collection. Each subject was pretreated for 1 week with professional dental hygiene. Before extraction, the dental crown was covered with a 0.3% chlorhexidine gel (Forhans, New York, NY) for 2 min. After mechanical fracturing, dental pulp was obtained by means of a dentinal excavator or a Gracey curette. The pulp was gently removed and immersed for 1 h at 37uC in a digestive solution: 100U/mL penicillin, 100 mg/mL streptomycin, 0.6 mL of 500 mg/mL clarithromycin, 3 mg/mL type I collagenase, and 4 mg/mL dispase in 4 mL of 1 M PBS. Once digested, the solution was filtered through 70mm Falcon strainers (Becton & Dickinson, Franklin Lakes, NJ) (Ferroni et al. 2015).

3.1.2.5 Immunocytochemical staining

DPSCs were layered over cover slip, fixed with absolute acetone for 10 min at room temperature and cryopreserved at − 20 C° until use. The following markers were visualized with immunofluorescence: SH2, SH3, SH4, CD14, CD34; CD45 (monoclonal mouse anti-human; SIGMA). Briefly, after non-specific antigen sites were saturated with 1/20 serum in 0.05 M maleate.
TRIZMA (Sigma; pH 7.6) for 20 s, 1/100 primary monoclonal anti-human Ab (Sigma) was added to the samples. After incubation, immunofluorescence staining was performed with fluorescein (anti-mouse) secondary antibody.

3.1.2.6 Karyotype analysis

After 45 days of culture on DPSc were exposed to colchicine (Sigma- Aldrich, St. Louis, MO, USA) for 6 h, washed in PBS, dissociated with trypsin (Lonza S.r.l), and centrifuged at 300 g for 5 min. Colchicine is needed to perform karyotyping analyses of the cells, because we need to stop cell mitosis in the metaphase stage. It is during this stage of nuclear division that the chromosomes are most condensed and, as a result, visible with a light microscope. After the cells have been arrested in this stage, they are then placed into a hypotonic solution, which causes water to enter and enlarge the cells. The cells are then placed into a chemical fixative to maintain this condition. Following this procedure, the cells can be "splatted" onto microscope slides, stained, and viewed microscopically. The pellet was carefully suspended and incubated in 1% sodium citrate for 15 min at 37°C, then fixed and spread onto −20 °C cold glass slides. Metaphases of cells were Q-banded and karyotyped in accordance with the international system for human cytogenetic nomenclature recommendations. Twenty five metaphases were analyzed for three expansions.

3.1.2.7 Growth curve and doubling time

Cells were seeded into the implants at an initial density of $5\times10_4$. When cells reached confluence, they were detached, counted and reseeded at a density of $5\times10_4$. The PDT of the cells was calculated according to the formula:

$$PDT = (T0\text{-}T1)\ \log2\ /\ (\log N_t - \mathrm{Log}Nt_1)$$

where PDT represents the cell doubling time, t represents the duration of cell culture, and N0 and Nt represent the cell number after seeding and the cell number after culturing for t hours, respectively (Bressan et al. 2012).

Sequence (5′-3′)	FOR	REV	Product length (bp)
OSTEOCALCIN	GCAGCGAGGTAGTGAAGAGAC	AGCAGAGCGACACCCTA	193
OSTEONECTIN	TGCATGTGTCTTAGTCTTAGTCACC	GCTAACTTAGTGCTTACAGGAACCA	183
OSTEOPONTIN	TGGAAAGCGAGGAGTTGAATGG	GCTCATTGCTCTCATCATTGGC	192
COLL I	TGAGCCAGCAGATCGAGA	ACCAGTCTCCATGTTGCAGA	178
RUNX2	AGCCTTACCAAACAACACAACAG	CCATATGTCCTCTCAGCTCAGC	175
GAPDH	TCAACAGCGACACCCAC	GGGTCTCTCTCTTCCTCTTGTG	203

Table 1. Human primer sequences

3.1.2.8 MTT assay

To determine the proliferation rate of cells growth on titanium disks with or without treatment, the MTT-based (methyl thiazolyl-tetrazolium) cytotoxicity assay was performed according to the method of Denizot and Lang with minor modifications [Denizot]. The test is based on mitochondria viability, i.e., only functional mitochondria can oxidize an MTT solution, giving a typical blue-violet end product. After harvesting the culture medium, the cells were incubated for 3 h at 37 °C in 1 mL of 0.5 mg/mL MTT solution prepared in PBS solution. After removal of the MTT solution by pipette, 0.5 mL of 10% dimethyl sulfoxide in isopropanol (iDMSO) was added for 30 min at 37 °C. For each sample, absorbance values at 570 nm were recorded in duplicate on 200 µL aliquots deposited in 96-well plates using a multilabel plate reader (Victor 3 Perkin Elmer, Milano, Italy). All samples were examined after 15 and 30 days of culture

(Gardin et al. 2012).

3.1.2.9 Senescence-associated beta-galactosidase staining

Beta-galactosidase staining was performed using a senescence-associated β-galactosidase (SA-β-Gal) staining kit (Cell Signaling Technology, Danvers, MA, USA) for 12 h. Briefly, human adipose-derived stem cells were cultured with 5, 10, 15, and 20 passages with or without REAC exposure in 6-well plates (3 × 103 per well) for 12 h, fixed with a fixative solution, and then processed according to the kit instructions. All of the experiments were repeated three times, and one representative set of results is shown. The cells were then photographed under an inverted microscope at 100 × magnification for a qualitative detection of SA-β-Gal activity. The numbers of positive (blue) and negative cells were counted in five random fields under the microscope (at 200 × magnification and bright field illumination), and the percentage of SA-β-Gal-positive cells was calculated as the number of positive cells divided by the total number of cells counted (Zhou et al. 2016).

3.1.2.10 ROS measurements

The OxiSelect™ ROS Assay Kit is a cell-based assay for measuring hydroxyl, peroxyl, and other ROS activity within a cell. The assay employs the cell-permeable fluorogenic probe DCFH-DA, which diffuses into cells and is deacetylated by cellular esterases into the non-fluorescent DCFH. In the presence of ROS, DCFH is rapidly oxidized to highly fluorescent DCF, and the fluorescence is read on a standard fluorometric plate reader.

3.1.2.11 RNA extraction and first-strand cDNA synthesis

Total RNA was extracted with RNeasy Mini Kit (Qiagen), including DNase digestion with the RNase-Free DNase Set (Qiagen) from implant cultured with DPSCs for 15 and 25 days. The RNA quality and concentration of the samples was measured using the NanoDrop™ ND-1000 (ThermoScientific).

For the first-strand cDNA synthesis, 200 ng of total RNA of each sample was reverse transcribed with M-MLV Reverse Transcriptase (Invitrogen), following the manufacturer's protocol.

3.1.2.12 Real-time PCR

Human primers were selected for each target gene with Primer 3 software (Table 1). Real-time PCRs were carried out using the designed primers at a concentration of 300 nM and FastStart SYBR Green Master (Roche) on a Rotor-Gene 3000 (Corbett Research, Sydney, Australia). Thermal cycling conditions were as follows: 15 min denaturation at 95 °C; followed by 40 cycles of 15 s denaturation at 95 °C; annealing for 30 s at 60 °C; and 20 s elongation at 72 °C. Differences in gene expression were evaluated by the 2ΔΔCt method, using DPSCs cultured onto non treated titanium disks for 15 days as control. Values were normalized to the expression of the glyceraldehyde-3-phosphate dehydrogenase (GAPDH) internal reference, whose abundance did not change under our experimental conditions. Experiments were performed with 3 different cell preparations and repeated at least 3 times.

3.1.2.13 Lactate dehydrogenase activity (LDH activity)

LDH activity was measured using a specific LDH Assay Kit (Sigma-Aldrich, St. Louis, MO,

USA) according to the manufacturer's instructions. All conditions were tested in duplicate. The culture medium was re- served to determine extracellular LDH. The intracellular LDH was estimated after cells lysis with the assay buffer contained in the kit. All samples were incubated with a supplied reaction mixture, resulting in a product whose absorbance was measured at 450 nm using a Victor 3 multilabel plate reader.

3.1.2.14 ALP activity measurements

The alkaline phosphatase (ALP) activity was measured up to weeks of cell culture to evaluate the initial differentiation of ADSc into preosteoblasts. Abcam's alkaline phosphatase kit (colorimetric) has been used to detect the intracellular and extracellular ALP activity. The kit uses p-nitrophenyl phosphate (pNPP) as a phosphatase substrate, which adsorbed at 405 nm when dephosphorylated by ALP. According to the manufacturer protocol, the culture medium from each sample group was collected and pooled together. At the same time, cells were washed with PBS and then homogenized with ALP Assay Buffer (300 µL in total for each group) and centrifuged at 13,000 rpm for 3 min to remove insoluble material. Different volumes of samples (medium and cells) were then added into with Assay Buffer. 80 µL of fresh medium was also utilized as sample background control. Thereafter, 50 µL of 5 mM pNPP solution was added to each well containing test samples and background control and incubated for 60 min at 25 °C, protecting the plate from the light. A standard curve of 0, 4, 6, 12, 16, and 20 nmol/ well was generated from 1 mM pNPP standard solution bringing the final volume to 120 µL with Assay Buffer. All reactions were then stopped by adding 20 µL of Stop solution into each standard and sample reaction except the sample background control reaction. Optical density was read at 405 nm in a microplate reader (Victor). The results were normalized subtracting the value derived from the zero standards from all standards, samples and sample background control. The pNP standard curve was plotted to identify the pNP concentration in each sample. ALP activity of the test samples was calculated as follow:

$$\text{APL activity (U/mL)} = A/V/T$$

where:

A is the amount of pNP generated by samples (in µmol).

V is the amount of sample added in the assay well (in mL).

T is the reaction times (in minutes)

3.1.2.15 Scanning electron microscopy (SEM)

Quantitative evaluation of surface roughness has been conducted in accordance with ISO 4287, providing values for all the parameters de- fined in the standard. As described before, data were obtained by Stereo SEM, generating three dimensional images from a stereo pair made up by two SEM images of the same field of view, obtained at 2000× with a tilting angle of 5°.

For SEM imaging, DPSCs grown on control and treated Ti surfaces for 15 and 25 days were fixed in 2.5% glutaraldehyde in 0.1 M cacodylate buffer for 1 h, then progressively dehydrated in ethanol. Control and treated Ti surfaces without cells were also examined. The SEM analysis

was carried out at the Interdepartmental Service Center C.U.G.A.S. (University of Padova, Italy).

3.1.2.16 Determination of scavenging effect on DPPH radicals

250 mL of 1, 10-diphenyl-2-picrylhydrazyl (DPPH, Sigma) solution (0.1 mM, in 95 wt% ethanol) was added into Ti control or OGI samples, and deionized water as the control. The mixture was shaken and kept at room temperature in the dark. After 30 min, the absorbance was measured at 517 nm by a spectrophotometer. The DPPH radicals scavenging effect (%) of Ti control surfaces and OGI can be calculated using the equation:

$$\text{Scavenging effect \%} = \frac{A_{control} - A_{sample}}{A_{control}} 100$$

3.1.2.17 Statistical analysis

One-way analysis of variance (ANOVA) was used for data analyses. The Levene's test was used to demonstrate the equal variances of the variables. Repeated-measures ANOVA with a post-hoc analysis using Bonferroni's multiple comparison was performed. *t*-Tests were used to determine significant differences (p,0.05). Repeatability was calculated as the standard deviation of the difference between measurements. All testing was performed in SPSS 16.0 software (SPSS Inc., Chicago, Illinois, USA) (license of the University of Padua, Italy).

3.1.3 Results

3.1.3.1 XPS analysis

The XPS analysis method was used to evaluate the surface composition: no aluminum from blasting residuals was detected suggesting that all residuals were removed in processing and cleaning steps

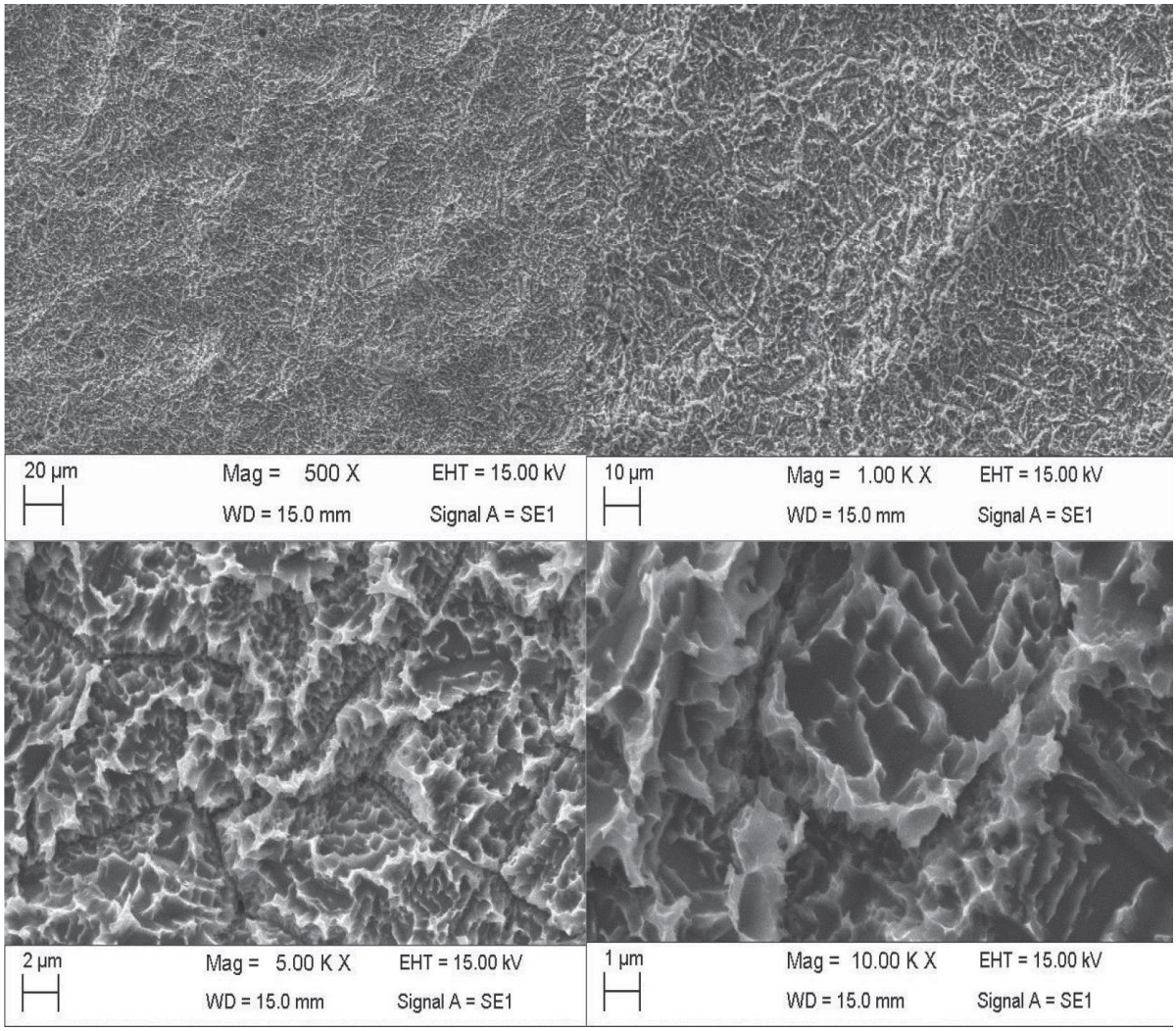

Figure 13. Figure 13 a–d shows microscopic views of the OGI surface. They confirm that the surface is free from dirt and particles, as suggested by XPS data, in particular from blasting residuals.

Parameter	OGI surfaces	Control
Ra	1.61 +/− 0.31	1.72 +/ 0.19
Rq	1–86 +/− 0.41	1.90 +/− 0.41
Rz	11.24 +/− 0.31	10.54 +/− 0.44
Rp	6.24 +/− 0.21	6.40 +/− 0.65
Rv	5.00 +/ 0.51	4.13 +/− 0.43
Rc	5.21 +/− 0.11	5.63 +/− 0.67

Where the definition of the various parameters are as follow

Parameter	
Ra	Average of roughness profile
Rq	Root mean square roughness of profile
Rz	Maximum height of roughness of profile
Rp	Maximum peak height of roughness of profile
Rv	Maximum valley depth of roughness profile
Rc	Mean height of profile irregularities of roughness

Table 2. A typical three-dimensional description of the OGI surface

3.1.3.2 SEM analysis

Figure 13 a–d show microscopic views of the OGI surface. They confirm that the surface is free from dirt and particles, as suggested by XPS data, in particular from blasting residuals. The whole surface is homogeneously treated. The peculiar features of the OGI surface are highlighted by the typical topography, which shows both big “holes” due to large-grit sandblasting on which the microroughness due to acid etching is superimposed. Figures show the typical nice tri-dimensional topography, which imparts to these surfaces spongy-like characteristics. Short peak-to-peak distance, of the order of about 1 μm, are also present. This combination of long-range (large grit sandblasting) and short range (acid etching) roughness is a feature of OGI surfaces (Table 2).

A typical three-dimensional view of the OGI surface in shown in Figure 14, that once again shows the co-existence of long-range and short range roughness.

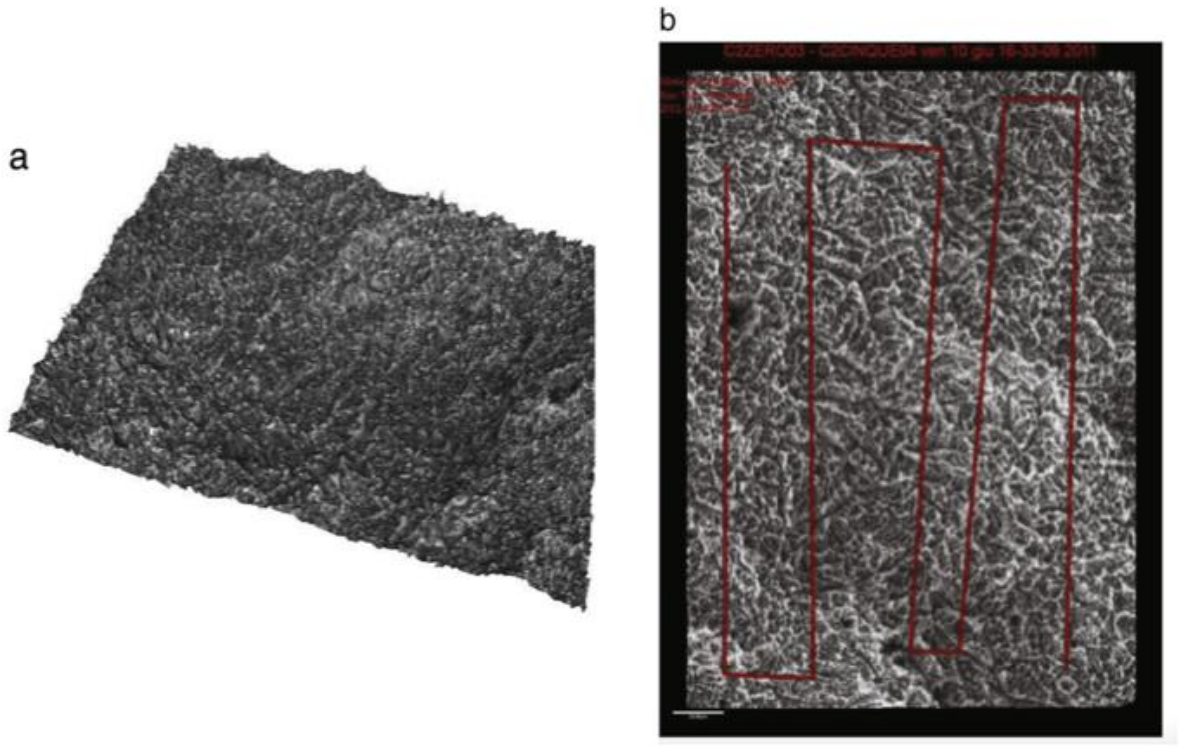

Figure 14. A typical three-dimensional view of the OGI surface in shown in Figure 14.

3.1.3.3 Dental pulp extraction and differentiation

Figure 15a illustrates the phenotypic characterization of culture-expanded human MSCs (hMSC) by immunofluorescence analysis. Cells were consistently positive for β1 integrin SH2 (93.22%), SH3 (96,63%) and SH4 (89,35%). Specific hematopoietic markers such as CD 14, CD34 and CD45 were consistently negative. The chromosomal stability of DPSc cultured in vitro up to 45 days was analyzed by means of karyotyping. As reported in Figure 15b, no chromosomal alterations are present in DPSc after long term in vitro cultures.

3.1.3.4 Proliferative activity

In order to evaluate proliferation activity of MSC on OGI titanium surfaces we have performed both Population doubling time (PDT) and MTT test. PDT is usually used to evaluate the ability of the cell to duplicate in number and is therefore a direct marker of the proliferative ability of the cell. In this experiment, we analyzed the PDT of MSC cultured in the titanium surfaced treated with OGI and in control (titanium surfaces not treated with OGI). PDT was evaluated at 5 different in vitro passages (p) of the cultures after 3, 7, 14, 21, 28 days. As reported in Figure 16a, we observed well-defined cell growth for each passage in both surfaces. On each sample moreover proliferative ability decreased in time and during in vitro aging and during the osteogenic commitment. Proliferative ability has been moreover evaluated by the MTT test (Figure 16b). The rising in MTT values confirmed that the cells were alive. When cells started the commitment, about after 14–18 days, the MTT value reach a steady state strongly related to the commitment in an adult phenotype of stem cell.

3.1.3.5 Senescence and ROS production

Normal somatic cells invariably enter a state of irreversibly arrested growth and altered function after a finite number of divisions. This process, is thought to be an underlying cause of aging. Studies on cells cultured from donors of different ages, genetic backgrounds, or species suggest that senescence occurs in vivo and that organismic lifespan and cell replicative lifespan are under common genetic control. However, senescent cells cannot be distinguished from quiescent or terminally differentiated cells in tissues. Thus, evidence that senescent cells exist and accumulate with age in vivo is lacking. There is a simple test that is based on the evidence that several human cells express a beta-galactosidase, histochemically detectable at pH 6, upon senescence in culture. This marker was expressed by senescent, but it was also absent from immortal cells. In our samples there was an in vitro-age-dependent increase in this marker in MSC. This marker provides in situ evidence that senescent cells may exist and accumulate with age in vitro. This senescence activity of stem cell due to their in vitro cultures has been evaluated by β-galactosidase staining detected at fixed time points of (3, 7, 21, 12, and 28 days) into both surfaces (Figure 17a). In particulars our results show that cells cultured on OGI surfaces have a significative higher value compared to the cells cultured on the control one, suggesting that a less aging could be occurred thanks to OGI treatment. The values of SA-β-Gal-staining were increase for every time point in both conditions and this result became more pronounced as the culture time in- creased. Moreover, a less significant increase in the intensity of the staining in the cultures on OGI surfaces was observed.

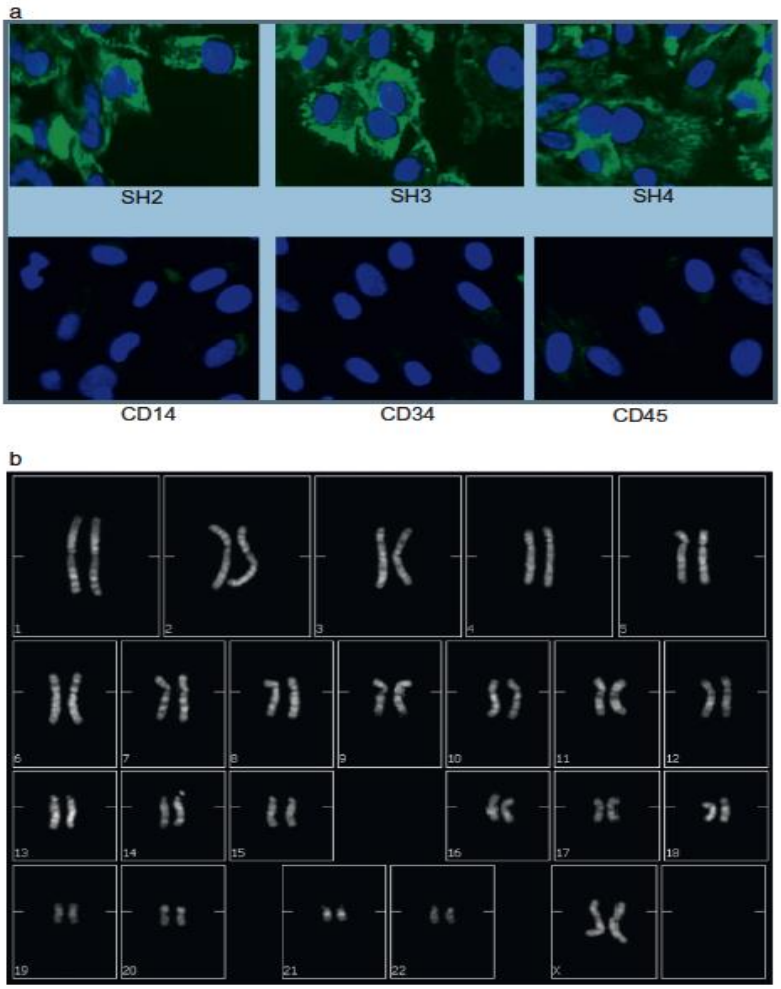

Figure 15. a) Immunofluorescence analysis of SH2; SH3; SH4; CD 14; CD 34; and CD 45. Cell in green are positive for SH2, SH3 SH4 and negative con CD14, CD34 and CD45 as no green staining is present. Fibroblast is used as negative controls (data not shown). b) Karyotype analysis of DPSCs cultured in vitro for 45 days. No chromosomal alterations are present. (For interpretation of the references to color in this figure legend, the reader is referred to the web version of this article.

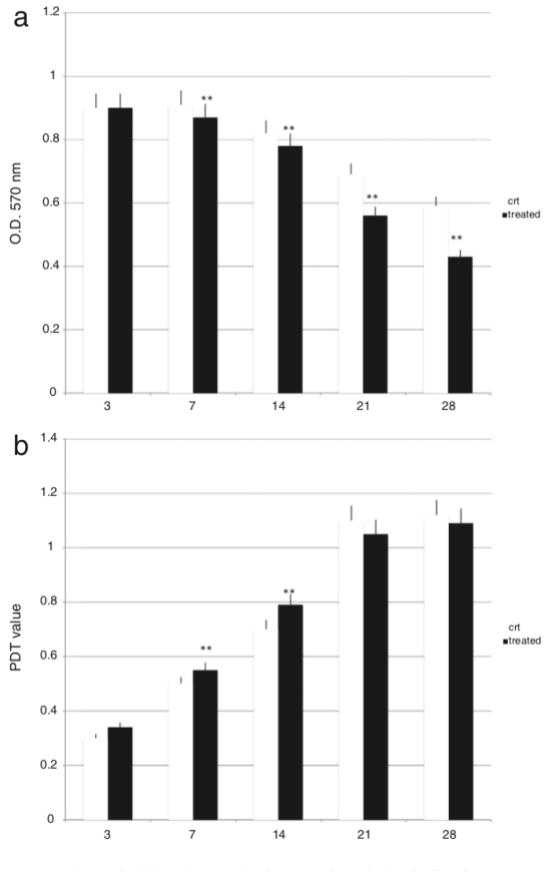

Figure 16

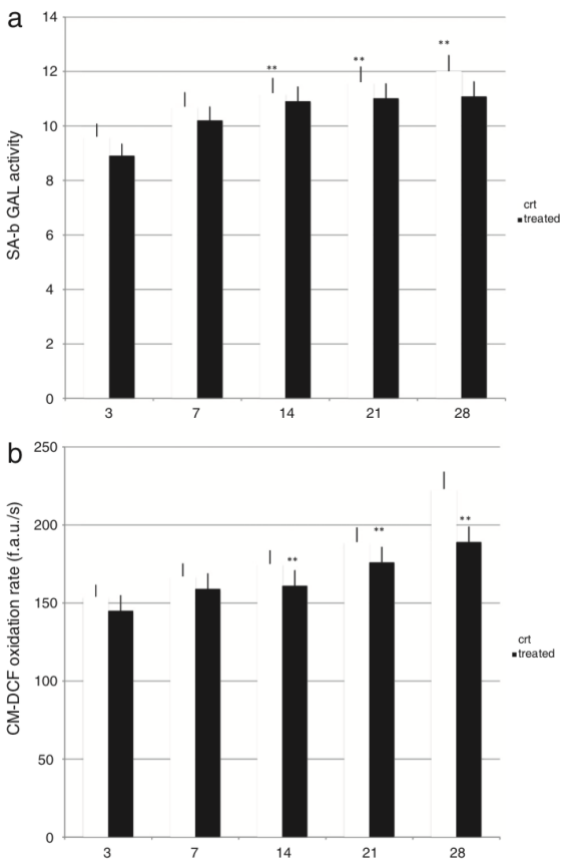

Figure 17

Figure 16. a) Population doubling time (PDT) of DPSCs cultured in both of surfaces in presence of osteogenic medium. The graph shows in vitro passage and tested at each time point. t- Tests were used to determine significant differences (p,0.05). *p,0,05; **p,0,01; ***p,0,001. b) MTT assay of DPSCs cultured on the control and treated Ti surfaces. DPSCs MTT related values are higher on the treated disks in the first periods of in vitro cultures and decrease when cells start the commitment respect to the control one at each time points of detection.

Figure 17. a) Senescence-associated β-galactosidase (SA β-Gal) staining in DPSc seeded onto both surfaces at fixed time points of 3, 7, 14, 21 and 28 days. A time-dependent increase in metabolic activity related to the in vitro aging is observable in both surfaces, weather the lower values are presents only is DPSc where cultured on OGI surfaces. b) ROS production in cells cultured onto both surfaces due to the in vitro aging of the cells, was observed: *t*-tests were used to determine significant differences (p b 0.05); *p b 0.05, **p b 0.01, ***p b 0.001. Lower ROS values were detected in presence of OGI treatment.

3.1.3.6 ROS measurement

To test whether the OGI treatment influence cell aging activity, we assessed ROS generation. Under environmental stress, the cells increased ROS production, leading to an imbalance between ROS generation and its neutralization by anti-oxidative enzymes and low molecular weight antioxidants, such as glutathione. This disturbance in the redox equilibrium is defined as oxidative stress. Under conditions of oxidative stress, the cell accumulates ROS, and the anti-oxidative response that follows involves modifications in signaling pathways. As reported in Figure 17b a time dependent increase in metabolic activity was observed in cells seeded onto both surfaces. When the MSC were cultured on OGI surfaces a well-defined decrease in ROS production was revealed, and this finding confirms the ability of OGI to influence the aging of the cells through mitochondrial function.

3.1.3.7 DPPH assay

DPPH radical scavenging assay is the most widely used method for screening antioxidant activity, since it can accommodate many samples in a short period and detect active ingredients at low concentration. The scavenging ability of antioxidants on DPPH radicals is thought to be due to their hydrogen donating ability. On our samples the DPPH radical scavenging effects (%) of Ti control surfaces and OGI surfaces are very low: 0.37% in control versus 0,41% on OGI surfaces.

3.1.3.8 Gene expression

Real-time PCR was performed on MSC cultures in both surfaces in presence of osteoinductive factors (Figure 18) after 28 days of cultures on control and OGI surfaces in presence of osteoinductive medium. The gene expression detected by means of the molecular markers selected can provide information on the mature osteogenic phenotype (osteocalcin; osteoectin; osteopontin; RUNX2; COL1A1; Wnt; Foxo 1; ALP; BMP2; BMP7).

As shown in Figure 18, the presence of osteoinductive medium was able to induce a good osteogenic commitment of the MSC in both conditions. Greater level of expression has been detected Indeed, the expression profile for osteopontin, osteonectin, osteocalcin, runx, FOX, bone morphogenic protein (BMP 2 and 7), and collagen type I is higher when cells are present on OGI surfaces compared to control.

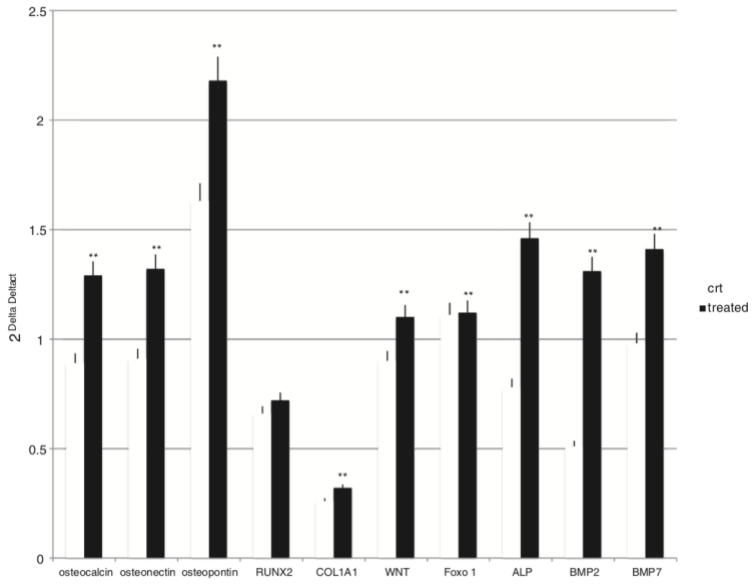

Figure 18. Gene expression by real-time PCR on DPSCs in control and OGI surfaces monolayers and in nanostructured scaffolds. Markers selected were bone morphogenic protein (BMP) 2, BMP-3, cathepsin B (CTSB), CTSD, collagen type I (Col1A1), collagen type III (Col3A1), Distal-less homeobox (DLX) 1, DLX5, fibroblast growth factor (FGF), transforming growth factor b1 (TGFb1), receptor activator of nuclear factor kappa-B (RANK), osteopontin, osteonectin, and osteocalcin. The results for each experiment are from quadruplicate experiments. Values are expressed as the mean 6 SD. *t*-Tests were used to determine significant differences (p,0.05). *p,0,05; **p,0,01; ***p,0,001.

3.1.3.9 ALP activity measurements

To confirm the early differentiation of MSC towards osteoblast phenotype, the ALP activity (expressed as U/mL that is the amount of enzyme causing the hydrolysis of 1 µmol of pNPP per units per mL) was quantified both into cells and in culture medium. Particularly, the intracellular ALP activity was 0.41 U/mL into MSC grown on OGI surfaces and 0.38 U/mL in MP group. Even the extracellular ALP was higher in OGI (0.29 U/mL) than the MP group, where it was slightly lower (0.21 U/mL). No statistical differences were observed between the groups.

3.1.3.10 Intracellular and extracellular lactate dehydrogenase activity (LDH activity)

In order to overcome the controversial results of the MTT assay related to the decreasing in time of the value, the LDH activity assay was also performed on the cells. Figure 19a shows the intracellular LDH activity of the cells seeded on both surfaces: the graph proves that cells were able to produce metabolites, with improved results after seven days from seeding. As reported in Figure 19b, extracellular LDH activity, generally related to a membrane damage related to the scaffolds, was also measured on the culture medium: the graph confirms that metabolites were secreted by the same cells with no difference between the surfaces.

3.1.3.11 Morphological analyses

SEM has evaluated morphological analyses of MSC seeded onto Ti surfaces. In Figure 20a–d and SEM images revealed how cells attached to the surface for the samples: control (a–c) and OGI (b–d). After 5 day of culture, cells in all cases, were characterized by short and thin filopodia and characterized by a good distribution for both samples. This observation is confirmed by the measurements with ImageJ software, showing that the area of the cell cultured for 5 day on control surfaces is approximately equal (199.33 μm_2) than that cultured on OGI (189.29 μm_2). It can be moreover observed that MSC appears spread, overlapped, which enable communication with each other and develop well-defined phyllopod (black arrows).

3.1.4 Discussion

In the present study we have investigated the osteogenic response of dental pulp Mesenchymal Stem Cells to an OGI titanium based surfaces. The surface Nano topography and chemistry would influence the interfacial cellular interaction and then its commitment if they were in a stemness condition. In the current study, proliferation analyses related to stem cells seeded onto the treated surfaces demonstrate some little differences between the OGI surfaces with the control.

In order to evaluate the osteogenic influence of the titanium surfaces, protocol requires a long-term in vitro cultures up to 28 days. The aging process related to this condition, has been evaluated and results showed that long-term in vitro cultures was strongly influenced by OGI surfaces. A slow-down in the aging process is indeed closely associated with the presence of OGI treatment. Moreover, this treatment exerts a positive effect on mitochondrial homeostasis, as shown by a decrease in ROS production related to environmental stress on the mitochondria. The presence of antioxidant effect of the surfaces has been moreover evaluated by DPPH assay that confirm the surfaces does not exert per se any direct antioxidant ability at extracellular level.

In brief, the DPSC cultured on the OGI surfaces appeared more spread in comparison to those grown on control titanium surface and had developed longer filopodia, which is an indication that OGI treatment is appropriate materials for cell colonization. In the meantime real time PCR data sets clearly demonstrated the osteoconductive properties of the OGI structure in terms of gene expression. Particularly, osteopontin presented a greater tendency of expression in cells cultured in the presence of OGI compared to the other genes.

These date are is also ascertained by the results of ALP activity test since ALP represents a key enzyme secreted by osteoblast in the early stages of differentiation, which provides high concentration of phosphate at the sites of mineral depositions. The mineralization process, related to matrix and mineral deposit, instead, is a process that occurs in the presence of mature osteoblasts during new bone formation.

Our results suggest that mesenchymal stem cells sensitively respond to surface properties related to OGI treatment enhancing their osteogenic activities. In order to explain how OGI surface could act this increasing on osteogenic commitment trough and antiaging ROS dependent way, we have postulated that the extracellular matrix environment of OGI could affect Wnt family receptor modifying the final commitment of MSC.MSCs, a non-hematopoietic

stem cell population are multipotent cells able to differentiate into mature cells of several mesenchymal tissues, such as fat and bone. As common progenitor cells of adipocytes and osteoblasts, MSCs are delicately balanced for their differentiation commitment. This event is important in bone environment. The dysregulation of the adipo-osteogenic balance has been linked to several pathophysiologic processes, osteopenia, osteopetrosis, and osteoporosis. Several investigations have demonstrated that fat-induction factors inhibit osteogenesis, and, conversely, bone-induction factors hinder adipogenesis (Gibon et al. 2016). Indeed a variety of external cues contribute to the delicate balance of adipo-osteogenic differentiation of MSCs, including chemical, physical, and biological factors. Among these, aging is note to cause a decrease in the number of bone-forming osteoblasts and an increase in the number of adipocytes. It is well known that the generation of reactive oxygen species (ROS) can lead to mitochondrial dysfunction, DNA damage, and the promotion of aging–dependent processes (Zhou et al. 2016).

More over as reported by Galli et al. (Galli et al. 2010, 2011) little is known about how surface topography can modulate mesenchymal cell responses to oxygen-related stress occurring with age, or during the early phases of wound healing or inflammation. To antagonize Reactive Oxygen Species (ROS), cells resort to defense mechanisms, relying on β-catenin, a molecular switch between a TCF-mediated pathway, which promotes cells proliferation and commitment, and an alternative one controlled by FoxO, which induces quiescence and defenses against ROS. It is known that the roughness of titanium surfaces affects cell proliferation and differentiation. However, the mechanisms mediating the cellular responses to surface topography are only partially understood. Galli et al. showed that surface roughness modulates the responsiveness of mesenchymal cells to Wnt3a, that this requires the control of β-catenin degradation, and that the control of β-catenin signaling by surface topography is accountable for at least part of the effects of surface on cell differentiation.

The potential for differentiation of MSCs according to age is controversial, but most of the studies have shown a decrease in their capacity to undergo osteogenic differentiation [20]. Recent studies have demonstrated that the Wnt/β-catenin signaling plays an important role in stem cell aging. However, the mechanisms of cell senescence induced by Wnt/β-catenin signaling are still poorly understood. Zang et al. has indicated that activated Wnt/β-catenin signaling can induce MSC aging. In this study, the authors reported that the Wnt/β-catenin signaling was a potent activator of reactive oxygen species (ROS) generation in MSCs (Du et al. 2016). These results indicated that the Wnt/β-catenin signaling could induce MSC aging through promoting the intracellular production of ROS, and ROS may be the main mediators of MSC aging induced by excessive activation of Wnt/β-catenin signaling. There is evidence that, during aging, the status of mMSC changes with respect to both their intrinsic differentiation potential and production of signaling molecules that contribute to the formation of a specific marrow microenvironment necessary for maintenance of bone homeostasis. With aging, the number of mMSC committed to the adipocytic lineage increases, whereas the number of mMSC committed to the osteoblastic lineage decreases. Increased expression of the adipocyte-specific transcription factor PPAR-γ2 and increased production of its activator might be a driving force forpro-adipocytic and anti-osteoblastic changes in the differentiation potential of mMSC (Du et al. 2016).

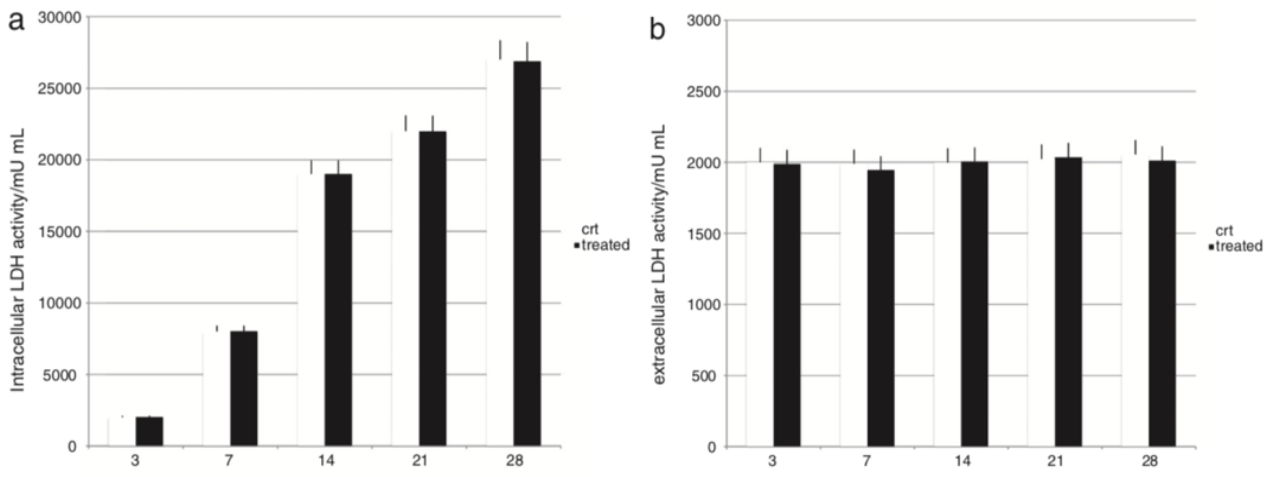

Figure 19. a) Intracellular LDH activity assay. b) Extracellular LDH activity assay.

Having said this, it is well established that extracellular matrix (ECM) stiffness plays a significant role in regulating the phenotypes and behaviors of many cell types. However, the mechanism underlying the sensing of mechanical cues and subsequent elasticity-triggered pathways remains largely unknown. Du et al. observed that stiff ECM significantly enhanced the expression level of several members of the Wnt/β-catenin pathway (Zhang et al. 2013).

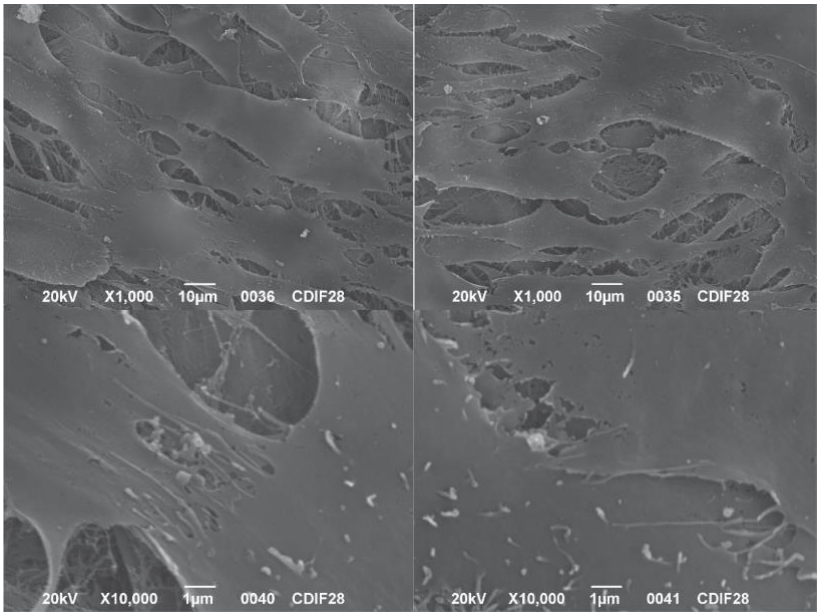

Figure 20. SEM analyses of MSC seeded onto Ti surfaces. a–b: SEM images of MSC attached to the surface of control surfaces c–d: SEM images of MSC attached to the surface of OGI surfaces. After 5 days of culture, cells in all cases, were characterized by short and thin filopodia and characterized by a good distribution for both samples.

In the end, with propose that OGI could affect the osteogenic commitment of MSC stimulating an ECM environment that reduces the aging of MSC.

3.2 The biological properties of OGI surfaces positively act on osteogenic and angiogenic commitment of mesenchymal stem cells

Ghensi P, Bressan E, Gardin C, Ferroni L, Soldini MC, Mandelli F, Soldini C, Zavan B

The biological properties of OGI surfaces positively act on osteogenic and angiogenic commitment of mesenchymal stem cells

Materials (Basel) (2017)

Abstract

Osteogenesis process displays a fundamental role during dental implant osseointegration. In the present work, we studied the influence of Osteo Growth Induction (OGI) surface properties on the angiogenic and osteogenic behaviors of Mesenchymal Stem cells (MSC). MSC derived from dental pulp and HUVEC (Human Umbilical Vein Endothelial Cells) were grown on OGI titanium surfaces, and cell proliferation and DNA synthesis were evaluated by MTT [3-(4,5-dimethylthiazol-2yl)-2,5-diphenyltetrazolium bromide] test and DNA quantification. Gene expression has been performed in order to evaluate the presence of mRNA related to endothelial and osteogenesis markers. Moreover, morphological and biochemical analyses of osteogenesis commitments have been performed. On OGI surfaces, MSC and HUVEC are able to proliferate. Gene expression profiler confirms that MSC on OGI surfaces are able to express endothelial and osteogenic markers, and that these expression are higher compared the expression on control surfaces. In conclusion on OGI surfaces proliferation, expression and morphological analyses of angiogenesis-associated markers in MSC are promoted. This process induces an increasing on their osteogenesis commitment.

Keywords: titanium surface; dental implant; MSC

3.2.1 Introduction

An adequate amount of bone tissue surrounding dental implants is fundamental to reach a satisfactory treatment outcome in the long-term period (Aghaloo and Moy 2007; Burgos et al. 2011; Scarano et al. 2014). Therefore, there is a need to further improve the performance of the implants particularly in a bad bone conditions and to optimize the time of osseointegration process (Terheyden et al. 2012; Bressan et al. 2013a, 2013b).

Osseointegration is defined as a “direct structural and functional connection between ordered living bone and the surface of a load-carrying implant.” Although osseointegration was meant originally to describe a biologic fixation of the titanium dental implants, it is now used to describe the attachment of other materials used for dental and orthopedic applications as well. Analyses of material-bone interface showed that osseointegrated implants can have an intervening fibrous layer or direct bone apposition characterized by bone-bonding depending on the composition and surface properties of the biomaterial. Research on dental implant designs, materials, and techniques has increased in the past few years and is expected to expand in the future due to the recent growth of the global market for dental implants and the

rising in the demand for cosmetic dentistry.

In order to increase the success rate of dental implants, research has focused on the control of surface properties such as morphology, topography, roughness, chemical composition, surface energy, residual stress, the existence of impurities, thickness of Ti oxide film, and the presence of metallic and nonmetallic compounds on the surface. These properties profoundly influence the osseous and tissue response to the implant by either increasing or decreasing healing times and osseointegration. Research has shown that osteoblastic cells adhere more quickly to rough surfaces than to smooth surfaces (Aghaloo and Moy 2007). This property can also produce orientation and guide locomotion of specific cell types and has the ability to directly affect cell shape and function.

The biological events during the early step of osseointegration are directly influenced by the osseous microenvironment (i.e., cells, matrix and signaling molecules) into which the implant is inserted and have several analogies with general wound healing mechanisms (Street et al. 2002; Carano and Filvaroff 2003; Figallo et al. 2007; Khalil et al. 2011; Ferroni et al. 2013; Shanbhag et al. 2015). From a clinical point of view, it is observed that the neo vascularization of the implant bed plays a key-role in bone tissue formation and this dynamic process is the result of complex biological phases (Abrahamsson et al. 2004; Bosshardt et al. 2011; Lang et al. 2011b; Silva-Correia et al. 2013). It is demonstrated that the first days of healing are crucial for the survival of the implant osseointegration whereby bone formation and remodeling occur in parallel around the implant (Lakey et al. 2000; Huang et al. 2005; Casadei et al. 2012; Saghiri et al. 2016).

Angiogenesis, the formation of new blood vessels from pre-existing capillaries, has a significant effort to inflammatory and regenerative processes in the body's tissues including bones (Gardin et al. 2012; Saghiri et al. 2015). Blood vessels are the fundamental component of bone formation, and maintenance and formation of an adequate vascular bed is a key-factor to support the metabolic needs of the newly forming tissues (Nobuto et al. 2005; Abshagen et al. 2009). Consequently, it is evident how angiogenesis temporally precedes osteogenesis. In fact the formation of new bone, bone modeling and remodeling and also osseointegration after dental implant placement need a blood supply to guarantee nutrition, oxygen, and osteoprogenitor cells through the newly formed blood vessels (Mijiritsky et al. 2017).

The primary cells implicated in angiogenesis are endothelial cells. They are involved on the realization of the microvasculature that is responsible for the supply of nutrients and oxygen and for the elimination of the waste. Moreover they participate in the tissue response thanks to expression of osteoblast adhesion molecules and by the releasing of pro-inflammatory factors (Peters et al. 2003). In the end there is an intimate connection between endothelial cells and bone cells, and information of blood vessels in bone enhances osteogenesis that takes place in the neighborhood of newly formed vessels (Eckardt et al. 2003). Several titanium surfaces are available, and in this scenario in the present work we have better characterized the biological properties of a novel dental surfaces OGI that we have previously characterized (Ghensi et al. 2017a) by mechanical point of view. OGI implants are characterized by a large-grit sandblasted and acid etched surface (Ra. 0.31–1.61). SEM (scanning electron microscope) and XPS (X-ray photoelectron spectroscopy) analyses have previously demonstrated this where the presence of both big "holes" due to large grit sandblasting on which the micro roughness due to acid etching is superimposed has been confirmed.

Moreover, tridimensional topography, which imparts to these surfaces spongy-like characteristics, has been confirmed thanks to the short peak-to-peak distance, on the order of about 1 µm. According to this close relationship between osteogenesis, angiogenesis, and osseointegration, the aim of the present study is to demonstrate through molecular, biochemical, and morphological analysis how an Osteon Growth Induction (OGI) titanium implant surface is able to own angiogenic properties that positively act on osteogenic commitment of mesenchymal stem cells (MSCs) and consequently on the osteointegration process.

3.2.2 Results

3.2.2.1 Proliferative Activity

In Figure 21, proliferative activity of MSC (in the presence of non-differentiation medium), MSC cultured in the presence of osteoinductive medium (representing here osteoblastic like cell population) and HUVEC (representing here endothelial cells population) have been detected employing MTT test, DNA content, and population doubling time (PDT) value.

As reported in Figure 21C, a well-defined cell growth on the OGI surfaces for each passage for each cells group is observed. The cells are able to well proliferate, increasing in number as demonstrated by the MTT test Figure 21A and the DNA content (Figure 21B). The rising MTT values confirmed that the cells were alive when cultured onto OGI surfaces, whether their ability to proliferate is confirmed by the increase in DNA content. These dates are also supported by the population doubling time (PDT) that is a direct marker of the proliferative ability of the cell since it is used to evaluate the ability of the cell to duplicate in number. In our experiment, we analyzed the PDT of the different cell populations at three different time: 3, 7 and 14 days.

As reported in Figure 21C, it is observed a well-defined cell growth for each passage for each cells group. When the cells are in a mesenchymal stage (MSC) a high PDT value was maintained in all cell passages confirming the right proliferative ability of the cells when are in a stem cells phenotype. For the other cells population (related to a committed one), both osteoblastic-like and endothelial one (HUVEC) proliferative ability decreased in time and during in vitro commitment.

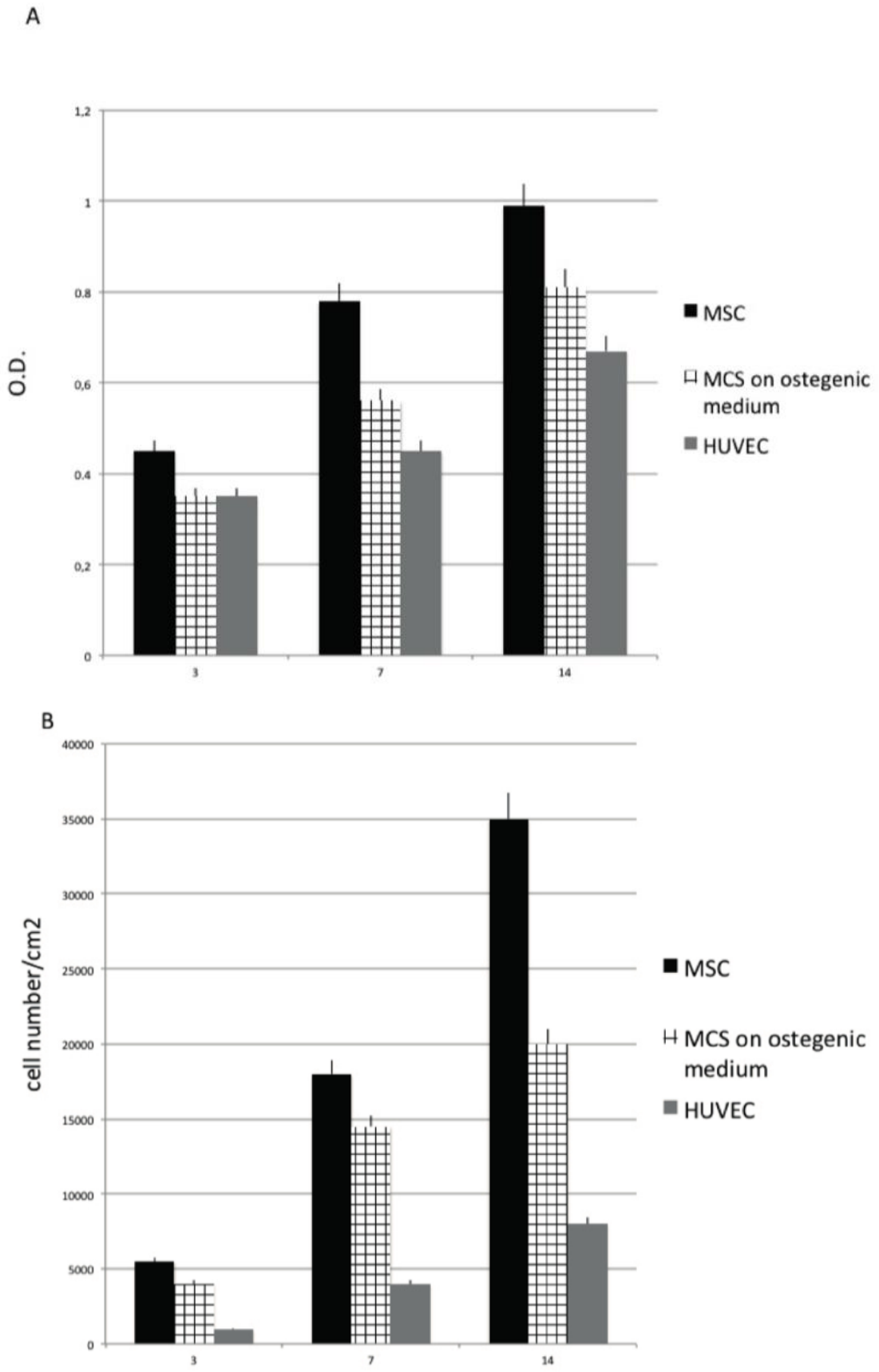
A
O.D.
1,2
1
0,8
0,6
0,4
0,2
0
3
7
14
MSC
MCS on ostegenic medium
HUVEC
B
cell number/cm2
40000
35000
30000
25000
20000
15000
10000
5000
0
3
7
14
MSC
MCS on ostegenic medium
HUVEC

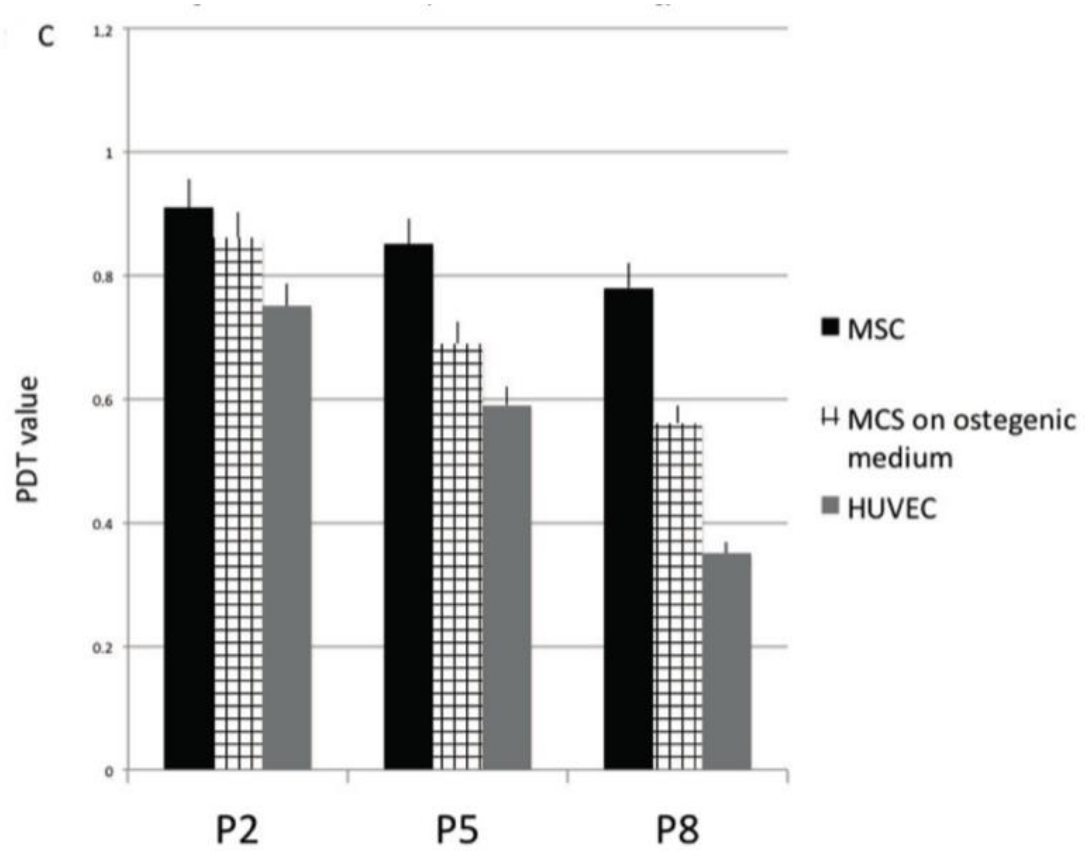

Figure 21. Proliferative activity of Mesenchymal Stem cells (MSC) detected by means of MTT test (A), DNA content (B) population doubling time (PDT) value (C). MSC cultured in presence of nondifferentiative medium: (black bars), osteoinductive medium (squared bars), HUVEC (Human Umbilical Vein Endothelial Cells) (grey bars.).

3.2.2.2 Endothelial Cells

To determine how OGI features affect the morphology of HUVECs, HUVECs were analyzed for morphological responses Figure 22 after 14 days of culture. Our results show that on OGI surfaces HUVECs were able adhere and to spread well. Cells were flattened with pronounced protrusion of philopodia. Cells were able to attach tightly to OGI surfaces and covered a great area. This has been confirmed by means of the morphology, by the enhancement of cell-cell communication, and by the cell-substrate adhesion. In Figure 22A SEM test and in Figure 2B immunohistochemical test against CD31 (in green) clearly show that cells can attach onto the surface organizing in capillary like structures (red circles). Maintaining of the correct phenotype also confirmed by the presence of CD31 receptor (typical of mature endothelial cells) onto the surface (in green). As reported in Figure 22, HUVEC are able to attach to the OGI surface and organized themselves into capillary like structures (red circles), as SEM analyses revealed. Positivity for CD31 (in green) confirms that HUVEC can maintain their endothelial phenotype.

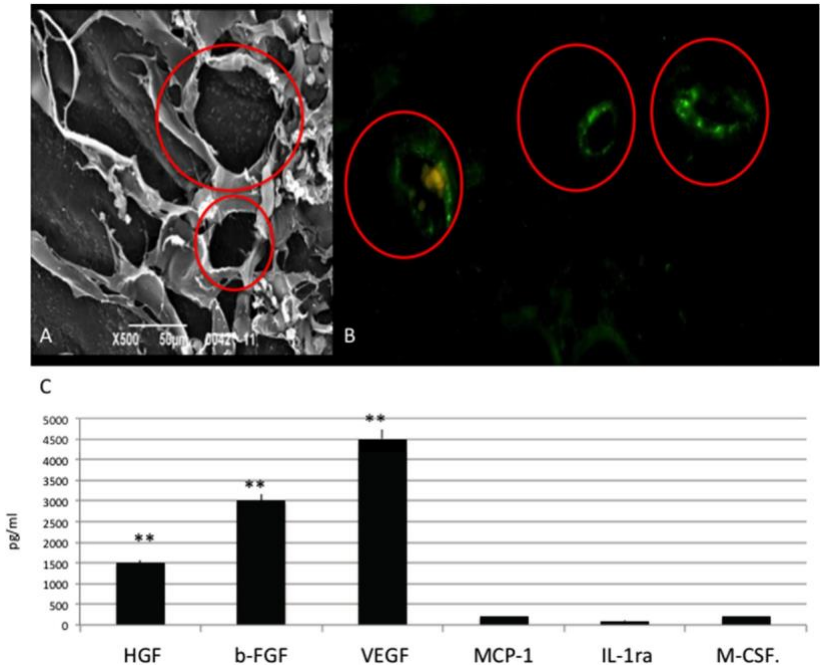

Figure 22. (**A**) SEM (scanning electron microscope) analyses of HUVEC cultured onto Osteon Growth Induction (OGI) surfaces; (**B**) immunohistochemical test against CD31 (in green), capillary like structures (red circles) as SEM analyses revealed; (**C**) Quantification of growth factor release pg/mL. Statistically significant differences are indicated as ** $p < 0.01$.

In Figure 22 C results related to ELISA (enzyme-linked immunosorbent assay) assay direct to evaluate quantitatively the secretion of the VEGF and bFGF proteins over 14 days are reported. For VEGF and bFGF protein secretion, it is clear that their level is significantly higher compared to the other protein secreted typical of a non-endothelial phenotype.

3.2.2.3 Osteoblastic Like Cells

When MSC are cultured into osteogenesis medium are able to attach into all the surfaces as electro-microscopy (Figure 23A) and immunohistochemical analyses for phalloidine (Figure 23B in red) analyses confirm. Cell spread well and colonized all the surface. Well-defined phyllopodia, ensuring the attached, are well evident by the positivity for phalloidin (in red. Figure 23B) shows.

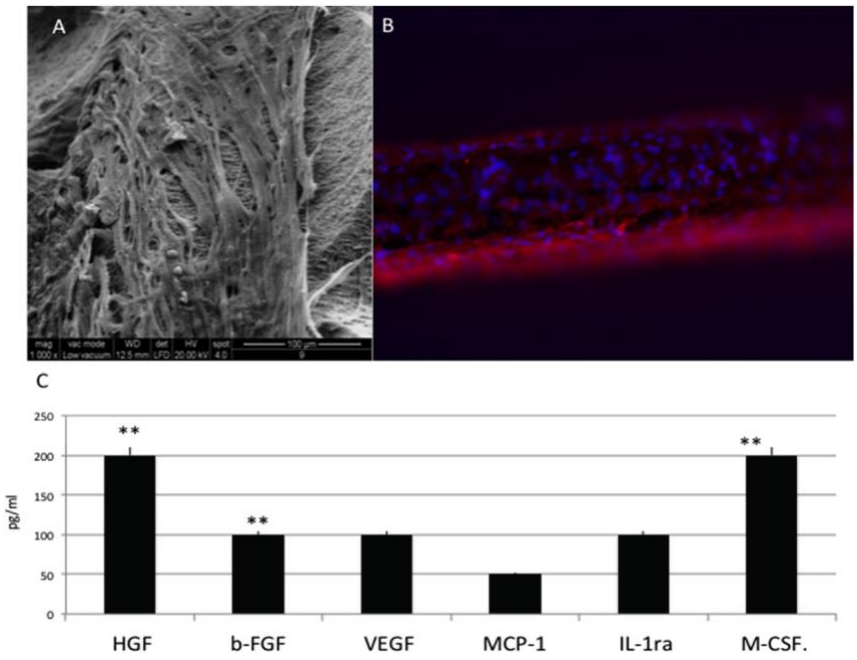

Figure 23. (**A**) SEM analyses of MSC in presence of osteoinductive medium cultured onto OGI surfaces; (**B**) immunohistochemical test against phalloidine (red) (**C**) Quantification of growth factor release pg/mL. Statistically significant differences are indicated as ** $p < 0.01$.

To assess differences between HUVEC, MSC and osteoblastic like cells regarding the release of paracrine factors with several supportive effects such as antiapoptotic, immunomodulatory, antifibrotic, angiogenic, chemoattractive, and hematopoiesis, the following factors were quantified: Hepatocyte growth factor (HGF), basic fibroblast growth factor (b-FGF), vascular endothelial growth factor (VEGF), monocyte chemotactic protein-1 (MCP-1), stromal cell-derived factor 1-alpha (SDF-1a), interleukin 1 receptor antagonist (IL-1ra) and macrophage colony-stimulating factor (M-CSF) (Figure 23C). In this cells cultures, lower factors related to endothelial phenotype such as VEGF and bFGF, whether typical markers of osteoblast such as Hepatocyte growth factor (HGF) and colony stimulating factor 1 (M-CSF), are significantly expressed. Cells of mesenchymal origin, and osteoblasts/osteocytes and bone marrow stromal cells originate from mesenchymal cells are able to mainly produce HGF. M-CSF is released by osteoblasts and exerts effects on osteoclasts thank to its paracrine effect. M-CSF binds to receptors on osteoclasts are able to induce differentiation, and to lead the increasing of plasma calcium levels.

3.2.2.4 MSC

Mesenchymal stem cells cultured in a no differentiative medium Cells reached a continuous cell layer on day 14 (Figure 24A–C), with a confluent cell monolayer as SEM (Figure 25A–B) and positivity for phalloidine staining (red) (Figure 5C).

Several paracrine factors secreted by MSCs have been selected and detected by ELISA test

are reported on Figure 25D where is evident that a good production of HGF, bFGF, and VEGF is present.

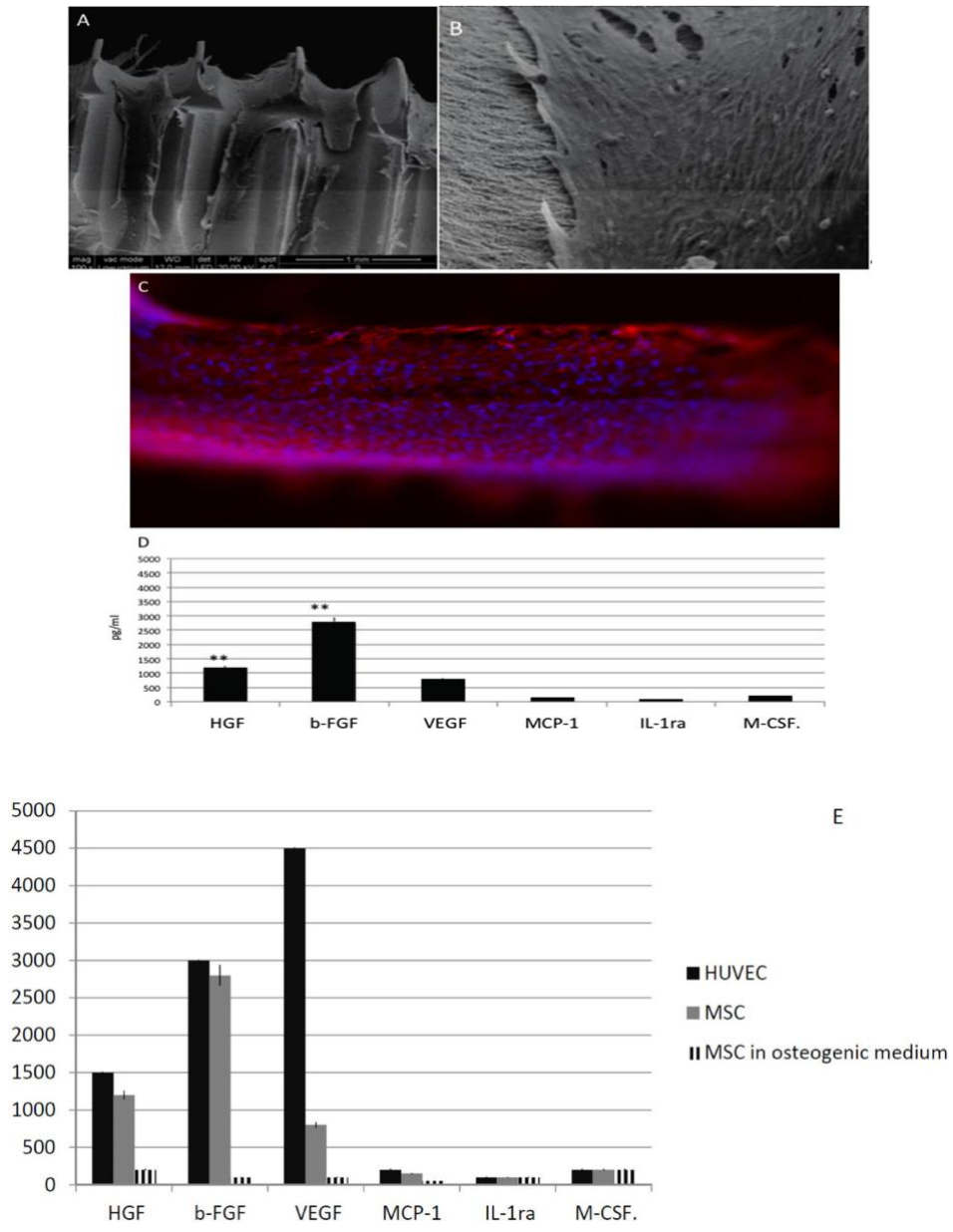

Figure 24. (**A**,**B**) SEM analyses of MSC in presence of no differentiative medium cultured onto OGI surfaces; (**C**) immunohistochemical test against phalloidine (red) (**D**) Quantification of growth factor release pg/mL. Statistically significant differences are indicated as ** $p < 0.01$; (**E**) Summarized graph about the quantification of growth factor release from the MSCs, osteoblastic like cells, and HUVEC cells.

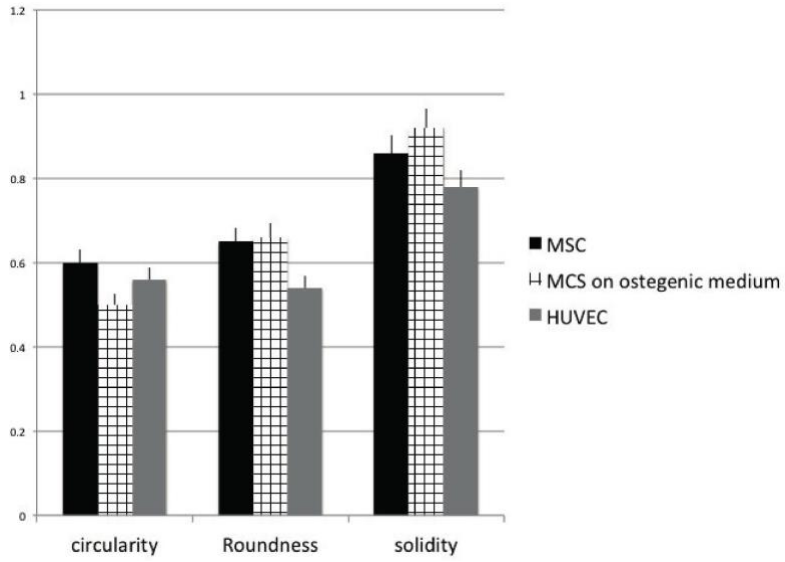

Figure 25. Analysis of the circularity, roundness, and solidity cell shape parameters after 14 days of culture onto OGI surfaces. MSC cultured in presence of nondifferentiative medium: (black bars), osteoinductive medium (squared bars); HUVEC (grey bars).

3.2.2.5 Cell Shape

In order to quantify the right phenotype of the cells we have performed an analyses of cells shape. We started from the axiom that endothelial cells have a small fusiform shape, osteoblastic cells a start-like phenotype, and MSC a fusiform shape. If cells maintain their right phenotype, they will be able to exert their function on osteogenesis (osteoblastic and MSC activity) and angiogenesis (MSC and endothelial cell activity). Figure 25 is related to the analysis of cell shape. Focused has been related to three parameters: circularity, roundness, and solidity. The circularity and roundness calculated values confirm that when endothelial cells were seeded onto the OGI implants and cultured for 14 days, they assumed an elongated morphology. They also have the lesser solidity value. Osteoblastic cells acquire a less rounded morphology with the highest value on solidity. MSC has a more rounded aspect typical for a staminal phenotype.

3.2.2.6 ALP Activity

The alkaline phosphatase (ALP) activity of the cells seeded onto OGI surface was quantified and reported in Figure 26 in order confirm the possible early differentiation. Results confirm that ALP was higher when MSC were in pre osteoblastic like cell (0.25 U/mL) compare when cell are in a non-differentiative medium (0.24 U/mL) whether in HUVEC cells was slightly lower.

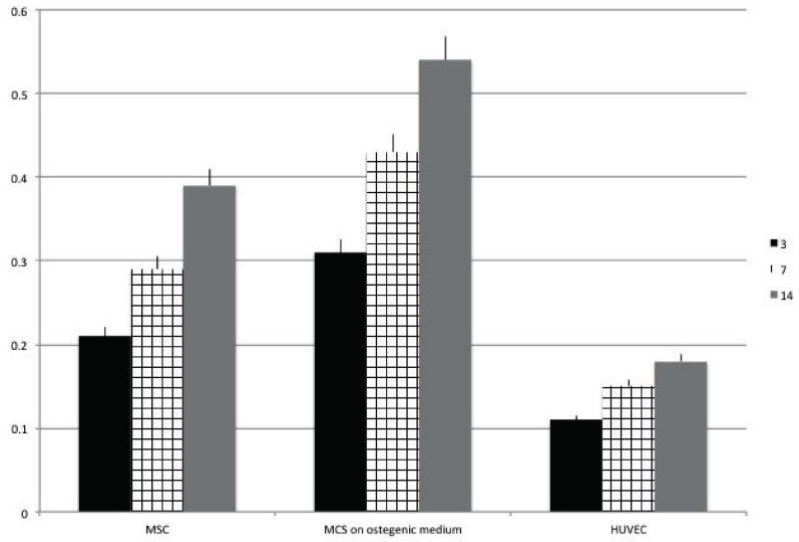

Figure 26. Analysis of ALP activity after 3 (black bars), 7 (squared bars), 14 (grey bars) days of culture onto OGI surfaces of MSC cultured in presence of nondifferentiative medium, osteoinductive medium; HUVEC

3.2.2.7 PCR

Moreover, the preservation or acquisition of endothelial cell phenotype on OGI surfaces was confirmed by the presence of angiogenic-osteogenic-cell adhesion endogenic cell-specific markers, at transcription levels using real-time RT-PCR (real time polymerase chain reaction), respectively, after cultured for 14 days on both control and OGI surfaces (Figure 27).

Our data show that the expression levels of angiogenic markers were higher on HUVEC compare in osteoblastic like cells. A well-defined expression is present on MSC cultures.

The osteoinductive properties of the OGI implants used in the present study were evaluated by means of the gene expression level of osteoblast markers. The expression of selected genes (COL1A1, OCN, ON, OPN, RUNX) was evaluated about the expression of a reference gene (GAPDH) and compared the cultures on controls Titanium surfaces. As shown in Figure 27, the expression of some osteoblast markers in MSC in a osteoblastic-like trend is higher compared to the HUVEC and to a MSC control condition. In particular, high gene expression levels were observed for COL1A1, OPN, and RUNX.

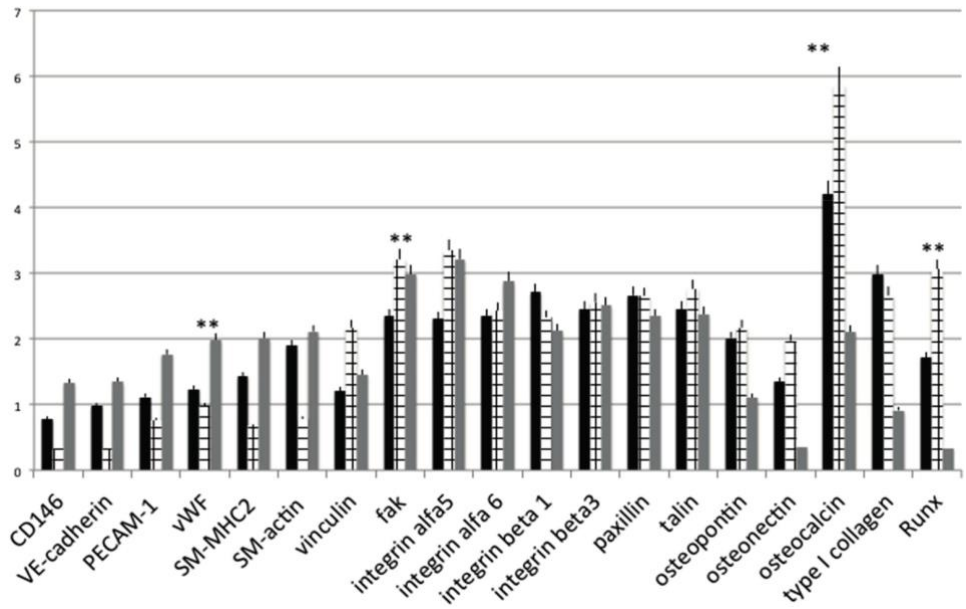

Figure 27. Gene expression profiles of osteogenic, cell adhesion molecules and endothelial differentiation markers in MSC cultured in presence of non-differentiative medium: (black bars), osteoinductive medium (squared bars); HUVEC (grey bars.) seeded onto control or OGI surfaces. Values are expressed as $2_{\Delta\Delta Ct}$. Statistically significant differences are indicated as ** $p < 0.01$.

The results related to the cell adhesion markers showed β1 and β3 integrin increase in osteoblastic differentiation markers on OGI surface. Moreover the same trend is present for integrin Alfa 5 and 6 that mediate adhesion of MSC cells to matrix proteins, and that are necessary for cell-matrix interactions in bone. Our results, confirm that in all cell types present in OGI surface gene expression of beta 1 and alpha 5 integrin are present. Osteoblasts uniformly expressed the alpha V.

3.2.3 Discussion

Cell-surface interactions could be considered as the primary factors of the long-term performance and bio functionality of dental devices since surfaces properties are able to promote osteoblast specific adhesion and enhance differentiation (Scarano et al. 2014), increasing the exogenesis of mineralized matrix, bone tissue formation, and deposition. An adverse event such as fibrous encapsulation is further known to occur with both different surfaces (Burgos et al. 2011). This could reduce biocompatibility. However, OGI Titanium (Ti) surface microarchitecture has been shown to increase osteoblast differentiation by our previous publication (Zavan et al. 2007; Bressan et al. 2012; Gardin et al. 2015; Caroprese et al. 2017; Ghensi et al. 2017a).

However, clinical success of implanted materials is related to osteointegration and on neovascularization in the peri-implant bone. Here, we tested the hypothesis that OGI Ti surface is able to regulate up the expression and secretion of angiogenic growth factors on HUVEC

cells, MSC in an undifferentiated state, and on a pre-osteoblastic feature have been seeded and analyzed on an OGI surface.

The values of secretion and expression ion of VEGF-A, and of FGF-2, confirmed the right endothelial activity of HUVEC when they are seeded onto an OGI surface. These factors were undetectable in osteoblastic-like cells cultures. These results show that the Ti surface modulates the secretion of angiogenic growth factors by osteoblasts. VEGF and b-FGF that are the most potent and widely investigated pro-angiogenic growth factors are produced by HUVECs when cultured on OGI surfaces in higher levels than those cells cultured on the control surface.

On this basis, we can conclude that OGI surfaces enhance the ability of HUVECs in producing angiogenic factors in vitro. This event has been moreover confirmed by the analyses of gene expression of other markers of the endogenic-associated genes, such as VWF, and PECAM-1. Moreover as revealed in Figure 27, position expression of VWF gene expression on the OGI surfaces suggest that HUVECs had some endothelial characteristics and functions after culturing on this surfaces. As evidenced from Figure 27, PECAM-1 expression on OGI surfaces was generally higher than that of the control surface, indicating increased endothelial cell proliferation and migration on the OGI surfaces, which is in good agreement with our cell proliferation results as shown in Figure 21. In order to evaluate the ability of the OGI surface to increase cells attachment of the “right cells” needed for osteointegration, an analyses of morphology and mediator of cell attachment was performed. The expressions of other markers related to cells attachment associated genes such as vincula, FAK, and integrin. The osteogenic influence of the surface has been in the end confirmed by the ability acquired by MSC to secreted typical osteoblastic factor such as HGF and MCSF by the production of ALP and by the gene expression related to osteogenic commitment such as osteopontin, osteonectin, and RUNKX. These data imply a better angiogenic and osteogenic potential of the as-grown OGI over the control counterpart.

In a biomaterials setting, mesenchymal stem cells have been shown to undergo osteospecific differentiation and functional tissue formation when cultured on topographies that increase focal adhesion frequency and reinforcement. Our results confirm that on OGI surface MSC and osteoblastic like cells are able to increase focal adhesion and its related activation of RUNX pathway.

These results support the preclinical in-vivo (animal) evidence of the good osteoproperties of OGI surface by Caroprese et al (Caroprese et al. 2017) that analyzed in the osseointegration of implants with OGI surface installed using a standard bed preparation in sites of different bone morphology. Results confirmed that the final insertion torque was 50–55 Ncm at the premolar and 30–35 Ncm at the molar sites. Mean osseointegration in percentage reached 61.5 ± 11.5% and 63.3 ± 10.1% at the premolar and molar sites, respectively. Mineralized bone density evaluated from the implant surface up to a distance of about 0.6 mm lateral to the implant surface was 63.0 ± 7.4% and 65.4 ± 17.7% at the premolar and molar sites, respectively. The authors conclude that similar implant bed preparations performed at premolar and molar sites with different bone morphology, yielding insertion torque values of about 30–35 and 50–55 Ncm, respectively, did not affect osseointegration after four months at non-submerged implants.

3.2.4 Materials and Methods

3.2.4.1 Dental Pulp Mesenchymal Stem Cells

Human dental pulps were extracted from healthy molar teeth, which had been extracted because of mucosal inflammation (impacted teeth with pericoronitis) or for orthodontic reasons from adult subjects aged 16 to 66. The pulps were classified into 6 age groups (12 teeth per group). Each subject gave informed written consent for the use of his or her dental pulps. The Ethical Committee of Padua Hospital approved the research protocol. Before extraction, each subject was checked for systemic and oral infections or diseases. Only disease-free subjects were selected for pulp collection. Each subject was pretreated for one week with professional dental hygiene. Before extraction, the dental crown was covered with a 0.3% chlorhexidine gel (Forhans, New York, NY, USA) for 2 min. After mechanical fracturing, dental pulp was obtained by means of a dentinal excavator or a Gracey curette. The pulp was gently removed and immersed for 1 h at 37 ◦C in a digestive solution: 100 U/mL penicillin, 100 mg/mL streptomycin, 0.6 mL of 500 mg/mL clarithromycin, 3 mg/mL type I collagenase, and 4 mg/mL dispase in 4 mL of 1 M PBS. Once digested, the solution was filtered through 70mm Falcon strainers (Becton & Dickinson, Franklin Lakes, NJ, USA) (Lang et al. 2011b).

3.2.4.2 Human Umbilical Vein Endothelial Cells (HUVEC)

HUVEC were prepared from Umbilical cords that were freshly supplied by the local Obstetrics and Gynecology Division. Briefly, after perfusion of the vein with a metal gauge, the vein was rinsed twice with saline solution (PBS, phosphate buffered saline without Ca^{2+} and Mg^{2+}). Endothelial cells were separated from the vein walls by collagenase type IA (Sigma, Kawasaki-shi, Japan) digestion (1 mg/mL; 300–400 U/mg) for 10 min at 371 ◦C in physiological solution. The reaction was terminated by adding complete Medium 199 (Seromed, Istanbul, Turkey) (M199 plus 2 mm L-glutamine, 1/2100 U/mL; 1/2100 mg/mL penicillin/streptomycin, 2:5 mg/mL amphotericin B, i.e., cM199) supplemented with 20% FBS without growth factors. A maximum of three passages were allowed before seeding of endothelial cells into the OGI surfaces.

3.2.4.3 Cell Medium

Non-differentiative medium: Non-hematopoietic (NH) stem cell expansion medium (Miltenyi Biotec, Bergisch Gladbach, Germany).

Osteogenic differentiation medium: NH OsteoDiff Medium (Miltenyi Biotec, Bergisch Gladbach, Germany).

Endothelial differentiation medium: DMEM containing 10% FBS plus 0.1 ng/mL human recombinant ECGF, 10 mg/mL human bFGF (Calbiochem, San Diego, CA, USA) and 100 mg/mL porcine heparin (Seromed; Berlin, Germany).

3.2.4.4 MTT Test

Cell proliferation rates were determined by the MTT [3-(4,5-dimethylthiazol-2yl)-2,5-diphenyltetrazolium bromide)-based cytotoxicity test using the Denizot and Lang method with minor modifications (Zavan et al. 2007).

3.2.4.5 DNA Content

DNA content was determined using a DNeasy kit (Qiagen, Hilden, Germany) to isolate total DNA from cell cultures following the manufacturer's protocol for tissue isolation, using overnight incubation in proteinase K (Qiagen). The concentration of DNA was detected by measuring the absorbance at 260 nm in a spectrophotometer. Cell number was then determined from a standard curve (microgram DNA vs. cell number) generated by DNA extraction from counted cells. The standard curve was linear over the tested range of 5–80 µg DNA ($r = 0.99$) [30].

3.2.4.6 Growth Curve and Doubling Time

Cells were seeded into OGI dishes at an initial density of 5 × 104. When cells reached confluence, they were detached, counted and re-seeded at a density of 5 × 104. The PDT of the cells was calculated according to the formula:

$$PDT = (T - T_0)\ \log 2/(\log N_t - \log N_0) \quad (1)$$

where PDT represents the cell doubling time, T represents the duration of cell culture, and N and N represent the cell number after seeding and the cell number after culturing for t hours, respectively [31].

3.2.4.7 Quantification of Secreted Factors

Secreted factors have been evaluated from culture supernatants. Cells (HUVEC, MSC; and osteoblast like cells) were seeded at a density of 50,000 cells/cm^2 onto OGI surfaces. After 24 h, cells were washed twice with standard culture medium w/o FBS.

Hepatocyte growth factor (HGF), basic fibroblast growth factor (b-FGF), vascular endothelial growth factor (VEGF), monocyte chemotactic protein-1 (MCP-1), stromal cell-derived factor 1-alpha (SDF-1a), interleukin 1 receptor antagonist (IL-1ra), and macrophage colony-stimulating factor (M-CSF) were quantified using the respective Bio-Plex assay (Bio-Rad) according to manufacturer's protocol.

3.2.4.8 Real-Time PCR

Human primers were selected for each target gene with Primer 3 software. Real-time PCRs were carried out using the designed primers at a concentration of 300 nM and FastStart SYBR Green Master (Roche) on a Rotor-Gene 3000 (Corbett Research, Sydney, Australia). Thermal cycling conditions were as follows: 15 min denaturation at 95 °C; followed by 40 cycles of 15 s denaturation at 95 °C; annealing for 30 s at 60 °C; and 20 s elongation at 72 °C. Differences in gene expression were evaluated by the $2^{\Delta\Delta Ct}$ method, using DPSCs cultured onto non treated titanium disks for 15 days as control. Values were normalized to the expression of the glyceraldehyde-3-phosphate dehydrogenase (GAPDH) internal reference, whose abundance did not change under our experimental conditions. Experiments were performed with three different cell preparations and repeated at least three times.

3.2.4.9 Scanning Electron Microscopy (SEM)

For SEM imaging, DPSCs grown on control and treated Ti surfaces for 15 and 25 days were

fixed in 2.5% glutaraldehyde in 0.1 M cacodylate buffer for 1 h, then progressively dehydrated in ethanol. Control and treated Ti surfaces without cells were also examined. The SEM analysis was carried out at the Interdepartmental Service Center C.U.G.A.S. (University of Padova, Padova, Italy).

3.2.4.10 Statistical Analysis

One-way analysis of variance (ANOVA) was used for data analyses. The Levene's test was used to demonstrate the equal variances of the variables. Repeated-measures ANOVA with a post-hoc analysis using Bonferroni's multiple comparison was performed. *T*-tests were used to determine significant differences (p, 0.05). Repeatability was calculated as the standard deviation of the difference between measurements. All testing was performed in SPSS 16.0 software (SPSS Inc., Chicago, IL, USA) (license of the University of Padua, Padova, Italy).

3.2.4.11 ALP Activity Measurements

The alkaline phosphatase (ALP) activity was measured after 2 weeks of cell culture to evaluate the initial differentiation of MSC into preosteoblasts. Abcam's Alkaline phosphatase kit (colorimetric) has been used to detect the intracellular and extracellular ALP activity. The kit uses p-nitrophenyl phosphate (pNPP) as a phosphatase substrate which adsorbed at 405 nm when dephosphorylated by ALP. According to the manufacturer protocol, the culture medium from each sample group was collected and pooled together. At the same time, cells were washed with PBS and then homogenized with ALP Assay Buffer (300 µL in total for each group) and centrifuged at 13,000 rpm for 3 min to remove insoluble material. Different volumes of samples (medium and cells) were then added into 96-well plate, bringing the total volume in each well up to 80 µL with Assay Buffer. 80 µL of fresh medium was also utilized as sample background control. Thereafter, 50 µL of 5 mM pNPP solution was added to each well containing test samples and background control and incubated for 60 min at 25 ◦C, protecting the plate from the light. A standard curve of 0, 4, 6, 12, 16, and 20 nmol/well was generated from 1 mM pNPP standard solution bringing the final volume to 120 µL with Assay Buffer. All reactions were then stopped by adding 20 µL of Stop solution into each standard and sample reaction except the sample background control reaction. Optical density was read at 405 nm in a microplate reader (Victor). The results were normalized subtracting the value derived from the zero standards from all standards, samples and sample background control. The pNP standard curve was plotted to identify the pNP concentration in each sample. ALP activity of the test samples was calculated as follow

$$\text{ALP activity (U/mL)} = A/V/T \qquad (2)$$

where:

A is the amount of pNP generated by samples (in µmol).

V is the amount of sample added in the assay well (in mL).

T is the reaction times (in minutes).

3.2.4.12 Cell Shape Analyses

Cell area and different shape descriptors were calculated with ImageJ software (National Institutes of Health) (http://rsb.info.nih.gov/ij). In particular, the solidity (S), circularity (C), and

roundness (R) of cells were investigated according to the following equations:

$$\text{Roundness } R = a/b \quad (3)$$

where a and b are the width and length of the minimum bounding (the smallest rectangle enclosing the selection), respectively,

$$\text{Circularity } C = 4A/P2 \quad (4)$$

where P is the perimeter and A is the cell area, and

$$\text{Solidity } S = A/\text{ConvexA} \quad (5)$$

where ConvexA is the area enclosed by the smallest shell that borders all the points of the cell.

3.2.4.13 Immunofluorescence

Cells were fixed in 4% paraformaldehyde in PBS for 10 min, then incubated in 2% bovine serum albumin (BSA, Sigma-Aldrich, Saint Louis, MO, USA) in PBS for 30 min at room temperature. Cells were then incubated with primary antibodies in 2% BSA solution in a humidified chamber for 12 h at 4 °C. The following primary antibodies were used: rabbit polyclonal antihuman phalloidine antibody (Millipore Corporation, Boston, MA, USA) and mouse polyclonal anti-human VEGF antibody (Sigma-Aldrich, Boston, MA, USA). Immunofluorescence staining was performed using the secondary antibodies DyLight 549-labeled anti-rabbit IgG (H + L) (KPL, Gaithersburg, MD, USA diluted 1/1000 in 2% BSA for 1 h at room temperature. Nuclear staining was performed with 2 µg/mL Hoechst H33342 (Sigma-Aldrich) solution for 2 min.

3.2.5 Acknowledgments

The work has been supported by Zavan Barbara University of Padova grant 2016.

4. A pilot study to develop a promising sericin-based coating with anti-biofilm properties for dental implants

Rationale

At the dawn of modern implantology implant surfaces were machined, later, in an attempt to enhance the osseointegration process and to shorten treatment times, surfaces with greater roughness were developed through titanium plasma spray and hydroxyapatite coatings (Barfeie et al. 2015). Microstructured and nanostructured surfaces developed later have been shown to induce cell differentiation toward a population of osteoblasts, thus promoting osseointegration (Bressan et al. 2013a). The negative aspect of surfaces with increased roughness, however, lies, in the case of exposure to the oral environment, in the difficulty in removing bacteria accumulated in the anfractuosities, with consequent worsening of the prognosis in case of onset of peri-implantitis (Carcuac et al. 2016).

Given the difficulty or impossibility to regain implant osseointegration, in the last few years materials and strategies have been tested that are potentially able to prevent peri-implant diseases by inhibiting bacterial colonization and promoting at the same time the growth of body tissues. Such strategies can act through different mechanisms including anti-bioadhesive coatings able to induce surface energy alteration (Price et al. 1996; Verran and Whitehead 2005; Antoci et al. 2007)), surface coating with molecules with bactericidal or photocatalytic activity (e.g. Vancomycin, Ag, Zn) (Price et al. 1996; Verran and Whitehead 2005; Antoci et al. 2007) or coatings (e.g. calcium phosphate, polylactic acid, chitosan) with controlled release of antimicrobial agents (Price et al. 1996; Verran and Whitehead 2005; Antoci et al. 2007). The future of research, however, consists in the development of surfaces able of inhibiting the biofilm formation or of being bioresponsive towards the biofilm formation, that is, to assume bactericidal properties in the presence of infection.

In this chapter, I present an *in-vitro* study conducted in collaboration with the BIOtech center at the Department of Industrial Engineering of the University of Trento in which we tested a new potential anti-biofilm coating based on sericin, one of the two main silk proteins, whose antibacterial efficacy is still debated. Different experimental protocols to obtain a sericin-based coating on medical grade titanium (Ti) were tested and one of them, that with glutaraldehyde-bound sericin after silanization in the vapor phase, showed a promising and significant biofilm inhibition activity of 53% using a standard biofilm producer strain of *Staphylococcus aureus* (ATCC 6538). These results represent a significant starting point to further test and elucidate such promising sericin-based coating with specific peri-implant-relevant microorganisms. This work has been recently published in *Materials* journal.

My contribution

My contribution to the pilot study contained in this chapter was mainly to elaborate the study design, to discuss the methodologies, and to critically analyze the experimental data.

The chapter is based on the following article:

Ghensi P, Bettio E, Maniglio D, Bonomi E, Piccoli F, Gross S, Caciagli P, Segata N, Nollo G, Tessarolo F

Dental implants with anti-biofilm properties: a pilot study for developing a new sericin-based coating

Materials (Basel) (2019)

4.1 Dental implants with anti-biofilm properties: a pilot study for developing a new sericin-based coating

Ghensi P, Bettio E, Maniglio D, Bonomi E, Piccoli F, Gross S, Caciagli P, Segata N, Nollo G, Tessarolo F

Dental implants with anti-biofilm properties: a pilot study for developing a new sericin-based coating

Materials (Basel) (2019)

Abstract

Aim: Several strategies have been tested in recent years to prevent bacterial colonization of dental implants. Sericin, one of the two main silk proteins, possesses relevant biological activities and literature reports also about its potential antibacterial properties, but results are discordant and not yet definitive. The aim of this study was to evaluate the effectiveness of different experimental protocols in order to obtain a sericin-based coating on medical grade titanium (Ti) able to reduce microbial adhesion to the dental implant surface. Materials and Methods: Different strategies for covalent bonding of sericin to Ti were pursued throughout a multi-step procedure on Ti disks. The surface of grade 5 Ti was initially immersed in NaOH solution to obtain the exposure of functional -OH groups. Two different silanization strategies were then tested using aminopropyltriethoxysilane (APTES). Eventually, the bonding between silanized Ti and sericin was obtained with two different crosslinking process: glutaraldehyde (GLU) or carbodiimide/N-Hydroxy-succinimide (EDC/NHS). Micro-morphological and compositional analyses were performed on the samples at each intermediate step to assess the most effective coating strategy able to optimize silanization and bioconjugation processes. Microbiological tests on the coated Ti disks were conducted *in-vitro* using a standard biofilm producer strain of *Staphylococcus aureus* (ATCC 6538) to quantify the inhibition of microbial biofilm formation (anti-biofilm efficacy) at 24 hours. Results: Both silanization techniques resulted in a significant increase of silicon (Si) on the Ti surfaces etched with NaOH. Differences were found between GLU and EDC/NHS bioconjugation strategies in terms of composition, surface micro-morphology and anti-biofilm efficacy. Titanium samples coated with GLU-bound sericin after silanization obtained via vapor phase deposition proved that this technique is the most convenient and effective coating strategy, resulting in a bacterial inhibition of about 53% in respect to the uncoated titanium disks. Conclusions: The coating with glutaraldehyde-bound sericin after silanization in the vapor phase showed promising bacterial inhibition values with a significant reduction of *S. aureus* biofilm. Further studies including higher number of replicates and more peri-implant-relevant microorganisms are needed to evaluate the applicability of this experimental protocol to dental implants.

4.1.1 Introduction

Bacterial biofilm formation on oral surfaces constitutes the starting point of the most common oral diseases, including caries, gingivitis, periodontitis and, when dental implants are involved, mucositis and peri-implantitis (Lang et al. 2011a; Do et al. 2013). Peri-implantitis is considered

today a major problem in dentistry and it is of growing importance as the number of patients treated with implant therapy increases. In a recent systematic review, Derks and Tomasi reported a prevalence of peri-implantitis of 22% (95% confidence interval, 14% to 30%) (Derks and Tomasi 2015). Untreated peri-implantitis can lead to detrimental effects on osseointegration, ultimately resulting in the so called “biological” implant failure (in opposition to “mechanical” failure), since it is related to biological processes (Quirynen et al. 2002, 2006; Romeo et al. 2004; Klinge et al. 2005)[. The treatment of this pathology is arduous and constitutes an important issue in modern clinical practice. Prevention strategies have therefore become extremely important. Numerous scientific researches are nowadays focused on the development of new methods to prevent bacterial adhesion and implant infection (Harris and Richards 2006).

The coating of dental implants with bioactive molecules is a recent approach to modify pristine titanium biochemical properties and hinder bacterial colonization of implant surface (Beutner et al. 2010). Implant coatings are essentially based on two strategies: drugs or biomolecules are mixed within the bulk of the device and released through diffusion or degradation of the matrix, or they can be grafted to the implant surface (Simchi et al. 2011). With the purpose of preventing implant infection, these strategies have been implemented using different drugs and molecules or constructs to obtain anti-bio-adhesive coatings, antimicrobial coatings (e.g. Vancomycin, Ag, Zn) or coatings (e.g. calcium phosphate, polylactic acid, chitosan) with controlled release of antimicrobial agents (Norowski and Bumgardner 2009).

A natural biomolecule which has shown to possess interesting biological characteristics is silk sericin. Silk produced by the silkworm is composed of two main proteins: the fibroin which forms the internal part and has a structural function, and sericin, a family of rubber-like coating proteins which constitutes 25-30% of the weight of the silk secreted by the *Bombyx mori* worm (Zhang 2002).

Sericin is currently a waste product of the textile silk industry since it is removed from fibroin in a process called “degumming”, to allow fiber acquiring luster, softness, smoothness, whiteness and dyeability. Sericin has been recently revalued due to its properties when in contact with biological materials, making it usable in the pharmacological, cosmetic and biotechnological fields. While some positive biological effects, as for example antioxidant or anti-inflammatory behavior, have been proven, the anti-bacterial efficacy of sericin is still debated and it is described by studies that often provide contrasting results (Aramwit et al. 2012; Gupta et al. 2013; Lamboni et al. 2015).

The aim of this study was to evaluate *in-vitro* the effectiveness of different experimental protocols to obtain a sericin-based coating on medical grade titanium (Ti) able to reduce microbial adhesion and biofilm formation on the dental implant surface.

4.1.2 Materials and Methods

4.1.2.1 Study Design

This *in-vitro* study was composed by two main phases. In the first phase, a multi-step procedure was implemented with the aim to bond covalently the sericin to the Ti disk surface. In this procedure, after a preliminary alkaline etching conditioning of the titanium surface, four different coating strategies were implemented combining two different silanization techniques

and two different bioconjugation processes (Figure 29). With the aim of controlling the process in an incremental way, samples were produced and analyzed after both an intermediate step of preparation and at completion of the coating strategies. Based on the results obtained from micromorphological and compositional analysis, the best performing coating strategy has been identified. Disk produced according to the best protocol were further checked for their ability to inhibit formation of microbial biofilm at their surface in a controlled microbiological experiment with a standard strain recognized for its ability to form biofilm.

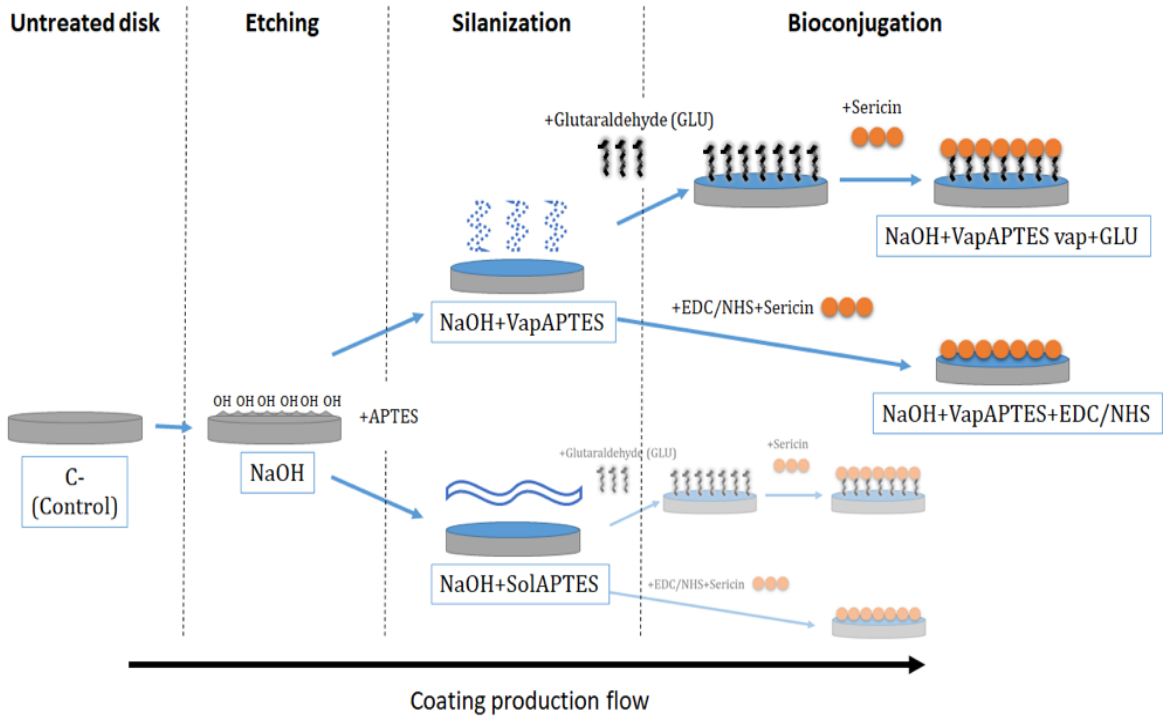

Figure 29. Diagram of the four investigated coating strategies obtained by combining different silanization (VapAPTES or SolAPTES) and bio conjugations (GLU or EDC/NHS) process after a preliminary etching phase (NaOH).

4.1.2.2 Chemicals

Sericin (Pure Sericin™ Seiren Co., Ltd), aminopropyltriethoxysilane, carbodiimide, N-Hydroxy-succinimide, and glutaraldehyde (Sigma Aldrich, St Louise, USA) were analytical grade.

4.1.2.3 Titanium substrate preparation

Titanium 6Al-4V alloy grade 5 disks (CLC scientific, Italy) 10 mm in diameter and 2 mm in thickness were produced by computer numerical control machining and cleaned using the same standards for dental abutments.

The disks were polished with increasing fine-grained abrasive paper up to 4000 grit to remove any possible manufacturing irregularities and undertook three washing steps to remove any

impurity and grinding residues. Washing was realized by sonication for 15 minutes each in three consecutive solutions: acetone, 70% ethanol in double distilled water (ddw) and pure ddw.

4.1.2.4 NaOH etching

The disks were immersed for 24 hours in a 2.5 M solution of sodium hydroxide (NaOH) at 60°C to expose -OH functional groups. NaOH etched disks were then thoroughly washed twice in ddw.

4.1.2.5 Silanization

Silanization with aminopropyltriethoxysilane (APTES) was realized according to two different protocols: i) deposition in organic/aqueous solvent (SolAPTES) and ii) vapor-phase deposition (VapAPTES).

SolAPTES deposition was realized by immersing the etched disks in a solution of water (5% v/v) and APTES (5% v/v) in ethanol at pH 4.5 - 5.5 for 2 hours. The silanized samples were then sonicated in ethanol to remove the excess of physio-absorbed molecules and cured at 110° in air for 30 minutes. VapAPTES was realized by exposing etched disks to a saturated vapor of APTES for 24 hours at room temperature.

4.1.2.6 Bioconjugation

The covalent bond between silane and sericin was obtained by either using glutaraldehyde (GLU) or carbodiimide/N-Hydroxy-succinimide (EDC/NHS).

The GLU bioconjugation strategy was obtained by immersing silanized disks in a solution of glutaraldehyde (2% v/v in ddw) for 24 hours at room temperature. The disks were then washed in ddw and transferred into a solution of sericin (1% w/v in ddw) at 37 ° C for 2 hours.

Bioconjugation using EDC/NHS was realized by immersing silanized disks in a sericin solution (10 mg/ml) in PBS at pH 7.4. EDC and NHS were then added into the solution up to a final concentration of 0.1 M and 0.025M respectively and left for 2 hours at room temperature.

Sericin coated samples were rinsed twice in ddw to remove the unattached sericin protein.

4.1.2.7 Micromorphological and compositional surface characterization

Micromorphology and composition of disks at each intermediate production step and after completion of all different sericin coating strategies reported in Figure 29 were studied by multiple investigation techniques. A XL30 ESEM FEG (FEI-Philips, Eindhoven, the Nederland) scanning electron microscope (SEM) equipped with energy dispersive X-rays spectroscopy (EDXS) (EDAX, Mahwah, NJ) was used to investigate microstructure and elemental composition of the samples surface. Secondary electrons and backscattered electrons images were collected at magnifications ranging from 50 to 20000 times using low energy primary electron beam. Surface topography was measured by Atomic Force Microscopy (AFM, Solver pro, NT-MDT Spectrum Instruments, Moscow, Russia) using a silicon nitride tip (NT-MDT NSG-11B, 10 nm tip radius, 181 kHz resonance frequency), scanning areas 20 µm x 20 µm wide in semi-contact mode. X-ray Photoelectron Spectroscopy (XPS) was also used to have a more quantitative evaluation of the elemental composition at the sample surface.

Samples were investigated by XPS measurements with a Φ 5600ci Perkin-Elmer spectrometer, using a standard aluminium (Al Kα) source, with an energy of 1486.6 eV operating at 200 W. The X-ray source employed was located at 54.7° relative to the analyser axis. The working pressure was < 5·10-8 Pa ~10^{-11} Torr. The calibration was based on the binding energy (B.E.) of the Au4f7/2 line at 83.9 eV with respect to the Fermi level. The standard deviation for the B.E. values was 0.15 eV. The reported B.E. were corrected for the B.E. charging effects, assigning the B.E. value of 284.6 eV to the C1s line of carbon (Craig 1991). Survey scans were obtained in the 0-1350 eV range (pass energy 58.7 eV, 0.5 eV/step, 25 ms/step). Detailed scans (11.75-29.35 eV pass energy, 0.1 eV/step, 50-150 ms/step) were recorded for relevant regions (O1s, C1s, Si2p, N1s, Na1s, Ti2p) depending on the sample. The atomic composition, after a Shirley-type background subtraction, (Shirley 1972) was evaluated using sensitivity factors supplied by Perkin-Elmer (Moulder et al. 1992). Assignment of the peaks was carried out according to literature data and available database (Wagner 1990)].

Comparative data analysis was performed along the production flow to reveal the added value of each incremental step (e.g. C- vs NaOH) and across different process options to identify the most effective treatment (e.g. NaOH+SolAPTES vs NaOH+VapAPTES).

4.1.2.8 Microbiological test

A microbiological test was designed and performed using a bioreactor model to stimulate the sessile adhesion and growth of a biofilm former microbial strain. In order to quantify the surface ability to inhibit the biofilm adhesion and formation (anti-biofilm activity), microbiological tests were conducted in parallel on untreated titanium disk and on disk subjected to intermediate and complete treatment for sericin coating. Namely, the following samples were produced for microbiological testing: untreated controls (C-), NaOH etched disks (NaOH), etched and vapor phase silanized disks (NaOH+VapAPTES), etched silanized and sericin coated disk using glutaraldehyde (NaOH+VapAPTES+GLU), and etched silanized and sericin coated disk using carbodiimide/N-Hydroxysuccinimide (NaOH+VapAPTES+EDC/NHS).

Tests were conducted in triplicate using 24-well polystyrene plates. *Staphylococcus aureus* ATCC 3568 was used as a recognized standards strain able to form thick biofilm. A refrigerated strain stock was thawed and plated on sheep blood agar plate. Colonies obtained after incubation at 36°C for 24h have been used to prepare a bacterial suspension with a final concentration of 10_7 CFU/mL in trypticase soy broth supplemented with 1% dextrose. One disk per each well was positioned using sterile pliers. An aliquot of 1 mL of bacterial suspension was poured over each disk. The plate was covered with lid and incubated for 24 h at 37° C.

At the end of the incubation period, the bacterial suspension was removed using a pipette and the disks were gently washed 3 times adding 1 mL of PBS per each well in order to remove any planktonic or poorly adherent microbial cell from the disk surface. To quantify the adherent biofilm biomass, each disk was then immersed into 1 mL of crystal violet (0.2% in water) for 10 minutes. Disks were then removed from the dye solution, immersed twice in water to remove excess of dye and allowed to dry for about 1h under a fume hood. Dried disks were moved in a new multi-well plate and 1 mL of acetic acid solution (33% in water) was added to each well in order to resuspend the biofilm-related dye. Dye concentration, representative for the biofilm biomass, was quantified spectrophotometrically by quantifying absorbance at 570 nm.

Absorbance data were averaged over triplicate samples and presented as mean and standard error. Relative amount of biofilm biomass was presented as percentages by normalizing data to the absorbance value of the untreated controls. Inhibition efficacy was calculated by using the following formula.

$$Inhibition\ (\%)=100-\ Biofilm\ Biomass\ (\%)$$

Absorbance data obtained from NaOH+VapAPTES+GLU and NaOH+VapAPTES+EDC/NHS disks was compared to untreated control for statistical significance. Student-t test was used with a significance for $p<0.05$.

4.1.3 Results

4.1.3.1 Morphology and surface composition

4.1.3.1.1 NaOH Etching

The untreated sample (Figure 30a), presented a uniform surface to the SEM analysis with minor parallel grooves related to the polishing with carbide sandpaper. Surface composition assessed by EDX (Figure 31a) is typical for an environmentally oxidized titanium Ti6Al4V alloy.

The NaOH treatment induced a clear morphological change at the surface, showing creation of micro and nano-crevices related to the chemical etching of the NaOH solution. The new micro and nano-morphology was diffused and uniform over the whole disk surface. Representative images were obtained by SEM (Figure 30b) and AFM (Figure 32a) respectively. Comparison of compositional analysis before and after NaOH treatment, evidenced a substantial increase in surface oxidation and the appearance of sodium among the minor surface components. Qualitative EDX spectra are reported in Figure 30a and 30b for the untreated and NaOH etched surfaces, evidencing a higher peak for the oxygen and the appearance of a sodium peak in the NaOH sample. Compositional atomic percentages obtained with XPS on NaOH etched surface were 52.5% and 11.7% for O and Na respectively (Table 7), showing a relevant increase, as expected, for sodium and a corresponding increase also of titanium (from 5 to 17.6%), this latter related to the etching of the surface contamination (C% from 58.2% to 16.9%).

4.1.3.1.2 Silanization

Both VapAPTES and SolAPTES silanization processes did not resulted in further changes of the surface morphology as shown in Figure 30c and 30a. Anyhow, a clear increase of silicon was documented. Qualitative spectra obtained at EDX showed the presence of the Si peak. Figure 31c and 31d report qualitative compositional data for disks treated according to NaOH+VapAPTES and NaOH+SolAPTES protocols respectively. Quantitative compositional analysis performed with XPS reported an atomic percentage of Si of 4.4% and 2.9% for samples underwent to silanization by vapor or solvent deposition (Table 7), respectively, therefore showing a more efficient silanization by vapor phase. By XPS, an increase in nitrogen and carbon, both elements present in the APTES molecule, was also detected, therefore demonstrating the anchoring of the APTES molecule. In Figure 33, the surveys corresponding to NaOH+VapAPTES and NaOH+SolAPTES samples are exemplarily superimposed. Based on the compositional data and considering that VapAPTES protocol resulted in a lower risk of

surface contamination and required a lower volume of APTES, silanization via vapor phase deposition was considered for the following bioconjugation procedures in this study.

4.1.3.1.3 Bioconjugation

The two bioconjugation strategies implemented in the study resulted in minor or non-detectable micro-morphological differences at SEM (Figure 30d). However, appreciable nano-morphological changes were visible at AFM images (Figure 32b and 32c). The sharp peaks induced by NaOH treatment were still present after the silanization process (Figure 32a), but appeared smoothed and rounded after sericin bioconjugation, in agreement with the expected deposition of the protein on a globular form. The low electron density of the protein layer did not permit proper SEM imaging. On the contrary, AFM images obtained in semi-contact mode, allowed reliable imaging of soft surface organic structures. Moreover, AFM elicited a uniform morphological pattern on the NaOH+VapAPTES+GLU samples (Figure 32b), while evidencing areas with different morphologies at the surface of the NaOH+VapAPTES+EDC/NHS samples (Figure 32c). Results of the compositional analysis realized by XPS on the bioconjugated surfaces are supportive of sericin deposition (Table 7). The protein bioconjugation resulted in different extent by using GLU or NHS/EDC protocols. NaOH+VapAPTES+GLU samples showed a clear reduction in the atomic percentages for titanium and silicon, and an increase of the amount of nitrogen and carbon (Table 7), suggesting the effective coverage of the titanium surface with the anchored molecules. Being XPS a surface sensitive method, the contribution of only the outermost layers is enhanced. Differently, compositional values for NaOH+VapAPTES+EDC/NHS samples evidenced no major variations in the same elements, in this case instead suggesting that the titanium surface was not effectively derivatized, this outlined also by the relatively low silicon content. In summary, XPS results were in agreement with AFM findings, showing a more effective and uniform protein coating after GLU bioconjugation protocol, but uneven coating after EDC/NHS protocol.

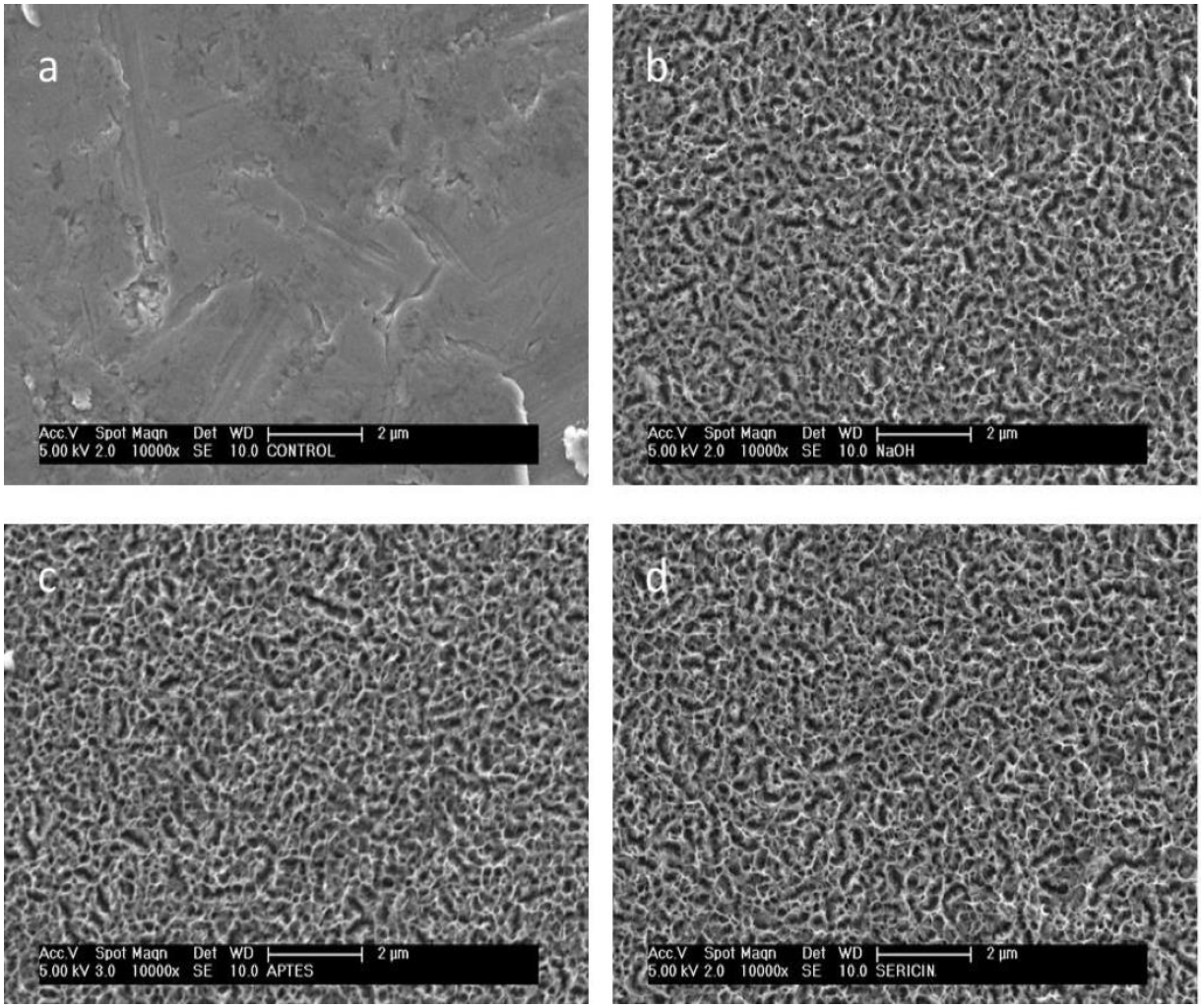

Figure 30. Micromorphology of the disk surface at different production step: a) untreated control, b) after etching (NaOH), c) after etching and silanization (NaOH+VapAPTES), d) after etching, silanization and sericin bioconjugation with glutaraldehyde (NaOH+VapAPTES+GLU). Images c) and d) are representative also for the micromorphology of disks subjected to the alternative silanization (SolAPTES) and bioconjugation (EDC/NHS) processes respectively. Scanning electron microscopy, secondary electrons detector signal, original magnification 10000x.

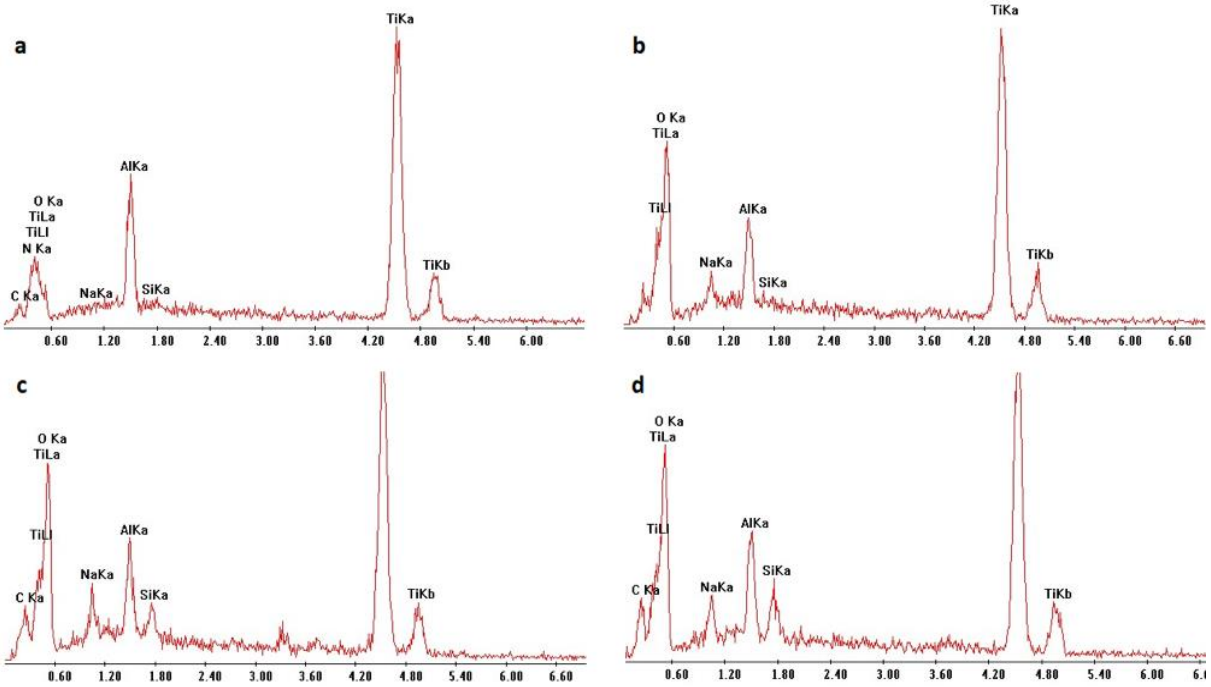

Figure 31. Surface compositional analysis of titanium disks subjected to different surface treatments: a) untreated control, b) after etching (NaOH), c) after etching and silanization by vapour deposition (NaOH+VapAPTES), d) after etching and silanization by solvent deposition (NaOH+SolAPTES). Sodium (Na) and oxygen (O) are introduced by the etching phase and Silicon (Si) by silanization phase. Energy dispersive spectroscopy. Primary electron beam energy was set to 15 KeV. Spectra are collected over an area of 25 μm_2. Integration time 200 s.

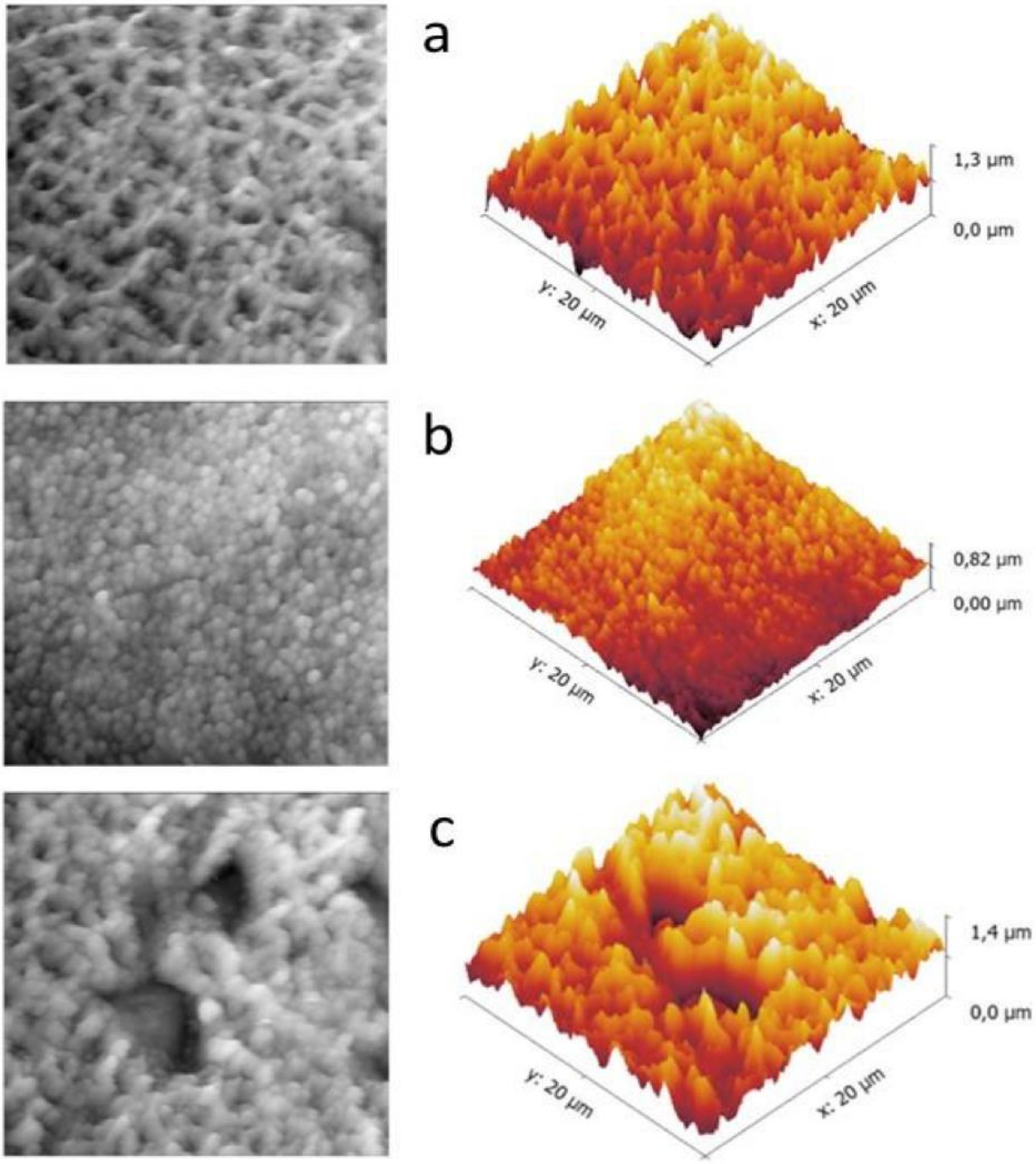

Figure 32. Nano-morphology (2D images on the left and 3D reconstructions on the right) of the disk surface at different production step: a) after etching and silanization (NaOH+VapAPTES), b) after etching, silanization and sericin bioconjugation with glutaraldehyde (NaOH+VapAPTES+GLU), c) after etching, silanization and sericin bioconjugation with EDC/NHS (NaOH+VapAPTES+NDC/NHS). Atomic force microscopy, semi-contact mode.

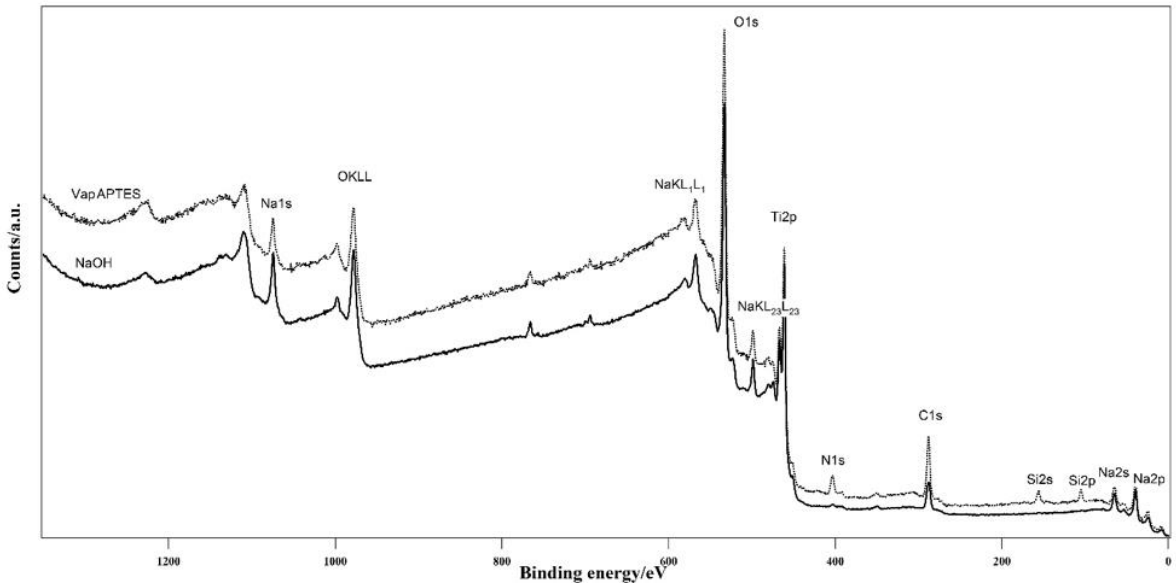

Figure 33. Comparison of the survey spectra of the samples after NaOH etching but before functionalization (NaOH) and after APTES (VapAPTES) functionalization. Successful attachment of APTES is evidenced by the presence of nitrogen and silicon species, which were not present on the bare titanium surface.

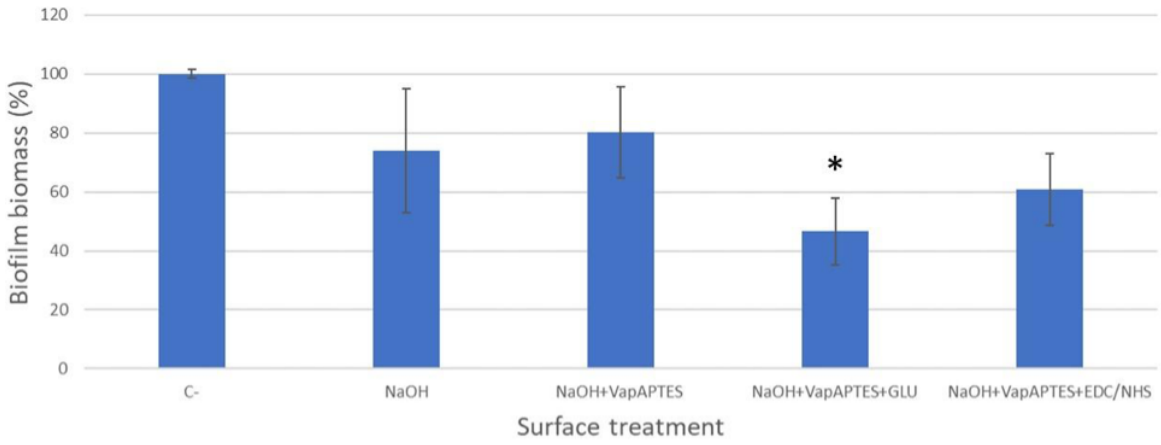

Figure 34. Biofilm biomass (%) of *Staphylococcus aureus* ATCC 6538 formed at 24 h of incubation on the surface of titanium disks subjected to different surface treatments. Data are normalized to untreated controls (C-). *p<0.05.

	C 1s	N 1s	O 1s	Na 1s	Si 2p	S 2p	Ti 2p
C-	58.2		34.1	1.5		1.15	5.0
NaOH	16.9	0.9	52.5	11.7	0.4		17.6
NaOH+VapAPTES	26.1	5.4	49.8		4.4		14.4
NaOH+SolAPTES	22.5	3.5	55.0		2.9		16.1
NaOH+VapAPTES vap+GLU	49.6	8.5	33.8		2.4		5.7
NaOH+VapAPTES vap+EDC/NHS	22.0	5.3	54.7		0.5		17.5

Table 7. Surface atomic percentages on samples at different steps of the production process. Composition was obtained for the most relevant elements identified by XPS.

4.1.3.2 Anti-biofilm activity

The bioreactor model was able to promote the *Staphylococcus aureus* biofilm formation at the disks surface within 24 h of incubation. Absorbance values at 570 nm varied among the different tested samples in the range between 1.11 and 2.38. Mean absorbance values and standard errors over the three replicates are reported in Table 8.

The highest absorbance value was obtained for the untreated disks, confirming the absence of any antibacterial and antibiofilm property of controls. The biofilm biomass percentage of controls was then set to 100% and inhibition values were calculated with respect to controls (Table 8).

Values of the biofilm biomass obtained for all tested samples are reported in Figure 34, for ease of comparison. Although minor variation in the absorbance and biofilm biomass could be related to the NaOH etching and to the silanization process, the lowest values were obtained from the samples subjected to sericin bioconjugation.

Statistical comparison between untreated samples and bioconjugated disks evidenced a statistically significant difference ($P = 0.041$) in the absorbance values of the NaOH+VapAPTES+GLU treated disks, documenting a biofilm inhibition activity of 53% for the process based on the glutaraldehyde bioconjugation of sericin.

	Absorbance @540 nm		Biofilm biomass (% in respect to controls)	Biofilm inhibition (% in respect to controls)
	Mean	S.E.	Mean	Mean
C-	2,38	0,04	100	0
NaOH	1,76	0,50	74	26
NaOH+VapAPTES	1,91	0,37	80	20
NaOH+VapAPTES vap+GLU	1,11	0,27	47	53
NaOH+VapAPTES vap+EDC/NHS	1,45	0,29	61	39

Table 8. Results summary of the microbiological tests. Mean and standard error (S.E.) values of the biofilm absorbance measured in triplicate experiments at different steps of the production process. Estimated biofilm biomass and inhibition percentages are calculated in respect to biofilm amount grown on controls.

4.1.4 Discussion

Numerous techniques have been developed over the years to coat or chemically modify titanium implantable surfaces for dental applications in order to improve the implant response to the oral microbiota. The objective of these interventions, in most cases, is achieved as a secondary effect for having enhanced the osseointegration process (Puleo et al. 2002; Gan and Pilliar 2004; Cai et al. 2006; Vanzillotta et al. 2006; Lindgren et al. 2009). The risk of an early implant infection is indeed reduced by shortening the time for eukaryotic cells adhesion and osseointegration. This approach revealed to be effective for protecting the implant immediately after implantation, but has a comparably lower impact on microbial colonization and infections occurring late after implant placement.

The present work was aimed at coupling a functional biomolecule to the titanium functionalized surface. The coupling agent was a silane (APTES), covalently bonded to the hydroxyl groups of the titanium oxidized surface, previously exposed via chemical etching using NaOH. Eventually sericin was immobilized to the silanes functional groups by using either a cross-linker (glutaraldehyde) or catalyzing a direct covalent bonding with EDC/ NHS. We followed and checked morphological and compositional evolution of the titanium surface at every step by realizing a battery of instrumental characterization techniques such as SEM, EDXS, AFM

and XPS.

In literature the activation of the surface with NaOH is reported to have a double function: allowing to incorporate -OH groups, thus making the surface more hydrophilic, and increasing the micro- and nano-surface roughness (Kim et al. 1996; Wang et al. 2000; Pattanayak et al. 2011; Rodríguez-Contreras et al. 2016). It has been also reported an increase in surface energy and consequently an increased bioactivity (Lindahl et al. 2013). In the present work, we highlighted a micro and nano-morphological modification by SEM and a compositional enrichment in oxygen by XPS and EDXS that is consistent with the expected increase of hydroxyl groups. The presence of adventitious carbon at this stage was considered a natural contaminant in the XPS analysis and is commonly used for the calibration of the instrument (Robinson and Sherwood 1984). Differently, sodium was an unexpected element found by both EDX and XPS on the titanium surface after the NaOH etching. Although the sodium concentration could be probably reduced by extending or improving the washing procedure after the NaOH treatment, remnants did not appear to have interfered with the silanization reactions and bioconjugation.

Silanization is the most used and consolidated method for immobilizing biological molecules on model inorganic surfaces (Chan et al. 2011). In this study, APTES was linked to the activated titanium surfaces using two strategies: deposition in organic-aqueous solvent and vapor deposition. The effectiveness of both techniques was documented by the increase of silicon using both XPS (Table 7) and EDXS (Figure 31). It should be outlined that, whereas XPS is surface sensitive and its sampling depth is limited to the first few nanometers, EXDS instead probes a sampling depth which is much higher, reaching the micrometer range. This treatment did not introduce substantial micro-morphological modification according to the SEM and AFM investigations. The microstructure induced by the NaOH etching was still present after both the silanization tested strategies.

The mere physical adsorption of proteins at the titanium surface is not suitable for use in the oral environment because fluids that are present at the peri-implant region can easily remove the protein by spreading it away from the implant site, especially in the case of a water-soluble protein such as sericin. Furthermore, it has been found that physical adsorption can lead to a conformational change of the protein denaturing it and altering its properties (Darst et al. 1988; Lee and Belfort 1989; Cheng et al. 1994; Bekos et al. 1995; Puleo 1995, 1996). On the other end, the covalent bond represents a valuable option for a stable and long-lasting attachment, with promising properties towards early and late implant microbial complications.

In order to covalently immobilize biological material on substrates bearing functional groups, coupling with terminal amino groups has been frequently used. The use of glutaraldehyde as a coupling agent provides satisfactory results for immunocytochemistry or in situ hybridization and for the maintenance of biological activity of a given molecule *in-vitro* (Werb et al. 1990; Larsson et al. 1994; Puleo 1995, 1996). Other studies have shown that the combined use of silanization and glutaraldehyde are effective techniques to immobilize immunoglobulins on glass (Ahluwalia et al. 1992). In this study, the use of glutaraldehyde appeared to be effective in binding the protein to the silane. The increase in carbon and the decrease in titanium at XPS after the bioconjugation with glutaraldehyde confirm this hypothesis and the AFM analysis shows uniformly distributed globular aggregates on the surface.

The other bioconjugation technique used here was based on crosslinking via carbodiimides.

The reaction mediated by EDC converts the carboxyl group into an intermediate of O-acylisourea which readily reacts with the amino group, resulting in covalent amide bond between the biomolecules and the surface (Tack et al. 2015). The effectiveness of protein conjugation was investigated by XPS analysis and showed the achievement of a less effective protein coating with a lower masking action of the underlying titanium substrate. This was further confirmed by AFM recognition of an irregularly patterned surface, including areas without the sericin aggregate at the surface. The AFM analysis also shows jagged peaks and large depressions that make the surface much less uniform than the bioconjugate samples with glutaraldehyde by suggesting the exposure of the Ti surface in some areas. In summary, these results evidenced that titanium samples in this study were more effectively coated by sericin using the NaOH+VapAPTES+GLU protocol and by using the vapor-based approach. Microbiological test provides further evidence of the higher effectiveness of this coating protocol for obtaining an antibiofilm surface.

In the literature, the anti-microbial and antibiofilm efficacy of sericin, is reported with contrasting results. Nuchadomrong et al. evaluated the influence of different degumming methods on the anti-bacterial capacity of the *Samia ricini* sericin comparing it with the *Bombix mori* sericin. *Escherichia coli*, *Salmonella choleraesuis* and *Bacillus subtilis* strains were found to be susceptible, at certain concentrations, to both sericins, while only the *S. ricini* sericin showed an inhibitory effect on *S. aureus* (Takechi et al. 2014). Other studies reported an anti-bacterial effect of *S. ricini* (Panthong et al. 2015) and *B. mori* sericin (Pandiarajan et al. 2011; Khalifa et al. 2012; Rajendran et al. 2012).

Nevertheless, Seves et al. observed that the raw silk buried in the ground has a bacterial growth greater than the degummed one, supposing that this result was due to the presence of sericin that is used by the bacteria for their growth (Seves et al. 1998). Similarly, Akiyama et al. they found the growth of gram-positive bacteria on the silk thread used for stitching mouse skin (Akiyama et al. 1993). Kaur et al. conducted *in-vitro* studies using gram-negative *E. coli* bacteria in order to determine if some components of the cocoon resist the colonization of microorganisms. Their results demonstrate that no component of the cocoon (including sericin) hinders the growth of such bacteria suggesting that the previously reported anti-bacterial properties are actually derived from chemicals used to separate or purify the elements of the cocoon (Kaur et al. 2014).

Considering such contrasting results reported in the literature and that characteristics other than antibacterial effect could be responsible for an antibiofilm property, it was decided to design and carry on a specific test to explore the anti-biofilm properties of the pure sericin coating. The realized biofilm model allowed the development of *S. aureus* (ATCC 6538) microbial biofilms at the surface of titanium disks and allowed to put on evidence differences between sericin-coated and untreated surfaces.

Titanium discs coated with glutaraldehyde-bound sericin resulted in a significant biofilm inhibition of approximately 53% compared to the untreated titanium. Samples obtained by bioconjugating sericin via EDC/NHS showed a lower inhibition possibly due to the inhomogeneous and incomplete surface coating.

Further experiments must be carried out in order to support the data so far produced and to better understand the most critical points of the coating protocol that can reduce the anti-biofilm effectiveness.

4.1.5 Conclusions

Both aqueous-organic solvent and vapor phase treatments were found effective for the surface silanization. Information provided by compositional and morphological analysis suggest that the use of glutaraldehyde can be more effective in forming a uniform protein coating on Ti-6Al-4V, while the use of EDC-NHS did not produce satisfactory results in terms of uniform protein coating.

The coating with glutaraldehyde-bound sericin after silanization in the vapor phase showed promising bacterial inhibition values with a significant reduction of *S. aureus* biofilm. Further studies including a higher number of replicates and a range of peri-implant relevant microorganisms are needed to evaluate the applicability and exploitability of this experimental protocol during dental implants production.

4.1 Acknowledgments

Dr. Stefano Diodati (DiSC, University of Padova) is gratefully acknowledged for his support in determination of XPS quantitative analysis. Titanium disks used in the study were kindly provided by CLC scientific, Padova, Italy.

The work was supported by SIdP (Italian Society of Periodontology and Implantology) and it is part of the IRCS-HTA special project, funded in part by the Autonomous Province of Trento.

5. Strong microbial and functional signatures characterize mucositis and peri-implantitis

Rationale

Investigations of the oral microorganisms with crucial roles in oral diseases are being performed since decades, but the recent revolution in technologies for “reading” the DNA material revolutionized the field. By directly sequencing the genetic material present in an oral sample (e.g. from a swab of the supragingival or subgingival plaque) it is possible to study the ecosystem of bacterial, viral, micro-eukaryotic, and archaeal organisms - the microbiome - present in the dental environment. Such techniques, called metagenomics, have the crucial advantage that they avoid completely the cultivation step which is very time consuming and can target only a small fraction of microbes with known cultivation protocols (Segata et al. 2013; Quince et al. 2017). This led to the recent definition of the current map of the microbiome in healthy individuals (Segata et al. 2012b) within the largest metagenomic sequencing effort performed so far (the Human Microbiome Project) (Consortium and The Human Microbiome Project Consortium 2012).

Despite the precise etiology of peri-implant diseases remains still not completely known, it is well established that mucositis and peri-implantitis are microbial biofilm-induced ((Takanashi et al. 2004; Tabanella et al. 2009; Rakic et al. 2016; Lafaurie et al. 2017; Teles 2017)). To date, however, at the best of our knowledge, no high resolution microbiome investigations have been performed in connection with peri-implant diseases, leaving thus unaddressed crucial aspects such as whether the microbial risk factors for peri-implantitis are similar to those of periodontitis (Takanashi et al. 2004; Tabanella et al. 2009; Rakic et al. 2016; Lafaurie et al. 2017; Teles 2017). Based on the lessons learned from microbiology and microbial epidemiology applied on microbial-associated human diseases, also in mucositis and peri-implantitis crucial microbial features associated with disease could be strongly strain-dependent. In other words, the potential pathogenicity of some species could depend on the specific variant (strain) of the organism of that species present in the subject. Moreover, it is now unclear which are the most relevant microbial organisms from which the implant material should try to be protective; such knowledge may allow the development of specific materials that are most effective against the most harmful bacterial organisms.

In this chapter, I present an *in-vitro* study conducted in the Laboratory of Computational Metagenomics of University of Trento in which we investigated the plaque microbiome associated with peri-implant diseases to identify specific microbial organisms, genes, and virulence factors associated with these conditions. Our study design included peri-implantitis patients as well as healthy patients and patients with mucositis. The contralateral tooth with respect to the implant one was also sampled to adjust for the high inter-subject variability. In this project we applied high-resolution shotgun metagenomics to analyze the plaque microbiome at the level of single strains. This shotgun metagenomic sequencing approach coupled with the novel computational methods developed in the lab had never been used to study peri-implant diseases and has allowed us to identify robust biomarkers for diseases and new potential therapeutic targets. Our work also set-up the path toward a personalized medicine approach at oral diseases and peri-implant diseases specifically.

My contribution

My contribution to the scientific work included in this chapter was as main investigator. I contributed collecting the grants to support the research, I designed the study, I performed a pilot study to test materials and methods, I recruited, trained and monitored the study centers. I personally performed several laboratory procedures and then I worked on writing the article by interpreting the data coming from the computational analysis. The work was supervised by Nicola Segata and Paolo Manghi performed part of the computational analysis.

Ghensi P*, Manghi P*, Zolfo M, Armanini F, Pasolli E, Bertelle A, Dell'Acqua F, Dellasega E, Waldner R, Soldini C, Tessarolo F, Tomasi C, Segata N

Microbial complexes in mucositis and peri-implantitis are strongly associated with disease status as seen through strain-resolution metagenomics of the submucosal oral plaque

Under submission

5.1 Microbial complexes in mucositis and peri-implantitis are strongly associated with disease status as seen through strain-resolution metagenomics of the submucosal oral plaque

Ghensi P*, Manghi P*, Zolfo M, Armanini F, Pasolli E, Bertelle A, Dell'Acqua F, Dellasega E, Waldner R, Soldini C, Tessarolo F, Tomasi C, Segata N

Microbial complexes in mucositis and peri-implantitis are strongly associated with disease status as seen through strain-resolution metagenomics of the submucosal oral plaque

Under submission

Abstract

Dental implants are commonly installed in the oral cavity of an increasing number of patients worldwide. Mucositis and peri-implantitis are common diseases affecting the tissues that surround the implant and are a major medical and socioeconomic burden. Although microbial colonization is required for the onset of peri-implant diseases, the precise composition of the microbiome associated with them remains largely unknown. We thus performed a metagenomic investigation of the plaque associated with peri-implant health, mucositis and peri-implantitis in a cohort of 72 patients. By sequencing main and contralateral sites (n=113), we found dramatic differences between healthy and diseased implants, with a newly defined Peri-implant Red Complex (PiRC) composed by the 7 most discriminative species that are on average 3.6 times enriched in peri-implantitis. The peri-implantitis microbiome is more conserved across individuals than the healthy microbiome, and it is strongly site-specific with contralateral healthy sites showing no microbial evidence of disease. Mucositis has an intermediate microbiome composition and it is characterized by high abundances of *Fusobacterium nucleatum* which appears to be a first step toward peri-implantitis development. Microbiome-based classifiers showed very high diagnostic power for peri-implant diseases especially when considering also clinical parameters such as peri-implant probing depth and the mucositis-associated microbiome further showed prognostic potential. Strain-level investigation of *F. nucleatum* identified the *F. nucleatum* subspecies nucleatum and another newly discovered subspecies to be the only ones associated with disease within the species. Altogether, we provide evidence of a very strong association between the plaque microbiome and peri-implant diseases and microbes such as those in the PiRC set can potentially be targeted for diagnostic, prognostic and therapeutic strategies.

5.1.1 Introduction

Since the late 70s, the use of dental implants to replace missing teeth has become an increasingly common clinical practice and continuous technological innovations have now made implant therapy more reliable and accessible to the population (Quirynen et al. 2014; Darcey and Eldridge 2016; Buser et al. 2017; Block 2018). Approximately 12 million implants are placed every year worldwide (Albrektsson et al. 2014; Khalil and Hultin 2019) but the past

3 decades have seen the emergence of two new oral diseases: peri-implantitis which affects both the soft and hard tissues surrounding the implant, and mucositis which precedes peri-implantitis and involves instead only the soft tissues (Heitz-Mayfield 2008; Lindhe et al. 2008; Zitzmann and Berglundh 2008; Ramanauskaite et al. 2018; Renvert et al. 2018). Mucositis affects more than 50% of the implants, while almost 20% of implants consequently develop peri-implantitis (Derks and Tomasi 2015; Derks et al. 2016; Berglundh et al. 2018; Heitz-Mayfield and Salvi 2018; Schwarz et al. 2018). A fifth of all inserted dental implants are thus suffering from a disease, leading in most cases to implant loosening or to the need for implant removal (Greenstein and Cavallaro 2014; Sinjab et al. 2018) with very large clinical and socio-economical costs and serious impairment of patients' quality of life (Mombelli and Cionca 2013; Abrahamsson et al. 2017; Insua et al. 2017; Kane et al. 2018).

It is now established that the onset and progression of peri-implant diseases is connected with the microbial population of the plaque (Berglundh et al. 2018; Heitz-Mayfield and Salvi 2018; Schwarz et al. 2018), in principle similarly to what has been shown for gingivitis and periodontitis (Belibasakis 2014; Belibasakis et al. 2015; Robitaille et al. 2016). However, despite many years of research on periodontal pathogens the recent emergence of peri-implantitis prevented comparably similar efforts in the past. Although some known periodontal pathogens may also be associated with the etiology of peri-implant diseases, different microorganisms are likely to be involved in these two clinically distinct conditions (Charalampakis and Belibasakis 2015; Faveri et al. 2015; Rakic et al. 2016; Lafaurie et al. 2017; Teles 2017). A thorough profiling of the microbiome associated with peri-implant diseases is thus the first step to undertake toward the development of novel diagnostic, preventive and therapeutic approaches.

Currently available studies investigating the link between the plaque microbiome and peri-implantitis have, however, important limitations. First, they all rely on the 16S rRNA sequencing approach (Hamady and Knight 2009) to profile the plaque microbiome (Koyanagi et al. 2010, 2013; Faveri et al. 2011, 2015; Heuer et al. 2012; Kumar et al. 2012a; Dabdoub et al. 2013b; Tamura et al. 2013; Maruyama et al. 2014; Schaumann et al. 2014; Albertini and López-Cerero 2015; Jakobi et al. 2015; Li et al. 2015; Tsigarida et al. 2015a; Zheng et al. 2015; Belibasakis et al. 2016; Shiba et al. 2016; Yu et al. 2016, 2019; Apatzidou et al. 2017; Sanz-Martin et al. 2017; Schincaglia et al. 2017; Sousa et al. 2017; Al-Ahmad et al. 2018; Belkacemi et al. 2018; Kröger et al. 2018; Pimentel et al. 2018). In contrast to the more powerful shotgun metagenomic approach (Tyson et al. 2004; Venter et al. 2004; Quince et al. 2017), this cost-effective technique cannot identify most microbes at the species level and cannot profile the overall functional potential of the microbial community as they target the ribosomal 16S gene only. Second, the variability of the oral human microbiome (Segata et al. 2012a; Donati et al. 2016) requires large sample sizes and intra-subject microbiome controls (i.e. contralateral sites) that are not considered in the vast majority of the available studies (Yu et al. 2019; Al-Ahmad et al. 2018; Apatzidou et al. 2017; Schincaglia et al. 2017; Yu et al. 2016; Dabdoub et al. 2013; Albertini et al. 2015; Belkacemi et al. 2018; Jakobi et al. 2015). A recent exception is a study sampling multiple implants from the same individual but on a small cohort (n = 18) of also periodontal patients (Yu et al. 2019). Third, mucositis and peri-implantitis are very related diseases that should be considered together, but the only two works in which both conditions were sampled focused specifically on the role of smoking on the plaque microbiome (Tsigarida et al. 2015b) or had a very small sample size not including intra-subject microbiome controls

(Zheng et al. 2015). There is thus the need of a high-resolution metagenomic investigation of a large cohort including both mucositis and peri-implantitis and controlling for inter-subject variability.

In this work, we investigated the plaque microbiome associated with peri-implantitis and mucositis in a cohort of 72 patients by sequencing a total of 113 metagenomes to identify specific microbial organisms features associated with peri-implant diseases. Our study design included, as controls, both healthy implants and teeth that were sampled both from healthy sites from healthy individuals and from the contralateral healthy site with respect to the mucositis or peri-implantitis sites. The analysis included not only the investigation of the quantitative taxonomic composition of the plaque microbiome, but advanced computational methods allowed us to explore the functional potential of the microbiome and to study some members of the microbial communities at the resolution of single strains.

5.1.2 Results and Discussion

In order to study the role of the oral microbiome in peri-implant diseases (mucositis and peri-implantitis), we performed shotgun metagenomic sequencing (Quince et al. 2017) of the plaque microbiome of 113 samples from individuals with dental implants. We profiled subjects with only healthy implants (H group, n= 35), at least an implant with mucositis (M group, n= 37) and at least an implant with peri-implantitis (P group, n=41) (Table 14). Submucosal and subgingival plaque samples were collected with sterile Gracey curettes at the time of diagnosis by expert periodontists in six Italian dental private practices following the same standardized and validated protocol. For each patient, two distinct sites were sampled: the implant in one of the three conditions and the healthy contralateral implant. The contralateral tooth was sampled only when a contralateral implant was not available (Suppl. Table S1-S2). The inclusion of subjects in one of the three study groups was based on radiographic evaluation of the marginal bone level around the implant, inflammation status (bleeding on probing), and presence of pus (suppuration) according to the current validated clinical criteria at the time when the study was designed (Consensus Report on Peri-implant Diseases, Lindhe et al. 2008, see Methods).

Study groups significantly differed between each other for the main known clinical parameters of disease, namely peri-implant probing depth (PPD), bleeding on probing (BOP), suppuration (SUP), and peri-implant bone loss (see Methods). The three clinical conditions were not confounded by other factors as no biases for demographic, anamnestic, clinical and implant-related characteristics were identified (see Table 14 and Suppl. Table S1-2). Shotgun metagenomics produced a total of 113 quality-controlled samples for a total of ~111*10^9 Gbases (Suppl. Table S3)

	Healthy	Mucositis	Peri-implantitis	p-value
N. of subjects	24	24	24	-
Age (mean (range))	62 (45-77)	63 (43-86)	62 (42-78)	0.83
Gender (M/F)	14/10	10/14	14/10	0.41
History of periodontitis (Y/N)	5/19	11/13	11/13	0.12
Smoking (Y/N)	2/22	7/17	7/17	0.13
Diabetes (n cases)	1	0	2	0.16
N. of implants (mean (SD))	3.6 (2.5)	3.8 (2.2)	4.1 (3.0)	0.82

Table 14. Demographic, anamnestic and clinical characteristics of the sampled population

5.1.2.1 A strong microbiome signature in peri-implantitis sites

Analysis of the quantitative taxonomic composition of the plaque microbiome obtained using a MetaPhlAn2-based metagenomic pipeline (see Methods), highlighted a clear distinction between the plaque from sites with peri-implantitis and from healthy implants in healthy individuals (Figure 52a, Permanova p-value < 0.001). The overall functional potential of the microbial communities of the plaque assessed using HUMAnN2 (see Methods) was also clearly distinctive for the two conditions (Permanova p-value < 0.001) at the level of abundance of single gene families (Figure 52b) as well as whole microbial pathways (Suppl. Figure 5a). The two conditions showed distinct alpha diversity profiles of the biofilm, with the richness of species, genes, and pathways substantially reduced in peri-implantitis compared to controls (Figure 52c-d, Suppl. Figure 1b), although inter-subject variability of alpha-diversity prevents strong statistical support (Wilcoxon sign-rank p-value = 0.064 and 0.056 for species and gene family richness, respectively). This trend points at a plaque microbiome in peri-implantitis composed by fewer dominant species that are encoding a smaller number of functions. The healthy plaque was not only richer, but also more variable among individuals (Figure 52f-g) while diseased implants were characterized by microbiome structures converging toward a more well-defined composition (Wilcoxon sign-rank p-value = 9.07e-26, p-value = 2.25e-11 on beta-diversity groups when considering taxonomic and functional potential profiles, respectively). At the whole microbiome level, peri-implantitis is thus associated with a relatively low diversity microbiome with a well-defined set of and inter-patient conserved set of bacterial taxa.

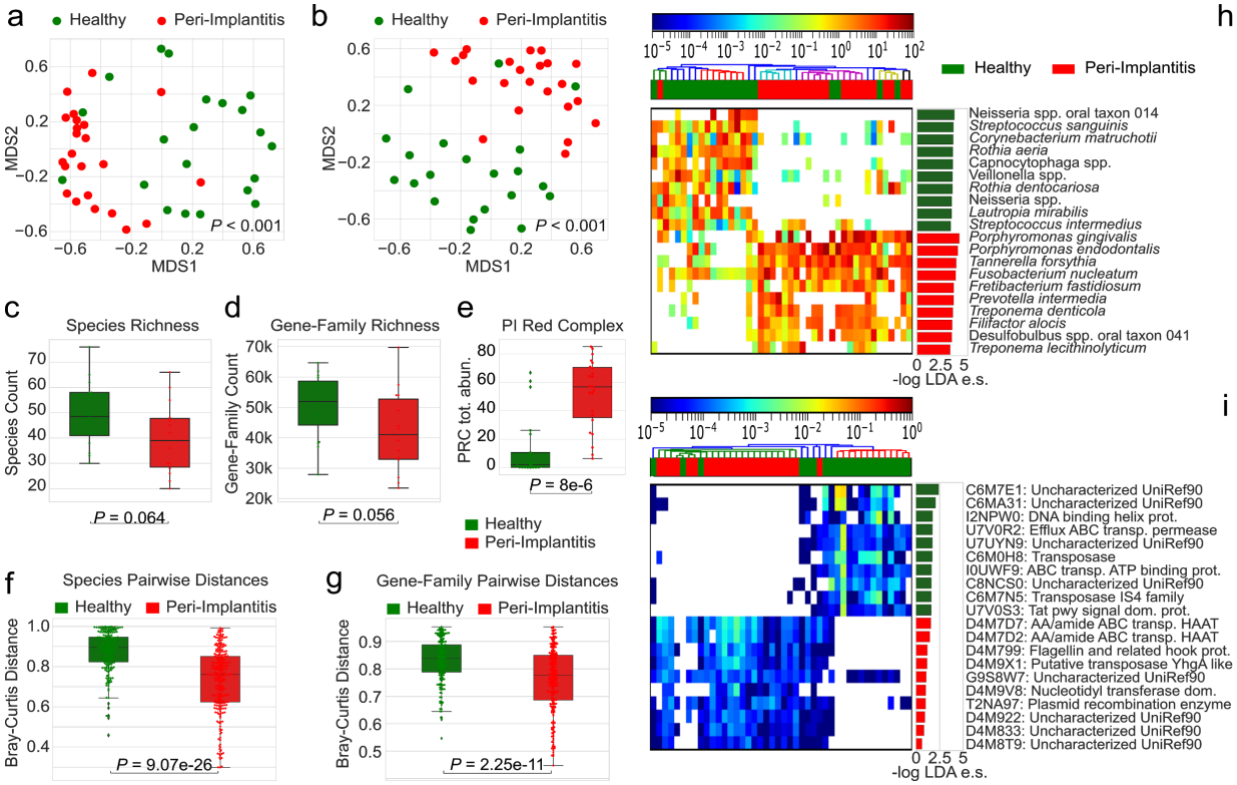

Figure 52. The plaque microbiome strongly differs in healthy and peri-implantitis sites. a) Multidimensional scaling (MDS) ordination plot of healthy and peri-implantitis sites based on the Bray-Curtis distance between microbiome samples highlights a strong condition-specific clustering. P-values were obtained by Permanova. b) Ordination plot (MDS) of healthy and peri-implantitis metagenomic samples based on the abundance of microbial UniProt90 gene families. P-values were obtained by Permanova. c) Alpha diversity distributions computed after rarefaction to the same sequencing depth and estimated as the richness of species and d) as richness of UniProt90 gene families show a trend of decreased diversity in peri-implantitis sites. P-values were obtained by the two-tailed Wilcoxon signed-rank test. e) Distribution of PiRC index values (the total abundance species in the Peri-implantitis Red Complex) in healthy and peri-implantitis samples. P-value was obtained by the two-tailed Wilcoxon signed-rank test. f) Intra-condition beta-diversity (Bray-Curtis dissimilarity) for microbial species and g) gene families points at a converging microbiome structure in diseased peri-implantitis sites. P-values were obtained by two-tailed Wilcoxon signed-rank test. h) Relative abundances (log scale) and effect sizes (LDA score from LEfSe) of the 10 microbial species and i) gene families most strongly associated with either the healthy sites or the sites with peri-implantitis (top 10 species/gene families effect sizes per class).

The taxonomic composition of the peri-implant microbiome was characterized by 71 species that were differentially abundant (Wilcoxon test p-value < 0.05) between the disease and healthy state, with 54 of them passing multiple hypothesis testing correction (FDR q < 0.1, Suppl. Table S4-5). Among them, 12 species were enriched in peri-implantitis and accordingly had very high prevalence in diseased sites with 10 of these 12 species at >73% prevalence in

peri-implantitis ranging from the 100% of *Tannerella forsythia* to 52% of *Treponema lecithinolyticum*. The same species had lower but nonetheless not negligible prevalence in the control sites with *Tannerella forsythia*, *Treponema socranskii* e *Fusobacterium nucleatum* exceeding 50% prevalence in healthy conditions (Suppl. Table S4). The highest effect size was detected for *Porphyromonas gingivalis* and *Porphyromonas endodontalis* (Figure 52h), but all the 12 peri-implantitis-associated species are substantially more abundant in the disease compared to the healthy state with mean enrichments above 10X for *Treponema maltophilum*, *Fretibacterium fastidiosum*, *Pseudoramibacter alactolyticus*, and *Treponema lecithinolyticum*. Conversely, 16 species significantly associated with the healthy implants and with >40% prevalence in controls were never detected in the peri-implantitis group, suggesting that several different taxa including multiple *Capnocytophaga* (*C. gingivalis*, *C. granulosa*, *C. ochracea*) and *Selenomonas* (*S. noxia*, *S. artemidis*) species characterize the complex and diverse healthy plaque. Most healthy-associated species belonged to the genera *Actinomyces* (7 species), *Capnocytophaga* (4 species), *Neisseria* (4 species), *Rothia* (3 species) and *Streptococcus* (5 species) that have no species associated with peri-implantitis. The different taxonomic composition in the two disease states were reflected at the level of the functional repertoire of the species with many gene families differentially abundant and very clearly differentiating the two conditions (Figure 52i, Suppl. Table S6). Overall, statistical significant biomarkers (Figure 52h-i, Suppl. Figure 1d) of either peri-implantitis or healthy implants constituted a large fraction of the plaque microbiome (average 63.6% s.d. 23.9% relative abundance when considering the 54 FDR-corrected species), indicating profound differences in bacterial populations associated with peri-implantitis and healthy conditions.

5.1.2.2 The “Peri-implantitis Red Complex (PiRC)” comprises the 7 most disease-associated species

The set of species that are most associated with peri-implantitis is partially overlapping with the sets (“complexes”) of bacteria originally linked by the group of Socransky to periodontitis (Socransky et al. 1998a). Considering the 10 most peri-implantitis-associated species according to LEfSe (Figure 52h), the three species in the Socransky’s Red Complex are ranked first (*Porphyromonas gingivalis*), third (*Tannerella forsythia*) and seventh (*Treponema denticola*) based on their effect size. This highlighted that *Porphyromonas endodontalis* (second in the ranking) and *Fretibacterium fastidiosum* (fifth) should be considered in the same class of key species. The other three bacteria in the 10 most peri-implantitis-associated species (*Filifactor alocis*, *Desulfobulbus* spp. oral taxon 041, and *Treponema lecithinolyticum*) are also newly associated with the disease but because they show a smaller effect size compared to the bacteria in the Socransky’s Red Complex we considered them comparatively less discriminative. We thus suggest to define the “Peri-implantitis Red Complex” (PiRC) of species strongly characterizing peri-implantitis sites as the set of microbes composed by the three bacteria in the Socransky’s Red Complex, by the two newly associated *P. endodontalis* and *F. fastidiosum* species, and by the *Prevotella intermedia* and *Fusobacterium nucleatum* species that are both part of the Socransky’s Orange Complex and found associated with peri-implantitis at higher effect size than Treponema denticola, the third bacterium in the Socransky’s “Red Complex”. The PiRC index defined as the cumulative abundance of the species in the PiRC complex is highly discriminative for the two conditions (Figure 52e) and may be a relevant single-value index for clinical evaluation of the peri-implant microbiome.

5.1.2.3 The peri-implantitis microbiome signature is site specific

Peri-implantitis may affect independently different dental implants inside the same oral cavity, but whether the associated microbiome is also site-specific is currently unclear and debated (Kumar et al. 2012b; Dabdoub et al. 2013; Schaumann et al. 2014; Padial-Molina et al. 2016; Zhuang et al. 2016; Pokrowiecki et al. 2017; Stokman et al. 2017; Monje et al. 2019). We thus considered samples from healthy contralateral implants (n=10) and teeth (n=22) in the same volunteers that were sampled from healthy and diseased implants (Figure 53a). Contralateral implants and teeth were considered together because we observed no significant difference in the microbiome associated with main healthy sites and contralateral healthy implants both taxonomically and functionally (Suppl. Figure 3 a, b,c, p-value = 0.637). We found that the microbiome samples of contralateral healthy sites cluster together with the healthy samples regardless of the disease status of the main sites. Indeed, while as expected healthy main sites and their healthy contralateral sites in subjects without peri-implantitis do not have different microbiomes (Permanova p-value = 0.58, no differential species after FDR correction), the healthy contralateral sites of main peri-implantitis sites do not differ from main healthy sites in volunteers without peri-implantitis (Permanova p-value = 0.55 with no differential species after FDR correction) nor from the healthy contralateral sites of healthy sites (Permanova p-value = 0.53, no FDR-corrected differential species). Peri-implant sites have instead clearly distinct microbiomes from their healthy contralateral sites (Permanova p-value < 0.001, 7 FDR-corrected differential species), from main sites of healthy subjects (Permanova p-value < 0.001, 11 FDR-corrected differential species), and from contralateral sites of healthy subjects (Permanova p-value = 0.001, 6 FDR-corrected differential species). These findings were confirmed by the analysis of the functional potential of the microbiome (Figure 53b and Suppl. Figure 2a). The peri-implantitis microbiome is thus strongly site-specific as the microbial composition of the plaque of healthy implants is generally consistent regardless of the presence of peri-implant sites in the same individuals.

Site-specificity of the peri-implantitis microbiome is further confirmed by beta-diversity analysis (Figure 53c). The Bray-Curtis microbiome distances between main and contralateral sites were significantly lower when both sides are healthy reflecting the peri-implantitis shift in microbiome composition. This holds true also when considering the abundance of gene families (Figure 53d) and whole microbial pathways (Suppl. Figure 2b). Inter-subject taxonomic and functional microbiome distances (Figure 53c-d) also confirm that peri-implantitis associated microbiomes tend to converge toward a specific configuration whereas the subgingival microbiome of healthy sites is more diverse and different between subjects. It is also of note that for healthy sites (main or contralateral), the plaque microbiome of implants and teeth is not distinguishable (Suppl. Figure 3a-b-c) which is further reinforcing the site-specificity of the detected peri-implantitis microbiome signature.

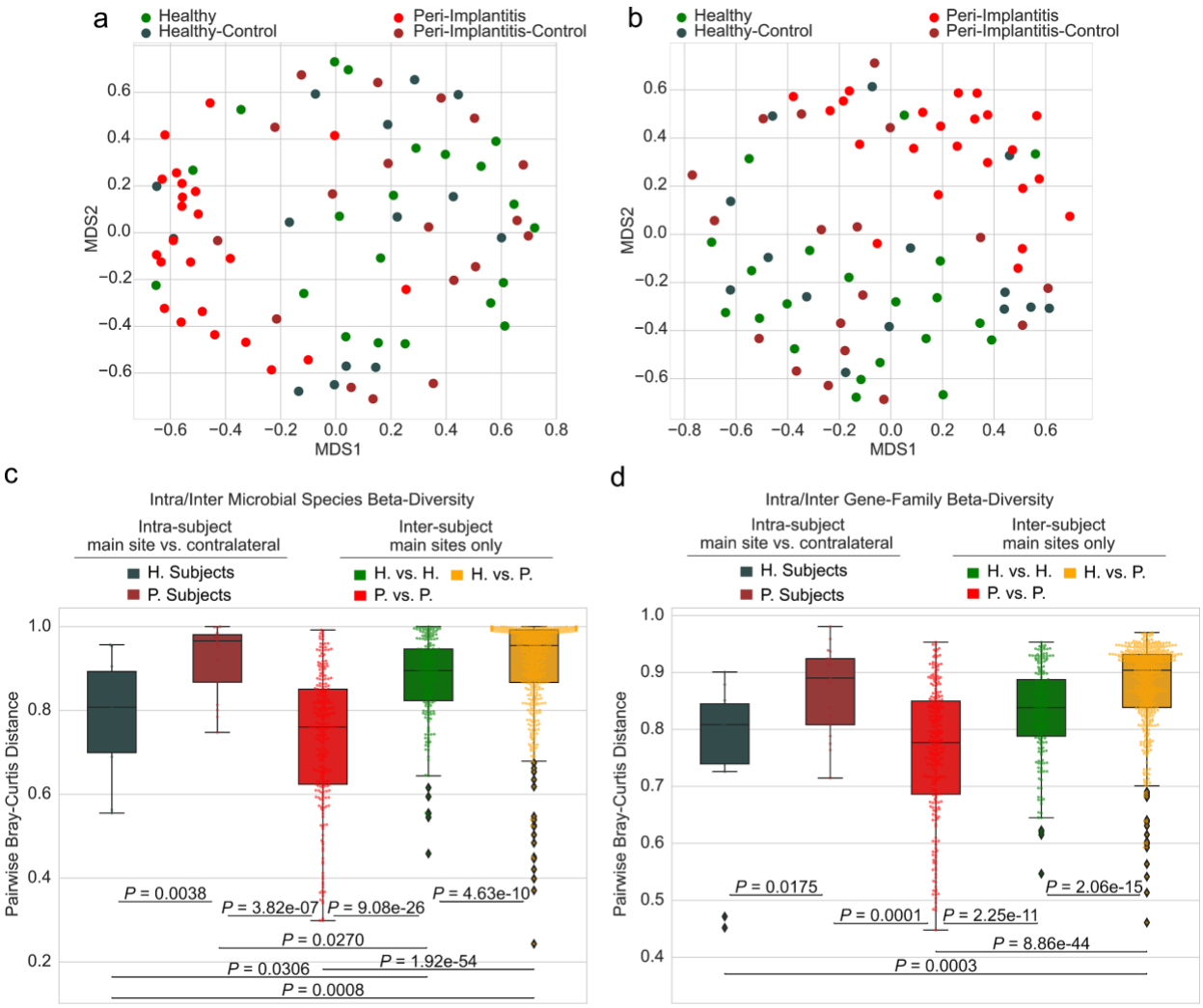

Figure 53. The microbiome in peri-implantitis patients is site specific and peri-implantitis sites are microbially consistent across individuals. a) Ordination plot (MDS) of peri-implantitis and healthy metagenomic samples (main and contralateral) based on the Bray-Curtis distances highlights the clustering of healthy contralateral samples in peri-implantitis with the samples from healthy individuals. b) Ordination analysis as per panel (a) obtained using microbial gene-family abundances instead of taxonomic profiles. c) Beta-diversities estimated with the Bray-Curtis dissimilarity metric for intra- and inter-condition comparisons in the diseased and healthy conditions estimated using as the taxonomic microbial composition and the d) functional microbial gene families composition. P-values were obtained by two-tailed Wilcoxon signed-rank test and reported if considered significant (<0.05).

5.1.2.4 Fusobacterium nucleatum as a key species in the intermediate microbial signature of mucositis

Mucositis is an inflammatory intermediate condition that is a prerequisite for peri-implantitis (Berglundh et al. 2018; Heitz-Mayfield and Salvi 2018b; Renvert et al. 2018). To characterize its associated microbiome, we sampled the plaque of 20 mucositis-affected implants (and their

non-diseased contralateral sites) and assessed its structure as compared to healthy individuals and peri-implantitis patients. Quantitative microbiome profiles (Suppl. Figure S4d-e, S5) highlighted how the mucositis-associated microbiome is not clearly distinct from the plaque microbiome from sites with peri-implantitis and from healthy implants in healthy individuals. Ordination analysis based on taxonomic (Figure 54a) and functional potential profiles (Figure 54b and Suppl. Figure 4a) did not highlight a clear discrete sample clustering distinctive for this condition. Despite its intermediate position, mucositis still however significantly differs in its associated microbiome compared to both the peri-implantitis group (Permanova p-value = 0.008) and healthy implants control group (Permanova p-value = 0.001). When looking at the microbiome alpha-diversity, the mucositis-associated microbiome resembled that of the peri-implantitis group with species, gene-families, and pathways richness (Figure 54c-d and Suppl. Figure 4b) substantially depleted compared to the healthy subgingival microbiome. This is in line with the hypothesis of a biofilm composed by fewer dominant species in disease, and a consequent small number of detected functions. On inter-subject microbiome divergence, mucositis is again in between healthy and peri-implantitis sites both from the taxonomic (Figure 54e) and functional potential viewpoint (Suppl. Figure 4c), suggesting that the mucositis-associated microbiome has a converging composition and structure that is less marked than in full-disease states.

Among the five most discriminating species between mucositis and health sites, there are no species belonging to the Socransky's Red Complex and only one, *F. nucleatum*, belonging to the orange complex (Figure 54f). In addition to *F. nucleatum*, only *T. denticola* is within the 10 most mucositis/healthy discriminative species and also in the 7-species Peri-implantitis Red Complex (PiRC) defined above. Conversely, the four of the five species that better distinguish peri-implantitis with respect to mucositis all belong to the PiRC and to either the Red Complex or to the Orange Complex, with only *F. nucleatum* not present in the list (Figure 54g). These observations suggest that *F. nucleatum* is the first species the increases in abundance inside the plaque microbiome along the mucositis - peri-implantitis axis and is then followed by more strongly peri-implantitis characterizing species at later stages of the disease. The microbiome signatures of mucositis and peri-implantitis are thus distinct and understanding the transition from the first to the second could provide important therapeutic targets.

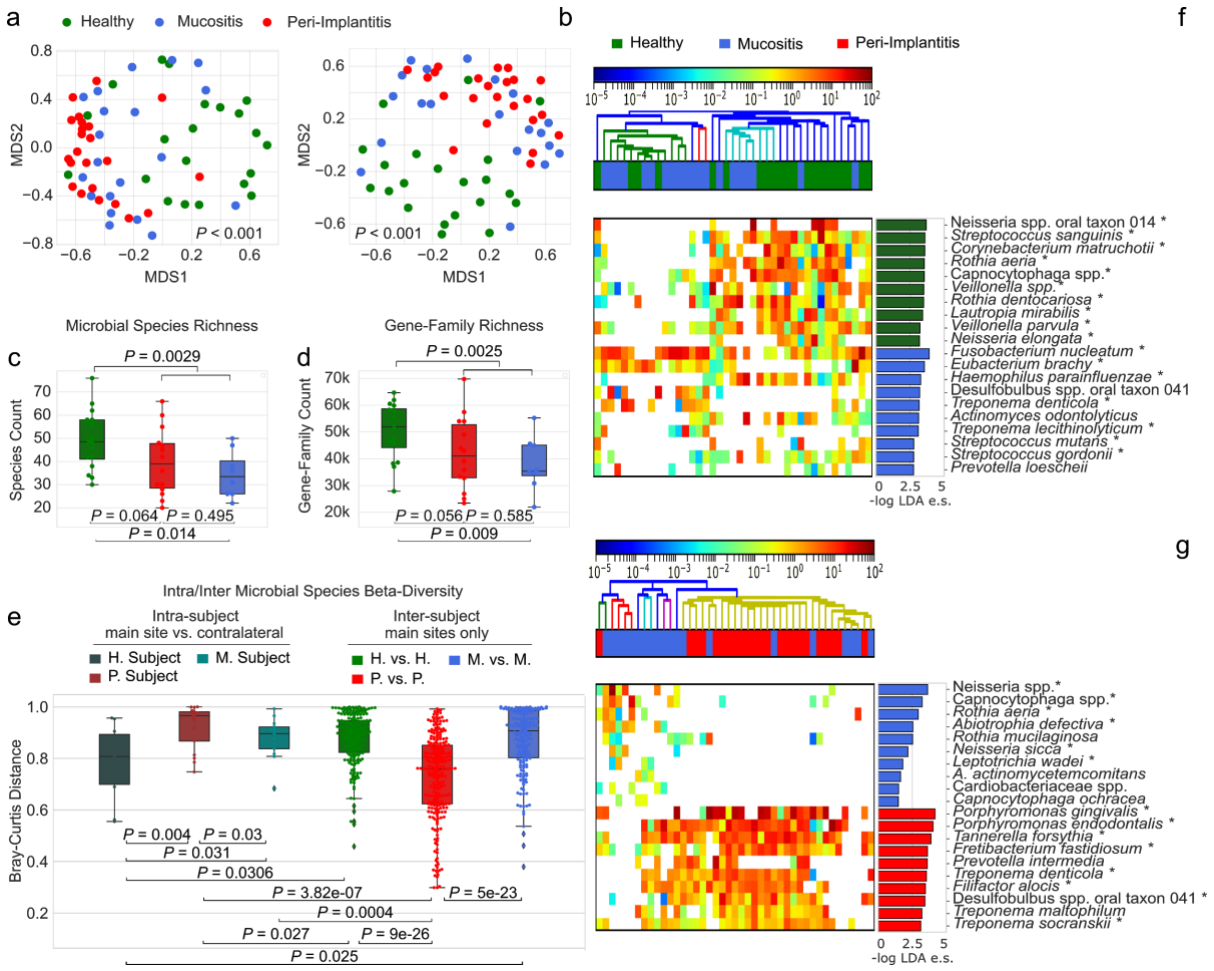

Figure 54. Mucositis shows and intermediate microbial signature between peri-implantitis and healthy sites. a) Ordination plot (MDS) of healthy, mucositis and peri-implantitis samples based on taxonomic abundance profiles and b) microbial gene family profiles. c) Alpha diversity distributions estimated as species richness and d) richness of UniProt90 gene families. e) Beta-diversity distributions estimated with the Bray-Curtis dissimilarity metric for intra- and inter-condition comparisons in the three conditions. f) Relative abundances (log scale) and effect sizes (LDA score from LEfSe) of the 10 microbial species most strongly associated with mucositis in comparison with healthy sites and g) peri-implantitis sites (top 10 species/gene families effect sizes per class).

5.1.2.5 Microbiome-based classifiers can accurately predict clinical peri-implant conditions and 6-month improvements of clinical parameters in mucositis affected implants

We then assessed the potential diagnostic and prognostic potential of the plaque microbiome for mucositis and peri-implantitis. Using a machine learning approach based on the random forest classifier applied in cross validation (see Methods) as performed for other predictive metagenomic tasks (Thomas et al. 2019), we found that peri-implantitis can be predicted at high accuracy, with an area under the receiver operating characteristic curve (AUC) of 0.91 (Figure 55a). Mucositis was also clearly associated with its microbiome but with comparably

less precision and recall for the task of predicting mucositis versus healthy conditions (AUC 0.81) and mucositis versus peri-implantitis (AUC 0.77). Similar classification performances were obtained when using gene families for training the classifier (Figure 55a) suggesting that the species that are discriminative for the disease conditions possess distinctive sets of genes.

An important parameter that is collected when assessing and monitoring the clinical condition of an implant is the peri-implant probing depth (PPD) at multiple sites around the implant. Such parameter is clearly distinctive for peri-implantitis but weaker for mucositis (Figure 55b-c). Mean PPD alone can reach an AUC of 0.95 in predicting peri-implantitis versus healthy sites, but for mucositis it reached worse performances than the microbiome-based classifier (AUC 0.73 vs AUC 0.81). When combining the microbiome taxonomic features with the PPD values the classifier outperformed the microbiome-based and PPD-based classifiers with very high AUCs for all pairs of conditions (Figure 55d). With a AUC 0.98 for the combined classifier, microbiome and clinical parameters thus provide complementary lines of evidence for the implant disease status, and when combined can provide very strong diagnostic tools.

Because mucositis is the most critical clinical condition for its risk of evolution in peri-implantitis, we then tested whether the microbiome associated with mucositis can be a good proxy for the severity of the condition. First, for the mucositis samples we analyzed (that were not used in the definition of the PiRC), we found that the PiRC index is correlated with mean PPDs for the mucositis samples (Figure 55e, Pearson's R = 0.44, P-value = 0.049). Second, using PPD values at 6-month re-evaluation from the sample collection and therapy of mucositis to establish improvement or worsening of the clinical condition, we found that the machine learning classifier trained in cross validation on the mucositis microbiome was predictive for positive or negative PPD variation at six months (AUC 0.88, Figure 55f). This was confirmed by the use in the classifier of the 7 species in the PiRC alone (AUC 0.90, Figure 55f) as well as just using the PiRC index (AUC 0.70, Figure 55f). This demonstrates that the plaque microbiome associated with mucositis is predictive for the variation in clinical parameters, and can potentially be used as a tool for testing the severity of the clinical condition.

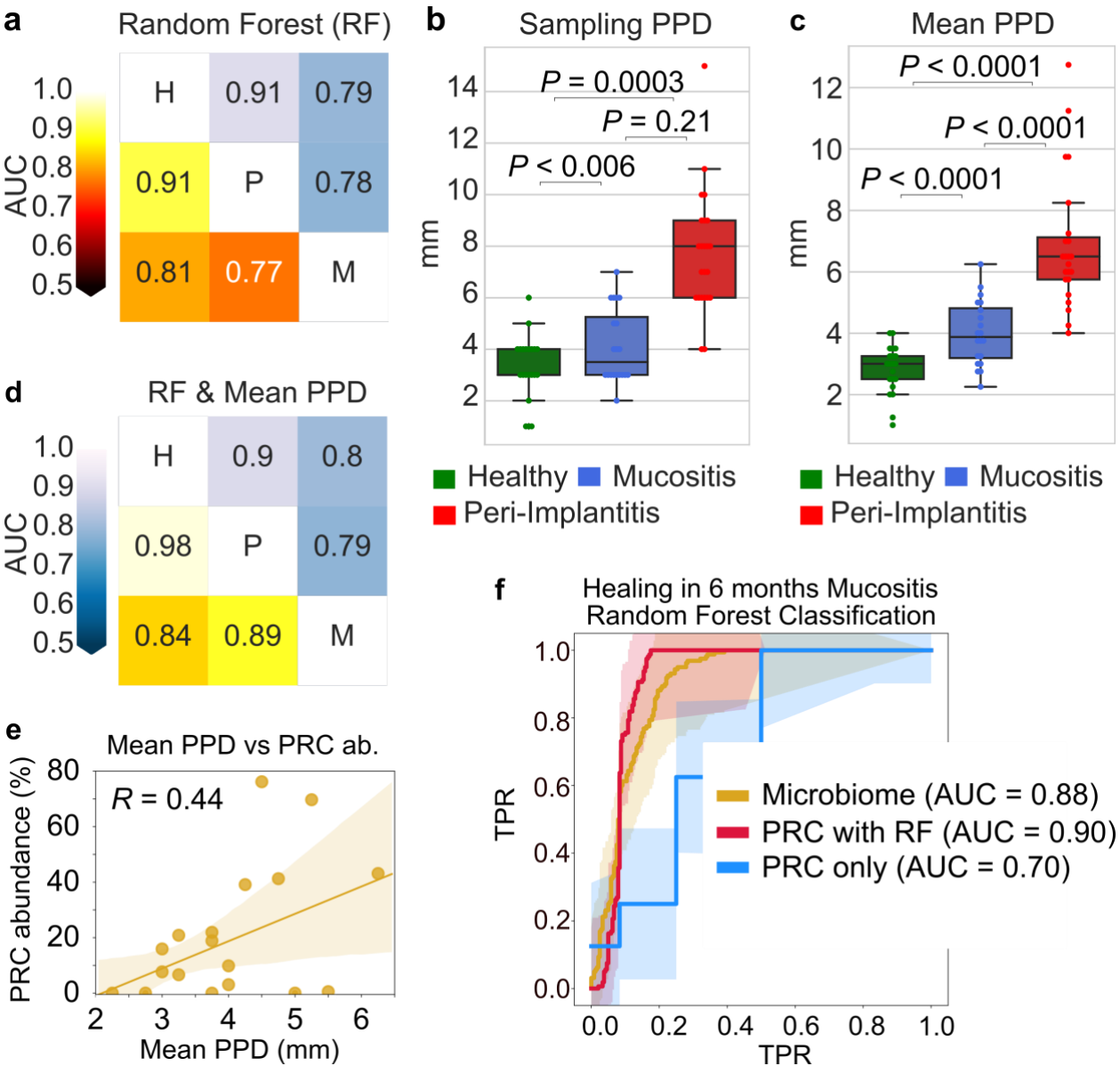

Figure 55. Diagnostic and prognostic metagenomic machine learning signatures for mucositis and peri-implantitis. a) AUC prediction matrix between pairs of conditions (H-healthy, M-mucositis, P-Peri-implantitis) achieved by the random forest machine learning classifier using taxonomic species-level features (bottom left triangular matrix in black-red-yellow colormap) and functional gene family features (upper right triangular matrix in blue colormap). Classifiers are applied in 10-fold cross-validation repeated 20 times. b) Distribution of PPD values at the sampling site ("sampling PPD") and c) mean PPD for the three conditions considered in this study d) The same prediction matrix of panel a) but using a classifier trained both on microbiome features (species or gene-family abundance) and mean-PPD values. e) Correlation between mean-PPD at baseline and Peri-implantitis Red Complex (PiRC) index for the mucositis samples. Pearson's correlation coefficient is reported. f) Receiver Operating Characteristic (ROC) curves and AUC values for the cross-validation performance of the microbiome-based RF classifier in predicting improvements in

mean PPD values. The three models consider (i) all species (ii) the species in the PiRC, and (iii) the PiRC index as input features.

5.1.2.6 Specific Fusobacterium nucleatum subspecies are associated with mucositis and peri-implantitis

Fusobacterium nucleatum is a hallmark of periodontal diseases (Signat et al. 2011; Han 2015) that we showed here is also strongly associated also with peri-implant diseases and especially with mucositis. Given the diversity of the strains present in this species, we further investigated the subspecies structure of *F. nucleatum* in relation to peri-implantitis and mucositis (see Methods). By using a pangenome-based strain profiling tool (Scholz et al. 2016) we characterized the dominant *F. nucleatum* strains in the 113 samples considered in this study as well as in 135 additional plaque samples from an American healthy metagenomic cohort (Consortium and The Human Microbiome Project Consortium 2012) and 48 plaque samples from patients with periodontitis (Shi et al. 2015). We recovered a total of 208 *F. nucleatum* strain profiles that were clustered into five distinct subspecies (Suppl. Figure 7) plus an additional single strain not belonging to any of the subspecies. These clusters correctly recapitulated the known subspecies of *F. nucleatum* (Gharbia and Shah 1990; Kook et al. 2017) which are subspp. nucleatum, polymorphum, Vincentii, and animalis (Suppl. Figure 7), but also identify the presence of one additional yet-to-be-named subspecies without taxonomic annotations we provisionally named *F. nucleatum* Cluster5. We then profiled the strains also using the genetic variability of their core genome (Truong et al. 2017) that confirmed that *F. nucleatum* subspecies were phylogenetically well separated, with reference genomes monophyletically placed, and in agreement with the genomic-content clustering mentioned above. Metagenomes harboring strains of the “animalis” and “nucleatum” subspecies were mostly comprised in monophyletic subtrees, while samples with the “polymorphum” cluster were more diverse (Figure 56a).

We then tested the association of specific subspecies with the clinical conditions. Strains belonging to *F. nucleatum* subsp. nucleatum were significantly more associated with peri-implantitis or mucositis sites (p-value = 2.27E-4, two-tailed Fisher’s exact test) than healthy sites. Conversely, *F. nucleatum* subsp. polymorphum was enriched in healthy subjects and control sites. Interestingly, the newly identified and unexplored *F. nucleatum* cluster 5 was significantly associated with peri-implantitis and mucositis samples, when compared against healthy subjects and controls (p-value = 3.05E-5, two-tailed Fisher’s exact test). Three additional periodontitis samples harbored a member of Cluster 5, and the association of Cluster 5 with disease status held true even when including samples with periodontitis (p-value = 2.61E-5). Taken together, these results suggest that only a subset of *F. nucleatum* strains including a newly identified subspecies without cultivated representatives are associated with peri-implant diseases and identifying *Fusobacterium* subspecies in the clinic may have prognostic relevance.

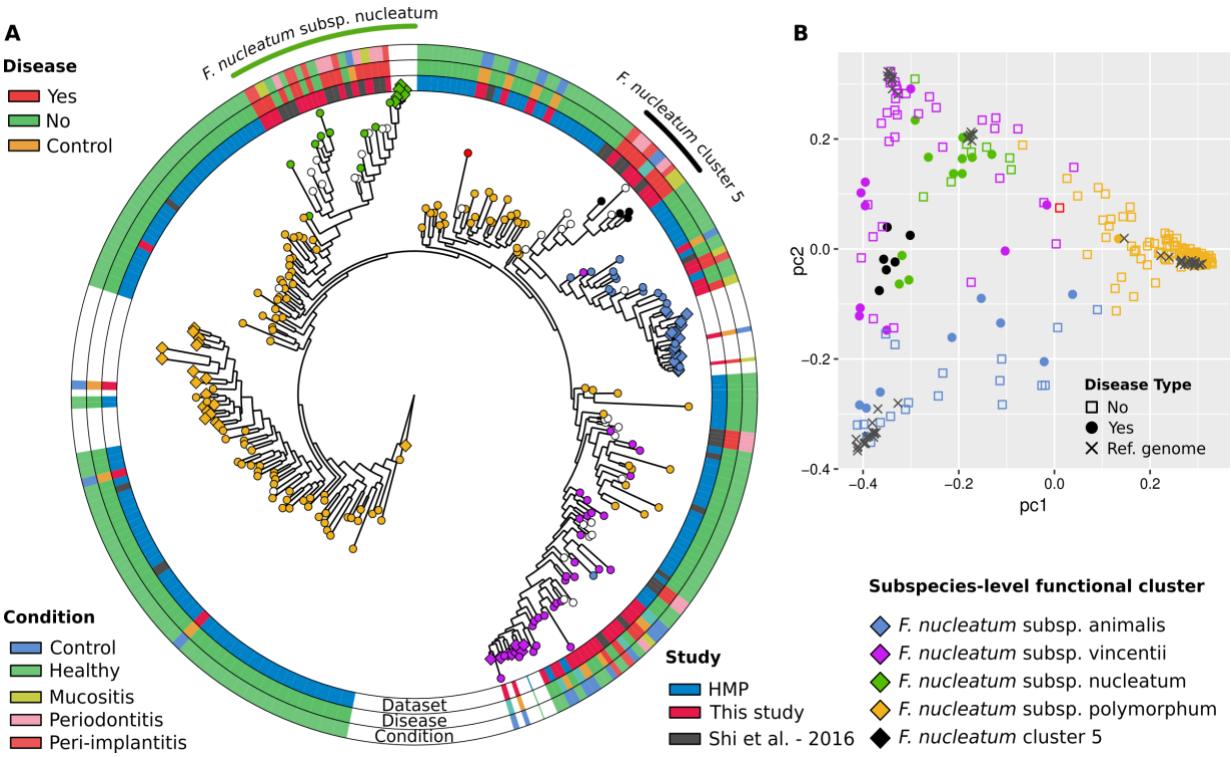

Figure 56. Strain level characterization of *Fusobacterium nucleatum* from metagenomes of the healthy, mucositis, peri-implantitis and periodontitis plaque. a) StrainPhlAn-based phylogenetic tree computed on the MetaPhlAn2 markers for *F. nucleatum*. Each node represents a single *F. nucleatum* strain reconstructed from a sample. Clinical metadata are reported in the three outer rings. Contralateral controls of healthy patients are labelled as "healthy". Nodes are coloured by genomic-content cluster (Methods, Suppl. Figure 7). White nodes reflect samples that could not be detected and typed by PanPhlan, and that were not clustered. Reference genomes are indicated by diamond leaf markers. The five colors of the markers refer to the five identified subtypes including the newly identified F. nucleatum Cluster 5 subspecies (see Methods). Subspecies significantly associated to peri-implant diseases are marked externally to the diagram. b) Clustering and principal coordinates analysis of the PanPhlAn-detected *F. nucleatum* strains. The analysis is performed on the gene presence-absence profiles of *F. nucleatum* pangenome. Points are coloured by genomic-content cluster (Methods, Suppl. Figure 7).

5.1.3 Conclusions

Our work provides the microbiome characterization of the plaque biofilm in implant diseases overcoming in resolution (shotgun metagenomics vs 16S rRNA sequencing), sample size (113 metagenomes), and inter-individual microbiome control (contralateral sites) existing investigations. We found strong taxonomic and functional biomarkers for disease and highlighted how peri-implantitis converges toward a low-diversity well-defined pathogenic set of taxa. The seven bacterial species we included in the "Peri-implantitis Red Complex" (PiRC) are appealing targets for diagnostic and prognostic assessment of the plaque microbiome and the basis for targeted more mechanistic investigation of the host-microbiome interaction

network in implant-associated diseases.

Our data also suggest that *Fusobacterium nucleatum* is a particularly relevant member of the PiRC because it appears to be the first biomarker of initial inflammation (mucositis). This species is indeed overly-abundant before the onset of peri-implantitis and the corresponding stronger microbial shift involving many taxa not very enriched in mucositis. *F. nucleatum* is a particularly diverse species, and of its known subspecies, only *F. nucleatum* subsp. nucleatum is connected with disease states. A new subspecies provisionally named *F. nucleatum* subsp. cluster5 is even more associated with peri-implantitis and mucositis and should be the basis for further characterization of this clade.

Mucositis is perhaps the more actionable disease state, and although even larger sample sizes are needed, its intermediary microbiome configuration in between the healthy plaque and the peri-implantitis plaque suggest that the mucositis microbiome has diagnostic and prognostic power. We indeed found that the improvement of clinical parameters associated with mucositis (such as probing depth) can be predicted starting from the microbiome structure at diagnosis. Specific microbiome-based therapeutic choices are not available, but the presence and abundance of *F. nucleatum* and other taxa of the PiRC might be associated with more or less favorable outcomes. More work is thus needed to correlated the structure of the mucositis-associated microbiome with the progress of the disease state.

The high-resolution characterization of the plaque microbiome in peri-implant diseases is the first step toward a more comprehensive understanding of the role of the microbiome in peri-implant diseases. Although the inter-subject diversity of the peri-implantitis microbiome is relatively low, the predominance of different taxa in the PiRC might open the door for disease stratification. Further studies are thus needed to define microbiome-dependent diseases subtypes and test the efficacy of existing and novel therapeutic strategies with respect of such subtypes.

5.1.4 Materials and Methods

5.1.4.1 Subject recruitment

This study was approved by the ethics committee of University of Trento (no. 2015-024) and was conducted in accordance with the guidelines of the world Medical Association Declaration of Helsinki. Male and female patients having dental implants and regular maintenance of their dental implants were recruited from six different private practices in the Province of Trentino (Italy) for this study. The study protocol was explained to each subject, and a signed informed consent was obtained. Inclusion criteria involved good general health as evidenced by the medical history, being at least 18 years of age, not fewer than 8 teeth, at least one functioning oral implant restored with crowns or prostheses for at least 1 yr, willingness to participate in the study. Exclusion criteria included pregnancy or lactation, HIV, use of immunosuppressant medications, bisphosphonates, or steroids, use of chlorhexidine mouthwash or gel during the previous 2 weeks, oral prophylactic procedures within the preceding 3 months, intake of systemic antibiotics or probiotics within the past 6 months.

Patients were identified and selected in the different private practices and were included in one of the following study groups according to the state of health of their dental implants: a) healthy (H, patients with at least one healthy implant and no implants with mucositis or peri-implantitis),

b) mucositis (M, patients with at least one implant with mucositis and no implants with peri-implantitis), c) peri-implantitis (P, patients with at least one implant with peri-implantitis). The selection and inclusion of patients in one of the groups was based on radiographic evaluation of the marginal bone level, clinical signs of inflammation, and/or presence of suppuration according to the criteria delineated by the Consensus Report on Peri-implant Diseases (Lindhe et al. 2008). In detail, peri-implant health was diagnosed when the implant was surrounded by healthy soft and hard tissues determined by absence of bleeding on probing (BOP) or suppuration (SUP) and visible/detectable radiographic bone loss. Implants with only clinical signs of inflammation in one or more sites (redness, swelling, BOP, SUP) and absence of radiographic bone loss following functional loading were classified as peri-implant mucositis, whereas implants with the presence in one or more sites of both clinical inflammation and radiographic evidence of more than 2 mm bone loss since the prosthesis installation (i.e. at least one-year after loading) were diagnosed as peri-implantitis.

5.1.4.2 Data Collection and clinical examination

Six experienced and calibrated periodontists examined all patients. The demographic parameters of gender and age and a comprehensive medical and dental history were recorded, followed by a full-mouth periodontal and implant clinical examination and, if necessary, a site-specific radiographic examination. Medical history comprised informations about smoking habit, diabetes, autoimmune diseases or other systemic diseases, alcohol consumption, medications taken. Dental history comprised informations about current and past periodontal status, number of remaining teeth, number of implants, previous peri-implantitis, frequency of home oral care, hours since last toothbrush, chlorhexidine usage. Clinical parameters included implant or tooth, site of sampling, diagnosis of implant age (time from installation), implant system used and nature of reconstruction (single implant, fixed or removable), type of implant retention (screw, cement, conometric), radiographic peri-implant bone loss, width of the keratinized mucosa (KM), as well as peri-implant probing pocket depth (PPD), plaque index (PI), bleeding on probing (BOP), and suppuration (SUP).

The latter four parameters were measured in each patient at the buccal, mesial, lingual, and distal sites of the experimental implant (healthy/mucositis/peri-implantitis) and of a healthy contralateral implant (if present) or tooth. PI, BOP and SUP were recorded on a binary scale (presence/absence) for each surface and PPD was measured to the nearest millimeter on the scale. In case of mucositis and peri-implantitis, any eventual subsequent therapy was noted. All patients were anonymized in the clinic assigning a unique patient ID to all subjects. All downstream analyses were performed using the anonymous IDs and anonymized metadata. The mapping between patients and IDs were stored and kept uniquely at the clinic with only the responsible of each centre allowed to have access to it.

5.1.4.3 Cohort and patient's clinical characteristics

In total, we enrolled for this study 80 patients (H: 28, M: 28, P: 24; 42 males, 38 females; mean age 60.29 ± 10.01 years) contributing with one implant per patient (two if the contralateral healthy site was an implant). 8 patients, 4 in the health group and 4 in the mucositis group, were excluded due to failure in DNA extraction or library preparation for sequencing.

Study groups comprising subjects with a healthy implant (H, N=24), an implant with mucositis (M, N=24) and an implant with peri-implantitis (P, N=24) were compared for demographic,

anamnestic and clinical characteristics (Table 14). The analysis of the sampled population showed that no differences were apparent between these three groups for age (p-value = 0.83), gender (p-value = 0.41), history of periodontitis (p-value = 0.12), smoking habit (p-value = 0.13), diabetes (p-value = 0.16), number of functioning implants (p-value = 0.82), number of residual teeth (p-value = 0.20), previous peri-implantitis (p-value = 0.30) and frequency of home oral care (p-value = 0.33). Extensive clinical data were registered both for experimental implants and contralateral implants or teeth (Suppl. Table S1, S2). When clinical parameters for the experimental implants were considered at the implant level, PPD, PI, BOP, SUP and bone loss were significantly higher in the peri-implantitis than in the peri-implant health group (p-value < 0.001). Significant differences between the groups were observed for the main clinical parameters that defined them, PPD, BOP, SUP and bone loss (p-value < 0.001). Plaque index was instead non significant (p-value = 0.20) among groups (Suppl. Table S1).

5.1.4.4 Sample collection, DNA extraction and Illumina shotgun sequencing

Microbiome samples were collected with a non-invasive procedure adopting a sampling protocol based on the one validated and adopted by the Human Microbiome Project (HMP) consortium (Consortium and The Human Microbiome Project Consortium 2012). Samples were collected with technical replicates (two per site) from a single implant and from the healthy contralateral/implant/tooth (if present, a healthy implant was preferred as contralateral healthy site) for each patient in each study group. If multiple implants with the same tested condition were present in a patient, one single implant was randomly selected for sampling. The selected sites were isolated using cotton rolls to prevent contamination with saliva and gentle dried with an air syringe, and supra-mucosal and supragingival plaque was removed using sterile cotton pellets. Submucosal and subgingival plaque samples were taken from the deepest probing site at each selected implant and tooth with individual sterile Gracey curettes and immediately placed in separate Eppendorf 1.5-mL microcentrifuge tubes (Eppendorf, Hamburg, Germany) containing sterile SCF-1 buffer solution (50mM Tris-HCl, pH 7.5; 1mM EDTA, pH 8.0; 0.5% Tween-20) (Tett et al. 2017) and frozen at −80 °C for later analysis. Total genomic DNA was isolated using the QIAamp DNA Mini kit (Qiagen, Hilden, Germany) with an additional mechanical disruption step for complete lysis of gram-positive and gram-negative species. Isolated DNA was stored at −20°C. Laboratory control extractions were also performed on prepared sample buffer to ascertain any potential contaminants. Each metagenome was first quantified and when there was sufficient material (> 1 ng) libraries were prepared using the Nextera-XT DNA kit (Illumina Inc., San Diego, CA, USA) using the manufacturer's protocol. Libraries were sequenced (2x 100 bp reads) on the Illumina HiSeq-2000 platform. Shotgun metagenomics produced initially a total of 140 samples that were reduced due to insufficient non-human DNA depth to 113 quality controlled samples for a total of 111*10^9 Gb and with at least 10 Mb of non-human reads.

5.1.4.5 Sequence preprocessing, taxonomic and functional potential profiling

The generated raw metagenomes were processed with FastqMcf (Aronesty 2013) by trimming positions with quality <15, removing low-quality reads (mean quality <25), and discarding reads shorter than 90 nt. Human and bacteriophage phiX174 DNA (Illumina spike-in) was then removed using BowTie2 (Langmead and Salzberg 2012) by mapping the reads against the corresponding reference genomes. We used MetaPhlAn 2 (Segata et al. 2012c; Truong et al. 2015) with default parameter settings for the taxonomical characterization of the sampled microbial community. HUMAnN2 (Abubucker et al. 2012) was used to generate normalised

pathways relative abundances and gene-families relative abundances tables according to the metagenome gene-contents.

5.1.4.6 Statistical analysis

We performed biomarker discovery using LefSe (Segata et al. 2011) on MetaPhlAn2 taxonomic abundance profiles and on HUMAnN2 pathway relative abundances and gene-families relative abundances profiles. Alpha-, beta-diversity and multi-dimensional scaling (MDS) analysis have been performed via custom python scripts based on Scipy, version 1.2.1, and Scikit-learn, version 0.20.3 (Varoquaux et al. 2015; Pasolli et al. 2016). Permutational Multivariate Analysis of Variance (PERMANOVA) was performed using the Scikit-bio python library, ver. 0.2.3, and 10.000 permutations.

For the computation of microbiome richness we subsampled the reads to one million reads per sample. Beta-diversity was computed using the Bray-Curtis dissimilarity index after log-transformation of the raw relative abundances to minimize the effect of compositionality. The two-tailed Wilcoxon rank-sum tests was used for the comparison unless otherwise stated. Metric MDS implementation which adopts the Scaling by MAjorizing a COmplicated Function algorithm to minimise the stress function was used setting the number of runs for the SMACOF to 4, the maximum number of iterations for each run to 5000, and the relative tolerance with respect to stress at which to declare convergence was set to 1e-09. Linear regression of the mean-PPD versus the Peri-implantitis Red Complex was computed and plotted together with 95% confidence intervals (Seaborn python library, ver. 0.9.0).

5.1.4.7 Machine learning analysis

We used a machine-learning framework similar to the one we employed in (Thomas et al. 2019), applying MetAML (Pasolli et al. 2016), which is based on the Scikit-Learn implementation (ver. 0.20.3) of random forest (Breiman 2001). We applied this framework on MetaPhlAn2 species-level abundance profiles, HUMANn2 gene-families relative abundances, PPD at the sampling site, mean-PPD across the four site of each implant, and on combinations of these feature sets. For each run we trained and tested the model in a 20-times repeated 10-fold stratified cross-validations, evaluating the resulting predictions through the mean Area Under The Roc curve (AUC).

5.1.4.8 Strain-level analysis of F. nucleatum

Strain-level profiling was performed by running StrainPhlAn (Truong et al. 2017) and PanPhlAn (Scholz et al. 2016) on the raw reads of the 113 samples considered in this study, plus 183 additional gingival plaque metagenomes from healthy and periodontitis subjects retrieved from publicly available datasets. Additionally, 56 reference genomes of *F. nucleatum* were retrieved from the NCBI Assembly database (Kitts et al. 2016) and incorporated in the strain-level analysis. For the strain-level profiling through StrainPhlAn, reads were preprocessed to remove short sequences (i.e. length < 90 nucleotides) and then mapped against the MetaPhlAn2 markes with Bowtie2 v. 2.3.4 (Langmead and Salzberg 2012). StrainPhlAn was applied with the following parameters: --marker_in_clade=0.2, --sample_in_marker=0.2, --N_in_marker=0.8 and --gap_in_sample=0.8. In total, *F. nucleatum* was detected in 208 out of 296 samples. The phylogenetic maximum likelihood tree was generated on the multiple sequence alignment using Muscle v3.8.425 (Edgar 2004) and RAxML v.8.1.15 (Stamatakis 2014) with the GTRCAT model. The phylogenetic tree was visualized with GraPhlAn v. 1.1.3

(Asnicar et al. 2015), using the genome of *Fusobacterium hwasookii* as an outgroup to root the tree. PanPhlAn was applied using default parameters on the same raw reads and reference genomes mentioned above. We build a custom *F. nucleatum* PanPhlAn pangenome from the 56 *F. nucleatum* reference genomes by annotating each genome with Prokka v1.12 (Seemann 2014) and by clustering annotated genes with Roary v. 3.8 (Page et al. 2015). Subspecies-level clusters were obtained by performing hierarchical clustering ("average" method) on the PanPhlAn presence-absence gene families matrix, and by cutting at an height of 0.45. Prior to clustering, we removed gene families that were present in less than three samples, or that were present in more than all-minus-three samples or reference genomes. The PCoA of Figure5b was computed on the same presence-absence matrix using the jaccard distance metric. Statistical analysis was performed with custom Python and R scripts.

5.1.4.9 Data availability

All metagenomes have been deposited and are available at the NCBI Sequence Read Archive under accession BioProject PRJNA547717).

5.1.5 Acknowledgments

We thank the members of the Segata laboratory for insightful discussions, all the clinicians and the personnel of the dental offices involved in the project, all the volunteers enrolled in the study, the NGS facility at the University of Trento for performing the metagenomic sequencing, and the HPC facility at the University of Trento for supporting the computational experiments.

This work was supported by the Italian Society of Periodontology and Implantology (SIdP) (Prot. 24/2015), Eklund Foundation (Prot. 2016/038), the International Team for Implantology (ITI) (No. 1107_2016) to P.G and N.S. The work was also supported by the European Research Council (project ERC- STG MetaPG-716575), the Italian Ministry of Research and University (MIUR RBFR13EWWI), and the EU-FP7 (PCIG13-GA-2013- 618833) to N.S.

5.1.6 Potential conflicts of interest

P. G. and N. S. are co-founders of Prebiomics, a company active in the fields of implantology and microbiome research.

5.1.7 Supplementary material

5.1.7.1 Supplementary figures

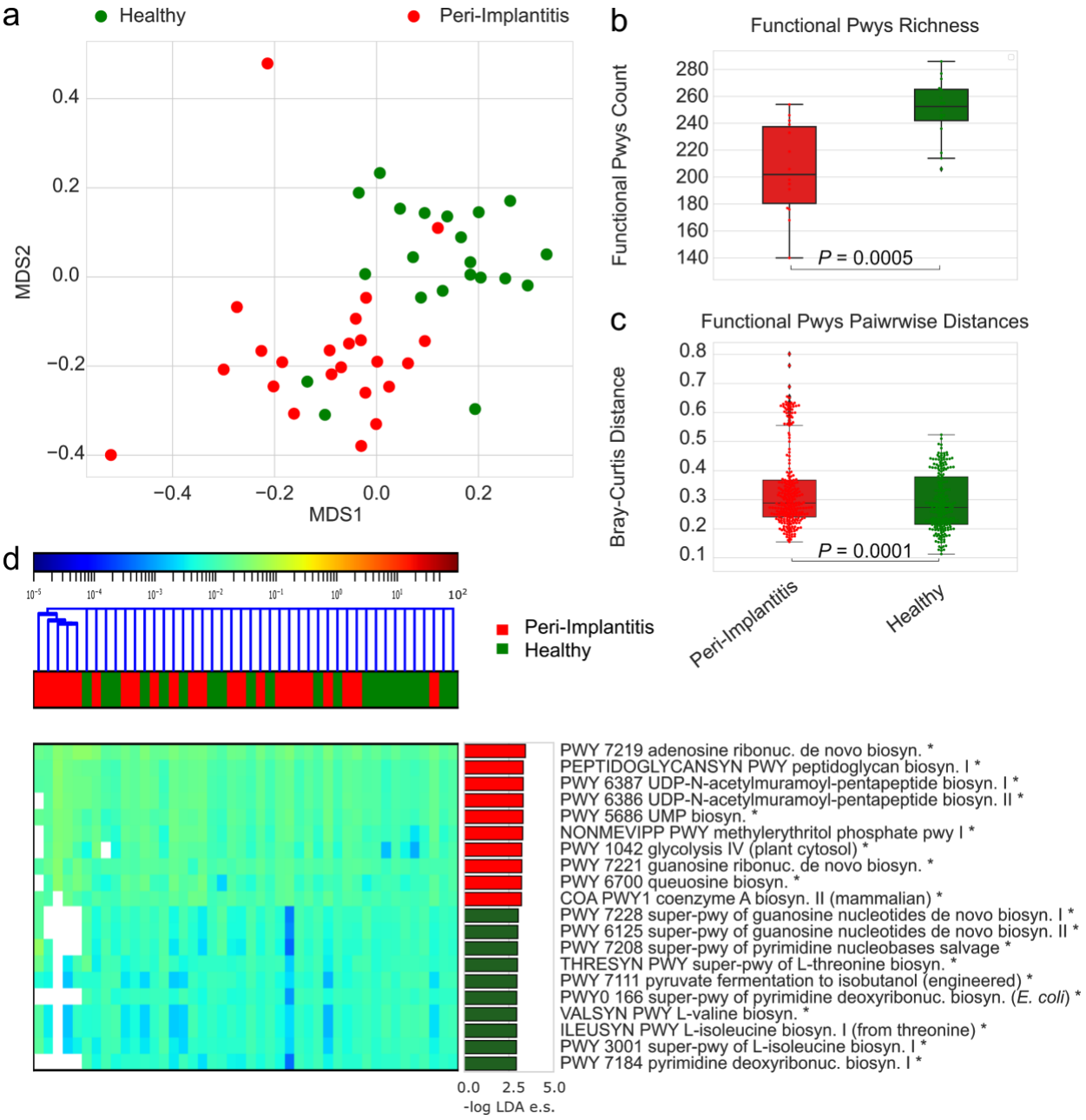

Supplementary Figure 1. Functional profiles are significantly richer but less heterogeneous among individuals in health status compared to peri-implantitis. a) Ordination plot (MDS) of healthy and peri-implantitis samples based on pathways after HUMAnN2 analysis. b) Rarefied Alpha diversities measured as the total number of pathways in each sample for the two conditions. c) Beta-diversities estimated with the Bray-Curtis dissimilarity metric for inter-condition comparisons in the two conditions as regard pathways. d) Relative abundances and effect sizes for the 10 pathways most strongly associated with either the healthy sites or the sites with peri-implantitis (top 10 species/gene families effect sizes per class).

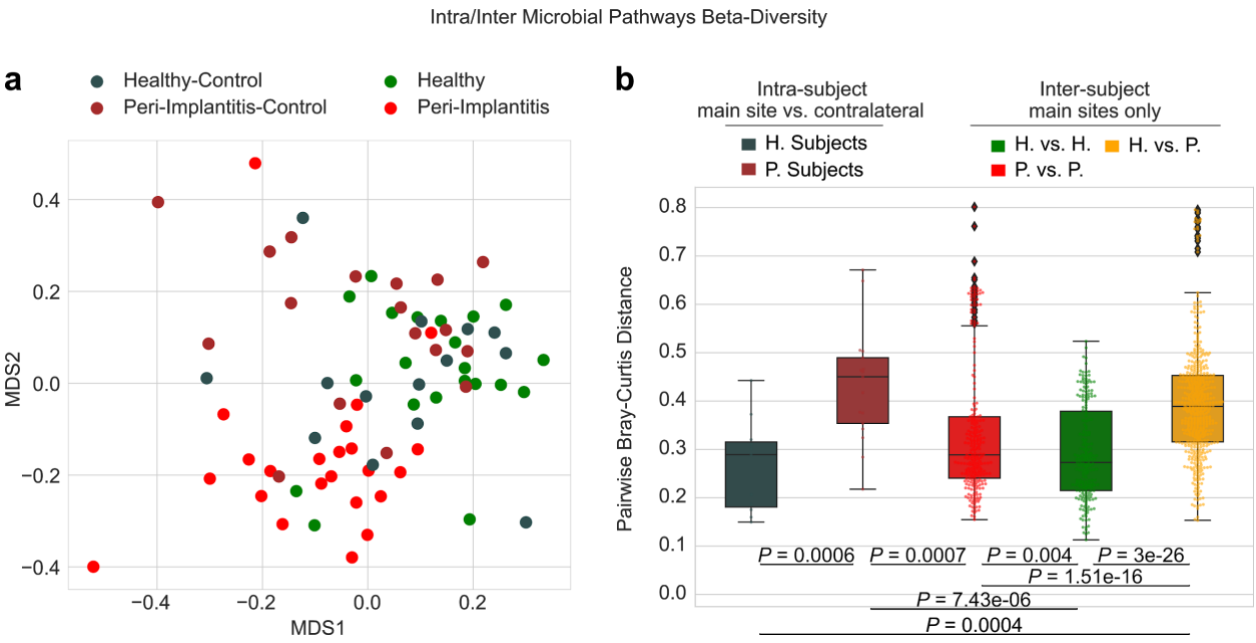

Supplementary Figure 2. The strong microbiome signature in peri-implantitis is also confirmed by pathways analysis. a) Ordination plot (MDS) of peri-implantitis and all healthy samples (test and contralateral) based on pathways. b) Intra and inter-subject Beta diversity analysis based on pathways.

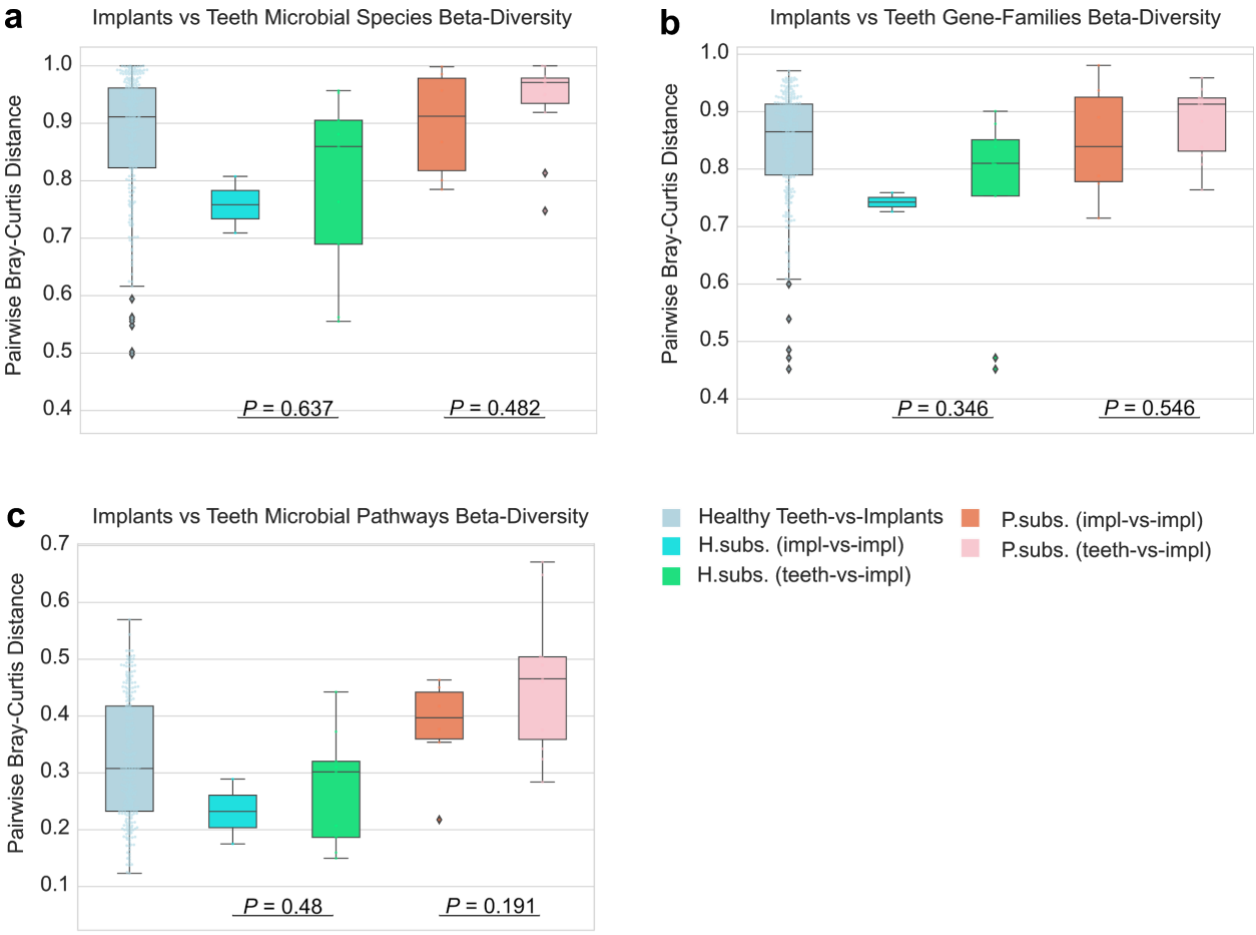

Supplementary Figure 3. Microbiome composition and functional potentials of healthy implants and teeth are not distinguishable. a) Beta-diversity analysis focused on Implant-Teeth Distances based on Metaphlan2. b) Beta-diversity analysis focused on Implant-Teeth Distances based on gene-families. c) Beta-diversity analysis focused on Implant-Teeth Distances based on pathways.

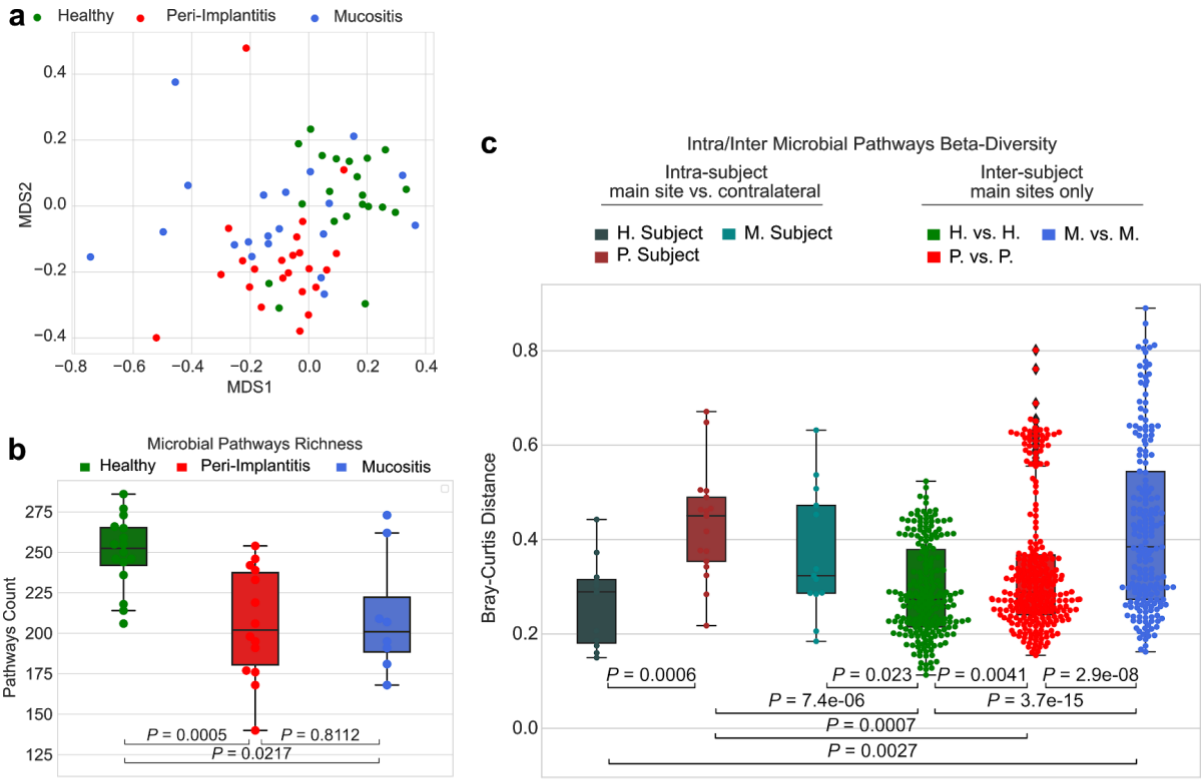
a
Healthy
Peri-Implantitis
Mucositis
MDS2
MDS1
b
Microbial Pathways Richness
Pathways Count
P = 0.0005
P = 0.8112
P = 0.0217
c
Intra/Inter Microbial Pathways Beta-Diversity
Intra-subject
main site vs. contralateral
Inter-subject
main sites only
H. Subject
M. Subject
P. Subject
H. vs. H.
M. vs. M.
P. vs. P.
Bray-Curtis Distance
P = 0.0006
P = 0.023
P = 0.0041
P = 2.9e-08
P = 7.4e-06
P = 3.7e-15
P = 0.0007
P = 0.0027

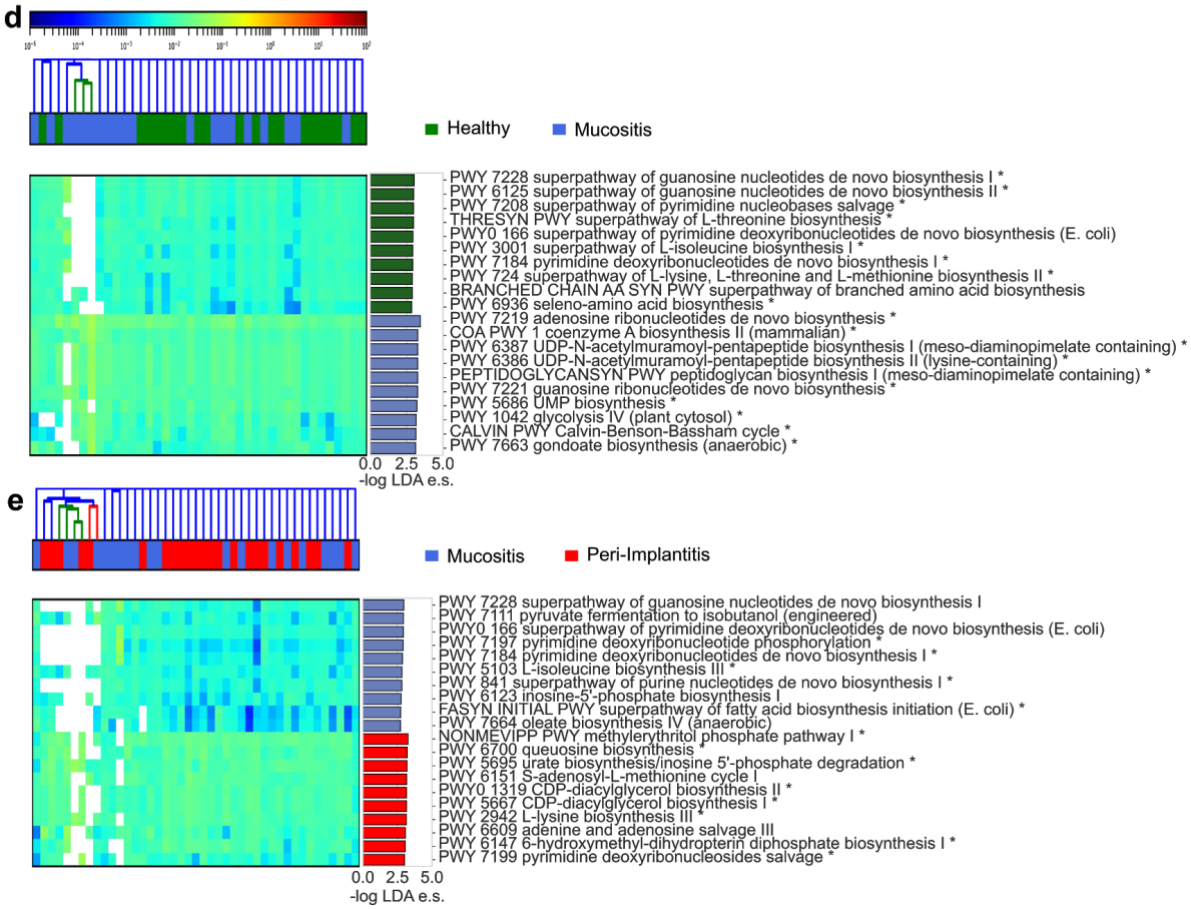
d
Healthy
Mucositis
PWY 7228 superpathway of guanosine nucleotides de novo biosynthesis I *
PWY 6125 superpathway of guanosine nucleotides de novo biosynthesis II *
PWY 7208 superpathway of pyrimidine nucleobases salvage *
THRESYN PWY superpathway of L-threonine biosynthesis *
PWY0 166 superpathway of pyrimidine deoxyribonucleotides de novo biosynthesis (E. coli)
PWY 3001 superpathway of L-isoleucine biosynthesis I *
PWY 7184 pyrimidine deoxyribonucleotides de novo biosynthesis I *
PWY 724 superpathway of L-lysine, L-threonine and L-methionine biosynthesis II *
BRANCHED CHAIN AA SYN PWY superpathway of branched amino acid biosynthesis
PWY 6936 seleno-amino acid biosynthesis *
PWY 7219 adenosine ribonucleotides de novo biosynthesis *
COA PWY 1 coenzyme A biosynthesis II (mammalian) *
PWY 6387 UDP-N-acetylmuramoyl-pentapeptide biosynthesis I (meso-diaminopimelate containing) *
PWY 6386 UDP-N-acetylmuramoyl-pentapeptide biosynthesis II (lysine-containing) *
PEPTIDOGLYCANSYN PWY peptidoglycan biosynthesis I (meso-diaminopimelate containing) *
PWY 7221 guanosine ribonucleotides de novo biosynthesis *
PWY 5686 UMP biosynthesis *
PWY 1042 glycolysis IV (plant cytosol) *
CALVIN PWY Calvin-Benson-Bassham cycle *
PWY 7663 gondoate biosynthesis (anaerobic) *
0.0 2.5 5.0
-log LDA e.s.

e
Mucositis
Peri-Implantitis
PWY 7228 superpathway of guanosine nucleotides de novo biosynthesis I
PWY 7111 pyruvate fermentation to isobutanol (engineered)
PWY0 166 superpathway of pyrimidine deoxyribonucleotides de novo biosynthesis (E. coli)
PWY 7197 pyrimidine deoxyribonucleotide phosphorylation *
PWY 7184 pyrimidine deoxyribonucleotides de novo biosynthesis I *
PWY 5103 L-isoleucine biosynthesis III *
PWY 841 superpathway of purine nucleotides de novo biosynthesis I *
PWY 6123 inosine-5'-phosphate biosynthesis I
FASYN INITIAL PWY superpathway of fatty acid biosynthesis initiation (E. coli) *
PWY 7664 oleate biosynthesis IV (anaerobic)
NONMEVIPP PWY methylerythritol phosphate pathway I *
PWY 6700 queuosine biosynthesis *
PWY 5695 urate biosynthesis/inosine 5'-phosphate degradation *
PWY 6151 S-adenosyl-L-methionine cycle I
PWY0 1319 CDP-diacylglycerol biosynthesis II *
PWY 5667 CDP-diacylglycerol biosynthesis I *
PWY 2942 L-lysine biosynthesis III *
PWY 6609 adenine and adenosine salvage III
PWY 6147 6-hydroxymethyl-dihydropterin diphosphate biosynthesis I *
PWY 7199 pyrimidine deoxyribonucleosides salvage *
0.0 2.5 5.0
-log LDA e.s.

Supplementary Figure 4. Pathways analysis confirm at large extent the intermediate signature of mucositis. a) Ordination plot (MDS) of healthy, mucositis and peri-implantitis samples based on pathways. b) Alpha diversities measured as the total number of pathways for the three conditions. c) Beta-diversities estimated with the Bray-Curtis dissimilarity metric for intra- and inter-condition comparisons in the three conditions based on pathways. d) Relative abundances (log scale) and effect sizes (estimated using the LDA score in LEfSe) of the 10 pathways most strongly discriminating healthy from mucositis sites. e) Relative abundances (log scale) and effect sizes (estimated using the LDA score in LEfSe) of the 10 pathways most strongly discriminating mucositis from peri-implantitis sites.

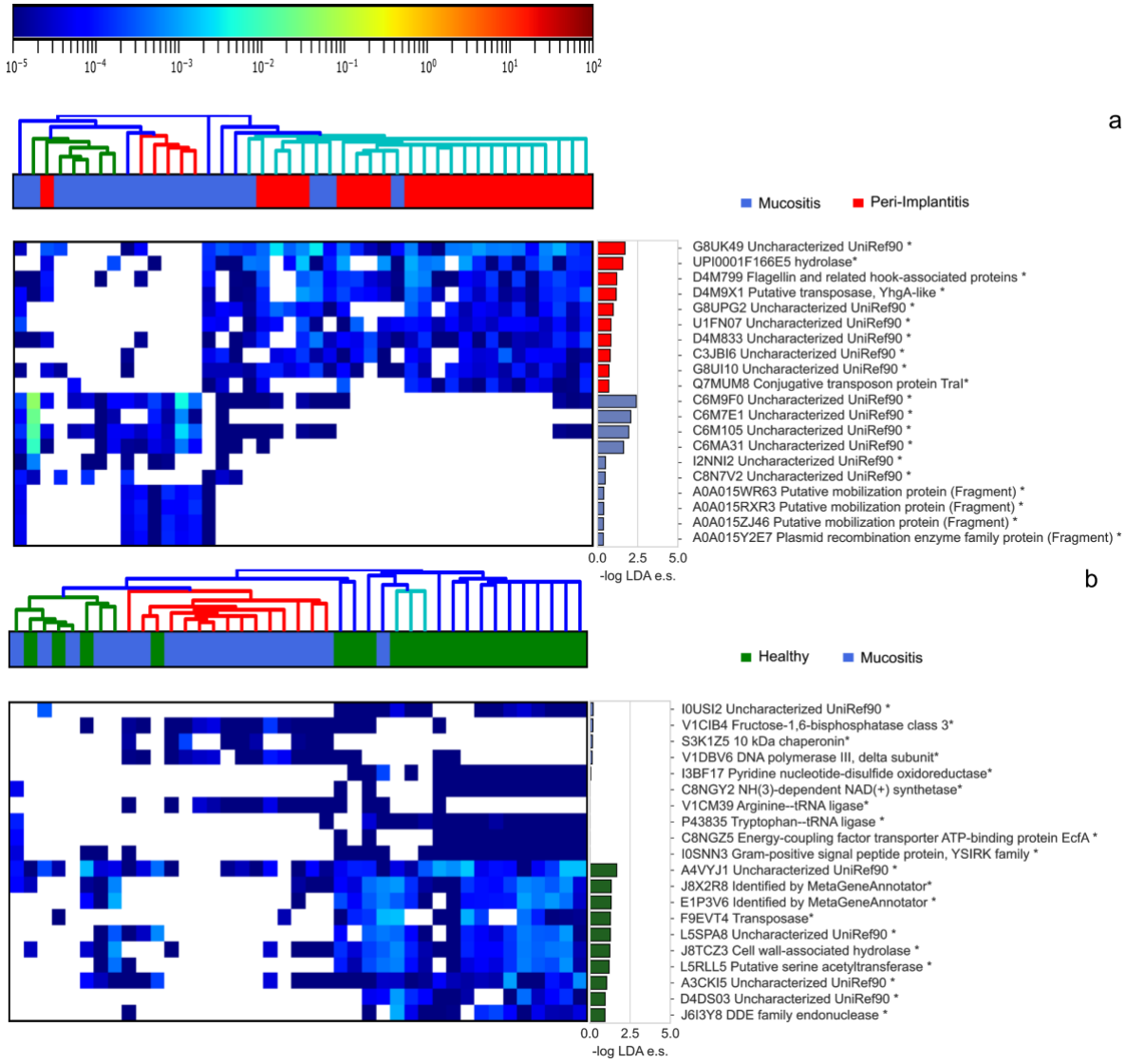

Supplementary Figure 5. Gene-families differential abundance analysis shows a larger similarity of mucositis to the healthy sites, with respect to peri-implantitis sites. a) Relative abundances (log scale) and effect sizes (estimated using the LDA score in LEfSe) of the 10 UniRef90 gene-families most strongly discriminating healthy from mucositis sites. b) Relative abundances (log scale) and effect sizes (estimated using the LDA score in LEfSe) of the 10 UniRef90 gene-families most strongly discriminating mucositis from peri-implantitis sites.

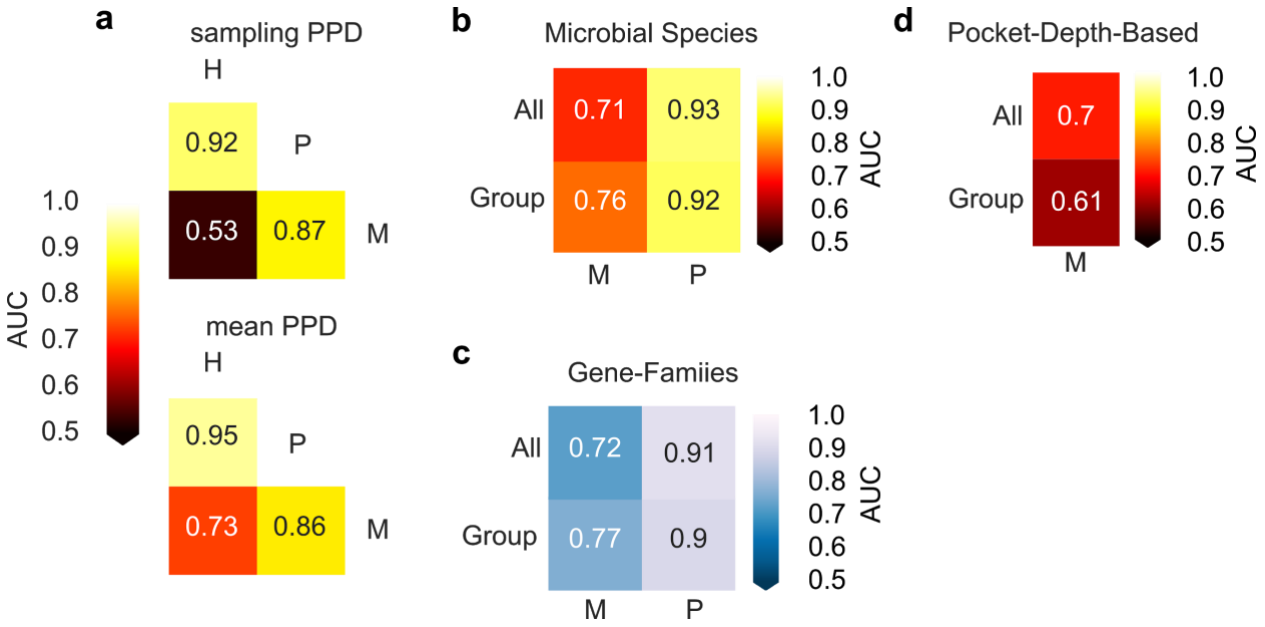

Supplementary Figure 6. PPD can't capture mucositis with respect to controls as good as microbiome can, a finding which holds true when mucositis is predicted against contralateral samples. a) Sampling-site PPD used as feature in a one-tree random forest for the prediction of peri-implantitis against healthy sites, mucositis against peri-implantitis, and mucositis against healthy implants (above). Mean-PPD used as feature in a one-tree random forest for the prediction of peri-implantitis against healthy sites, mucositis against peri-implantitis and mucositis against healthy implants (below). b) Microbial species random forests prediction of mucositis and peri-implantitis implants against the overall contralateral samples (all) and against the corresponding set of contralateral (group). c) Gene-families random forests prediction of mucositis and peri-implantitis implants against the overall contralateral samples (all) and against the corresponding set of contralateral (group). d) Mean PPD-based one-tree random forest prediction of mucositis against the entire set of contralateral samples (all) and the mucositis-group contralateral samples alone (group).

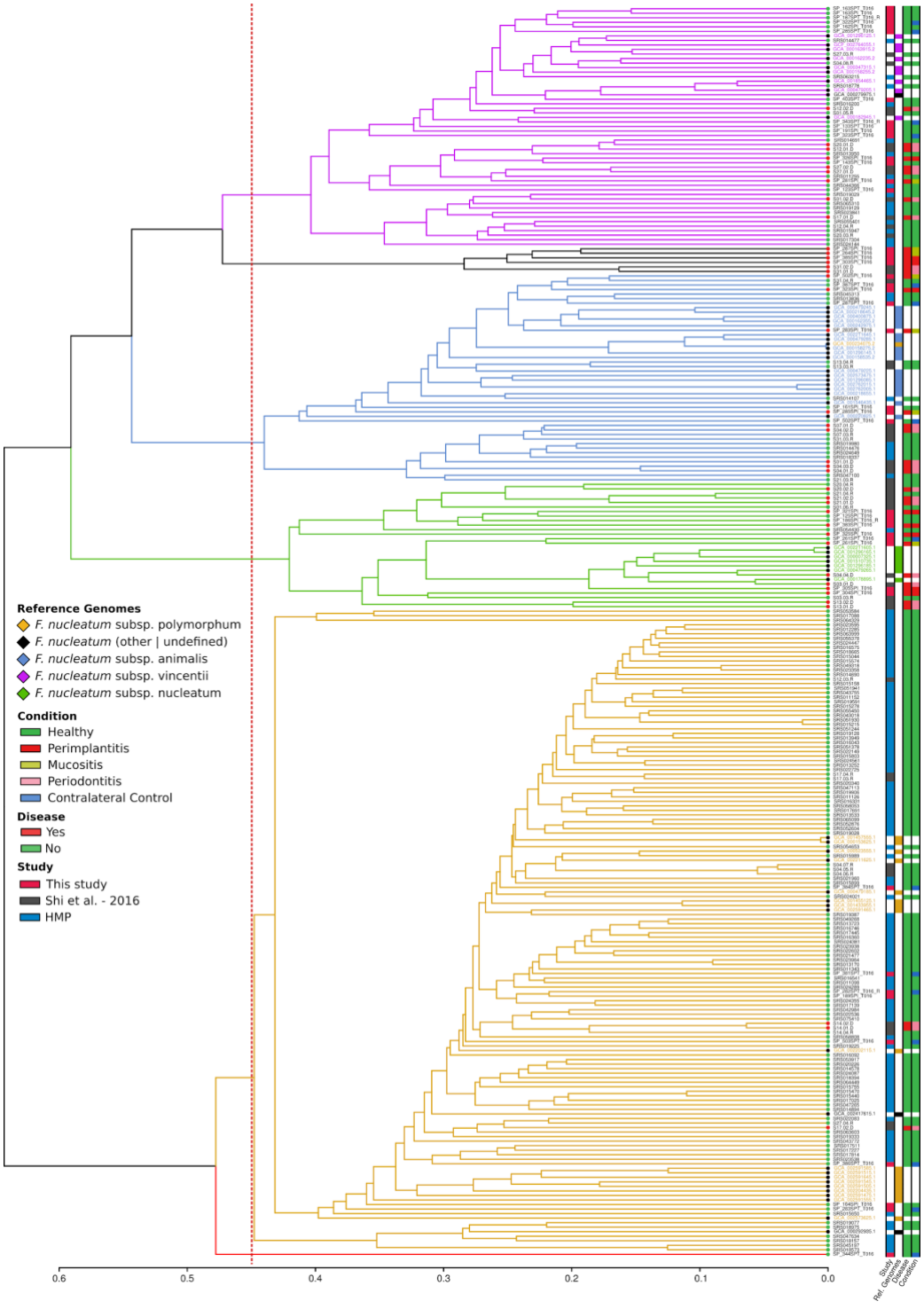

Supplementary Figure 7. Hierarchical clustering of samples basing on the genomic content of different F. nucleatum subspecies The hierarchical clustering is based on the presence-absence matrix of gene families on 208 metagenomes. Reference genomes are added and colored by subspecies. The associated clinical metadata are presented as color-bars on the right. Six clusters were derived by cutting at an height of 0.45 to recapitulate the division of the different F. nucleatum subspecies. Gene families present in less than three or more than all-minus-three samples were excluded. Leaves colors represent the disease status of each metagenomic sample.

5.1.7.2 Supplementary tables

Supplementary Table S1. Experimental implants' clinical and microbial characteristics

Supplementary Table S2 . Sampled teeth/implants characteristics

Supplementary Table S3. Cohort metadata

Supplementary Table S4. Statistical significance, FDR-correction, abundances and prevalences in the peri-implantitis/healthy implants comparison of microbial species

Supplementary Table S5. Lefse microbial species biomarkers for the peri-implantitis/healthy implants comparison.

Supplementary Table S6 . Lefse gene-families biomarkers for the peri-implantitis/healthy implants comparison.

Supplementary Table S7 . Statistical significance, FDR-correction, abundances and prevalences in the mucositis/healthy implants comparison of microbial species

Supplementary Table S8 . Statistical significance, FDR-correction, abundances and prevalences in the mucositis/peri-implantitis implants comparison of microbial species

6. Conclusions

Through the integrated approach that I employed in this thesis to study the multiple aspects related to peri-implant diseases, we were able to reach some interesting conclusions. Some of them confirm or reinforce what was already present in the literature, while others provide some interesting insights especially with a view to future perspectives.

I am exploiting below the most important aspects related to each chapter of the thesis.

In **Chapter 3** we evaluated the topic of implant surfaces, both in chemical and biological terms. Specifically, we focused on moderately rough surfaces, which, according to the literature, are suggested as an optimal compromise to be used in clinical practice, but of which there is less evidence about their biochemical characteristics. Our *in-vitro* data demonstrated that a specific moderately rough surface, such as OGI surface, has a bioactive behavior that increases its osteoconductive properties enhancing mesenchymal stem cells' osteogenic activities.

In **Chapter 4** we deepened the discussion on implant surfaces, believing that the possibility of introducing antibacterial surfaces for dental implants is not just a speculation. Starting from the debated antibacterial properties of silk, we developed and tested, through various procedures, a potential implant coating based on sericin, one of the two main silk proteins. The antibiofilm efficacy of this coating was very positive when its effect against standard biofilm producer strain of *Staphylococcus aureus* was tested. The next step to do will certainly be to test and further validate this sericin based-coating against specific bacteria related to peri-implant diseases.

In Chapter 5 we performed a metagenomic investigation of the plaque microbiome associated with peri-implant health, mucositis and peri-implantitis. We found dramatic differences between healthy and diseased implants with a newly defined Peri-implant Red Complex (PiRC) composed by the 7 most discriminative species. Mucositis had an intermediate microbiome composition and it was characterized by high abundances of *Fusobacterium nucleatum* which appears to be a first step toward peri-implantitis development. Altogether, we provided evidence of a very strong association between the plaque microbiome and peri-implant diseases and microbes such as those in the PiRC set can potentially be targeted for diagnostic, prognostic, and therapeutic strategies.

In conclusion, it is clear that peri-implant diseases have a multifactorial etiology and there are several elements involved in their onset and in their progression. In this thesis I focused mainly on implant surface, microbiome colonization and their relationship; it is clear, however, that other elements should be considered, above all the host response.

Despite these limitations, several interesting indications have still emerged that could be useful in decreasing the incidence of peri-implant diseases. The *in-vitro* evidence for excellent bioactive properties of moderately rough surfaces, able to reduce bacterial colonization in case they are exposed to the oral environment, is an important insight. Even more important it is the opportunity and the ability to unravel always in more detail the peri-implant microbiome in health and disease. If on the one hand it may be helpful in developing antibacterial materials specifically designed for oral implantology, on the other it may allow the application of personalized treatment protocols in clinical practice. This may be particularly useful in the near future in the diagnostic and preventive steps, for example in assessing the risk of evolution of peri-implant mucositis in peri-implantitis, as well as in active therapy.

6.1 Future works

The overall results obtained in this research project have been very satisfactory and therefore do not represent a point of arrival but a starting point for future research. Our future work will focus in particular 1) on the further development of antibacterial surfaces for dental implants and 2) on a wider investigation of the peri-implant microbiome with the aim of employing the results already obtained and the new ones for potential applications in daily dental clinical practice.

As for the surfaces, in addition to sericin, other substances and materials with potential antibacterial properties will be taken into consideration, such as oral biosurfactants. Thanks to our results on the disease-associated peri-implant microbiome, it will be possible to test *in-vitro* the efficacy of these coatings directly against PiRC, the complex of bacterial species most associated with peri-implant diseases.

As for the peri-implant microbiome, future works will be of two types. On the one hand we will implement our cohort of enrolled patients and therefore of samples collected in order to further strengthen our data and our predictive models. On the other hand we will prospectively evaluate the changes of healthy and diseased peri-implant microbiome also considering the influence on the microbial ecology of any therapies in cases of mucositis and peri-implantitis. From these results we expect to have enough data, adequate accuracy and solid predictive models to potentially introduce on the dental market clinical tests based on metagenomics that will be able to help dentists in diagnosis, prevention and therapy of peri-implant diseases.

7. Appendix

7.1 Other works

In this chapter, I report the other research works I was involved in during my doctoral studies and that I did not include in the main discussion of the thesis. For these works, I report the citation of the article and its abstract.

Mandelli F, Ghensi P, Traini T

Biomimetic implant restoration made of human enamel and CAD/CAM block: a short report

Quintessence International (2019)

Abstract - This short report describes a clinical case in which an implant-supported crown was made using an extracted natural tooth as the outer shell. The same tooth had been previously relined for immediate loading without occlusal contacts. Using digital software, a composite resin mesostructure was fabricated in order to place the crown in the correct occlusal position, and the natural crown was ground using a computer-controlled milling machine to perfectly fit on the mesostructure.

Pasolli E, Asnicar F, Manara S, Zolfo M, Karcher N, Armanini F, Beghini F, Tett A, Ghensi P, Collado MC, Rice BL, DuLong C, Morgan XC, Golden CD, Quince C, Huttenhower C, Segata N

Extensive Unexplored Human Microbiome Diversity Revealed by Over 150,000 Genomes from Metagenomes Spanning Age, Geography, and Lifestyle

Cell (2019)

Abstract - The body-wide human microbiome plays a role in health, but its full diversity remains uncharacterized, particularly outside of the gut and in international populations. We leveraged 9,428 metagenomes to reconstruct 154,723 microbial genomes (45% of high quality) spanning body sites, ages, countries, and lifestyles. We recapitulated 4,930 species-level genome bins (SGBs), 77% without genomes in public repositories (unknown SGBs [uSGBs]). uSGBs are prevalent (in 93% of well-assembled samples), expand underrepresented phyla, and are enriched in non-Westernized populations (40% of the total SGBs). We annotated 2.85 M genes in SGBs, many associated with conditions including infant development (94,000) or Westernization (106,000). SGBs and uSGBs permit deeper microbiome analyses and increase the average mappability of metagenomic reads from 67.76% to 87.51% in the gut (median 94.26%) and 65.14% to 82.34% in the mouth. We thus identify thousands of microbial genomes from yet-to-be-named species, expand the

pangenomes of human-associated microbes, and allow better exploitation of metagenomic technologies.

Ghensi P, Tonetto G, Soldini MC, Bettio E, Mortellaro C, Soldini C

Dental implants with a platform-switched Morse taper connection and an Osteo Growth Induction surface

Journal of Craniofacial Surgery (2019)

Abstract – Aim. The aim of this study was to analyze the clinical outcomes after using an innovative implant system characterized by a modern platform-switched Morse taper connection and an osteo growth induction titanium surface (a particular type of SLA surface). Peri-implant bone loss (PBL) and implant success rate were examined after a 1- to 3-year follow-up. **Methods.** The study was conducted as a cross-sectional analysis on all patients treated from January 2011 to December 2014 using CLC CONIC implants. Implants were divided into 3 main groups, based on the duration of the follow-up (1 year, 2 years, and 3 years), then subgrouped by diameter, length, and type of prosthetic rehabilitation to compare differences in PBL. X-rays were taken at the time of surgery, at prosthetic loading, at 1 year, and then annually thereafter. Previously-established success criteria were used to assess the implants. Frequency analyses and comparisons between the means (with 95% CI) were conducted for the statistical analysis of the data collected. **Results.** One hundred twenty patients met inclusion and exclusion criteria, and completed the follow-up, and were thus eligible for the study, with a total of 261 CLC CONIC implants. The mean follow-up was 22.45 months. No implants failed, giving an overall success rate of 100%. The average PBL at 1-year follow-up was 0.047 mm, at 2 years it was 0.128 mm, and at 3 years it was 0.236 mm. **Conclusions.** The CLC CONIC implant system had a high success rate after 1 to 3 years of follow-up, in line with previous reports in the scientific literature. Combining platform switching with the Morse taper connection enabled stable bone levels to be achieved in the short to medium term.

Ghensi P, Cucchi A, Bonaccorso A, Ferroni L, Gardin C, Mortellaro C, Zavan B

In Vitro Effect of Bromelain on the Regenerative Properties of Mesenchymal Stem Cells

Journal of Craniofacial Surgery (2018)

Abstract - Background. Bromelain belongs to a group of protein-digesting enzymes obtained commercially from the fruit or stem of pineapple. Several studies demonstrated that bromelain exhibits various fibrinolytic, anti-edematous, antithrombotic, and anti-inflammatory activities supporting its application for many therapeutic benefits. The aim of this study was to analyze the effects of bromelain on the pro-wound healing activities and the regenerative properties of

mesenchymal stem cells. **Methods.** Mesenchymal stem cells were treated in vitro with bromelain alone or combined with dexamethasone sodium phosphate. Real-time polymerase chain reaction was performed to profile the expression of extracellular matrix components and remodeling enzymes, and cytokines. **Results**. The combination of bromelain and dexamethasone sodium phosphate induced a great activation of mesenchymal stem cells with an increase in hyaluronan and collagen production and anti-inflammatory cytokines release. **Conclusions.** Based on the results of this in vitro study, the combined use of bromelain and dexamethasone sodium phosphate stimulated the pro-wound healing activities and the regenerative properties of mesenchymal stem cells better than bromelain and dexamethasone alone.

Malchiodi L, Moro T, Cattina DP, Cucchi A, Ghensi P, Nocini PF

Implant rehabilitation of the edentulous jaws: Does tilting of posterior implants at an angle greater than 45° affect bone resorption and implant success?: A retrospective study

Clinical Implant Dentistry and Related Research (2018)

Abstract - Purpose. This study aimed to (1) investigate the success of posterior implants tilted >45° when 4 immediately loaded implants were used to support full-arch prostheses, eliminating any distal cantilever and (2) examine the effect on marginal bone loss (MBL) of different combinations of anterior multi-unit abutment (MUA) angles and posterior implant tilting angles. **Materials and Methods.** Records of patients rehabilitated according to the Columbus Bridge Protocol were analyzed. Peri-implant bone levels (PBLs) and MBL were measured for each implant. The influence of posterior implant tilting angle on PBL, MBL, and implant and prosthetic success rate was investigated. The impact on the same endpoints of different anterior MUA angles, and different combinations of anterior MUA and tilted posterior implant angles was also examined. **Results.** Records of 41 patients were analyzed, for a total of 46 complete rehabilitations, and 142 implants (52 anterior, 63 posterior tilted ≤45° [group 1], and 27 posterior tilted >45° [group 2]). No implants were lost during the follow-up (25.9 months), and no prosthetic complications were reported. Success rate for posterior implants was 100% in group 1 and 96.3% in group 2. Mean MBL differed significantly between the 2 groups (0.45 mm in group 1, 0.66 in group 2 [P = .04]), but not when the analysis was limited to implants in the same jaw. Implant tilting angle did not correlate with MBL and the MUA angle had no effect on bone resorption around posterior implants, neither in the sample as a whole nor in individual patients. **Conclusions.** Posterior implants tilted >45° to eliminate distal cantilever may be as safe as those tilted less in severely atrophic jaws rehabilitated with immediately loaded, full-arch prostheses supported on 4 implants. Further prospective studies on larger samples of patients and implants and with longer follow-up are needed to confirm these findings.

Caricasulo R, Malchiodi L, Ghensi P, Fantozzi G, Cucchi A

The influence of implant-abutment connection to peri-implant bone loss: a systematic review and meta-analysis.

Clinical Implant Dentistry and Related Research (2018)

Aim - Purpose. Different implant-abutment connections are available and it has been claimed they could have an effect on marginal bone loss. The aim of this review is to establish if implant connection configuration influences peri-implant bone loss (PBL) after functional loading. **Methods.** A specific question was formulated according to the Population, Intervention, Control, and Outcome (PICO): Does the type of implant-abutment connection (external, internal, or conical) have an influence on peri-implant bone loss? A PubMed/MEDLINE electronic search was conducted to identify English language publications published in international journals during the last decade (from 2006 to 2016). The search was conducted by using the Medical Subject Headings (MeSH) keywords "dental implants OR dental abutment AND external connection OR internal connection OR conical connection OR Morse Taper." Selected studies were randomized clinical trials and prospective studies; in vitro studies, case reports and retrospective studies were excluded. Titles and abstracts and, in the second phase, full texts, were evaluated autonomously and in duplicate by two reviewers. **Results.** A total of 1649 articles were found, but only 14 studies met the pre-established inclusion criteria and were considered suitable for meta-analytic analysis. The network meta-analysis (NMA) suggested a significant difference between the external and the conical connections; this was less evident for the internal and conical ones. Platform-switching (PS) seemed to positively affect bone levels, non-regarding the implant-connection it was applied to. **Conclusions.** Within the limitations of this systematic review, it can be concluded that crestal bone levels are better maintained in the short-medium term when internal kinds of interface are adopted. In particular, conical connections seem to be more advantageous, showing lower peri-implant bone loss, but further studies are necessary to investigate the efficacy of implant-abutment connection on stability of crestal bone levels.

Bressan E, Venezze AC, Magaz VR, Lops D, Ghensi P

Fixed Conometric Retention with CAD/CAM Conic Coupling Abutments and Prefabricated Syncone Caps: A Case Series

International Journal of Periodontics and Restorative Dentistry (2018)

Abstract - The conometric retention system was proposed and described as a predictable alternative to retain fixed implant-supported complete dentures and, more recently, to retain fixed partial restorations. Currently available studies describe a technique based on the Ankylos (Dentsply) implant system and stock conic coupling abutments. The purpose of this case series study is therefore to demonstrate the possibility of using Atlantis computer-aided design/computer-assisted manufacture technology to produce Conus abutments (Dentsply)

and using the fixed conometric retention with other implant brands for which appropriate stock conic coupling abutments are not available.

Venezze AC, Ghensi P, Stellini E, Magaz VR, Bressan E

Double Duplicate Technique for CAD/CAM Full-Arch Immediate Loading: A Technical Description and Case Report

International Journal of Periodontics and Restorative Dentistry (2018)

Abstract - Full-arch fixed implant-supported prostheses have shown high biologic success rates after long-term follow-up, along with technical and prosthetic complications. Adequate planning is necessary for immediate implant occlusal loading in a completely edentulous maxilla or mandible. For totally edentulous patients, the main prosthetic problem is the transfer of diagnostic information to the master cast when an immediate loading approach is used. The aim of this clinical case report is to illustrate a new prosthetic protocol for immediate implant loading in edentulous or potentially edentulous patients. This innovative procedure can successfully guide the clinician step by step in a predictable way from diagnosis to delivery of an immediately loaded implant-supported full-arch rehabilitation.

Ghensi P, Stablum W, Bettio E, Soldini MC, Tripi TR, Soldini C

Management of the exposure of a dense PTFE (d-PTFE) membrane in guided bone regeneration (GBR): a case report

Oral Implantology (2017)

Abstract – Objective. Guided bone regeneration (GBR) is a well-established and generally predictable method for repairing alveolar ridge defects and preparing edentulous sites for implant placement. Standard GBR involves filling the space underneath a membrane with autogenous bone or a mixture composed of autogenous bone particles and allogeneic bone tissue or heterologous biomaterials. The use of a barrier membrane for GBR has sometimes been associated with complications, however - reportedly involving exposure, infection, and collapse - and the non-resorbable types of membrane seem to be involved more often than the resorbable solutions. Such complications may be severe enough to defeat the object of the GBR procedure. A non-resorbable high-density polytetrafluoroethylene (d-PTFE) membrane has recently been designed specifically for use in bone-augmentation procedures that seems to assure a good bone regeneration process even when the membrane is exposed to the oral cavity. This case report describes an exposure of a d-PTFE membrane occurring after a maxillary GBR procedure and how it was overcome successfully, enabling implants insertion.

Malchiodi L, Balzani L, Cucchi A, Ghensi P, Nocini PF

Primary and Secondary Stability of Implants in Postextraction and Healed Sites: A Randomized Controlled Clinical Trial

International Journal of Oral and Maxillofacial Implants (2016)

Abstract - Purpose. This randomized clinical trial aimed to investigate the relationships between insertion torque, implant stability quotient (ISQ), and crestal bone loss (CBL) of implants placed in fresh or 12-week healed extraction sites. **Materials and Methods.** Forty patients were randomly assigned to one of two groups and had one implant placed immediately (test group, n = 20) or 12 weeks after extraction (control group, n = 20) at premolar or molar sites. For all implants, insertion torque and ISQ scores at insertion and loading were recorded. Patients were followed for up to 12 months. **Results.** Implant success was 100% in both groups. No differences were observed concerning both ISQ at insertion and ISQ at loading. A stronger correlation was detected between ISQ at insertion and insertion torque in the postextractive group (R = 0.83), than in the delayed group (R = 0.39), while ISQ at loading and insertion torque showed no correlation. CBL at 12 months was significantly different between test (0.68 ± 0.43 mm) and control (0.40 ± 0.26 mm, P = .02) groups. **Conclusion.** Implant placement timing (immediate or delayed) may affect correlation between insertion torque and ISQ at insertion with ISQ at loading. While insertion torque influences ISQ at insertion, it does not affect ISQ at loading because of successful osseointegration. Postextraction and delayed implants seem to have similar ISQ at insertion and at loading, but different CBL after 12 months of follow-up because of postextraction bone remodeling.

Ghensi P, Cucchi A, Creminelli L, Tomasi C, Zavan B, Maiorana C

Effect of Oral Administration of Bromelain on Postoperative Discomfort After Third Molar Surgery

Journal of Craniofacial Surgery (2017)

Abstract - Introduction. The purpose of this prospective randomized controlled clinical trial was to evaluate the effect of oral administration of bromelain on discomfort after mandibular third molar surgery. **Materials and methods.** Eighty-four consecutive patients requiring surgical removal of a single mandibular impacted third molar under local anesthesia were randomly assigned to receiving no drug (control group, Group A), postoperative 40 mg bromelain every 6 hours for 6 days (Group B), preoperative 4 mg dexamethasone sodium phosphate as a submucosal injection (Group C), and preoperative 4 mg dexamethasone sodium phosphate as a submucosal injection plus postoperative 40 mg bromelain every 6 hours for 6 days (Group D). Standardized surgical and analgesic protocols were adopted. Maximum interincisal distance and facial contours were measured at baseline and on postoperative days

2 and 7. Pain was measured objectively by counting the number of analgesic tablets required. Patient perception of the severity of symptoms was assessed with a follow-up questionnaire (PoSSe scale). **Results.** On postoperative day 2, there was a statistically significant reduction in facial edema in both Groups C and D compared with the control group, but no statistically significant differences were observed between Group B and the control group. At evaluation on postoperative day 7, Group D showed a statistically significant reduction in postoperative swelling compared with the control group. The combined use of bromelain and dexamethasone (Group D) induced a statistically significant reduction in the total number of analgesic tablets taken after surgery compared with the control group. The treatment groups had a limited, nonsignificant effect on trismus when compared with the control group. **Conclusions.** Bromelain used singly showed moderate anti-inflammatory efficacy, reducing postoperative swelling, albeit not to any significant extent compared with no drug administration. The combined use of bromelain and dexamethasone sodium phosphate yielded the best results in terms of control of postoperative discomfort.

Rea M, Ricci S, Ghensi P, Lang NP, Botticelli D, Soldini C

Marginal healing using Polyetheretherketone as healing abutments: an experimental study in dogs

Clinical Oral Implants Research (2017)

Abstract - Objective. To evaluate the marginal soft and hard tissue healing at titanium and Polyetheretherketone (PEEK) healing implant abutments over a 4-month period. **Material and methods**. In six Labrador dogs, all mandibular premolars and first molars were extracted. After 4 months of healing, flaps were elevated, and two implants were installed at each side of the mandible, one in the premolar and the other in the molar regions. Four different types of healing abutments were positioned on the top of each implant: (i) titanium (Ti); (ii) PEEK material bonded to a base made of titanium (Ti-P), randomly positioned in the premolar region; (iii) PEEK, pristine (P); and (iv) PEEK, roughened (P-R), randomly positioned in the molar region. The flaps were sutured to allow a non-submerged healing, and after 4 months, the animals were sacrificed and ground sections obtained for histological evaluation. **Results.** A higher resorption of the buccal bone crest was observed at the PEEK bonded to a base made of titanium abutments (1.0 ± 0.3 mm) compared to those made of titanium (0.3 ± 0.4 mm). However, similar dimensions of the peri-implant mucosa and similar locations of the soft tissues in relation to the implant shoulder were observed. No statistically significant differences were seen in the outcomes when the pristine PEEK was compared with the roughened PEEK abutments. The mean apical extension of the junctional epithelium did not exceed the implant shoulder at any of the abutment types used. **Conclusions.** The coronal level of the hard and soft tissues allows the conclusion that the use of PEEK as healing abutments may be indicated.

Cucchi A, Caricasulo R, Ghensi P, Malchiodi L, Corinaldesi G

Prevention of BRONJ Using PRGF in a Totally Edentulous Patient Restored With Postextraction Implants: A Case Report

Journal of Oral Implantology (2016)

Abstract - The aim of this report was to show how a strict protocol based on recording CTX values and using PRGF to enhance healing processes enabled implant-supported prosthetic rehabilitation of a patient with a high risk of MRONJ.

8. References

Abrahamsson I, Berglundh T, Linder E, Lang NP, Lindhe J. Early bone formation adjacent to rough and turned endosseous implant surfaces. An experimental study in the dog. Clin Oral Implants Res. 2004;15:381–92.

Abrahamsson I, Berglundh T. Effects of different implant surfaces and designs on marginal bone-level alterations: a review. Clin Oral Implants Res. 2009; 20 Suppl 4:207-15.

Abrahamsson I, Berglundh T, Lindhe J. The mucosal barrier following abutment dis/reconnection. An experimental study in dogs. J Clin Periodontol. 1997;24:568–72.

Abrahamsson I, Berglundh T, Moon I-S, Lindhe J. Peri-implant tissues at submerged and non-submerged titanium implants. J Clin Periodontol. 1999;26:600–7.

Abrahamsson I, Berglundh T, Wennström J, Lindhe J. The peri-implant hard and soft tissues at different implant systems. A comparative study in the dog. Clin Oral Implants Res. 1996;7:212–9.

Abrahamsson KH, Wennström JL, Berglundh T, Abrahamsson I. Altered expectations on dental implant therapy; views of patients referred for treatment of peri-implantitis. Clin Oral Implants Res. 2017;28:437–42.

Abshagen K, Schrodi I, Gerber T, Vollmar B. In vivo analysis of biocompatibility and vascularization of the synthetic bone grafting substitute NanoBone®. Vol. 91A, Journal of Biomedical Materials Research Part A. 2009. p. 557–66.

Abubucker S, Segata N, Goll J, Schubert AM, Izard J, Cantarel BL, et al. Metabolic reconstruction for metagenomic data and its application to the human microbiome. PLoS Comput Biol. 2012;8:e1002358.

Aghaloo TL, Moy PK. Which hard tissue augmentation techniques are the most successful in furnishing bony support for implant placement? Int J Oral Maxillofac Implants. 2007;22 Suppl:49–70.

Aglietta M, Siciliano VI, Zwahlen M, Brägger U, Pjetursson BE, Lang NP, et al. A systematic review of the survival and complication rates of implant supported fixed dental prostheses with cantilever extensions after an observation period of at least 5 years. Vol. 20, Clinical Oral Implants Research. 2009. p. 441–51.

Aguirre-Zorzano LA, Estefanía-Fresco R, Telletxea O, Bravo M. Prevalence of peri-implant inflammatory disease in patients with a history of periodontal disease who receive supportive periodontal therapy. Clin Oral Implants Res. 2015;26:1338–44.

Ahluwalia A, De Rossi D, Ristori C, Schirone A, Serra G. A comparative study of protein immobilization techniques for optical immunosensors. Vol. 7, Biosensors and Bioelectronics. 1992. p. 207–14.

Akiyama H, Torigoe R, Arata J. Interaction of Staphylococcus aureus cells and silk threads in vitro and in mouse skin. Vol. 6, Journal of Dermatological Science. 1993. p. 73.

Albouy JP, Abrahamsson I, Berglundh T. Spontaneous progression of experimental peri-implantitis at implants with different surface characteristics: an experimental study in dogs. J Clin Periodontol. 2012;39(2):182-7.

Albrektsson T, Brånemark PI, Hansson HA, Lindström J. Osseointegrated titanium implants. Requirements for ensuring a long-lasting, direct bone-to-implant anchorage in man. Acta Orthop Scand. 1981;52:155–70.

Albrektsson T, Buser D, Sennerby L. Crestal bone loss and oral implants. Clin Implant Dent Relat Res. 2012;14:783–91.

Albrektsson T, Dahlin C, Jemt T, Sennerby L, Turri A, Wennerberg A. Is marginal bone loss around oral implants the result of a provoked foreign body reaction? Clin Implant Dent Relat Res. 2014;16:155–65.

Albrektsson T, Isidor F. Consensus report: implant therapy. In: Proceedings of the 1st European Workshop on Periodontology. Quintessence Berlin; 1994. p. 365–9.

Albrektsson T, Sennerby L. State of the art in oral implants. J Clin Periodontol. 1991;18:474–81.

Albrektsson T, Wennerberg A. Oral implant surfaces: Part 1--review focusing on topographic and chemical properties of different surfaces and in vivo responses to them. Int J Prosthodont. 2004;17:536–43.

Albrektsson T, Zarb GA. Determinants of correct clinical reporting. Ont Dent. 1999;76:29–33.

Albrektsson T, Zarb G, Worthington P, Eriksson AR. The long-term efficacy of currently used dental implants: a review and proposed criteria of success. Int J Oral Maxillofac Implants. 1986;1:11–25.

Almeida EO, Freitas AC Jr, Bonfante EA, Marotta L, Silva NRFA, Coelho PG. Mechanical testing of implant-supported anterior crowns with different implant/abutment connections. Int J Oral Maxillofac Implants. 2013;28:103–8.

Annibali S, Bignozzi I, Cristalli MP, Graziani F, La Monaca G, Polimeni A. Peri-implant marginal bone level: a systematic review and meta-analysis of studies comparing platform switching versus conventionally restored implants. J Clin Periodontol. 2012a;39:1097–113.

Annibali S, Cristalli MP, Dell'Aquila D, Bignozzi I, La Monaca G, Pilloni A. Short dental implants: a systematic review. J Dent Res. 2012b;91:25–32.

Antoci V Jr, King SB, Jose B, Parvizi J, Zeiger AR, Wickstrom E, et al. Vancomycin covalently bonded to titanium alloy prevents bacterial colonization. J Orthop Res. 2007;25:858–66.

Apatzidou D, Lappin DF, Hamilton G, Papadopoulos CA, Konstantinidis A, Riggio MP. Microbiome of peri-implantitis affected and healthy dental sites in patients with a history of chronic periodontitis. Arch Oral Biol. 2017;83:145–52.

Aramwit P, Siritientong T, Srichana T. Potential applications of silk sericin, a natural protein from textile industry by-products. Waste Manag Res. 2012;30:217–24.

Arnhart C, Kielbassa AM, Martinez-de Fuentes R, Goldstein M, Jackowski J, Lorenzoni M, et al. Comparison of variable-thread tapered implant designs to a standard tapered implant design after immediate loading. A 3-year multicentre randomised controlled trial. Eur J Oral Implantol. 2012;5:123–36.

Aronesty E. Comparison of Sequencing Utility Programs. Vol. 7, The Open Bioinformatics Journal. 2013. p. 1–8.

Asnicar F, Weingart G, Tickle TL, Huttenhower C, Segata N. Compact graphical representation of phylogenetic data and metadata with GraPhlAn. PeerJ. 2015;3:e1029.

Åstrand P, Ahlqvist J, Gunne J, Nilson H. Implant treatment of patients with edentulous jaws: a 20-year follow-up. Clin Implant Dent Relat Res. 2008;10:207–17.

Atieh MA, Ibrahim HM, Atieh AH. Platform switching for marginal bone preservation around dental implants: a systematic review and meta-analysis. J Periodontol. 2010;81:1350–66.

Atsuta I, Ayukawa Y, Kondo R, Oshiro W, Matsuura Y, Furuhashi A, et al. Soft tissue sealing around dental implants based on histological interpretation. J Prosthodont Res. 2016;60:3–11.

Barfeie A, Wilson J, Rees J. Implant surface characteristics and their effect on osseointegration. Br Dent J. 2015;218:E9.

Barros RRM, Novaes AB Jr, Muglia VA, Iezzi G, Piattelli A. Influence of interimplant distances and placement depth on peri-implant bone remodeling of adjacent and immediately loaded Morse cone connection implants: a histomorphometric study in dogs. Clin Oral Implants Res. 2010;21:371–8.

Bekos EJ, Ranieri JP, Aebischer P, Gardella JA, Bright FV. Structural Changes of Bovine Serum Albumin upon Adsorption to Modified Fluoropolymer Substrates Used for Neural Cell Attachment Studies. Vol. 11, Langmuir. 1995. p. 984–9.

Belibasakis GN. Microbiological and immuno-pathological aspects of peri-implant diseases. Arch Oral Biol. 2014;59:66–72.

Belibasakis GN, Charalampakis G, Bostanci N, Stadlinger B. Peri-implant infections of oral biofilm etiology. Adv Exp Med Biol. 2015;830:69–84.

Berglundh T, Abrahamsson I, Welander M, Lang NP, Lindhe J. Morphogenesis of the peri-implant mucosa: an experimental study in dogs. Clin Oral Implants Res. 2007;18:1–8.

Berglundh T, Armitage G, Araujo MG, Avila-Ortiz G, Blanco J, Camargo PM, et al. Peri-implant diseases and conditions: Consensus report of workgroup 4 of the 2017 World Workshop on the Classification of Periodontal and Peri-Implant Diseases and Conditions. J Clin Periodontol. 2018;45:S286–91.

Berglundh T, Lindhe J. Dimension of the periimplant mucosa. Vol. 23, Journal of Clinical Periodontology. 1996a. p. 971–3.

Berglundh T, Lindhe J. Dimension of the periimplant mucosa. Biological width revisited. J Clin Periodontol. 1996b;23:971–3.

Berglundh T, Lindhe J, Ericsson I, Marinello CP, Liljenberg B, Thomsen P. The soft tissue barrier at implants and teeth. Clin Oral Implants Res. 1991;2:81–90.

Berglundh T, Zitzmann NU, Donati M. Are peri-implantitis lesions different from periodontitis lesions? J Clin Periodontol. 2011;38 Suppl 11:188–202.

Beutner R, Michael J, Schwenzer B, Scharnweber D. Biological nano-functionalization of titanium-based biomaterial surfaces: a flexible toolbox. J R Soc Interface. 2010;7 Suppl 1:S93–105.

Bigerelle M, Anselme K, Noël B, Ruderman I, Hardouin P, Iost A. Improvement in the

morphology of Ti-based surfaces: a new process to increase in vitro human osteoblast response. Biomaterials. 2002;23:1563–77.

Block MS. Dental Implants: The Last 100 Years. J Oral Maxillofac Surg. 2018;76:11–26.

Bonfante EA, Coelho PG. A Critical Perspective on Mechanical Testing of Implants and Prostheses. Adv Dent Res. 2016;28:18–27.

Bosshardt DD, Chappuis V, Buser D. Osseointegration of titanium, titanium alloy and zirconia dental implants: current knowledge and open questions. Periodontol 2000. 2017;73:22–40.

Bosshardt DD, Salvi GE, Huynh-Ba G, Ivanovski S, Donos N, Lang NP. The role of bone debris in early healing adjacent to hydrophilic and hydrophobic implant surfaces in man. Clin Oral Implants Res. 2011;22:357–64.

Bouazza-Juanes K, Martínez-González A, Peiró G, Ródenas J-J, López-Mollá M-V. Effect of platform switching on the peri-implant bone: A finite element study. J Clin Exp Dent. 2015;7:e483–8.

Brånemark PI, Adell R, Breine U, Hansson BO, Lindström J, Ohlsson A. Intra-osseous anchorage of dental prostheses. I. Experimental studies. Scand J Plast Reconstr Surg. 1969a;3:81–100.

Brånemark P-I, -I. Brånemark P, Breine U, Adell R, Hansson BO, Lindström J, et al. Intra-Osseous Anchorage of Dental Prostheses:I. Experimental Studies. Vol. 3, Scandinavian Journal of Plastic and Reconstructive Surgery. 1969b. p. 81–100.

Breiman L. Random Forests. Mach Learn. 2001;45:5–32.

Bressan E, Carraro A, Ferroni L, Gardin C, Sbricoli L, Guazzo R, et al. Nanotechnology to drive stem cell commitment. Nanomedicine . 2013a;8:469–86.

Bressan E, Ferroni L, Gardin C, Pinton P, Stellini E, Botticelli D, et al. Donor age-related biological properties of human dental pulp stem cells change in nanostructured scaffolds. PLoS One. 2012;7:e49146.

Bressan E, Sbricoli L, Guazzo R, Tocco I, Roman M, Vindigni V, et al. Nanostructured Surfaces of Dental Implants. Vol. 14, International Journal of Molecular Sciences. 2013b. p. 1918–31.

Broggini N, McManus LM, Hermann JS, Medina R, Schenk RK, Buser D, et al. Peri-implant Inflammation Defined by the Implant-Abutment Interface. Vol. 85, Journal of Dental Research. 2006. p. 473–8.

Broggini N, McManus LM, Hermann JS, Medina RU, Oates TW, Schenk RK, et al. Persistent acute inflammation at the implant-abutment interface. J Dent Res. 2003;82:232–7.

Bumgardner JD, Adatrow P, Haggard WO, Norowski PA. Emerging antibacterial biomaterial strategies for the prevention of peri-implant inflammatory diseases. Int J Oral Maxillofac Implants. 2011;26:553–60.

Burgos PM, Meirelles L, Sennerby L. Influence of furrow width on the stability of titanium implants. A study in the rabbit. 1. 2011;3:2–9.

Buser D, Sennerby L, De Bruyn H. Modern implant dentistry based on osseointegration: 50 years of progress, current trends and open questions. Periodontol 2000. 2017;73:7–21.

Buser D, Broggini N, Wieland M, Schenk RK, Denzer AJ, Cochran DL, Hoffmann B, Lussi A, Steinemann SG. Enhanced bone apposition to a chemically modified SLA titanium surface. J Dent Res 2004;83:529–533.

Buser D, Weber HP, Brägger U, Balsiger C. Tissue integration of one-stage implants: three-year results of a prospective longitudinal study with hollow cylinder and hollow screw implants. Quintessence Int. 1994;25:679–86.

Buser D, Weber HP, Donath K. Soft tissue reactions to non-submerged unloaded titanium implants in beagle dogs. Journal of. 1992;

Cai K, Frant M, Bossert J, Hildebrand G, Liefeith K, Jandt KD. Surface functionalized titanium thin films: zeta-potential, protein adsorption and cell proliferation. Colloids Surf B Biointerfaces. 2006;50:1–8.

Camargos Gde V, do Prado CJ, das Neves FD, Sartori IA. Clinical outcomes of single dental implants with external connections: results after 2 to 13 years. Int J Oral Maxillofac Implants. 2012;27(4):935-44.

Canullo L, Peñarrocha-Oltra D, Covani U, Botticelli D, Serino G, Penarrocha M. Clinical and microbiological findings in patients with peri-implantitis: a cross-sectional study. Vol. 27, Clinical Oral Implants Research. 2016. p. 376–82.

Canullo L, Peñarrocha-Oltra D, Covani U, Rossetti P. Microbiologic and Clinical Findings of Implants in Healthy Condition and with Peri-Implantitis. Vol. 30, The International Journal of Oral & Maxillofacial Implants. 2015. p. 834–42.

Carano RAD, Filvaroff EH. Angiogenesis and bone repair. Drug Discov Today. 2003;8:980–9.

Carcuac O, Derks J, Charalampakis G, Abrahamsson I, Wennström J, Berglundh T. Adjunctive Systemic and Local Antimicrobial Therapy in the Surgical Treatment of Peri-implantitis: A Randomized Controlled Clinical Trial. J Dent Res. 2016;95:50–7.

Carcuac O, Abrahamsson I, Albouy JP, Linder E, Larsson L, Berglundh T. Experimental periodontitis and peri-implantitis in dogs. Clin Oral Implants Res. 2013;24(4):363-71.

Caricasulo R, Malchiodi L, Ghensi P, Fantozzi G, Cucchi A. The influence of implant-abutment connection to peri-implant bone loss: A systematic review and meta-analysis. Clin Implant Dent Relat Res. 2018;20:653–64.

Carlsson GE. Clinical morbidity and sequelae of treatment with complete dentures. J Prosthet Dent. 1998;79(1):17-23. Review.

Caroprese M, Soldini C, Ricci S, Rea M, Lang NP, Botticelli D. Healing at implants placed in bone of different morphology: an experimental study in dogs. Clin Oral Implants Res. 2017;28:961–5.

Carr AB. Successful long-term treatment outcomes in the field of osseointegrated implants: prosthodontic determinants. Int J Prosthodont. 1998;11:502–12.

Carr AB, Laney WR. Maximum occlusal force levels in patients with osseointegrated oral implant prostheses and patients with complete dentures. Int J Oral Maxillofac Implants. 1987;2(2):101-8.

Casadei A, Epis R, Ferroni L, Tocco I, Gardin C, Bressan E, et al. Adipose tissue regeneration: a state of the art. J Biomed Biotechnol. 2012;2012:462543.

Cassetta M, Di Mambro A, Giansanti M, Brandetti G, Calasso S. A 36-month follow-up prospective cohort study on peri-implant bone loss of Morse Taper connection implants with platform switching. J Oral Sci. 2016;58:49–57.

Cássio do Nascimento DMD, Paola Kirsten Miani DMD, Pedrazzi V, Gonçalves RB, Ribeiro RF, Faria ACL. Leakage of saliva through the implant-abutment interface: in vitro evaluation of three different implant connections under unloaded and loaded conditions. Int J Oral Maxillofac Implants. 2012;27:551–60.

Cavalcanti YW, Soare RV, Leite Assis MA, Zenóbio EG, Girundi FM. Titanium surface roughing treatments contribute to higher interaction with salivary proteins MG2 and lactoferrin. J Contemp Dent Pract. 2015;16(2):141–146

Ceruso FM, Barnaba P, Mazzoleni S, Ottria L, Gargari M, Zuccon A, et al. Implant-abutment connections on single crowns: a systematic review. Oral Implantol . 2017;10:349–53.

Chan RTH, Marçal H, Russell RA, Holden PJ, Foster LJR. Application of Polyethylene Glycol to Promote Cellular Biocompatibility of Polyhydroxybutyrate Films. Vol. 2011, International Journal of Polymer Science. 2011. p. 1–9.

Charalampakis G, Belibasakis GN. Microbiome of peri-implant infections: lessons from conventional, molecular and metagenomic analyses. Virulence. 2015;6:183–7.

Cheng S-S, Chittur KK, Sukenik CN, Culp LA, Lewandowska K. The Conformation of Fibronectin on Self-Assembled Monolayers with Different Surface Composition: An FTIR/ATR Study. Vol. 162, Journal of Colloid and Interface Science. 1994. p. 135–43.

Cho W-R, Huh Y-H, Park C-J, Cho L-R. Effect of cyclic loading and retightening on reverse torque value in external and internal implants. J Adv Prosthodont. 2015;7:288–93.

Chouirfa H, Bouloussa H, Migonney V, Falentin-Daudré C. Review of titanium surface modification techniques and coatings for antibacterial applications. Vol. 83, Acta Biomaterialia. 2019. p. 37–54.

Chrcanovic BR, Albrektsson T, Wennerberg A. Reasons for failures of oral implants. J Oral Rehabil. 2014;41:443–76.

Chrcanovic BR, Albrektsson T, Wennerberg A. Platform switch and dental implants: A meta-analysis. Vol. 43, Journal of Dentistry. 2015. p. 629–46.

Cochran DL, Schenk RK, Lussi A. Bone response to unloaded and loaded titanium implants with a sandblasted and acid-etched surface: A histometric study in the canine mandible. Research: An Official …. 1998a;.

Cochran DL, Schenk RK, Lussi A, Higginbottom FL, Buser D. Bone response to unloaded and loaded titanium implants with a sandblasted and acid-etched surface: a histometric study in the canine mandible. J Biomed Mater Res. 1998b;40:1–11.

Coelho PG, Granjeiro JM, Romanos GE, Suzuki M, Silva NRF, Cardaropoli G, et al. Basic research methods and current trends of dental implant surfaces. J Biomed Mater Res B Appl Biomater. 2009;88:579–96.

Çomut AA, Weber HP, Shortkroff S, Spector M, Cui F. Connective tissue orientation around

dental implants in a canine model. Clin Oral Implants Res. 2001;12:433–40.

Consortium THMP, The Human Microbiome Project Consortium. Structure, function and diversity of the healthy human microbiome. Vol. 486, Nature. 2012. p. 207–14.

Cooper LF, Tarnow D, Froum S, Moriarty J, De Kok IJ. Comparison of Marginal Bone Changes with Internal Conus and External Hexagon Design Implant Systems: A Prospective, Randomized Study. Int J Periodontics Restorative Dent. 2016;36:631–42.

Cooper L, Reside G, Stanford C, Barwacz C, Feine J, Nader S, et al. A Multicenter Randomized Comparative Trial of Implants with Different Abutment Interfaces to Replace Anterior Maxillary Single Teeth. Vol. 30, The International Journal of Oral & Maxillofacial Implants. 2015. p. 622–32.

Coppedê AR, Bersani E, de Mattos M da GC, Rodrigues RCS, de Mattias Sartori IA, Ribeiro RF. Fracture resistance of the implant-abutment connection in implants with internal hex and internal conical connections under oblique compressive loading: an in vitro study. Int J Prosthodont. 2009;22.

Craig JB. Practical surface analysis, volume 1—auger and x-ray photoelectron spectroscopy: D. Briggs and MP Seah (editors), Wiley, Chichester, 1990. Pages xiv+ 657.£ 85.00. Elsevier; 1991.

Crespi R, Capparè P, Gherlone E. Radiographic evaluation of marginal bone levels around platform-switched and non-platform-switched implants used in an immediate loading protocol. Int J Oral Maxillofac Implants. 2009;24:920–6.

Dabdoub SM, Tsigarida AA, Kumar PS. Patient-specific analysis of periodontal and peri-implant microbiomes. J Dent Res. 2013;92:168S – 75S.

Dalago HR, Filho GS, Rodrigues MAP, Renvert S, Bianchini MA. Risk indicators for Peri-implantitis. A cross-sectional study with 916 implants. Vol. 28, Clinical Oral Implants Research. 2017. p. 144–50.

Darcey J, Eldridge D. Fifty Years of Dental Implant Development: a Continuous Evolution. Dent Hist. 2016;61:75–92.

Darst SA, Robertson CR, Berzofsky JA. Adsorption of the protein antigen myoglobin affects the binding of conformation-specific monoclonal antibodies. Vol. 53, Biophysical Journal. 1988. p. 533–9.

Daubert DM, Weinstein BF, Bordin S, Leroux BG, Flemmig TF. Prevalence and Predictive Factors for Peri-Implant Disease and Implant Failure: A Cross-Sectional Analysis. Vol. 86, Journal of Periodontology. 2015. p. 337–47.

Davies J, Testori T, Del Fabbro M. Il ruolo delle superfici implantari. 2009;

De Bruyn H, Christiaens V, Doornewaard R, Jacobsson M, Cosyn J, Jacquet W, et al. Implant surface roughness and patient factors on long-term peri-implant bone loss. Periodontol 2000. 2017;73:218–27.

Degidi M, Nardi D, Piattelli A. One abutment at one time: non-removal of an immediate abutment and its effect on bone healing around subcrestal tapered implants. Clin Oral Implants Res. 2011;22:1303–7.

Deligianni DD, Katsala N, Ladas S, Sotiropoulou D, Amedee J, Missirlis YF. Effect of surface

roughness of the titanium alloy Ti–6Al–4V on human bone marrow cell response and on protein adsorption. Biomaterials. 2001;22:1241–51.

Derks J, Schaller D, Håkansson J, Wennström JL, Tomasi C, Berglundh T. Effectiveness of Implant Therapy Analyzed in a Swedish Population. Vol. 95, Journal of Dental Research. 2016. p. 43–9.

Derks J, Schaller D, Håkansson J, Wennström JL, Tomasi C, Berglundh T. Peri-implantitis - onset and pattern of progression. J Clin Periodontol. 2016 Apr;43(4):383-8.

Derks J, Tomasi C. Peri-implant health and disease. A systematic review of current epidemiology. J Clin Periodontol. 2015;42:S158–71.

Dibart S, Warbington M, Su MF, Skobe Z. In vitro evaluation of the implant-abutment bacterial seal: the locking taper system. Int J Oral Maxillofac Implants. 2005;20:732–7.

Donati C, Zolfo M, Albanese D, Tin Truong D, Asnicar F, Iebba V, et al. Uncovering oral Neisseria tropism and persistence using metagenomic sequencing. Nat Microbiol. 2016;1:16070.

Doornewaard R, Christiaens V. Long-term effect of surface roughness and patients' factors on crestal bone loss at dental implants. A systematic review and meta-analysis. Implant Dent. 2017;

Do T, Devine D, Marsh PD. Oral biofilms: molecular analysis, challenges, and future prospects in dental diagnostics. Clin Cosmet Investig Dent. 2013;5:11–9.

Du J, Zu Y, Li J, Du S, Xu Y, Zhang L, et al. Extracellular matrix stiffness dictates Wnt expression through integrin pathway. Sci Rep. 2016;6:20395.

Ebadian AR, Kadkhodazadeh M, Zarnegarnia P, Dahlén G. Bacterial analysis of peri-implantitis and chronic periodontitis in Iranian subjects. Acta Med Iran. 2012;50:486–92.

Eckardt H, Bundgaard KG, Christensen KS, Lind M, Hansen ES, Hvid I. Effects of locally applied vascular endothelial growth factor (VEGF) and VEGF-inhibitor to the rabbit tibia during distraction osteogenesis. Vol. 21, Journal of Orthopaedic Research. 2003. p. 335–40.

Eckert SE, Parein A, Myshin HL, Padilla JL. Validation of dental implant systems through a review of literature supplied by system manufacturers. J Prosthet Dent. 1997;77:271–9.

Edgar RC. MUSCLE: multiple sequence alignment with high accuracy and high throughput. Nucleic Acids Res. 2004;32:1792–7.

E. Jung R, Zembic A, Pjetursson BE, Zwahlen M, S. Thoma D. Systematic review of the survival rate and the incidence of biological, technical, and aesthetic complications of single crowns on implants reported in longitudinal studies with a mean follow-up of 5 years. Clin Oral Implants Res. 2012;23:2–21.

Elias CN, Lima JHC, Valiev R, Meyers MA. Biomedical applications of titanium and its alloys. JOM. 2008;60:46–9.

Ellingsen JE. A study on the mechanism of protein adsorption to TiO2. Biomaterials. 1991;12:593–6.

Ellingsen JE, Thomsen P, Lyngstadaas SP. Advances in dental implant materials and tissue regeneration. Periodontol 2000. 2006;41:136–56.

Eming SA, Krieg T, Davidson JM. Inflammation in wound repair: molecular and cellular mechanisms. J Invest Dermatol. 2007;127:514–25.

Ericsson I, Nilner K, Klinge B, Glantz P-O. Radiographical and histological characteristics of ssubmerged and nonsubmerged titanium implants. An experimental study in the Labrador dog. Clin Oral Implants Res. 1996;7:20–6.

Esposito M, Ardebili Y, Worthington HV. Interventions for replacing missing teeth: different types of dental implants. Cochrane Database Syst Rev. 2014;CD003815.

Esposito M, Grusovin MG, Worthington HV. Treatment of peri-implantitis: what interventions are effective? A Cochrane systematic review. Eur J Oral Implantol. 2012;5 Suppl:S21–41.

Esposito M, Maghaireh H, Pistilli R, Grusovin MG, Lee ST, Gualini F, et al. Dental implants with internal versus external connections: 1-year post-loading results from a pragmatic multicenter randomised controlled trial. Eur J Oral Implantol. 2015;8:331–44.

Esposito M, Maghaireh H, Pistilli R, Grusovin MG, Lee ST, Trullenque-Eriksson A, et al. Dental implants with internal versus external connections: 5-year post-loading results from a pragmatic multicenter randomised controlled trial. Eur J Oral Implantol. 2016;9 Suppl 1:129–41.

Faveri M, Figueiredo LC, Shibli JA, Pérez-Chaparro PJ, Feres M. Microbiological diversity of peri-implantitis biofilms. Adv Exp Med Biol. 2015;830:85–96.

Feller L, Jadwat Y, Khammissa RAG, Meyerov R, Schechter I, Lemmer J. Cellular responses evoked by different surface characteristics of intraosseous titanium implants. Biomed Res Int. 2015;2015:171945.

Fernández-Formoso N, Rilo B, Mora MJ, Martínez-Silva I, Díaz-Afonso AM. Radiographic evaluation of marginal bone maintenance around tissue level implant and bone level implant: a randomised controlled trial. A 1-year follow-up. Vol. 39, Journal of Oral Rehabilitation. 2012. p. 830–7.

Ferreira SD, Silva GLM, Cortelli JR, Costa JE, Costa FO. Prevalence and risk variables for peri-implant disease in Brazilian subjects. J Clin Periodontol. 2006;33:929–35.

Ferroni L, Gardin C, Sivolella S, Brunello G, Berengo M, Piattelli A, et al. A hyaluronan-based scaffold for the in vitro construction of dental pulp-like tissue. Int J Mol Sci. 2015;16:4666–81.

Ferroni L, Gardin C, Tocco I, Epis R, Casadei A, Vindigni V, et al. Potential for neural differentiation of mesenchymal stem cells. Adv Biochem Eng Biotechnol. 2013;129:89–115.

Figallo E, Flaibani M, Zavan B, Abatangelo G, Elvassore N. Micropatterned biopolymer 3D scaffold for static and dynamic culture of human fibroblasts. Biotechnol Prog. 2007;23:210–6.

Fleck C, Eifler D. Corrosion, fatigue and corrosion fatigue behaviour of metal implant materials, especially titanium alloys. Int J Fatigue. 2010;32:929–35.

Freitas AC Jr, Bonfante EA, Rocha EP, Silva NRFA, Marotta L, Coelho PG. Effect of implant connection and restoration design (screwed vs. cemented) in reliability and failure modes of anterior crowns. Eur J Oral Sci. 2011;119:323–30.

Freitas-Júnior AC, Almeida EO, Bonfante EA, Nelson R F, Coelho PG. Reliability and failure

modes of internal conical dental implant connections. Vol. 24, Clinical Oral Implants Research. 2013. p. 197–202.

Fu J-H, Hsu Y-T, Wang H-L. Identifying occlusal overload and how to deal with it to avoid marginal bone loss around implants. Eur J Oral Implantol. 2012;5 Suppl:S91–103.

Galli C, Macaluso GM, Piemontese M, Passeri G. Titanium Topography Controls FoxO/β-catenin Signaling. J Dent Res. 2011;90:360–4.

Galli C, Passeri G, Ravanetti F, Elezi E, Pedrazzoni M, Macaluso GM. Rough surface topography enhances the activation of Wnt/β-catenin signaling in mesenchymal cells. Vol. 95A, Journal of Biomedical Materials Research Part A. 2010. p. 682–90.

Gan L, Pilliar R. Calcium phosphate sol–gel-derived thin films on porous-surfaced implants for enhanced osteoconductivity. Part I: Synthesis and characterization. Vol. 25, Biomaterials. 2004. p. 5303–12.

Gardin C, Bressan E, Ferroni L, Nalesso E, Vindigni V, Stellini E, et al. In Vitro Concurrent Endothelial and Osteogenic Commitment of Adipose-Derived Stem Cells and Their Genomical Analyses Through Comparative Genomic Hybridization Array: Novel Strategies to Increase the Successful Engraftment of Tissue-Engineered Bone Grafts. Vol. 21, Stem Cells and Development. 2012. p. 767–77.

Gardin C, Ricci S, Ferroni L, Guazzo R, Sbricoli L, De Benedictis G, et al. Decellularization and Delipidation Protocols of Bovine Bone and Pericardium for Bone Grafting and Guided Bone Regeneration Procedures. PLoS One. 2015;10:e0132344.

Gardner DM. Platform switching as a means to achieving implant esthetics. N Y State Dent J. 2005;71:34–7.

Gharbia SE, Shah HN. Heterogeneity within Fusobacterium nucleatum, proposal of four subspecies. Lett Appl Microbiol. 1990;10:105–8.

Ghensi P, Bressan E, Gardin C, Ferroni L, Ruffato L, Caberlotto M, et al. Osteo Growth Induction titanium surface treatment reduces ROS production of mesenchymal stem cells increasing their osteogenic commitment. Vol. 74, Materials Science and Engineering: C. 2017a. p. 389–98.

Ghensi P, Bressan E, Gardin C, Ferroni L, Soldini MC, Mandelli F, et al. The Biological Properties of OGI Surfaces Positively Act on Osteogenic and Angiogenic Commitment of Mesenchymal Stem Cells. Materials . 2017b;10.

Ghensi P, Stablum W, Bettio E, Soldini MC, Tripi TR, Soldini C. Management of the exposure of a dense PTFE (d-PTFE) membrane in guided bone regeneration (GBR): a case report. Oral Implantol . 2017c;10:335–42.

Ghensi P, Tonetto G, Soldini C, Bettio E, Mortellaro C, Soldini C. Dental Implants With a Platform-Switched Morse Taper Connection and an Osteo Growth Induction Surface. J Craniofac Surg. 2018;

Gibon E, Lu L, Goodman SB. Aging, inflammation, stem cells, and bone healing. Stem Cell Res Ther. 2016;7:44.

Glibert M, Vervaeke S, Jacquet W, Vermeersch K, Östman P-O, De Bruyn H. A randomized controlled clinical trial to assess crestal bone remodeling of four different implant designs. Clin Implant Dent Relat Res. 2018;20:455–62.

Goiato MC, Pellizzer EP, da Silva EVF, Bonatto L da R, dos Santos DM. Is the internal connection more efficient than external connection in mechanical, biological, and esthetical point of views? A systematic review. Oral Maxillofac Surg. 2015;19:229–42.

Gotfredsen K, Berglundh T, Lindhe J. Anchorage of titanium implants with different surface characteristics: an experimental study in rabbits. Clin Implant Dent Relat Res. 2000;2:120–8.

Gotfredsen K, Wiskott A, Working Group. Consensus report - reconstructions on implants. The Third EAO Consensus Conference 2012. Vol. 23, Clinical Oral Implants Research. 2012. p. 238–41.

Gracis S, Michalakis K, Vigolo P, Vult von Steyern P, Zwahlen M, Sailer I. Internal vs. external connections for abutments/reconstructions: a systematic review. Clin Oral Implants Res. 2012;23 Suppl 6:202–16.

Grassi S, Piattelli A, de Figueiredo LC, Feres M, de Melo L, Iezzi G, et al. Histologic evaluation of early human bone response to different implant surfaces. J Periodontol. 2006;77:1736–43.

Greenberg AM. Dental Implants and Evolving Discipline. Vol. 27, Oral and Maxillofacial Surgery Clinics of North America. 2015. p. ix – x.

Gruber R, Bosshardt DD. Dental Implantology and Implants - Tissue Interface. Stem Cell Biology and Tissue Engineering in Dental Sciences. 2015. p. 735–47.

Guillaume B. Dental implants: A review. Morphologie. 2016;100:189–98.

Gultekin BA, Alper Gultekin B, Gultekin P, Leblebicioglu B, Basegmez C, Yalcin S. Clinical Evaluation of Marginal Bone Loss and Stability in Two Types of Submerged Dental Implants. Vol. 28, The International Journal of Oral & Maxillofacial Implants. 2013. p. 815–23.

Gupta D, Agrawal A, Chaudhary H, Gulrajani M, Gupta C. Cleaner process for extraction of sericin using infrared. J Clean Prod. 2013;52:488–94.

Gurgel BC de V, de Vasconcelos Gurgel BC, Montenegro SCL, Dantas PMC, de Barros Pascoal AL, Lima KC, et al. Frequency of peri-implant diseases and associated factors. Vol. 28, Clinical Oral Implants Research. 2017. p. 1211–7.

Hallgren Höstner C. On the bone response to different implant textures. A 3D analysis of roughness, wavelength and surface pattern of experimental implants. 2001.

Hamady M, Knight R. Microbial community profiling for human microbiome projects: Tools, techniques, and challenges. Genome Res. 2009;19:1141–52.

Hammerle CH, Chen ST, Wilson TG Jr, Others. Consensus statements and recommended clinical procedures regarding the placement of implants in extraction sockets. Int J Oral Maxillofac Implants. 2004;19:26–8.

Hämmerle CHF, Jung RE, Sanz M, Chen S, Martin WC, Jackowski J, et al. Submerged and transmucosal healing yield the same clinical outcomes with two-piece implants in the anterior maxilla and mandible: interim 1-year results of a randomized, controlled clinical trial. Clin Oral Implants Res. 2012;23:211–9.

Hansson S. Implant-abutment interface: biomechanical study of flat top versus conical. Clin Implant Dent Relat Res. 2000;2:33–41.

Hansson S. A conical implant–abutment interface at the level of the marginal bone improves the distribution of stresses in the supporting bone: An axisymmetric finite element …. Clin Oral Implants Res. 2003a;.

Hansson S. A conical implant--abutment interface at the level of the marginal bone improves the distribution of stresses in the supporting bone: An axisymmetric finite element analysis. Clin Oral Implants Res. 2003b;14:286–93.

Han YW. Fusobacterium nucleatum: a commensal-turned pathogen. Curr Opin Microbiol. 2015;23:141–7.

Harder S, Dimaczek B, Açil Y, Terheyden H, Freitag-Wolf S, Kern M. Molecular leakage at implant-abutment connection—in vitro investigation of tightness of internal conical implant-abutment connections against endotoxin penetration. Vol. 14, Clinical Oral Investigations. 2010. p. 427–32.

Harris LG, Richards RG. Staphylococci and implant surfaces: a review. Injury. 2006;37 Suppl 2:S3–14.

Hartman GA, Cochran DL. Initial implant position determines the magnitude of crestal bone remodeling. J Periodontol. 2004;75:572–7.

Heitz-Mayfield LJA. Diagnosis and management of peri-implant diseases. Aust Dent J. 2008;

Heitz-Mayfield LJA. Peri-implant diseases: diagnosis and risk indicators. J Clin Periodontol. 2008;35:292–304.

Heitz-Mayfield LJA, Lang NP. Comparative biology of chronic and aggressive periodontitis vs. peri-implantitis. Periodontol 2000. 2010;53:167–81.

Heitz-Mayfield LJA, Needleman I, Salvi GE, Pjetursson BE. Consensus Statements and Clinical Recommendations for Prevention and Management of Biologic and Technical Implant Complications. Int J Oral Maxillofac Implants. 2013;

Heitz-Mayfield LJA, Salvi GE. Peri-implant mucositis. J Clin Periodontol. 2018b;45:S237–45.

Hermann JS, Buser D, Schenk RK, Cochran DL. Crestal Bone Changes Around Titanium Implants. A Histometric Evaluation of Unloaded Non-Submerged and Submerged Implants in the Canine Mandible. Vol. 71, Journal of Periodontology. 2000. p. 1412–24.

Hermann JS, Cochran DL, Hermann JS, Buser D, Schenk RK, Schoolfield JD. Biologic Width around one- and two-piece titanium implants. A histometric evaluation of unloaded nonsubmerged and submerged implants in the canine mandible. Vol. 12, Clinical Oral Implants Research. 2001. p. 559–71.

Hermann JS, Cochran DL, Nummikoski PV, Buser D. Crestal bone changes around titanium implants. A radiographic evaluation of unloaded nonsubmerged and submerged implants in the canine mandible. J Periodontol. 1997;68:1117–30.

Hernigou P, Queinnec S, Flouzat Lachaniette CH. One hundred and fifty years of history of the Morse taper: from Stephen A. Morse in 1864 to complications related to modularity in hip arthroplasty. Int Orthop. 2013;37:2081–8.

Herrero-Climent M, Ruiz M, Díaz-Castro C, Bullón P, Ríos-Santos J. Influence of Two Different Machined-Collar Heights on Crestal Bone Loss. Vol. 29, The International Journal of Oral & Maxillofacial Implants. 2014. p. 1374–9.

Heuer W, Kettenring A, Stumpp SN, Eberhard J, Gellermann E, Winkel A, et al. Metagenomic analysis of the peri-implant and periodontal microflora in patients with clinical signs of gingivitis or mucositis. Clin Oral Investig. 2012;16:843–50.

Hosseini MM, Sodek J, Franke RP, Davies JE. The structure and composition of the bone-implant interface. Bone engineering Toronto: em squared Inc. 2000;295–304.

Hsu Y-T, Chan H-L, Rudek I, Bashutski J, Oh W-S, Wang H-L, et al. Comparison of Clinical and Radiographic Outcomes of Platform-Switched Implants with a Rough Collar and Platform-Matched Implants with a Smooth Collar: A 1-Year Randomized Clinical Trial. The International Journal of Oral & Maxillofacial Implants. 2016. p. 382–90.

Huang Y-C, Kaigler D, Rice KG, Krebsbach PH, Mooney DJ. Combined angiogenic and osteogenic factor delivery enhances bone marrow stromal cell-driven bone regeneration. J Bone Miner Res. 2005;20:848–57.

Hürzeler M, Fickl S, Zuhr O, Wachtel HC. Peri-Implant Bone Level Around Implants With Platform-Switched Abutments: Preliminary Data From a Prospective Study. Vol. 65, Journal of Oral and Maxillofacial Surgery. 2007. p. 33–9.

Insua A, Monje A, Wang H-L, Inglehart M. Patient-Centered Perspectives and Understanding of Peri-Implantitis. J Periodontol. 2017;88:1153–62.

Ivanoff CJ, Sennerby L, Johansson C, Rangert B, Lekholm U. Influence of implant diameters on the integration of screw implants. An experimental study in rabbits. Int J Oral Maxillofac Surg. 1997;26:141–8.

Ivanovski S, Lee R. Comparison of peri-implant and periodontal marginal soft tissues in health and disease. Periodontol 2000. 2018;76:116–30.

Jansen VK, Conrads G, Richter EJ. Microbial leakage and marginal fit of the implant-abutment interface. Int J Oral Maxillofac Implants. 1997;12:527–40.

Jaworski ME, Melo AC, Picheth CM, Sartori IA. Analysis of the bacterial seal at the implant-abutment interface in external-hexagon and Morse taper-connection implants: an in vitro study using a new methodology. Int J Oral Maxillofac Implants. 2012 Sep-Oct;27(5):1091-5.

Jemat A, Ghazali MJ, Razali M, Otsuka Y. Surface Modifications and Their Effects on Titanium Dental Implants. Biomed Res Int. 2015;2015:791725.

Jo D-W, Yi Y-J, Kwon M-J, Kim Y-K. Correlation between interimplant distance and crestal bone loss in internal connection implants with platform switching. Int J Oral Maxillofac Implants. 2014;29:296–302.

Jordana F, Susbielles L, Colat-Parros J. Periimplantitis and Implant Body Roughness: A Systematic Review of Literature. Implant Dent. 2018;27:672–81.

Jr ABN, Novaes AB Jr, de Souza SLS, de Barros RRM, Pereira KKY, Iezzi G, et al. Influence of implant surfaces on osseointegration. Vol. 21, Brazilian Dental Journal. 2010. p. 471–81.

Jung RE, Pjetursson BE, Glauser R, Zembic A, Zwahlen M, Lang NP. A systematic review of the 5-year survival and complication rates of implant-supported single crowns. Clin Oral Implants Res. 2008;19:119–30.

Kane G, Fang V, Simon S, Girdler J, Adeyinka O, Alhilou A. A Survey Exploring the Experiences & Attitudes of Dental Implant Clinicians in the Management of Peri-implantitis

within the United Kingdom. Eur J Prosthodont Restor Dent. 2018;26:46–52.

Kaur J, Rajkhowa R, Afrin T, Tsuzuki T, Wang X. Facts and myths of antibacterial properties of silk. Vol. 101, Biopolymers. 2014. p. 237–45.

Khalifa IB, Belhaj Khalifa I, Ladhari N, Touay M. Application of sericin to modify textile supports. Vol. 103, Journal of the Textile Institute. 2012. p. 370–7.

Khalil D, Hultin M. Peri-implantitis Microbiota. In: Ahmad Almasri M, editor. An Update of Dental Implantology and Biomaterial. IntechOpen; 2019.

Khalil G, Lorthois S, Marcoux M, Mansat P, Swider P. Wave front migration of endothelial cells in a bone-implant interface. J Biomech. 2011;44:1980–6.

Kielbassa AM, Fuentes RM, Goldstein M, Arnhart C, Barlattani A, Jackowski J, et al. Randomized controlled trial comparing a variable-thread novel tapered and a standard tapered implant: Interim one-year results. Vol. 101, The Journal of Prosthetic Dentistry. 2009. p. 293–305.

Kieswetter K, Schwartz Z, Dean DD, Boyan BD. The role of implant surface characteristics in the healing of bone. Crit Rev Oral Biol Med. 1996;7:329–45.

Kim H, Choi S-H, Ryu J-J, Koh S-Y, Park J-H, Lee I-S. The biocompatibility of SLA-treated titanium implants. Biomed Mater. 2008;3:025011.

Kim HM, Miyaji F, Kokubo T, Nakamura T. Preparation of bioactive Ti and its alloys via simple chemical surface treatment. J Biomed Mater Res. 1996;32:409–17.

Kingston G, Webster C. Heroes of implant dentistry: osseointegration and titanium. Prim Dent J. 2013;2:74–5.

Kitts PA, Church DM, Thibaud-Nissen F, Choi J, Hem V, Sapojnikov V, et al. Assembly: a resource for assembled genomes at NCBI. Nucleic Acids Res. 2016;44:D73–80.

Klinge B, Flemming T, Cosyn J, De Bruyn H, Eisner BM, Hultin M, et al. The patient undergoing implant therapy. Summary and consensus statements. The 4th EAO Consensus Conference 2015. Clin Oral Implants Res. 2015;26 Suppl 11:64–7.

Klinge B, Hultin M, Berglundh T. Peri-implantitis. Dent Clin North Am. 2005;49:661–76, vii – viii.

Klinge B, Klinge A, Bertl K, Stavropoulos A. Peri-implant diseases. Vol. 126, European Journal of Oral Sciences. 2018. p. 88–94.

Koizumi H, Takeuchi Y, Imai H, Kawai T, Yoneyama T. Application of titanium and titanium alloys to fixed dental prostheses. J Prosthodont Res. 2019;63(3):266-270.

Kook JK, Park SN, Lim YK, Cho E, Jo E, Roh H, et al. Genome-Based Reclassification of Fusobacterium nucleatum Subspecies at the Species Level. Curr Microbiol. 2017;74:1137–47.

Koo K-T, Lee E-J, Kim J-Y, Seol Y-J, Han JS, Kim T-I, et al. The Effect of Internal Versus External Abutment Connection Modes on Crestal Bone Changes Around Dental Implants: A Radiographic Analysis. Vol. 83, Journal of Periodontology. 2012. p. 1104–9.

Koutouzis T. Implant-abutment connection as contributing factor to peri-implant diseases. Periodontol 2000. 2019 Oct;81(1):152-166.

Koutouzis T, Neiva R, Nonhoff J, Lundgren T. Placement of implants with platform-switched Morse taper connections with the implant-abutment interface at different levels in relation to the alveolar crest: a short-term (1-year) randomized prospective controlled clinical trial. Int J Oral Maxillofac Implants. 2013;28:1553–63.

Koutouzis T, Wallet S, Calderon N, Lundgren T. Bacterial Colonization of the Implant–Abutment Interface Using an In Vitro Dynamic Loading Model. J Periodontol. 2011;82:613–8.

Koyanagi T, Sakamoto M, Takeuchi Y, Maruyama N, Ohkuma M, Izumi Y. Comprehensive microbiological findings in peri-implantitis and periodontitis. J Clin Periodontol. 2013;40:218–26.

Kumar PS, Mason MR, Brooker MR, O'Brien K. Pyrosequencing reveals unique microbial signatures associated with healthy and failing dental implants. Vol. 39, Journal of Clinical Periodontology. 2012a. p. 425–33.

Kumar PS, Mason MR, Brooker MR, O'Brien K. Pyrosequencing reveals unique microbial signatures associated with healthy and failing dental implants. J Clin Periodontol. 2012b;39:425–33.

Lafaurie GI, Sabogal MA, Castillo DM, Rincón MV, Gómez LA, Lesmes YA, et al. Microbiome and Microbial Biofilm Profiles of Peri-Implantitis: A Systematic Review. J Periodontol. 2017;88:1066–89.

Lakey LA, Akella R, Ranieri JP. Angiogenesis: implications for tissue repair. Bone engineering Toronto: Em Squared Incorporated. 2000;137–42.

Lamboni L, Gauthier M, Yang G, Wang Q. Silk sericin: A versatile material for tissue engineering and drug delivery. Biotechnol Adv. 2015;33:1855–67.

Langmead B, Salzberg SL. Fast gapped-read alignment with Bowtie 2. Nat Methods. 2012;9:357–9.

Lang NP, Berglundh T, on Periodontology WG 4. of TSEW. Periimplant diseases: where are we now?--Consensus of the Seventh European Workshop on Periodontology. J Clin Periodontol. 2011a;38:178–81.

Lang NP, Jepsen S. Implant surfaces and design (Working Group 4). Vol. 20, Clinical Oral Implants Research. 2009. p. 228–31.

Lang NP, Pun L, Lau KY, Li KY, Wong MCM. A systematic review on survival and success rates of implants placed immediately into fresh extraction sockets after at least 1 year. Vol. 23, Clinical Oral Implants Research. 2012. p. 39–66.

Lang NP, Salvi GE, Huynh-Ba G, Ivanovski S, Donos N, Bosshardt DD. Early osseointegration to hydrophilic and hydrophobic implant surfaces in humans. Clin Oral Implants Res. 2011b;22:349–56.

Larsson C, Thomsen P, Aronsson BO, Rodahl M, Lausmaa J, Kasemo B, et al. Bone response to surface-modified titanium implants: studies on the early tissue response to machined and electropolished implants with different oxide thicknesses. Biomaterials. 1996;17:605–16.

Larsson L-I, -I. Larsson L, Hougard DM. Glass slide models for immunocytochemistry and in situ hybridization. Vol. 101, Histochemistry. 1994. p. 325–31.

Lazzara RJ, Porter SS. Platform switching: a new concept in implant dentistry for controlling postrestorative crestal bone levels. Int J Periodontics Restorative Dent. 2006;26:9–17.

Lee CS, Belfort G. Changing activity of ribonuclease A during adsorption: a molecular explanation. Vol. 86, Proceedings of the National Academy of Sciences. 1989. p. 8392–6.

Lee J-S, Kim H-M, Kim C-S, Choi S-H, Chai J-K, Jung U-W. Long-term retrospective study of narrow implants for fixed dental prostheses. Clin Oral Implants Res. 2013;24:847–52.

Lemos CAA, Ferro-Alves ML, Okamoto R, Mendonça MR, Pellizzer EP. Short dental implants versus standard dental implants placed in the posterior jaws: A systematic review and meta-analysis. J Dent. 2016;47:8–17.

Lemos CAA, Verri FR, Bonfante EA, Santiago Júnior JF, Pellizzer EP. Comparison of external and internal implant-abutment connections for implant supported prostheses. A systematic review and meta-analysis. J Dent. 2018;70:14–22.

Lindahl C, Engqvist H, Xia W. Influence of Surface Treatments on the Bioactivity of Ti. Vol. 2013, ISRN Biomaterials. 2013. p. 1–13.

Lindgren M, Astrand M, Wiklund U, Engqvist H. Investigation of boundary conditions for biomimetic HA deposition on titanium oxide surfaces. J Mater Sci Mater Med. 2009;20:1401–8.

Lindhe J, Berglundh T, Ericsson I, Liljenberg B, Marinello C. Experimental breakdown of peri-implant and periodontal tissues. A study in the beagle dog. Clin Oral Implants Res. 1992;3:9–16.

Lindhe J, Meyle J, Group D of European Workshop on Periodontology. Peri-implant diseases: Consensus Report of the Sixth European Workshop on Periodontology. J Clin Periodontol. 2008;35:282–5.

Lin M-I, Shen Y-W, Huang H-L, Hsu J-T, Fuh L-J. A retrospective study of implant-abutment connections on crestal bone level. J Dent Res. 2013;92:202S – 7S.

Liu X, Chu PK, Ding C. Surface modification of titanium, titanium alloys, and related materials for biomedical applications. Mater Sci Eng R Rep. 2004;47:49–121.

Li ZJ, Wang SG, Li YH, Tu DX, Liu SY, Nie HB, et al. Study on microbial diversity of peri-implantitis subgingival by high-throughput sequencing. Sichuan da xue xue bao Yi xue ban= Journal of Sichuan University Medical science edition. 2015;46:568–72.

Lohmann CH, Tandy EM, Sylvia VL, Hell-Vocke AK, Cochran DL, Dean DD, et al. Response of normal female human osteoblasts (NHOst) to 17?-estradiol is modulated by implant surface morphology. Vol. 62, Journal of Biomedical Materials Research. 2002. p. 204–13.

Machado LS, Bonfante EA, Anchieta RB, Yamaguchi S, Coelho PG. Implant-Abutment Connection Designs for Anterior Crowns. Vol. 22, Implant Dentistry. 2013. p. 540–5. http://dx.doi.org/10.1097/id.0b013e31829f1f2d

Malchiodi L, Cucchi A, Ghensi P, Bondì V. A case of rapidly progressive peri-implantitis around a short sintered porous-surfaced implant. J Indiana Dent Assoc. 2009;88:33–5.

Malchiodi L, Cucchi A, Ghensi P, Consonni D, Nocini PF. Influence of crown-implant ratio on implant success rates and crestal bone levels: a 36-month follow-up prospective study. Vol. 25, Clinical Oral Implants Research. 2014. p. 240–51.

Malchiodi L, Cucchi A, Ghensi P, Nocini PF. Evaluation of the esthetic results of 64 nonfunctional immediately loaded postextraction implants in the maxilla: correlation between interproximal alveolar crest and soft tissues at 3 years of follow-up. Clin Implant Dent Relat Res. 2013;15:130–42.

Malchiodi L, Ghensi P, Cucchi A, Pieroni S, Bertossi D. Peri-implant conditions around sintered porous-surfaced (SPS) implants. A 36-month prospective cohort study. Clin Oral Implants Res. 2015;26:212–9.

Mangano C, Iaculli F, Piattelli A, Mangano F. Fixed restorations supported by Morse-taper connection implants: a retrospective clinical study with 10--20 years of follow-up. Clin Oral Implants Res. 2015;26:1229–36.

Mangano C, Mangano F, Piattelli A, Iezzi G, Mangano A, La Colla L. Prospective clinical evaluation of 307 single-tooth morse taper-connection implants: a multicenter study. Int J Oral Maxillofac Implants. 2010;25:394–400.

Mangano C, Mangano F, Shibli JA, Luongo G, De Franco M, Briguglio F, et al. Prospective clinical evaluation of 201 direct laser metal forming implants: results from a 1-year multicenter study. Lasers Med Sci. 2012;27:181–9.

Martines RT, Sendyk WR, Gromatzky A, Cury PR. Sandblasted/Acid-Etched vs Smooth-Surface Implants: Implant Mobility and Clinical Reaction to Experimentally Induced Peri-Implantitis in Beagle Dogs. J Oral Implantol. 2008;34:185–9.

Maruyama N, Maruyama F, Takeuchi Y, Aikawa C, Izumi Y, Nakagawa I. Intraindividual variation in core microbiota in peri-implantitis and periodontitis. Sci Rep. 2014;4:6602.

de Medeiros RA, Pellizzer EP, Vechiato Filho AJ, Dos Santos DM, da Silva EVF, Goiato MC. Evaluation of marginal bone loss of dental implants with internal or external connections and its association with other variables: A systematic review. J Prosthet Dent. 2016;116:501–6.e5.

Mei DM, Zhao B, Xu H, Wang Y. Radiographic and clinical outcomes of rooted, platform-switched, microthreaded implants with a sandblasted, large-grid, and acid-etched surface: A 5-year prospective study. Clin Implant Dent Relat Res. 2017;19:1074–81.

Meng H-W, Chien EY, Chien H-H. Dental implant bioactive surface modifications and their effects on osseointegration: a review. Biomark Res. 2016;4:24.

Merz BR, Hunenbart S, Belser UC. Mechanics of the implant-abutment connection: an 8-degree taper compared to a butt joint connection. Int J Oral Maxillofac Implants. 2000;15:519–26.

Mijiritsky E, Ferroni L, Gardin C, Bressan E, Zanette G, Piattelli A, et al. Porcine Bone Scaffolds Adsorb Growth Factors Secreted by MSCs and Improve Bone Tissue Repair. Materials . 2017;10.

Misch CE. Generic root form components terminology. Contemporary Implant Dentistry. 2014;3:26–38.

Mishra SK, Chowdhary R, Kumari S. Microleakage at the Different Implant Abutment Interface:

A Systematic Review. J Clin Diagn Res. 2017;11(6):ZE10-ZE15.

Moher D, Liberati A, Tetzlaff J, Altman DG. Preferred reporting items for systematic reviews and meta-analyses: The PRISMA statement. Vol. 8, International Journal of Surgery. 2010. p. 336–41.

Mombelli A, Cionca N. The prevalence of peri-implantitis: how big is the problem. In: Forum Implantologicum. 2013. p. 12–9.

Mombelli A, Marxer M, Gaberthüel T, Grunder U, Lang NP. The microbiota of osseointegrated implants in patients with a history of periodontal disease. J Clin Periodontol. 1995;22:124–30.

Monje A, Insua A, Wang H-L. Understanding Peri-Implantitis as a Plaque-Associated and Site-Specific Entity: On the Local Predisposing Factors. J Clin Med Res. 2019;8.

Monje A, Pommer B. The Concept of Platform Switching to Preserve Peri-implant Bone Level: Assessment of Methodologic Quality of Systematic Reviews. Int J Oral Maxillofac Implants. 2015;30:1084–92.

Moraschini V, Poubel LA da C, Ferreira VF, Barboza E dos SP. Evaluation of survival and success rates of dental implants reported in longitudinal studies with a follow-up period of at least 10 years: a systematic review. Int J Oral Maxillofac Surg. 2015;44:377–88.

Morra M, Cassinelli C, Bruzzone G, Carpi A, Di Santi G, Giardino R, et al. Surface chemistry effects of topographic modification of titanium dental implant surfaces: 1. Surface analysis. Int J Oral Maxillofac Implants. 2003;18:40–5.

Moulder JF, Stickle WF, Sobol PE. Poly (iso-butyl methacrylate) by XPS. Vol. 1, Surface Science Spectra. 1992. p. 356–60.

Mumcu E, Bilhan H, Cekici A. Marginal Bone Loss Around Implants Supporting Fixed Restorations. Vol. 37, Journal of Oral Implantology. 2011. p. 549–58.

do Nascimento C, Ikeda LN, Pita MS, Pedroso e Silva RC, Pedrazzi V, de Albuquerque Junior RF, et al. Marginal fit and microbial leakage along the implant-abutment interface of fixed partial prostheses: An in vitro analysis using Checkerboard DNA-DNA hybridization. J Prosthet Dent. 2015;114:831–8.

Nassar HI, Abdalla MF. Bacterial leakage of different internal implant/abutment connection. Vol. 1, Future Dental Journal. 2015. p. 1–5.

Nobuto T, Suwa F, Kono T, Taguchi Y, Takahashi T, Kanemura N, et al. Microvascular Response in the Periosteum Following Mucoperiosteal Flap Surgery in Dogs: Angiogenesis and Bone Resorption and Formation. Vol. 76, Journal of Periodontology. 2005. p. 1346–53.

Norowski PA Jr, Bumgardner JD. Biomaterial and antibiotic strategies for peri-implantitis: A review. Journal of Biomedical Materials Research Part B: Applied Biomaterials: An Official Journal of The Society for Biomaterials, The Japanese Society for Biomaterials, and The Australian Society for Biomaterials and the Korean Society for Biomaterials. 2009;88:530–43.

Norton MR. Assessment of cold welding properties of the internal conical interface of two commercially available implant systems. J Prosthet Dent. 1999;81:159–66.

Ogle OE. Implant surface material, design, and osseointegration. Dent Clin North Am.

2015;59:505–20.

Oh T-J, Yoon J, Misch CE, Wang H-L. The causes of early implant bone loss: myth or science? J Periodontol. 2002;73:322–33.

Orsini G, Assenza B, Scarano A, Piattelli M, Piattelli A. Surface analysis of machined versus sandblasted and acid-etched titanium implants. Int J Oral Maxillofac Implants. 2000;15:779–84.

Öztürk VÖ, Emingil G, Bostanci N. Impact of implant–abutment connection on osteoimmunological and microbiological parameters in short implants: a randomized controlled clinical trial. Clin Oral Implants Res. 2017;

Padial-Molina M, López-Martínez J, O'Valle F, Galindo-Moreno P. Microbial Profiles and Detection Techniques in Peri-Implant Diseases: a Systematic Review. J Oral Maxillofac Res. 2016;7:e10.

Page AJ, Cummins CA, Hunt M, Wong VK, Reuter S, Holden MTG, et al. Roary: rapid large-scale prokaryote pan genome analysis. Bioinformatics. 2015;31:3691–3.

Palmquist A, Omar OM, Esposito M, Lausmaa J, Thomsen P. Titanium oral implants: surface characteristics, interface biology and clinical outcome. J R Soc Interface. 2010;7 Suppl 5:S515–27.

Pandiarajan J, Cathrin BP, Pratheep T, Krishnan M. Defense role of the cocoon in the silk worm Bombyx mori L. Vol. 25, Rapid Communications in Mass Spectrometry. 2011. p. 3203–6.

Panthong J, Program of Food Engineering, Department of Food Science and Technology, Faculty of Agro-Industry, Kasetsart University, Bangkok, et al. Effect of spray drying conditions on the characteristics of sericin powder from eri silk boiling water. Vol. 1, life: International Journal of Health and Life-sciences. 2015. p. 151–60.

Pasolli E, Truong DT, Malik F, Waldron L, Segata N. Machine Learning Meta-analysis of Large Metagenomic Datasets: Tools and Biological Insights. PLoS Comput Biol. 2016;12:e1004977.

Pattanaik B, Pawar S, Pattanaik S. Biocompatible implant surface treatments. Indian J Dent Res. 2012;23:398–406.

Pattanayak DK, Yamaguchi S, Matsushita T, Kokubo T. Nanostructured positively charged bioactive TiO2 layer formed on Ti metal by NaOH, acid and heat treatments. Vol. 22, Journal of Materials Science: Materials in Medicine. 2011. p. 1803–12.

Peñarrocha-Diago MA, Flichy-Fernández AJ, Alonso-González R, Peñarrocha-Oltra D, Balaguer-Martínez J, Peñarrocha-Diago M. Influence of implant neck design and implant-abutment connection type on peri-implant health. Radiological study. Clinical Oral Implants Research. 2012.

Pérez-Chaparro PJ, Duarte PM, Shibli JA, Montenegro S, Lacerda Heluy S, Figueiredo LC, et al. The current weight of evidence of the microbiologic profile associated with peri-implantitis: A systematic review. J Periodontol. 2016;87:1295–304.

Persson LG, Lekholm U, Leonhardt Å, Dahlen G, Lindhe J. Bacterial colonization on internal surfaces of Brånemark system® implant components. Clin Oral Implants Res. 1996;7:90–5.

Pessoa RS, Muraru L, Júnior EM, Vaz LG, Sloten JV, Duyck J, et al. Influence of implant connection type on the biomechanical environment of immediately placed implants--CT-based nonlinear, three-dimensional finite element analysis. Clin Implant Dent Relat Res. 2010;12:219–34.

Pessoa RS, Sousa RM, Pereira LM, Neves FD, Bezerra FJB, Jaecques SVN, et al. Bone Remodeling Around Implants with External Hexagon and Morse-Taper Connections: A Randomized, Controlled, Split-Mouth, Clinical Trial. Vol. 19, Clinical Implant Dentistry and Related Research. 2017. p. 97–110.

Peters K, Unger RE, Brunner J, Kirkpatrick CJ. Molecular basis of endothelial dysfunction in sepsis. Cardiovasc Res. 2003;60:49–57.

Pi B, Hansson BO, Adell R, Breine U, Lindström J, Hallén O, et al. Osseointegrated implants in the treatment of the edentulous jaw. Experience from a 10-year period. Scand J Plast Reconstr Surg Suppl. 1977;16:1–132.

Pier-Francesco A, Adams RJ, Waters MGJ, Williams DW. Titanium surface modification and its effect on the adherence of Porphyromonas gingivalis: an in vitro study. Clin Oral Implants Res. 2006;17:633–7.

Pieri F, Aldini NN, Marchetti C, Corinaldesi G. Influence of implant-abutment interface design on bone and soft tissue levels around immediately placed and restored single-tooth implants: a randomized controlled clinical trial. Int J Oral Maxillofac Implants. 2011;26:169–78.

Pieri F, Siroli L, Forlivesi C, Corinaldesi G. Clinical, esthetic, and radiographic evaluation of small-diameter (3.0-mm) implants supporting single crowns in the anterior region: a 3-year prospective study. Int J Periodontics Restorative Dent. 2014;34:825–32.

Pinchi V, Varvara G, Pradella F, Focardi M, Donati MD, Norelli G. Analysis of professional malpractice claims in implant dentistry in Italy from insurance company technical reports, 2006 to 2010. Int J Oral Maxillofac Implants. 2014;29:1177–84.

Pokrowiecki R, Mielczarek A, Zaręba T, Tyski S. Oral microbiome and peri-implant diseases: where are we now? Ther Clin Risk Manag. 2017;13:1529–42.

Pozzi A, Agliardi E, Tallarico M, Barlattani A. Clinical and Radiological Outcomes of Two Implants with Different Prosthetic Interfaces and Neck Configurations: Randomized, Controlled, Split-Mouth Clinical Trial. Vol. 16, Clinical Implant Dentistry and Related Research. 2014a. p. 96–106.

Pozzi A, Tallarico M, Moy PK. Three-year post-loading results of a randomised, controlled, split-mouth trial comparing implants with different prosthetic interfaces and design in partially posterior edentulous mandibles. Eur J Oral Implantol. 2014b;7:47–61.

Pozzi A, Tallarico M, Moy PK. Immediate loading with a novel implant featured by variable-threaded geometry, internal conical connection and platform shifting: three-year results from a prospective cohort study. Eur J Oral Implantol. 2015;8:51–63.

Price JS, Tencer AF, Arm DM, Bohach GA. Controlled release of antibiotics from coated orthopedic implants. J Biomed Mater Res. 1996;30:281–6.

Prosper L, Redaelli S, Pasi M, Zarone F, Radaelli G, Gherlone EF. A randomized prospective multicenter trial evaluating the platform-switching technique for the prevention of postrestorative crestal bone loss. Int J Oral Maxillofac Implants. 2009;24:299–308.

Puleo D. Biochemical surface modification of Co_Cr_Mo. Vol. 17, Biomaterials. 1996. p. 217–22.

Puleo DA. Activity of enzyme immobilized on silanized Co-Cr-Mo. Vol. 29, Journal of Biomedical Materials Research. 1995. p. 951–7.

Puleo DA, Kissling RA, Sheu MS. A technique to immobilize bioactive proteins, including bone morphogenetic protein-4 (BMP-4), on titanium alloy. Biomaterials. 2002;23:2079–87.

Qin S, Xu K, Nie B, Ji F, Zhang H. Approaches based on passive and active antibacterial coating on titanium to achieve antibacterial activity. Vol. 106, Journal of Biomedical Materials Research Part A. 2018. p. 2531–9.

Quaranta A, Piattelli A, Scarano A, Quaranta M, Pompa G, Iezzi G. Light-microscopic evaluation of the dimensions of peri-implant mucosa around immediately loaded and submerged titanium implants in monkeys. J Periodontol. 2008;79:1697–703.

Quince C, Walker AW, Simpson JT, Loman NJ, Segata N. Shotgun metagenomics, from sampling to analysis. Nat Biotechnol. 2017;35:833–44.

Quirynen M, De Soete M, van Steenberghe D. Infectious risks for oral implants: a review of the literature. Clin Oral Implants Res. 2002;13:1–19.

Quirynen M, Herrera D, Teughels W, Sanz M. Implant therapy: 40 years of experience. Vol. 66, Periodontology 2000. 2014. p. 7–12. http://dx.doi.org/10.1111/prd.12060

Quirynen M, Van Steenberghe D. Bacterial colonization of the internal part of two-stage implants. An in vivo study. Clin Oral Implants Res. 1993;4:158–61.

Quirynen M, Vogels R, Peeters W, van Steenberghe D, Naert I, Haffajee A. Dynamics of initial subgingival colonization of “pristine”peri-implant pockets. Clin Oral Implants Res. 2006;17:25–37.

Rajendran R, Balakumar C, Sivakumar R, Amruta T, Devaki N. Extraction and application of natural silk protein sericin fromBombyx morias antimicrobial finish for cotton fabrics. Vol. 103, Journal of the Textile Institute. 2012. p. 458–62.

Rakic M, Grusovin MG, Canullo L. The Microbiologic Profile Associated with Peri-Implantitis in Humans: A Systematic Review. Int J Oral Maxillofac Implants. 2016;31.

Ramanauskaite A, Becker K, Schwarz F. Clinical characteristics of peri-implant mucositis and peri-implantitis. Vol. 29, Clinical Oral Implants Research. 2018. p. 551–6. http://dx.doi.org/10.1111/clr.13152

Rea M, Ricci S, Ghensi P, Lang NP, Botticelli D, Soldini C. Marginal healing using Polyetheretherketone as healing abutments: an experimental study in dogs. Clin Oral Implants Res. 2017;28:e46–50.

Renouard F, Nisand D. Impact of implant length and diameter on survival rates. Clin Oral Implants Res. 2006;17 Suppl 2:35–51.

Renvert S, Persson GR, Pirih FQ, Camargo PM. Peri-implant health, peri-implant mucositis, and peri-implantitis: Case definitions and diagnostic considerations. J Periodontol. 2018;89 Suppl 1:S304–12.

Renvert S, Polyzois I. Treatment of pathologic peri-implant pockets. Vol. 76, Periodontology

2000. 2018. p. 180–90.

Renvert S, Samuelsson E, Lindahl C, Persson GR. Mechanical non-surgical treatment of peri-implantitis: a double-blind randomized longitudinal clinical study. I: clinical results. J Clin Periodontol. 2009;36:604–9.

Rissin L, House JE, Manly RS, Kapur KK. Clinical comparison of masticatory performance and electromyographic activity of patients with complete dentures, overdentures, and natural teeth. J Prosthet Dent. 1978;39(5):508-11.

Robinson KS, Sherwood PMA. X-Ray photoelectron spectroscopic studies of the surface of sputter ion plated films. Vol. 6, Surface and Interface Analysis. 1984. p. 261–6.

Robitaille N, Reed DN, Walters JD, Kumar PS. Periodontal and peri-implant diseases: identical or fraternal infections? Mol Oral Microbiol. 2016;31:285–301.

Rodríguez-Ciurana X, Vela-Nebot X, Segalà-Torres M, Rodado-Alonso C, Méndez-Blanco V, Mata-Bugueroles M. Biomechanical repercussions of bone resorption related to biologic width: a finite element analysis of three implant-abutment configurations. Int J Periodontics Restorative Dent. 2009;29:479–87.

Rodríguez-Contreras A, Marqués-Calvo MS, Gil FJ, Manero JM. Modification of titanium surfaces by adding antibiotic-loaded PHB spheres and PEG for biomedical applications. J Mater Sci Mater Med. 2016;27:124.

Rokn A, Aslroosta H, Akbari S, Najafi H, Zayeri F, Hashemi K. Prevalence of peri-implantitis in patients not participating in well-designed supportive periodontal treatments: a cross-sectional study. Clin Oral Implants Res. 2017;28:314–9.

Romanos GE, Weitz D. Therapy of peri-implant diseases. Where is the evidence? J Evid Based Dent Pract. 2012;12:204–8.

Romeo E, Ghisolfi M, Carmagnola D. Peri-implant diseases. A systematic review of the literature. Minerva Stomatol. 2004;53:215–30.

Romeo E, Ghisolfi M, Rozza R, Chiapasco M, Lops D. Short (8-mm) dental implants in the rehabilitation of partial and complete edentulism: a 3- to 14-year longitudinal study. Int J Prosthodont. 2006;19:586–92.

Rupp F, Liang L, Geis-Gerstorfer J, Scheideler L, Hüttig F. Surface characteristics of dental implants: A review. Dent Mater. 2018;34:40–57.

Saghiri M-A, Asatourian A, Garcia-Godoy F, Sheibani N. The role of angiogenesis in implant dentistry part I: Review of titanium alloys, surface characteristics and treatments. Med Oral Patol Oral Cir Bucal. 2016;21:e514–25.

Saghiri MA, Asatourian A, Sorenson CM, Sheibani N. Role of angiogenesis in endodontics: contributions of stem cells and proangiogenic and antiangiogenic factors to dental pulp regeneration. J Endod. 2015;41:797–803.

Sailer I, Sailer T, Stawarczyk B, Jung RE, Hämmerle CHF. In vitro study of the influence of the type of connection on the fracture load of zirconia abutments with internal and external implant-abutment connections. Int J Oral Maxillofac Implants. 2009;24:850–8.

Sakka S, Baroudi K, Nassani MZ. Factors associated with early and late failure of dental implants. J Investig Clin Dent. 2012;3:258–61.

Salvi GE, Cosgarea R, Sculean A. Prevalence and Mechanisms of Peri-implant Diseases. J Dent Res. 2017;96:31–7.

Santiago JF, Verri FR, de Faria Almeida DA, de Souza Batista VE, Lemos CAA, Pellizzer EP. Finite element analysis on influence of implant surface treatments, connection and bone types. Vol. 63, Materials Science and Engineering: C. 2016. p. 292–300.

Sanz-Martin I, Doolittle-Hall J, Teles RP, Patel M, Belibasakis GN, Hämmerle CHF, et al. Exploring the microbiome of healthy and diseased peri-implant sites using Illumina sequencing. J Clin Periodontol. 2017;44:1274–84.

Sanz M, Chapple IL, on behalf of Working Group 4 of the VIII European Workshop on Periodontology*. Clinical research on peri-implant diseases: consensus report of Working Group 4. Vol. 39, Journal of Clinical Periodontology. 2012. p. 202–6.

Sanz M, Ivanoff C-J, Weingart D, Wiltfang J, Gahlert M, Cordaro L, et al. Clinical and Radiologic Outcomes after Submerged and Transmucosal Implant Placement with Two-Piece Implants in the Anterior Maxilla and Mandible: 3-Year Results of a Randomized Controlled Clinical Trial. Vol. 17, Clinical Implant Dentistry and Related Research. 2015. p. 234–46.

Sanz M, Noguerol B, Sanz-Sanchez I, Hammerle CHF, Schliephake H, Renouard F, et al. European Association for Osseointegration Delphi study on the trends in Implant Dentistry in Europe for the year 2030. Clinical Oral Implants Research. 2019.

Sasada Y, Cochran DL. Implant-Abutment Connections: A Review of Biologic Consequences and Peri-implantitis Implications. Int J Oral Maxillofac Implants. 2017;32:1296–307.

Scarano A, Perrotti V, Artese L, Degidi M, Degidi D, Piattelli A, et al. Blood vessels are concentrated within the implant surface concavities: a histologic study in rabbit tibia. Odontology. 2014;102:259–66.

Schaumann S, Staufenbiel I, Scherer R, Schilhabel M, Winkel A, Stumpp SN, et al. Pyrosequencing of supra- and subgingival biofilms from inflamed peri-implant and periodontal sites. Vol. 14, BMC Oral Health. 2014.

Schincaglia GP, Hong BY, Rosania A, Barasz J, Thompson A, Sobue T, et al. Clinical, Immune, and Microbiome Traits of Gingivitis and Peri-implant Mucositis. J Dent Res. 2017;96:47–55.

Schmitt CM, Nogueira-Filho G, Tenenbaum HC, Lai JY, Brito C, Döring H, et al. Performance of conical abutment (Morse Taper) connection implants: a systematic review. J Biomed Mater Res A. 2014;102:552–74.

Scholz M, Ward DV, Pasolli E, Tolio T, Zolfo M, Asnicar F, et al. Strain-level microbial epidemiology and population genomics from shotgun metagenomics. Nat Methods. 2016;

Schroeder A, Stich H, Straumann F. The accumulation of osteocementum around a dental implant under physical loading. Revue mensuelle suisse …. 1978;

Schulte W. Tübingen implant made of Frialit: 5 years of experience. Dtsch Zahnarztl Z. 1981;36:544–50.

Schwartz Z, Nasazky E, Boyan BD. Surface microtopography regulates osteointegration: the role of implant surface microtopography in osteointegration. Alpha Omegan. 2005;98:9–19.

Schwarzer G, Carpenter JR, Rücker G. Meta-Analysis with R. Use R! 2015.

Schwarz F, Becker K, Sahm N, Horstkemper T, Rousi K, Becker J. The prevalence of peri-implant diseases for two-piece implants with an internal tube-in-tube connection: a cross-sectional analysis of 512 implants. Vol. 28, Clinical Oral Implants Research. 2017. p. 24–8.

Schwarz F, Derks J, Monje A. Peri-implantitis. Journal of clinical. 2018;

Sculean A, Gruber R, Bosshardt DD. Soft tissue wound healing around teeth and dental implants. J Clin Periodontol. 2014;41 Suppl 15:S6–22.

Seemann T. Prokka: rapid prokaryotic genome annotation. Bioinformatics. 2014;30:2068–9.

Segata N, Boernigen D, Tickle TL, Morgan XC, Garrett WS, Huttenhower C. Computational meta'omics for microbial community studies. Mol Syst Biol. 2013;9:666.

Segata N, Haake SK, Mannon P, Lemon KP, Waldron L, Gevers D, et al. Composition of the adult digestive tract bacterial microbiome based on seven mouth surfaces, tonsils, throat and stool samples. Genome Biol. 2012a;13:R42.

Segata N, Haake S, Mannon P, Lemon KP, Waldron L, Gevers D, et al. Composition of the adult digestive tract bacterial microbiome based on seven mouth surfaces, tonsils, throat and stool samples. Vol. 13, Genome Biology. 2012b. p. R42.

Segata N, Izard J, Waldron L, Gevers D, Miropolsky L, Garrett WS, et al. Metagenomic biomarker discovery and explanation. Genome Biol. 2011;12:R60.

Segata N, Waldron L, Ballarini A, Narasimhan V, Jousson O, Huttenhower C. Metagenomic microbial community profiling using unique clade-specific marker genes. Nat Methods. 2012c;9:811–4.

Serrano-Sánchez P, Calvo-Guirado JL, Manzanera-Pastor E, Lorrio-Castro C, Bretones-López P, Pérez-Llanes JA. The influence of platform switching in dental implants. A literature review. Med Oral Patol Oral Cir Bucal. 2011;16:e400–5.

Seves A, Romanò M, Maifreni T, Sora S, Ciferri O. The microbial degradation of silk: a laboratory investigation. Vol. 42, International Biodeterioration & Biodegradation. 1998. p. 203–11.

Shanbhag S, Shanbhag V, Stavropoulos A. Genomic analyses of early peri-implant bone healing in humans: a systematic review. Int J Implant Dent. 2015;1:5.

Shemtov-Yona K, Rittel D. An Overview of the Mechanical Integrity of Dental Implants. Biomed Res Int. 2015;2015:547384.

Shi B, Chang M, Martin J, Mitreva M, Lux R, Klokkevold P, et al. Dynamic changes in the subgingival microbiome and their potential for diagnosis and prognosis of periodontitis. MBio. 2015;6:e01926–14.

Shibli JA, Grassi S, de Figueiredo LC, Feres M, Marcantonio E, Iezzi G, et al. Influence of implant surface topography on early osseointegration: A histological study in human jaws. Vol. 80B, Journal of Biomedical Materials Research Part B: Applied Biomaterials. 2007. p. 377–85.

Shibli JA, Melo L, Ferrari DS, Figueiredo LC, Faveri M, Feres M. Composition of supra- and subgingival biofilm of subjects with healthy and diseased implants. Vol. 19, Clinical Oral

Implants Research. 2008. p. 975–82.

Shirley DA. High-Resolution X-Ray Photoemission Spectrum of the Valence Bands of Gold. Vol. 5, Physical Review B. 1972. p. 4709–14.

Shuster JJ. Review: Cochrane handbook for systematic reviews for interventions, Version 5.1.0, published 3/2011. Julian P.T. Higgins and Sally Green, Editors. Vol. 2, Research Synthesis Methods. 2011. p. 126–30.

Signat B, Roques C, Poulet P, Duffaut D. Role of Fusobacterium nucleatum in periodontal health and disease. Curr Issues Mol Biol. 2011;13:25–36.

Silva-Correia J, Zavan B, Vindigni V, Silva TH, Oliveira JM, Abatangelo G, et al. Biocompatibility Evaluation of Ionic- and Photo-Crosslinked Methacrylated Gellan Gum Hydrogels: In Vitro and In Vivo Study. Vol. 2, Advanced Healthcare Materials. 2013. p. 568–75.

Silverstein LH, Lefkove MD, Garnick JJ. The use of free gingival soft tissue to improve the implant/soft-tissue interface. J Oral Implantol. 1994;20:36–40.

Simchi A, Tamjid E, Pishbin F, Boccaccini AR. Recent progress in inorganic and composite coatings with bactericidal capability for orthopaedic applications. Nanomedicine. 2011;7:22–39.

Simion M, Benigni M, Al-Hezaimi K, Kim DM. Early bone formation adjacent to oxidized and machined implant surfaces: a histologic study. Int J Periodontics Restorative Dent. 2015a;35:9–17.

Simion M, Gionso L, Grossi GB, Briguglio F, Fontana F. Twelve-year retrospective follow-up of machined implants in the posterior maxilla: Radiographic and peri-implant outcome. Clin Implant Dent Relat Res. 2015b;17:e343–51.

Smeets R, Henningsen A, Jung O, Heiland M, Hammächer C, Stein JM. Definition, etiology, prevention and treatment of peri-implantitis--a review. Head Face Med. 2014;10:34.

Smith DC, Pilliar RM, Chernecky R. Dental implant materials. I. Some effects of preparative procedures on surface topography. J Biomed Mater Res. 1991;25:1045–68.

Socransky SS, Haffajee AD. Dental biofilms: difficult therapeutic targets. Periodontol 2000. 2002;28:12-55.

Socransky SS, Haffajee AD, Cugini MA, Smith C, Kent RL. Microbial complexes in subgingival plaque. J Clin Periodontol. 1998a;25:134–44.

Socransky SS, Haffajee AD, Cugini MA, Smith C, Kent RL Jr. Microbial complexes in subgingival plaque. J Clin Periodontol. 1998b;25:134–44.

Stamatakis A. RAxML version 8: a tool for phylogenetic analysis and post-analysis of large phylogenies. Bioinformatics. 2014;30:1312–3.

van Steenberghe D, Klinge B, Lindén U, Quirynen M, Herrmann I, Garpland C. Periodontal indices around natural and titanium abutments: a longitudinal multicenter study. J Periodontol. 1993;64:538–41.

Steinebrunner L, Wolfart S, Bössmann K, Kern M. In vitro evaluation of bacterial leakage along the implant-abutment interface of different implant systems. Int J Oral Maxillofac Implants.

2005;20:875–81.

Stokman MA, van Winkelhoff AJ, Vissink A, Spijkervet FKL, Raghoebar GM. Bacterial colonization of the peri-implant sulcus in dentate patients: a prospective observational study. Clin Oral Investig. 2017;21:717–24.

Street J, Bao M, deGuzman L, Bunting S, Peale FV Jr, Ferrara N, et al. Vascular endothelial growth factor stimulates bone repair by promoting angiogenesis and bone turnover. Proc Natl Acad Sci U S A. 2002;99:9656–61.

Sykaras N, Iacopino AM, Marker VA, Triplett RG, Woody RD. Implant materials, designs, and surface topographies: their effect on osseointegration. A literature review. Int J Oral Maxillofac Implants. 2000;15:675–90.

Tabanella G, Nowzari H, Slots J. Clinical and microbiological determinants of ailing dental implants. Clin Implant Dent Relat Res. 2009;11:24–36.

Tack L, Schickle K, Böke F, Fischer H. Immobilization of specific proteins to titanium surface using self-assembled monolayer technique. Vol. 31, Dental Materials. 2015. p. 1169–79.

Takanashi K, Kishi M, Okuda K, Ishihara K. COLONIZATION BY *PORPHYROMONAS GINGIVALIS* AND *PREVOTELLA INTERMEDIA* FROM TEETH TO OSSEOINTEGRATED IMPLANT REGIONS. Vol. 45, The Bulletin of Tokyo Dental College. 2004. p. 77–85.

Takechi T, Wada R, Fukuda T, Harada K, Takamura H. Antioxidant activities of two sericin proteins extracted from cocoon of silkworm (Bombyx mori) measured by DPPH, chemiluminescence, ORAC and ESR methods. Vol. 2, Biomedical Reports. 2014. p. 364–9.

Tallarico M, Canullo L, Xhanari E, Meloni SM. Dental implants treatment outcomes in patient under active therapy with alendronate: 3-year follow-up results of a multicenter prospective observational study. Clin Oral Implants Res. 2016;27:943–9.

Tarnow DP. Increasing Prevalence of Peri-implantitis: How Will We Manage? J Dent Res. 2016;95:7–8.

Teles FRF. The Microbiome of Peri-implantitis: Is It Unique? Compend Contin Educ Dent. 2017;38:22–5.

Telleman G, Raghoebar GM, Vissink A, Meijer HJA. Impact of Platform Switching on Peri-Implant Bone Remodeling around Short Implants in the Posterior Region, 1-Year Results from a Split-Mouth Clinical Trial. Vol. 16, Clinical Implant Dentistry and Related Research. 2014. p. 70–80.

Terheyden H, Lang NP, Bierbaum S, Stadlinger B. Osseointegration--communication of cells. Clin Oral Implants Res. 2012;23:1127–35.

Tett A, Pasolli E, Farina S, Truong DT, Asnicar F, Zolfo M, et al. Unexplored diversity and strain-level structure of the skin microbiome associated with psoriasis. Vol. 3, npj Biofilms and Microbiomes. 2017.

Teughels W, Assche N, Sliepen I, Quirynen M. Effect of material characteristics and/or surface topography on biofilm development. Clin Oral Implants Res 2006;17(suppl 2):68–81.

Thomas AM, Manghi P, Asnicar F, Pasolli E, Armanini F, Zolfo M, et al. Metagenomic analysis of colorectal cancer datasets identifies cross-cohort microbial diagnostic signatures and a link with choline degradation. Vol. 25, Nature Medicine. 2019. p. 667–78.

Tolentino L, Sukekava F, Seabra M, Lima LA, Garcez-Filho J, Araújo MG. Success and survival rates of narrow diameter implants made of titanium-zirconium alloy in the posterior region of the jaws - results from a 1-year follow-up. Clin Oral Implants Res. 2014;25:137–41.

Tomasi C, Derks J. Clinical research of peri-implant diseases--quality of reporting, case definitions and methods to study incidence, prevalence and risk factors of peri-implant diseases. J Clin Periodontol. 2012;39:207–23.

Tomasi C, Tessarolo F, Caola I, Piccoli F, Wennström JL, Nollo G, et al. Early healing of peri-implant mucosa in man. J Clin Periodontol. 2016;43:816–24.

Tomasi C, Tessarolo F, Caola I, Wennström J, Nollo G, Berglundh T. Morphogenesis of peri-implant mucosa revisited: an experimental study in humans. Clin Oral Implants Res. 2014;25:997–1003.

Tonetti MS, Greenwell H, Kornman KS. Staging and grading of periodontitis: Framework and proposal of a new classification and case definition. J Periodontol. 2018;89 Suppl 1:S159–72.

Trisi P, Rao W, Rebaudi A. A histometric comparison of smooth and rough titanium implants in human low-density jawbone. Int J Oral Maxillofac Implants. 1999;14:689–98.

Trombelli L, Farina R, Silva CO, Tatakis DN. Plaque-induced gingivitis: Case definition and diagnostic considerations. Vol. 45, Journal of Clinical Periodontology. 2018. p. S44–67.

Truong DT, Franzosa EA, Tickle TL, Scholz M, Weingart G, Pasolli E, et al. MetaPhlAn2 for enhanced metagenomic taxonomic profiling. Vol. 12, Nature Methods. 2015. p. 902–3.

Truong DT, Tett A, Pasolli E, Huttenhower C, Segata N. Microbial strain-level population structure and genetic diversity from metagenomes. Genome Res. 2017;27:626–38.

Tsigarida AA, Dabdoub SM, Nagaraja HN, Kumar PS. The Influence of Smoking on the Peri-Implant Microbiome. J Dent Res. 2015;94:1202–17.

Tyson GW, Chapman J, Hugenholtz P, Allen EE, Ram RJ, Richardson PM, et al. Community structure and metabolism through reconstruction of microbial genomes from the environment. Nature. 2004;428:37–43.

Vandenbroucke JP, von Elm E, Altman DG, Gøtzsche PC, Mulrow CD, Pocock SJ, et al. Strengthening the Reporting of Observational Studies in Epidemiology (STROBE): explanation and elaboration. Int J Surg. 2014;12:1500–24.

Vandeweghe S, De Bruyn H. A within-implant comparison to evaluate the concept of platform switching: a randomised controlled trial. Eur J Oral Implantol. 2012;5:253–62.

Van Noort R. Titanium: The implant material of today. J Mater Sci. 1987;22:3801–11.

Vanzillotta PS, Sader MS, Bastos IN, Soares G de A. Improvement of in vitro titanium bioactivity by three different surface treatments. Dent Mater. 2006;22:275–82.

Varoquaux G, Buitinck L, Louppe G, Grisel O, Pedregosa F, Mueller A. Scikit-learn. Vol. 19, GetMobile: Mobile Computing and Communications. 2015. p. 29–33.

Vela-Nebot X, Rodríguez-Ciurana X, Rodado-Alonso C, Segalà-Torres M. Benefits of an implant platform modification technique to reduce crestal bone resorption. Implant Dent. 2006;15:313–20.

Veltri M, Ferrari M, Balleri P. One-year outcome of narrow diameter blasted implants for rehabilitation of maxillas with knife-edge resorption. Clin Oral Implants Res. 2008;19:1069–73.

Venter JC, Remington K, Heidelberg JF, Halpern AL, Rusch D, Eisen JA, et al. Environmental genome shotgun sequencing of the Sargasso Sea. Science. 2004;304:66–74.

Verran J, Whitehead K. Factors affecting microbial adhesion to stainless steel and other materials used in medical devices. Int J Artif Organs. 2005;28:1138–45.

Wagner CD. NIST x-ray photoelectron spectroscopy (XPS) database. 1990.

Wang XX, Hayakawa S, Tsuru K, Osaka A. Improvement of bioactivity of H(2)O(2)/TaCl(5)-treated titanium after subsequent heat treatments. J Biomed Mater Res. 2000;52:171–6.

Wang Y-C, Kan JYK, Rungcharassaeng K, Roe P, Lozada JL. Marginal bone response of implants with platform switching and non-platform switching abutments in posterior healed sites: a 1-year prospective study. Clin Oral Implants Res. 2015;26:220–7.

Weng D, Richter EJ. Die Implantat-Abutment-Verbindung-vom mechanischen zum biologischen Aspekt des Mikrospalts. Implantologie. 2005;13:125–30.

Wennerberg A, Albrektsson T. Effects of titanium surface topography on bone integration: a systematic review. Clin Oral Implants Res. 2009;20 Suppl 4:172–84.

Wennerberg A, Albrektsson T, Andersson B. Bone tissue response to commercially pure titanium implants blasted with fine and coarse particles of aluminum oxide. Int J Oral Maxillofac Implants. 1996a;11:38–45.

Wennerberg A, Albrektsson T, Lausmaa J. Torque and histomorphometric evaluation of cp titanium screws blasted with 25-and 75-µm-sized particles of Al2O3. Journal of Biomedical Materials Research: An Official Journal of The Society for Biomaterials and The Japanese Society for Biomaterials. 1996b;30:251–60.

Wennström JL, Ekestubbe A, Gröndahl K, Karlsson S, Lindhe J. Implant-supported single-tooth restorations: a 5-year prospective study. J Clin Periodontol. 2005;32:567–74.

Werb Z, Tremble P, Werb Z, Damsky CH, Tremble P, Damsky CH. Regulation of extracellular matrix degradation by cell—extracellular matrix interactions. Vol. 32, Cell Differentiation and Development. 1990. p. 299–306.

Wiskott HWA, Anselm Wiskott HW, Belser UC. Lack of integration of smooth titanium surfaces: a working hypothesis based on strains generated in the surrounding bone. Vol. 10, Clinical Oral Implants Research. 1999. p. 429–44.

Wojciechowski PW. Transport and adsorption of cells and proteins at interfaces. Interfacial phenomena and bioproducts. 1996;209–29.

Yeung SCH. Biological basis for soft tissue management in implant dentistry. Aust Dent J. 2008;53 Suppl 1:S39–42.

Yu X-L, Chan Y, Zhuang L-F, Lai H-C, Lang NP, Lacap-Bugler DC, et al. Distributions of Synergistetes in clinically-healthy and diseased periodontal and peri-implant niches. Microb Pathog. 2016;94:90–103.

Yu X-L, Chan Y, Zhuang L, Lai H-C, Lang NP, Leung WK, et al. Intra-oral single site

comparisons of periodontal and peri-implant microbiota in health and disease. Clin Oral Implants Res. 2019;

Zavan B, Giorgi C, Bagnara GP, Vindigni V, Abatangelo G, Cortivo R. Osteogenic and chondrogenic differentiation: comparison of human and rat bone marrow mesenchymal stem cells cultured into polymeric scaffolds. Eur J Histochem. 2007;51 Suppl 1:1–8.

Zavan B, Vindigni V, Vezzù K, Zorzato G, Luni C, Abatangelo G, et al. Hyaluronan based porous nano-particles enriched with growth factors for the treatment of ulcers: a placebo-controlled study. J Mater Sci Mater Med. 2009;20:235–47.

Zhang D-Y, Pan Y, Zhang C, Yan B-X, Yu S-S, Wu D-L, et al. Wnt/β-catenin signaling induces the aging of mesenchymal stem cells through promoting the ROS production. Vol. 374, Molecular and Cellular Biochemistry. 2013. p. 13–20.

Zhang Y-Q. Applications of natural silk protein sericin in biomaterials. Biotechnol Adv. 2002;20:91–100.

Zheng H, Xu L, Wang Z, Li L, Zhang J, Zhang Q, et al. Subgingival microbiome in patients with healthy and ailing dental implants. Sci Rep. 2015;5:10948.

Zhou Y, Zimber M, Yuan H, Naughton GK, Fernan R, Li W-J. Effects of Human Fibroblast-Derived Extracellular Matrix on Mesenchymal Stem Cells. Stem Cell Rev. 2016;12:560–72.

Zhuang L-F, Watt RM, Mattheos N, Si M-S, Lai H-C, Lang NP. Periodontal and peri-implant microbiota in patients with healthy and inflamed periodontal and peri-implant tissues. Clin Oral Implants Res. 2016;27:13–21.

Zipprich H, Miatke S, Hmaidouch R, Lauer HC. A New Experimental Design for Bacterial Microleakage Investigation at the Implant-AbutmentInterface: An In Vitro Study. Int J Oral Maxillofac Implants. 2016;31(1):37-44.

Zipprich H, Weigl P, Ratka C, Lange B, Lauer HC. The micromechanical behavior of implant-abutment connections under a dynamic load protocol. Clin Implant Dent Relat Res. 2018;20(5):814-823.

Zitzmann NU, Berglundh T. Definition and prevalence of peri-implant diseases. J Clin Periodontol. 2008a;35:286–91.